Regeneration of Articular Cartilage using Mesenchymal Stem Cells

by

Troy Douglas Bornes

A thesis submitted in partial fulfillment of the requirements for the degree of

Doctor of Philosophy

in

Experimental Surgery

Department of Surgery
University of Alberta

Abstract

Articular cartilage injury is a major risk factor for the development of osteoarthritis, a condition that results in significant patient morbidity and substantial cost to the healthcare system. Due to the limited capacity of articular cartilage to regenerate, early intervention is required to prevent the progression of focal chondral and osteochondral defects to advanced disease and joint degeneration. Effective management options are limited at present. Mesenchymal stem cell (MSC) transplantation is a promising treatment strategy given the high proliferative capacity of MSCs and their potential to differentiate into cartilage-producing cells. MSCs may be harvested through minimally invasive techniques, such as bone marrow aspiration, which do not require joint surgery or extraction of cells from healthy cartilage as required by other cell-based strategies. Although preclinical and clinical studies have demonstrated that MSCs are capable of producing hyaline-like repair tissue and improving functional outcome following transplantation into articular cartilage defects, tissue engineering and transplantation variables are actively being studied with the goal of optimizing this treatment modality.

The experiments of this thesis focused on the investigation of bone marrow-derived MSC (BMSC) isolation and expansion environment, biomaterial matrix composition and seeding density, and chondrogenic differentiation

conditions in BMSC-based cartilage engineering using *in vitro* and *in vivo* models. The first study involved an assessment of incubator oxygen tension during ovine BMSC isolation, expansion and differentiation on *in vitro* BMSC chondrogenesis within porous scaffolds composed of type I collagen or esterified hyaluronic acid. Hypoxic culture was shown to augment chondrogenesis. Differences in gene expression and construct size were noted between scaffolds, although extracellular matrix formation consistent with hyaline-like cartilaginous tissue was noted within each scaffold. This was followed by a second study that characterized contraction of collagen I scaffolds seeded with human BMSCs that were isolated and expanded under different oxygen tensions. During chondrogenesis, BMSC-seeded scaffolds increased in size initially and then progressively contracted to the end of the 30-day culture period. Scaffold-specific and cell-mediated diameter changes were elucidated. Hypoxic isolation and expansion significantly reduced scaffold contraction. Thereafter, a third study investigated *in vitro* chondrogenesis of ovine BMSCs within a collagen I scaffold following isolation and expansion in either two-dimensional or three-dimensional environments. Both protocols yielded cells with hyaline-associated gene expression and extracellular matrix molecule production. Optimal scaffold seeding densities for chondrogenesis were established. The final study utilized an *in vivo* sheep model with full-thickness articular cartilage defects to assess a novel protocol for BMSC transplantation that involved BMSCs that were isolated, expanded, seeded within an esterified hyaluronic acid scaffold, and chondrogenically primed for a short duration in chondrogenic medium prior to

implantation. The impact of oxygen tension during pre-implantation *ex vivo* culture on cartilaginous tissue formation was investigated. Implantation of BMSC-seeded scaffolds yielded repair tissues that varied in quality between hyaline-like cartilage and fibrocartilage. Defects implanted with cell-seeded scaffolds had significantly higher histological scores and repair tissue areas than cell-free controls. A consistent effect of oxygen tension was not established across animals.

The studies described in this thesis demonstrate methods of optimization of BMSC chondrogenesis within *in vitro* and *in vivo* models through modulation of tissue engineering variables. Although the outcomes of this work are promising, further investigation is required to establish techniques that may be used in BMSC transplantation protocols to promote the reproducible creation of tissue that resembles articular cartilage.

Preface

This thesis is an original work by Troy Douglas Bornes. The research project, of which this thesis is a part, received ethical approval from the University of Alberta's Research Ethics Office. The Health Research Ethics Board – Biomedical Panel provided ethical approval for the experimental use of human cells and tissue, Project Name "Regeneration of Articular Cartilage utilizing Chondrocytes and Mesenchymal Stem Cells", No. Pro00018778, October 24, 2012, which was revised to Project Name "Regeneration of Nasal and Articular Cartilage utilizing Chondrocytes and Mesenchymal Stem Cells", No. Pro00018778, November 13, 2015. The Animal Care and Use Committee provided ethical approval for the experimental use of animal models, Project Name "Joint Tissue Reconstruction Using Stem Cells", No. AUP00000764, October 9, 2013.

Chapter 2 of this thesis has been published in part as: T.D. Bornes, A.B. Adesida and N.M. Jomha, "Mesenchymal stem cells in the treatment of traumatic articular cartilage defects: a comprehensive review," *Arthritis Research & Therapy* 2014, volume 16, issue 5, pages 432 (1-19 online). T.D Bornes was responsible for study design, literature review, manuscript composition, and manuscript revision. A.B. Adesida and N.M. Jomha were supervisory authors and contributed to study design and manuscript revision.

Chapter 3 and Appendix 2 of this thesis have been published in part as: T.D. Bornes, N.M. Jomha, A. Mulet-Sierra, and A.B. Adesida, "Hypoxic culture of bone marrow-derived mesenchymal stromal stem cells differentially enhances *in vitro* chondrogenesis within cell-seeded collagen and hyaluronic acid porous scaffolds," *Stem Cell Research & Therapy* 2015, volume 6, issue 1, pages 84 (1-17 online). T.D. Bornes was responsible for study design, experimental methods, data collection, analysis, manuscript composition and manuscript revision. N.M. Jomha and A.B. Adesida were supervisory authors and contributed to study design and manuscript revision. A. Mulet-Sierra contributed to experimental methods.

Chapter 5 of this thesis has been published in part as: T.D. Bornes, N.M. Jomha, A. Mulet-Sierra, and A.B. Adesida, "Optimal Seeding Densities for In Vitro Chondrogenesis of Two- and Three-Dimensional-Isolated and -Expanded Bone Marrow-Derived Mesenchymal Stromal Stem Cells Within a Porous Collagen Scaffold," *Tissue Engineering Part C Methods* 2016, volume 22, issue 3, pages 208-220. T.D. Bornes was responsible for study design, experimental methods, data collection, analysis, manuscript composition and manuscript revision. N.M. Jomha and A.B. Adesida were supervisory authors and contributed to study design and manuscript revision. A. Mulet-Sierra contributed to experimental methods.

Appendix 1 of this thesis has been published in part as: T.D. Bornes, N.M. Jomha, A. Mulet-Sierra, and A.B. Adesida, “Porous Scaffold Seeding and Chondrogenic Differentiation of BMSC-seeded Scaffolds,” *Bio-protocol* 2015, volume 5, issue 24, page e1693. T.D. Bornes was responsible for manuscript composition and manuscript revision. N.M. Jomha and A.B. Adesida were supervisory authors and contributed to manuscript revision. A. Mulet-Sierra contributed to experimental methods related to this manuscript.

Dedication

This thesis is dedicated to my parents, Glenn and Barbara Bornes.

Acknowledgements

I extend my sincerest gratitude to my PhD Supervisors, Dr. Nadr Jomha and Dr. Adetola Adesida, for their guidance, mentorship and motivation throughout my research training. I thank Dr. Hasan Uludag, Dr. Gregory Korbutt and Dr. Thomas Churchill for their unique perspectives and constructive criticism during meetings, seminars and examinations. I thank Dr. Mark Hurtig for his stimulating questioning and discussion during my PhD defense. For their invaluable advice, technical support and company, I would like to recognize Aillette Mulet Sierra, Dr. Stephen Andrews, Joshua Hahn, Yan Liang, Dr. Leila Laouar, Enaam Idrees, Leiah Luoma, Rotem Lavy, Kirollos Labib, Anika Chowdhury, Alex Szojka, and Karamveer Lalh. I am grateful for the animal monitoring and care provided by Brenda Tchir. I thank Dr. Craig Wilkinson for providing expertise in veterinary medicine and guidance pertaining to the use of animals in our studies.

I wish to acknowledge some very important people outside of the laboratory. My family and friends have supported me throughout my training. I would like to recognize my parents, Glenn and Barbara Bornes, who have provided everlasting guidance and reassurance in all my endeavours. My brother, Cody Bornes, and grandmother, Anita Bornes, have encouraged me along the way. Finally, I wish to thank my girlfriend, Alicia Achen, who has inspired me to

continue to grow and improve. Her loving support during times of success and hardship is appreciated.

I am grateful for the stipend support from the Clinician Investigator Program at the University of Alberta, Alberta Innovates-Health Solutions and Canadian Institutes of Health Research. Research funding was provided by grants from the Edmonton Orthopaedic Research Committee, Canadian Institutes of Health Research and University Hospital Foundation in Edmonton, Alberta. Travel was funded by the Division of Orthopaedic Surgery, Faculty of Graduate Studies and Research, and Alberta Osteoarthritis Team. I would like to acknowledge the kind donations from several companies: Integra LifeSciences Corp. provided the collagen I matrix, Anika Therapeutics S.r.l. provided the esterified hyaluronic acid (HYAFF) matrix, and Baxter Corp. provided the Tisseel fibrin sealant for our studies.

Table of Contents

List of Figures

List of Tables

List of Abbreviations

2D : two-dimensional

3D: three-dimensional

α: alpha

ADAMTS: a disintegrin and metalloproteinase with thrombospondin motifs

AEC: aminoethylcarbazole

α-MEM: alpha-minimal essential medium

ACI: autologous chondrocyte implantation

ACT: autologous chondrocyte transplantation

AMIC: autologous matrix-induced chondrogenesis

ANOVA: analysis of variance

AOFAS: American Orthopaedic Foot and Ankle Society

β: beta

β-actin: beta-actin

BFOA: bipolar fresh osteochondral allograft

BLAST: Basic Local Alignment Search Tool

BMA: bone marrow aspirate

BMAC: bone marrow aspirate concentrate

BMC: bone marrow concentrate

BMDC: bone marrow-derived cell

BMP: bone morphogenic protein

BMNC: bone marrow-derived mononucleated cell

BMSC: bone marrow-derived mesenchymal stromal stem cell

CD: cluster of differentiation

CDM: cartilage-derived matrix

cDNA: complementary deoxyribonucleic acid

CFU-F: colony-forming unit fibroblastic

COMP: cartilage oligomeric matrix protein

CT: computed tomography

DAPI: 4',6-diamidino-2-phenylindole

DHT: dehydrothermal treatment

DMEM: Dulbecco's modified Eagle's medium

ECM: extracellular matrix

EDTA: ethylenediaminetetraacetic acid

FAAM: Foot and Ankle Ability Measures

FBS: fetal bovine serum

FGF-2: fibroblast growth factor-two, basic fibroblast growth factor

GAG: glycosaminoglycan

HA: hyaluronic acid

HEPES: 4-(2-hydroxyethyl)-1-piperazineethanesulfonic acid

HLA: human leukocyte antigen

HSS: Hospital for Special Surgery

IBMX: 3-isobutyl-1-methylxanthine

ICRS: International Cartilage Repair Society

IGF: insulin-like growth factor

IL: interleukin

ITS: insulin-transferrin-selenium

IKDC: International Knee Documentation Committee

ISCT: International Society for Cellular Therapy

KOOS: Knee Injury and Osteoarthritis Outcome Score

KS-F: Knee Society function

KSS: Knee Society Score

LEFS: Lower Extremity Functional Scale

MACI: matrix-associated autologous chondrocyte implantation

MACT: matrix-associated autologous chondrocyte transplantation

MMP: matrix metalloproteinase

MNC: mononucleated cell

MOCART: magnetic resonance observation of cartilage repair tissue

MRI: magnetic resonance imaging

mRNA: messenger ribonucleic acid

MSC: mesenchymal stem cell

NCBI: National Center for Biotechnology Information

OA: osteoarthritis

OATS: osteochondral autograft transplantation

OCA: osteochondral allograft transplantation

P: passage

PBS: phosphate-buffered saline

PCL: polycaprolactone

PDGF: platelet-derived growth factor

PGA: polyglycolic acid

PLA: polylactic acid

PLGA: polylactide-co-glycolide, polylacticglycolic acid

RNA: ribonucleic acid

RUNX2: Runt-related transcription factor-two

RT-qPCR: reverse-transcription quantitative real-time polymerase chain reaction

SD: standard deviation

SEM: standard error of the mean

SF-36: Short Form 36 Health Survey

SLRP: small leucine-rich repeat proteoglycan

SMA: smooth muscle actin

SOX: sex determining region Y (SRY)-box

SPECT-CT: single photon emission computed tomography-computed tomography

T150: 150-cm^2 tissue-culture flask

TEC: tissue-engineered construct

TGF-β: transforming growth factor-beta

UV: ultraviolet

VAS: visual analog scale

Vol: volume

Wt: weight

Chapter 1

Introduction

Troy D. Bornes

1.1 Thesis overview

Articular cartilage injury is a major risk factor for the development of osteoarthritis (OA), a condition that results in significant patient morbidity and substantial cost to the healthcare systems of several nations that include Canada, the United States of America, the United Kingdom, France, Italy, Spain, and Australia [1-19]. It is estimated that 10-25% of the adult population suffers from OA, with an increased prevalence noted in older age groups [7-11, 13, 14, 20-22]. OA is irreversible and eventually requires joint replacement for alleviation of pain and restoration of function as it progresses to end-stage disease [23-26]. Due to the limited capacity of articular cartilage to regenerate, early intervention is required to prevent the progression of focal cartilage injury to advanced disease and joint degeneration [27]. Effective management options are limited at present. Consequently, there has been a drive to develop novel tissue engineering techniques with the goal of resurfacing defects with bioengineered cartilage that recapitulates the properties of hyaline cartilage [28-30].

Transplantation of mesenchymal stem cells (MSCs) is a promising strategy given the high proliferative capacity of MSCs and their potential to differentiate into cartilage-producing cells [31-33]. MSCs have been historically harvested through bone marrow aspiration, which does not require invasive surgical intervention or cartilage extraction from other sites as required by other cell-based strategies [34]. Biomaterial matrices are commonly used in conjunction with MSCs to aid cell delivery and support chondrogenic differentiation, extracellular matrix (ECM) formation and three-dimensional (3D) tissue development [35]. A number of specific MSC transplantation protocols have successfully resurfaced articular cartilage in animals and humans to date [29, 36-38]. Arthroscopy, histologic staining and imaging have demonstrated that MSCs are capable of filling defects with hyaline-like cartilaginous repair tissue in clinical trials [38-44]. Positive functional outcomes have been reported at 12-54 months post-implantation, but future work is required to assess long-term outcomes in comparison to other treatment modalities [38, 39, 41, 45, 46]. Despite relatively positive outcomes, further investigation is required to establish a consensus on technique for treatment of chondral and osteochondral defects with respect to cell source, cell isolation and expansion environment, biomaterial matrix composition, matrix seeding, *in vitro* precultivation, and implantation. This will allow for optimization of MSC proliferation, chondrogenic differentiation, 3D tissue formation, bioengineered cartilage integration, and clinical outcome.

The objective of this thesis is to provide insight into variables that impact MSC transplantation with the goal of optimizing outcomes. The thesis will begin with an introduction to articular cartilage anatomy, physiology and injury, and current surgical treatment modalities for focal articular cartilage defects. This will be followed by a comprehensive review of the current preclinical and clinical literature pertaining to MSC-based cartilage engineering and transplantation. A series of experiments designed to investigate specific tissue engineering and transplantation variables using *in vitro* and *in vivo* models will be reported in subsequent chapters.

1.2 Anatomy and physiology of articular cartilage

Articular cartilage is a type of hyaline cartilage that forms the bearing surface of synovial joints and plays a crucial role in joint motion and load transfer [47-49]. The minimal friction created between smooth articular cartilage surfaces in conjunction with lubricating synovial fluid allows for movement between long bones that is unobstructed, pain-free and efficient [47]. On a macroscopic level, hyaline articular cartilage is a glossy, semi-transparent connective tissue that lacks blood vessels, lymphatic structures and nerves [50, 51]. Articular cartilage varies in thickness depending on its location. Within the weight-bearing articular surfaces of the human lower extremity, cartilage thickness has been measured at 1.7-2.7 mm on the femoral condyles, 1.5-3.5 mm on the tibial plateau, 1.1-1.6 mm on the tibial plafond, 0.9-1.6 mm on the talus, 1.4-2.4 on the femoral head, and 1.2-2.3 mm on the acetabulum of the pelvis [52].

Microscopically, hyaline articular cartilage is composed of cells and ECM that are organized into a complex 3D structure [50]. The chondrocyte – the specialized cell of articular cartilage – produces, organizes and maintains the abundant ECM, and these processes are modulated by extracellular cues such as mechanical loading and chemical mediators [53-55]. Chondrocytes have a mean diameter of 13 μm, but vary in size and shape depending on location [56, 57]. With a mean cell volume of 1748 μm^3, each chondrocyte controls 104,040 μm^3 of surrounding ECM territory [57]. Accordingly, there are roughly 10,000 chondrocytes per mm^3 of tissue with only 1-2% of the total volume of articular cartilage attributed to cellular volume [57, 58]. Although chondrocytes were once thought to be the only cell type in healthy articular cartilage, it is now apparent that multipotent progenitor cells with characteristics of MSCs exist within non-arthritic cartilage in humans and other mammals [59-62]. These cells demonstrate homing to cartilage defects following injury [63]. In the setting of OA, progenitor cells also presumably migrate into articular cartilage from subchondral bone through breaks in the tidemark and through sprouting blood vessels [64, 65].

The ECM of articular cartilage is made up of collagen, proteoglycans, hyaluronic acid, and various other proteins. A large amount of water accompanies these ECM components [66]. Type II collagen forms a network of macrofibrils within articular cartilage that provides strength and tensile stiffness, while types IX and XI regulate this network [56]. Types III and VI play roles within the

pericellular ECM [67, 68]. Type X is present around hypertrophic chondrocytes that reside in the growth plate prior to skeletal maturity and in arthritic cartilage [69, 70].

Proteoglycans, formed from glycosaminoglycans (GAGs) and proteins, interact with the collagen network and other macromolecules [71]. Aggrecan makes up 90% of the total proteoglycan mass in articular cartilage [56]. Within large aggregates, aggrecan associates with hyaluronic acid, a non-sulfated GAG that serves as a backbone molecule [72]. The fixed negative charge of aggrecan is key to the development of osmotic swelling and the resulting compressive strength conferred by articular cartilage [73]. Small leucine-rich repeat proteoglycans (SLRPs) such as decorin, fibromodulin and lumican regulate and protect the collagen network and interact with growth factors, fibrinogen and elastin [71].

Four anatomic layers or zones with characteristic cellular and extracellular patterns have been defined within articular cartilage [49, 53, 57, 74]. The superficial zone contains a relatively high number of flattened chondrocytes that are oriented parallel to the articular surface, and a low proteoglycan content. Collagen fibrils run parallel to the surface. The middle or transitional zone has more proteoglycans and less chondrocytes that are round in shape. Collagen fibrils occur in radial bundles or layers and are less organized in this zone. The deep or radial zone is composed of an abundance of proteoglycans and an even

lower density of round chondrocytes that are positioned perpendicularly to the articular surface. Radially configured large collagen fibrils are present, and these course through the tidemark into the underlying calcified zone to provide an anchoring effect. The calcified zone is a thin layer that contains hypertrophic chondrocytes and connects the three more superficial zones to subchondral bone. The mean combined thickness of the superficial, middle and deep zones has been measured at 2.4 mm in human femoral condyles, while the calcified cartilage layer and subchondral bone plate were 0.134 mm and 0.190 mm, respectively [57].

1.3 Articular cartilage injury and post-traumatic osteoarthritis

1.3.1 Pathogenesis of focal articular cartilage injury

Joint trauma resulting in an articular cartilage defect leads to a series of immediate, acute post-traumatic and chronic events at the cellular and tissue levels [75]. Much of our current knowledge pertaining to this process has been derived from *ex vivo* explant models and *in vivo* animal studies that have utilized simulated defects of articular cartilage. At the time of mechanical injury to articular cartilage, the collagen network of cartilage ruptures and this leads to exposure, swelling and loss of proteoglycans [76-78]. Chondrocyte death in the area of injury occurs through necrosis [79-83]. Hemarthrosis develops as blood enters the joint through ruptured vessels in the joint capsule, cruciate ligaments, synovium, or subchondral bone [84-86]. Leukocytes infiltrate and become

activated to produce reactive oxygen species and enzymes such as elastase that are capable of proteoglycan degradation [87].

The events of the acute post-traumatic period that occur in days-to-weeks following injury are variable and depend on whether a focal injury involves articular cartilage alone (chondral defect) or both articular cartilage and underlying subchondral bone (osteochondral defect) [88]. The reason for this is that articular cartilage is avascular, while subchondral bone has a rich blood supply [50]. In the context of a focal chondral defect, an inflammatory response occurs via vascularized tissues in the joint, such as the synovium, that have undergone traumatic insult although the response at the defect site is limited given that subchondral bone is intact [89, 90]. Chondrocytes in the area surrounding the defect proliferate and increase synthesis of ECM molecules [27, 80, 91]. Chondrogenic progenitor cells from adjacent cartilage migrate into the defect site and participate in tissue repair [63]. However, this reparative response is temporary and often insufficient to resurface the defect [1, 27]. Moreover, ongoing cell death occurs through apoptosis in the region surrounding the defect, which can increase the size of the defect with time [82, 92].

A focal osteochondral defect involves compromise of the subchondral bone plate that leads to an inflammatory response and allows for blood and marrow containing cells and chemical mediators to enter the defect site [86, 93]. Fibrin forms and platelets bind leading to the creation of a fibrin clot [86, 94].

Cells from the bone marrow that presumably include a population of MSCs enter the defect site, proliferate, differentiate and form repair tissue [27, 86, 94, 95]. After 6 weeks, cartilaginous repair tissue has features of mixed hyaline cartilage and fibrocartilage [86, 93, 94, 96-99]. Thereafter, remodeling occurs and repair tissue predominantly consists of fibrocartilage [94, 96, 97].

In the chronic period following articular cartilage injury, inflammation and tissue remodeling occur in a variable fashion [75]. Focal chondral defects that lacked repair tissue in the acute post-traumatic period remain empty given that the subchondral bone is intact [27]. Some degenerate leading to post-traumatic OA [3, 100]. Focal osteochondral lesions that were filled with fibrocartilaginous repair tissue either undergo further remodeling to restore the normal articular surface or deteriorate to OA [86, 101-103]. Studies that have assessed the natural history of articular cartilage injury in humans have demonstrated the spectrum of outcomes that exists with chondral and osteochondral defects.

1.3.2 Natural history of focal articular cartilage injury

Focal articular cartilage injury is a common issue following joint injury. With respect to the knee joint, the prevalence of articular cartilage injury has been reported to be 60-63% in two large studies involving over 25,000 patients assessed with arthroscopy [104, 105]. Widuchowski *et al.* reported focal chondral and osteochondral lesions in 67%, OA in 29%, osteochondritis dissecans in 2% and other defects in 1% of patients [104]. Of the patients with focal defects, 90%

had a history of knee trauma. Defect size was 0.5 cm^2 in 39%, 0.5-1 cm^2 in 25%, 1-2 cm^2 in 29%, and >2 cm^2 in 7% of patients. Based on the Outerbridge classification [106], 36% of patients had lesions of grade III or IV that could be considered operative. Other injuries were found in 70% of patients with the most common being medial meniscus tear (37%), anterior cruciate ligament (ACL) tear (36%) and lateral meniscus tear (17%).

The evolution of focal articular cartilage defects to osteoarthritis has been demonstrated in a large-animal study by Schinhan *et al.* [100]. Simulated full-thickness cartilage lesions with diameters of 7 mm and 14 mm were created on the medial femoral condyles of sheep. The sheep were mobilized and sacrificed after either 6 or 12 weeks. After 6 weeks, only minor degenerative changes were noted. After 12 weeks, unicompartmental OA was noted on femoral condyles in joints that were subjected to 7 mm-diameter defects. Joints that were injured with 14 mm-diameter defects had femoral condyle OA along with significant degenerative changes noted on the tibia and meniscus.

Multiple long-term clinical studies have demonstrated an association between traumatic articular cartilage defects and post-traumatic OA [3-5]. Maletius *et al.* retrospectively assessed patients with untreated traumatic articular cartilage defects of the knee localized to the weight-bearing zone of the femoral condyle based on arthroscopy [3]. At follow-up time of 12-15 years, 71% of patients with isolated chondral defects measuring at least one-third of the condyle

width had signs of OA on imaging. In contrast, OA was noted in non-operative knees in 43% of patients. Stufkens *et al.* studied a population of patients with ankle fractures requiring operative fixation [4]. Significantly worse radiographic and functional outcomes were noted at a mean follow-up time of 13 years when articular cartilage injury was noted at the time of fixation. Articular cartilage lesions on the anterior talus, lateral talus, and medial malleolus were associated with clinical signs of osteoarthritis. Messner *et al.* arthroscopically assessed 19 patients with post-traumatic chondral lesions, 6 patients with osteochondritis dissecans, and 3 patients with non-traumatic chondral lesions of the distal femur and tibial plateau [5]. At a mean follow-up duration of 14 years, 21% of patients had symptoms during activities of daily living. On radiographic assessment, 57% had signs of degenerative changes while 43% specifically had joint space narrowing. Gelber *et al.* followed 1321 medical students over a median of 36 years [107]. Knee injuries related to fracture, ligamentous injury, cartilage injury, gunshot wound, dislocation, and hemarthrosis were noted in 125 participants. The cumulative incidence of knee OA was significantly higher in subjects who had a history of knee injury (17%) versus those who did not (4%).

A number of long-term osteochondritis dissecans studies also demonstrate that without intervention, articular cartilage lesions degenerate to OA [108-110]. Twyman *et al*. followed 21 knees treated with excision or pinning for osteochondritis dissecans for a mean of 34 years and noted that 43% had poor functional scores [109]. On radiography, 72% of patients with defects localized to

the lateral femoral condyle or patellofemoral joint had signs of OA. However, no joint space narrowing was noted in participants with medial femoral condyle lesions. Anderson *et al*. treated 20 osteochondral defects of the femoral condyle with fragment excision and reported OA in 70% of radiographs at a mean follow-up of 9 years. Only 25% of patients could participate in strenuous activities. De Smet *et al.* assessed 14 knees treated non-operatively at a mean time of 4 years from diagnosis. All patients with either an articular cartilage surface defect or osteochondral fracture had poor clinical outcomes.

Other studies have assessed the short-term progression of focal articular cartilage defects using magnetic resonance imaging (MRI) [111, 112]. Wang *et al.* performed a longitudinal cohort study of patients who had chondral defects of the knee but lacked significant knee pain and previous significant injury [111]. Based on MRI performed at baseline and after 2 years, 49% of defects worsened, 42% did not change and 9% improved. Biswal *et al.* retrospectively assessed patients who had received serial MRIs for assessment of insults of the knee, most of which were related to trauma [112]. After a mean duration of 1.8 years, progression was seen in 19%, 28% and 17% of medial tibiofemoral lesions located in the anterior, central and posterior aspects of the joint. On the lateral side of the joint, progression was noted in 6%, 15% and 15% of lesions in the anterior, central and posterior aspects of the joint. Meniscal tears increased the likelihood of defect progression as 72% of articular cartilage lesions worsened when there was a concomitant meniscus injury, while 15% worsened in the absence of a meniscus

injury. With respect to the anterior cruciate ligament (ACL), progression was seen in 49% of patients with pathology and 33% of patients with an intact ACL.

The prevalence of post-traumatic OA was investigated by Brown *et al.* in a study of 662 patients with OA of the lower extremity who were candidates for total joint arthroplasty [2]. A significant portion of the all cases of OA was considered to be post-traumatic, as 9.8%, 79.5% and 1.6% of patients with knee, ankle and hip OA, respectively, had previously sustained a well-defined injury to the joint of interest. The overall percentage of OA in all three joints attributed to post-traumatic causes was estimated at 12%.

1.3.3 Evolution of focal articular cartilage injury to post-traumatic osteoarthritis

The evolution of focal articular cartilage defects to post-traumatic OA is believed to involve ongoing inflammation and tissue remodeling which are modulated by mechanical stress [75, 113]. The specific cellular basis and order of events have not been well defined and are currently under investigation [113]. Several pro-inflammatory cytokines are elevated in synovial fluid after joint injury [90]. Tumor necrosis factor-alpha (TNF-α), interleukin (IL)-1, IL-6, IL-8, and IL-17 have been implicated in down-regulating ECM molecule synthesis and promoting the production of enzymes that degrade articular cartilage [113, 114]. Mechanical injury to articular cartilage leads to release of matrix metalloproteinase (MMP)-1, MMP-3, MMP-9, MMP-13 and a disintegrin and metalloproteinase with

thrombospondin motifs (ADAMTS)-5 by chondrocytes in the region of injury [115]. Levels of degradative enzymes are elevated for years following joint injury and may lead to a catabolic imbalance that promotes progression to OA [116, 117].

A spectrum of outcomes exists following articular cartilage injury as some lesions degenerate slowly, while others progress rapidly to OA [111]. Several authors have reviewed our current knowledge of the factors that influence the development of post-traumatic OA and it is apparent that rigorous investigation and definitive conclusions are lacking [1, 75, 113, 118]. Clinical studies investigating post-traumatic OA have demonstrated that age is associated with degeneration of articular cartilage defects and the risk of OA progression following joint injuries [111, 119-121]. One reason for this could be a decreased reparative capacity with age that has been noted in an animal model [95]. Increased defect size appears to predispose a defect to degenerate based on animal studies [99, 100]. Preclinical and clinical studies have demonstrated that joint instability related to ligamentous rupture or meniscus injury leads to OA [122, 123], and increases the likelihood of progression to post-traumatic OA in joints with articular cartilage defects [3, 103, 112, 119]. Articular surface incongruity following injury has been established as a risk factor for degeneration during the investigation of tibial plateau fractures [119, 124]. Defect location, which could relate to congruity or load transmission, also appears to play a role in progression [112]. For example, in patients with medial femoral condyle cartilage injuries,

lesions located in the central region of the condyle were shown to be more likely to degenerate than lesions located anterior or posterior to this area [112]. Lastly, articular cartilage defects appear to be more likely to progress in males than females [111].

1.4 Current surgical treatment strategies for focal articular cartilage injury

The objectives of surgical management of focal articular cartilage defects are to: (1) alleviate pain and improve joint function in order to allow patients to perform activities of daily living and potentially return to higher levels of activity, and (2) restore joint congruity and avoid further injury with the goal of preventing progression to symptomatic joint degeneration and OA [125]. Current surgical treatment modalities include primary fixation, marrow stimulation, osteochondral tissue transplantation using autograft or allograft, cell-free biomaterial matrix implantation, and autologous chondrocyte transplantation. These treatment modalities have been investigated particularly in the context of focal chondral and osteochondral defects of the knee and ankle to date.

1.4.1 Primary fixation

Primary repair involves rigid fixation of large, loose osteochondral fragments with headless screws, pins or pegs [125-128]. This technique has been shown to yield positive outcomes in patients with acute injuries of the knee and ankle [129-134]. Successful fixation of chronic fragments has also been reported in the context of femoral condyle osteochondral fracture in young patients [135, 136].

1.4.2 Marrow stimulation

Marrow stimulation techniques involve penetration of the subchondral bone plate at the base of articular cartilage defects to allow bone marrow contents – including endogenous MSCs – from the subchondral bone to enter the defect [86]. Several techniques have been employed including Pridie drilling, abrasion arthroplasty and microfracture [137]. Microfracture is commonly used today and involves debridement of damaged cartilage out of the defect site followed by the creation of 1.5-2.0 mm-diameter holes in the subchondral bone with an awl and spacing the holes at a distance of 3 mm to create a density of 3-4 holes/cm^2 [138]. The major downside of this technique is that repair tissue formed predominantly consists of fibrocartilage, which has inferior mechanical properties to hyaline cartilage [98, 138-141]. Therefore, the procedure is typically used for treatment of small defects [125].

Variable outcomes following marrow stimulation techniques have been reported, and this may relate to patient age and pre-injury activity level, and defect size, location and depth [142-146]. Gudas *et al*. assessed microfracture for the treatment of chondral and osteochondral lesions of the knee with a mean area of 2.8 cm^2 in athletes [142]. Participants were assessed at 3 and 10 years post-procedure and function based on the International Cartilage Repair Society (ICRS) and Tegner scores was noted to decrease with time, although the 10-year outcome was relatively improved in comparison to pre-operative levels [142].

Outcomes were better for patients with age less than 25 years, chondral defects rather than osteochondral defects, and lesions less than 2 cm^2 in size. Radiographic OA was noted in 48% of patients at the 10-year follow-up, and a subsequent surgical procedure was required in 38% of patients. Kon *et al*. also showed reductions in International Knee Documentation Committee (IKDC) and Tegner scores at 7.5 years compared with 2 years after microfracture of chondral defects with a mean area of 2.5 cm^2 in athletes [145].

In contrast to these studies, Steadman *et al.* assessed a larger general population of patients with full-thickness chondral lesions of the knee (mean size of 2.8 cm^2) treated with microfracture [144]. The majority of subjects had stable function and pain based on several scales over time until final follow-up at a mean of 11 years. Only 2 of 72 patients required another procedure due to failure in this study. Sansone *et al.* evaluated outcomes over 20 years in patients treated with abrasion arthroplasty for full-thickness cartilage lesions of the femoral condyle [147]. At 20 years, a positive functional outcome – based on the presence of a high Knee Society Score (KSS) or absence of reoperation – was noted in 68% of patients. Survivorship at 20 years was 71% for all patients, 90% for patients under the age of 50 years and 56% for older patients. Outcomes were significantly better in patients with smaller defects (<4 cm^2) than larger defects.

The studies available in the ankle literature have relatively shorter follow-up periods than the knee literature. Becher *et al*. concluded that function based on

the Hannover Scoring System and pain based on the visual analog scale (VAS) improved after microfracture of chondral and osteochondral lesions of the talus smaller than 2 cm^2 and remained stable until final follow-up at 6 years [146]. MRI, defect filling and integration occurred in the majority of patients, but the quality of tissue was variable. Choi *et al*. showed similar positive outcomes based on the American Orthopaedic Foot and Ankle Society (AOFAS) Ankle-Hindfoot Scale and VAS at 4 years from microfracture and abrasion arthroplasty for treatment of defects with a mean area of 1 cm^2 [148].

Based on the evidence to date, marrow stimulation produces reasonable results in the short- to mid-term with respect to clinical outcome [144-146, 148-151]. However, after 5-10 years, functional scores decline and there is an increased likelihood of failure and signs of degenerative arthritis [142, 145, 151-153]. At present, this procedure is indicated as a first-line treatment for small cartilage defects with areas of <2-3 cm^2 in the knee and <1.5 cm^2 in the ankle [125, 134, 154].

1.4.3 Osteochondral autograft transplantation

Osteochondral autograft transplantation (OATS), also described as osteochondral autologous transplantation, is performed through transplanting osteochondral grafts from healthy, non-weight-bearing surfaces into chondral or osteochondral defects [155]. This procedure is routinely performed as a mosaicplasty in which multiple osteochondral cylindrical plugs with diameters of 2.5-10 mm are

implanted in a mosaic pattern [125, 156]. The plugs are derived from the intercondylar notch or margins of the medial and lateral condyles of the femur [157]. Prior to implantation, the defect site is drilled to create a recipient socket with vertical walls to facilitate congruency between the plugs and defect [125]. The downsides of this technique are donor site injury and donor-recipient mismatch [158, 159]. Although the majority of a defect is filled with grafts containing hyaline cartilage, the empty spaces left between the cylindrical plugs fill with fibrocartilage [150, 154].

Outcomes following OATS in the knee are positive within a few years of surgery but are variable and generally deteriorate with time [159-165]. Marcacci *et al*. showed improved IKDC and Tegner scores post-operatively following osteochondral mosaicplasty, although there was a decreasing trend between 2 and 7 years [159]. Visualization of the defect site using MRI assessment showed complete defect filling in 63%, complete cartilage integration in 75% and complete bone integration in 96% [159]. Solheim *et al.* described deterioration in Lysholm and VAS pain scores between 12 months and 5-9 post-operative years [161]. In a subsequent study, this group reported treatment failure in 45% of patients, and a poor Lysholm clinical score in 40% of patients after 10-14 years [160]. Similar to these findings, Gudas *et al*. found better Tegner scores at 3 years than 10 years [142]. At the 10-year follow-up, 25% of patients had signs of OA on radiography. However, in comparison to microfracture, OATS performed significantly better at all time points.

Hangody *et al*. assessed OATS in professional athletes with a mean defect area of 2.5 cm^2 after 9.6 years and reported good-to-excellent outcomes based on several scores in 91% of patients with femoral condyle defects, 86% of patients with proximal tibia defects and 74% of patients with patellofemoral defects [165]. However, Ollat *et al*. found that only 30% of patients returned to competitive sports following surgery with a mean follow up time of 8 years [162].

Across studies, improved outcomes with OATS have been associated with several patient and treatment characteristics including younger age, male gender, smaller defect size (area of <2-3 cm^2), pure chondral defect type, medial femoral defect location, and fewer number of osteochondral grafts used [159, 160, 162, 163, 165].

OATS has also been described for treatment of focal cartilage defects of the ankle. Hangody *et al.* reported good-to-excellent clinical outcomes based on the Hannover ankle score at 10 years in 92% of patients treated with OATS for cartilage lesions of the talus with an area of 1.2-2.1 cm^2 [165, 166]. Valderrabano *et al.* found a satisfaction rate of good-to-excellent in 92% and significantly improved AOFAS and VAS pain scores after 6 years in patients with osteochondral lesions of the talus with a mean area of 1.4 cm^2 [166]. However, sports activity scores and ankle dorsiflexion remained decreased. MRI and single photon emission computed tomography-computed tomography (SPECT-CT)

showed cartilage degenerative changes and discontinuity in the subchondral bone plate in 100% of images. At the donor site in the knee, 50% of patients had continuous pain at follow up. Gobbi *et al.* compared OATS to chondroplasty and microfracture for treatment of osteochondral lesions of the talus measuring 3.7-4.5 cm^2 in area and did not find a significant difference in AOFAS scores between these modalities of treatment at 24 months from the time of surgery [150]. Pain intensity was higher in OATS than the other groups. MRI demonstrated full bony integration but incomplete chondral integration with the presence of gaps.

The literature to date indicates that OATS leads to good short- and mid-term outcomes when used for treatment of small articular cartilage defects [159, 163, 165]. Longer-term outcomes appear to be less positive, although potentially better than with marrow stimulation techniques [163]. This procedure is currently indicated for small cartilage defects of the knee with areas of <2-3 cm^2 in high-demand patients such as competitive athletes or in patients who have had treatment failure following marrow simulation [125]. For treatment of focal articular cartilage injury of the talus, OATS is indicated for defect areas of 1.5-3 cm^2 [134, 154].

1.4.4 Osteochondral allograft transplantation

Osteochondral allograft transplantation (OCA) involves implantation of an allograft composed of viable articular cartilage and non-living subchondral bone from another human [167]. Benefits of this procedure include the capability to

resurface large cartilage defects with a graft has similar geometry and dimensions to the pre-injury native cartilage without the need for autologous tissue harvesting that would generate donor-site morbidity [168]. OCA restores the mature structure and function of hyaline cartilage to the defect site through the use of a cylindrical plug (dowel) or shell graft that is implanted in a press-fit fashion into a circular bed of healthy subchondral bone created at the defect site [169, 170]. The major downside of OCA is that it is logistically difficult given the need for donor-recipient size matching, testing for infectious diseases, sterilization, processing, and implantation within a short time frame following harvest to ensure chondrocyte viability [171]. Furthermore, a variable immune response is elicited in recipients although the transplanted graft is generally tolerated without obvious rejection [167].

Most allografts have been implanted fresh following storage at 4°C [172-174]. In this environment, there is an inverse relationship between storage time and outcomes of chondrocyte viability and ECM integrity [175-178]. Therefore, fresh allografts must be implanted within 14-28 days of procurement [175-178]. Although freezing of tissue allows for longer-term storage, outcomes have been shown to deteriorate quickly following implantation of frozen allografts [179, 180]. Cryopreservation could be a suitable alternative [181, 182]. However, this technique is still under investigation and not used widely.

The implantation of fresh osteochondral allografts stored for short periods at 4°C into articular cartilage defects of the knee has been shown to provide good long-term outcomes [170, 173, 174, 183, 184]. In patients diagnosed with traumatic osteochondral lesions with a diameter of ≥3 cm (area of ≥7 cm^2) and depth of ≥1 cm who were not previously treated with another cartilage repair procedure, Gross *et al.* reported 95%, 85% and 74% survival of femoral condyle grafts at 5, 10 and 15 years, respectively [174]. At a mean follow-up of 10 years, clinical scores on the modified Hospital for Special Surgery (HSS) scale were excellent in 61% and good in another 23% of patients, while 48% of radiographs had no signs of OA. With respect to tibial plateau grafts, survival was 95%, 80%, 65%, and 46% at 5, 10, 15, and 20 years, respectively. At a mean follow-up of 12 years, 86% of patients had good-to-excellent modified HSS scores and 61% of patients had no radiographic signs of OA. In another study, this group elucidated factors related to graft failure that included patient age over 50 years, concomitant (bipolar) defects of the femur and tibia, malaligned knees, and workers' compensation cases [185].

Levy *et al.* provided a long-term assessment of OCA for a heterogeneous group of patients with femoral condyle defects related to osteochondritis dissecans, traumatic cartilage injury, fracture and avascular necrosis [173]. The majority of patients had previous chondral debridement or marrow stimulation procedure. They reported survivorship of allografts with a mean area of 8.1 cm^2 was 82%, 74% and 66% at 10, 15 and 20 years from the time of transplantation.

Modified Merle d'Aubigné-Postel, IKDC pain, IKDC function and Knee Society function (KS-F) scores all improved significantly following surgery.

Treatment of patellofemoral defects of the knee using allograft transplantation as investigated by Jamali *et al*. [186]. Eight years following transplantation with allografts with a mean area of 7.1 cm^2, clinical outcome based on the modified Merle d'Aubigné-Postel score was improved compared to the pre-operative level. Good-to-excellent scores were found in 60% of patients. Allograft survival at 10 years was 67%.

Graticelli *et al.* assessed allograft transplantation as a salvage procedure after previous failed cartilage repair surgery of the knee using marrow stimulation, OATS and chondrocyte transplantation [170]. Survival of allografts with a mean area of 8.5 cm^2 was 82% at 10 years and 75% at 15 years. At a mean follow-up time of 8.5 years, clinical outcomes were improved compared to pre-OCA based on modified Merle d'Aubigné-Postel, IKDC, KS-F, and Knee Injury and Osteoarthritis Outcome Score (KOOS) scores. In a comparison of primary allograft transplantation and allograft transplantation after failure of marrow stimulation, there was similar survivorship at 10 years and no difference in pain and function [184].

Allograft transplantation has also been performed for treatment of articular cartilage defects of the ankle. Gross *et al.* evaluated OCA for treatment of

osteochondral lesions of the dome or shoulder of the talus (diameter of ≥1 cm and depth of ≥0.5 cm) in 9 patients, most of whom had a history of ostechondritis dissecans and trauma [187]. Their procedure involved restoration of the affected region of each talus with a portion of a size-matched allograft talus. Fusion of the ankle was required in 3 patients due to failure, while 6 patients had a graft *in situ* at 11 years. Within this latter group, 83% of patients tolerated walking for greater than an hour and had no pain, and 75% of allografts showed no radiographic evidence of resorption, fragmentation or degeneration. Adams *et al*. assessed OCA for treatment of uncontained talar shoulder osteochondral defects in 10 patients [188]. At a mean follow-up time of 4 years, pain was decreased and function improved on the Lower Extremity Functional Scale (LEFS). No patients had to undergo arthroplasty or arthrodesis for failure.

Ahmad *et al.* used cylindrical OCA plugs and compared these to OATS for treatment of osteochondral lesions of the talus with an area ≥1.5 cm^2 [189]. After 1 year, Foot and Ankle Ability Measures (FAAM) and VAS pain scores were not significantly different between the groups. Giannini *et al*. utilized bipolar fresh osteochondral allograft (BFOA) for treatment of unilateral ankle arthritis involving combined lesions of the talus and distal tibia [190]. At a mean follow-up of 31 months, 19% of patients had excellent results and 34% had good results based on AOFAS scores. Failure of this treatment modality occurred in 19% of patients.

In summary, allograft transplantation has produced good long-term results in the treatment of large articular cartilage defects of the knee [170, 173, 174, 183, 184]. Evidence also exists to suggest that it is a promising modality of treatment for large ankle defects [187, 189]. At present, OCA is indicated for treatment of knee lesions with an area of >2-3 cm^2 [125], and talus lesions with an area of >1.5 cm^2 or diameter of >1-1.5 cm [134, 154, 187, 191]. Defects of the talar shoulder are routinely treated with allograft transplantation given the anatomic complexity that may be difficult to recreate and outcomes that are poor with other modalities [191, 192]. OCA is also routinely used as a salvage procedure following failure of the other cartilage repair techniques including marrow stimulation, OATS and chondrocyte transplantation [125].

1.4.5 Biomaterial matrix implantation

Biomaterial matrices have been developed to mimic biochemical and biophysical properties of native osteochondral tissue, attract and situate endogenous cells and support the creation of 3D repair tissue [35, 193, 194]. Implantation of a matrix without concomitant cell transplantation is a relatively new modality of treatment for articular cartilage defects that has been assessed in the short- to mid-term to date.

Multilayer scaffolds used for treatment of osteochondral lesions have been designed with the goal of fostering the creation of separate chondral and osseous repair tissues within a defect site. Presumably, cells such as MSCs and growth

factors within subchondral marrow permeate the scaffold through breaks in the subchondral bone plate [195]. Two cell-free scaffolds, the TruFit plug and MaioRegen matrix, have been used clinically and investigated in multiple studies [194].

The TruFit plug is an acellular, cylindrical, synthetic bilayer scaffold composed of polylactic-co-glycolic acid (PLGA), polyglycolic acid (PGA) and calcium sulfate [195, 196]. Dell'Osso *et al.* utilized 1-2 TruFit plugs with diameters of 7-11 mm in the treatment of osteochondral lesions of the femoral condyle [197]. At 4 years, functional outcomes based on the Lysholm Knee Scoring Scale were significantly better than pre-operative levels. MRI showed progressive changes post-operatively at the defect site with time between 12 and 48 months suggestive of integration of the scaffold and formation of repair tissue. Gelber *et al.* treated chondral and osteochondral defect of the femoral condyles and trochlea with 1-4 TruFit plugs (diameter of 5-11 mm) per defect and followed patients to a mean of 45 months [198]. KOOS, Short Form 36 Health Survey (SF-36) and VAS pain scores were significantly better following surgery. Less improvement was noted in patients with larger defects. MRI assessment at 24 months from the time of surgery showed complete defect filling in only 9% of defects with heterogeneous cartilaginous repair tissue noted. The subchondral bone plate was not restored in 84% of defects, while all defect displayed subchondral changes of edema, cysts, granulation tissue, or sclerosis. Dhollander *et al.* treated patients with articular cartilage lesions of the femoral condyle,

patella or trochlea with mean area of 0.83 cm^2 with 1-2 TruFit plugs per lesion and followed them over 3 years [199]. VAS pain and KOOS scores improved significantly following surgery, although 30% of patients had treatment failure that warranted revision surgery. Magnetic resonance observation of cartilage repair tissue (MOCART) scores decreased over 24 months from the time of surgery, which suggested deterioration of the repair tissue.

The MaioRegen matrix is an acellular trilayer scaffold with a superficial chondral layer composed of type I collagen, middle tidemark layer consisting of 60% type I collagen and 40% hydroxyapatite, and deep osseous layer containing a mineralized blend of 30% type I collagen and 70% hydroxyapatite [200]. Kon *et al.* treated chondral and osteochondral defects of the femoral condyle, trochlea, patella, and tibial plateau with a mean area of 3.2 cm^2 with this scaffold and followed patients for 5 years [201]. Function based on IKDC and Tegner scores improved from pre-operative levels to post-operative levels at 2 and 5 years. There was significant improvement in the MOCART score and subchondral bone status between 2 and 5 years. Based on MRI at 5 years, 78% of defects were completely filled, 70% of defects had scaffolds that were completely integrated, and 61% of defects contained homogeneous repair tissue. Repair tissue was isotense relative to native cartilage in 65-70% of defects, which suggested the presence of cartilaginous tissue. However, intact subchondral lamina and bone were demonstrated in a minority of patients.

Biomaterial matrices have also been implanted in association with microfracture in a technique termed autologous matrix-induced chondrogenesis (AMIC) [30]. The rationale of this procedure is that endogenous MSCs within subchondral marrow enter the defect site through holes created in the subchondral plate and are contained at the defect site by a biomaterial membrane or populate a 3D scaffold that fills the defect site [202]. MSCs are thought to be directed to differentiate into cartilage-producing cells through local cues and stimulus from the biomaterial [203]. In the initial description of AMIC by Benthien and Behrens, a mixture of commercially available fibrin glue and autologous serum was used to adhere a collagen membrane to the defect site after microfracture was performed [30]. To date, matrices used have included a collagen I/III membrane (Chondro-Gide), a PGA scaffold treated with hyaluronan (chondrotissue) and a hyaluronic acid scaffold (Hyalofast composed of HYAFF) [30, 202, 204, 205].

Gille *et al.* used AMIC in the treatment of full-thickness articular cartilage defects of the femoral condyle, patella and trochlea with a mean area of 4.2 cm^2 [203]. Improvement in Lysholm, Tegner, Cincinnati and IKDC scores was noted within 24 months of the procedure compared to pre-operative levels, but there was a trend of decreased scores thereafter up to 36-48 months. MRI showed bone marrow lesions in 47% and greater than 50% defect fill was noted in 67% of defects. Two other studies demonstrated improvement in clinical outcomes at 2 years following AMIC for treatment of articular cartilage defects with an average

area of 2-2.3 cm^2 [205, 206]. MRI in both studies showed inconsistent defect filling with heterogeneous repair tissue and subchondral bone abnormalities.

The BST-CarGel system is an AMIC procedure in which a matrix composed of chitosan gel and peripheral blood is implanted into a defect following microfracture [140]. In a randomized controlled trial, Stanish *et al.* reported superior defect fill and repair tissue quality on MRI at 12 months with BST-CarGel in comparison to microfracture alone for treatment of femoral condyle articular cartilage defects with areas of 2-2.5 cm^2 [140]. Clinical outcomes based on the Western Ontario and McMaster Universities Osteoarthritis Index (WOMAC) were significantly improved following surgery for both BST-CarGel and microfracture with no difference between these groups. Methot *et al.* reported macroscopic and histological outcomes from a subset of patients that underwent elective second-look arthroscopy and osteochondral biopsy at 13 months from the time of surgery [207]. Defects treated with BST-CarGel had significantly higher ICRS macroscopic scores and histological subscores for surface characteristics and cell viability than defects treated with microfracture alone. Repair tissue derived from BST-CarGel was more organized than repair tissue derived from microfracture based on polarized light microscopy scoring.

AMIC has also been used in the treatment of articular cartilage lesions of the ankle [208, 209]. Kubosch *et al.* treated osteochondral lesions of the talar shoulder with a mean area of 2.4 cm^2 by debriding damaged cartilage and necrotic

subchondral bone, microfracturing sclerotic bone areas, recreating the outline of the shoulder with cancellous bone graft, and implanting a collagen I/III membrane using fibrin glue [210]. After a mean of 40 months from the time of surgery, AOFAS and VAS pain scores were significantly improved. Defect sizes of ≥3 cm^2 were associated with worse outcomes. MRI assessment showed complete defect filling with hypertrophy in 62% of defects, while 15% had complete filling to the level of adjacent cartilage. The T2 relaxation time of repair tissue was not significantly different than native cartilage, which suggested the presence of hyaline-like tissue.

Based on short- to medium-term clinical studies that have been performed, cell-free matrix implantation appears to be a suitable treatment option for small articular cartilage lesions. Future investigation is required to compare matrix implantation to modalities of treatment such as microfracture and cell transplantation that have been more rigorously tested to date. Although promising, the indications for multilayer scaffold implantation and AMIC are currently unclear.

1.4.6 Autologous chondrocyte transplantation

Autologous chondrocyte transplantation (ACT), also commonly referred to as autologous chondrocyte implantation (ACI), was first described by Brittberg *et al*. and involves biopsy of healthy hyaline cartilage, *ex vivo* chondrocyte isolation from this cartilage, expansion of chondrocytes within tissue-culture flasks,

implantation of chondrocytes into an articular cartilage defect, and coverage of the implanted cells with a sutured, autologous periosteal flap [28]. A variation of this technique involves implantation of chondrocytes into a defect and coverage with a collagen membrane – such as the bilayer collagen I/III membrane (Chondro-Gide) – to avoid the donor site morbidity and hypertrophic repair tissue associated with the transplanted periosteum [211].

In second-generation ACT, a collagen membrane is used as a carrier for implantation of chondrocytes rather than as a cover for these cells [212, 213]. *Ex vivo* isolated and expanded chondrocytes are cultured on the membrane for multiple days and implanted as part of the construct [213]. Membranes may be bilayer, as in the case of the collagen I/III membrane produced by Verigen (MACI), with one side engineered to promote cell adherence that is placed towards the defect and another side with a smooth surface facing the joint [214, 215]. Third-generation ACT involves cultivation and implantation of chondrocytes on a 3D biomaterial matrix [214, 216]. Presumably a 3D matrix promotes defect filling at the time of implantation and supports 3D tissue formation [214]. Several matrices have been used for third-generation ACT including a collagen I scaffold (Neocart), collagen I gel (CaReS), collagen-chondroitin sulfate scaffold (Novocart), agarose-alginate gel (Cartipatch), esterified hyaluronic acid scaffold (HYAFF in Hyalograft C), and polymer-based scaffold consisting of polyglycolic acid/polylactic acid and polydioxanone supplemented with fibrin glue (BioSeed-C) [35, 194, 217]. Second- and third-

generation ACT methods are collectively referred to as matrix-associated, matrix-assisted or matrix-induced ACT/ACI (MACT/MACI) [213]. Given that the cell-scaffold constructs in MACT are typically implanted and supported with fibrin glue rather than sutures, implantation can be performed through a mini-arthrotomy or via arthroscopy [216].

Characterized chondrocyte implantation (CCI) is a technical variation of ACT and MACT with the goal of optimizing the source of chondrocytes used for transplantation [218]. In this protocol, multiple populations of chondrocytes are isolated, expanded, subjected to a gene expression assay, and assessed with a score capable of predicting the capacity to form stable hyaline-like cartilage *in vivo* [219]. The selected population of chondrocytes is then implanted using conventional ACT or MACT methods [218, 220].

There is a growing body of evidence to suggest that ACT and MACT are effective options for surgical management of chondral and osteochondral lesions of the knee and ankle. Specifically, long-term outcomes are available from studies assessing first-generation ACT [40, 221, 222], and mid-term outcomes have been reported for MACT [223-225].

ACT for chondral and osteochondral lesions of the knee produced positive functional outcomes in the majority of patients when assessed at long-term follow-up of 10-20 years in several studies [221, 222, 226-228]. During this time

period, treatment failure occurred in 9-25% of patients [221, 222, 226, 228]. Minas *et al.* treated articular cartilage lesions of the knee with a mean area of 8.4 cm^2 with ACT and found significant improvements in function based on modified Cincinnati, KSS, SF-36, and WOMAC scores at a mean follow-up time of 12 years [221]. Graft survival was 79%, 71% and 71% at 5, 10 and 15 years following ACT. Patients less than 30 years of age had a 15-year graft survival of 84%, while patients aged 30-45 years and older than 45 years had reduced graft survival of 68% and 66%, respectively. Peterson *et al.* treated articular cartilage lesions of the knee with a mean area of 5.3 cm^2 with ACT and found significant improvements in function based on Lysholm, Tegner, and Brittberg-Peterson scores at a mean follow-up time of 13 years [227]. Moradi *et al.* assessed osteochondral lesions with mean area of 4.3 cm^2 at 1 year and 10 years from the time of ACT [222]. Tegner scores increased between these two time points, while other scores including Lysholm, IKDC and SF-36 trended downward. Mosely *et al.* treated articular cartilage lesions of the knee with a mean area of 5.2 cm^2 with ACT and found clinical improvement based on the modified Cincinnati Score in 69%, no change in 13% and failure in 17% of patients by 10 years [227]. Of the patients that had positive outcomes after 1-5 years, 13% did not sustain improvement by 6-10 years.

Based on the long-term ACT studies of the knee, several factors have been shown to negatively impact outcome following ACT including increased age, increased duration of symptoms, previous treatment with marrow stimulation,

defect location at the patellofemoral joint (versus tibiofemoral joint), presence of kissing lesions, and increased defect size [221, 226, 227, 229]. With respect to defect size, Minas *et al.* divided patients into defect areas of 1-5, 5-10, 10-15, and >15 cm^2 [221]. Implant survival at 15 years was significantly worse in defects >15 cm^2 (38%) than in defects ≤15 cm^2 (75%).

Tissue quality following knee ACT has been assessed in multiple studies using MRI and histological analysis [222]. On MRI, Moradi *et al.* found complete defect filling in 52%, homogeneous repair tissue in 29%, repair tissue that was isotense to native cartilage in 29%, complete integration of repair tissue with surrounding cartilage in 24%, and subchondral lamina intactness in 67% [222]. Defect filling correlated with Tegner scores but not Lysholm or IKDC scores. Vasiliadis *et al*. used delayed gadolinium-enhanced MRI and reported that quality of repair tissue at a mean of 13 years post-ACT was similar to surrounding native cartilage, although intralesional osteophytes, subchondral cysts and significant bone marrow edema were noted in 64%, 39% and 14% [230]. There was no correlation between MRI values and KOOS outcomes. Peterson *et al.* found hyaline-like cartilaginous tissue in the majority of biopsy specimens from ACT-derived repair tissue of the knee [229]. A correlation between histologic quality of repair tissue and clinical outcome was found.

MACT for treatment of articular cartilage lesions of the knee has been assessed in a number of mid-term studies [153, 224, 231, 232]. Kon *et al.*

performed MACT on defects of the femoral condyle and trochlea (2.2 cm^2 mean area) using an esterified hyaluronic acid scaffold (HYAFF in Hyalograft C) and found improved IKDC scores at 5 years from the time of surgery [153]. There was 100% graft survival in 40 patients. Using the same scaffold, Nehrer *et al*. reported increased IKDC, Lysholm and modified Cincinnati scores 5 years after MACT for treatment of knee defects with a mean area of 4.4 cm^2 [231]. Survival was 95% at 3 years and 90% at 5 years for primary MACT. In contrast, secondary indications of MACT such as complex defects and salvage led to significantly lower survival of 64% at 3 years and 0% at 5 years. Feruzzi *et al.* treated femoral condyle articular cartilage defects with a mean size of 5.9 cm^2 using arthroscopic MACT with Hyalograft C [224]. IKDC scores increased post-operatively and remained stable by 5 years. There were no treatment failures. MRI demonstrated well-integrated repair tissue in 93% of patients at final follow-up. Low signal intensity was noted on T2 images suggestive of hyaline-like tissue. This was confirmed with histological assessment performed on biopsied repair tissue from 10 patients that showed the presence of hyaline-related proteoglycans and type II collagen. Nawaz *et al.* reported improved modified Cincinnati, VAS pain and Stanmore functional scores at a mean follow-up duration of 6 years following MACT with a collagen I/III membrane for treatment of femoral condyle and patellofemoral defects [232]. Graft survivals of ACT and MACT in this study were equivalent at 78% at 5 years and 51% at 10 years.

Several groups have compared different generations of ACT in the treatment of knee lesions with variable outcomes reported [215, 224, 233, 234]. Zeifang *et al.* compared first-generation ACT to MACT with a polymer scaffold (BioSeed-C) [233]. First-generation ACT had better clinical outcomes at 12-24 months based on the Lysholm and Guilquist scores, while IKDC, SF-36 and Tegner scores were not different between groups. MACT led to superior MOCART scores at 6 months. Ergellet *et al.* compared the same treatment groups and found that clinical outcomes were similar at 2 years [234]. However, a higher number of revision procedures were required in patients treated with first-generation ACT. Bartlett *et al.* compared ACT involving transplantation of chondrocytes behind a sutured collagen I/III membrane (Marticel) to MACT involving implantation of chondrocytes on a bilayer collagen I/III membrane (MACI by Verigen) [215]. MACT led to non-significantly higher modified Cincinnati scores and less graft hypertrophy at 12 months, but appeared to produce inferior repair tissue quality based on arthroscopic and histologic assessment. Ferruzi *et al.* compared first-generation ACT to arthroscopic MACT with a hyaluronic acid scaffold (HYAFF in Hyalograft C) [224]. Patients who received MACT improved earlier on and had significantly better clinical outcomes on the IKDC scale at 6-18 months, but functional outcomes were similar between ACT and MACT thereafter to 5 years. MRI and histological analysis showed that both ACT and MACT produced repair tissue consistent with hyaline cartilage.

Chondrocyte transplantation has been compared to marrow stimulation by microfracture in the treatment of articular cartilage defects of the knee and shown to lead to favorable outcomes. Vanlauwe *et al.* compared ACT using characterized chondrocytes with microfracture in the treatment of femoral condyle lesions with areas of 1-5 cm^2 and found similar outcomes at 5 years [235]. At 5 years, ACT produced better outcomes based on the KOOS in patients who had surgery within 3 years of symptom onset. However, in patients with longer durations between symptom onset and surgery, there was not a significant difference between groups. Basad *et al.* compared MACT using a collagen membrane (MACI by Verigen) to microfracture in the treatment of large lesions of the femoral condyle and patella (4-10 cm^2) [236]. After 2 years, outcomes based on Lyholm, Tegner and ICRS scales were significantly better with MACT.

Kon *et al.* compared MACT using a hyaluronic acid scaffold (HYAFF in Hyalograft C) to microfracture for treatment of articular cartilage defects of the femoral condyles or trochlea (mean area of 1.9-2.5 cm^2) in two studies [153, 237]. In the first study involving active patients, IKDC scores were significantly higher at 5 years with MACT in comparison to microfracture [153]. Furthermore, return to sports was stable between 2 and 5 years for MACT, while this outcome deteriorated between the two time points for microfracture. In the second study involving competitive soccer players, MACT led to similar IKDC scores at 2 years between groups. At 7.5 years, IKDC scores were significantly better in

patients treated with MACT and outcomes worsened in the microfracture group at this time point.

Chondrocyte transplantation also appears to lead to superior outcomes in comparison to OATS (mosaicplasty) for the treatment of the knee. Bentley *et al*. compared first-generation ACT to OATS for treatment of articular cartilage lesions of the femur, patella and tibial plateau with a mean area of 4 cm^2 [226]. At 10 years, functional outcome based on the Cincinnati score was significantly improved following ACT in comparison to OATS. Failure of treatment was noted in 17% of patients treated with ACT and 55% of patients treated with OATS.

Chondrocyte transplantation appears to be a suitable treatment modality for articular cartilage defects of the ankle. Positive clinical outcomes based on several scores including the AOFAS ankle-hindfoot score, VAS pain score, Hannover ankle rating score, and Tegner score have been reported at a mean follow-up duration of 5-10 years following ACT [40, 238, 239] and 3-7 years following MACT of talus lesions with mean areas of 1.6-3.1 cm^2 [40, 225, 240-242]. In the longer-duration studies, no deterioration was noted in functional outcome [40, 239, 240]. Characteristics associated with worse outcomes include increased patient age, previous intervention and defect depth >5 mm [239-242]. With respect to tissue quality, MOCART scores improved with time following ACT and MACT [240]. MRI T2 mapping and histological assessment

demonstrated the presence of hyaline-like cartilaginous repair tissue following ACT and MACT in the majority of defects [239-242].

Based on the long-term outcomes reported for ACT and mid-term outcomes reported for MACT, chondrocyte transplantation is a cell-based option for treating articular cartilage defects that results in the creation of hyaline-like cartilaginous repair tissue and improved outcomes post-operatively [40, 221-225]. ACT and MACT are indicated for articular cartilage lesions >2-3 cm^2 in the knee and >1.5 cm^2 in the talus [125, 154]. There are several drawbacks of chondrocyte transplantation that should be considered in treatment planning. Two invasive surgical procedures are required to allow for cartilage harvesting, *ex vivo* chondrocyte isolation and expansion, and implantation [28]. Therefore, this protocol is time consuming and expensive [40]. Low chondrocyte yield may be an issue given the limited proliferative capacity of mature cells [243, 244]. With prolonged *ex vivo* cell expansion, chondrocytes lose the capacity to generate hyaline-like extracellular matrix (ECM) due to de-differentiation and chondrocyte senescence may occur, which reduce the potential of transplanted cells to generate desirable hyaline-like cartilaginous repair tissue [244-253].

1.4.7 Current treatment algorithms

Articular cartilage repair procedures in the knee are guided by defect size and patient characteristics [125]. Primary repair is used for treatment of osteochondral fragments that are amenable to fixation with an area of >1 cm^2 [125, 127, 128].

When primary repair is not possible, treatment with another modality is considered. For small defects with an area of <2-3 cm^2, marrow stimulation is the first-line treatment [125, 138]. OATS can be used for small defects of the knee in high-demand patients or in those who have failed marrow simulation [125, 155]. Cell-free matrix implantation and AMIC may be suitable options for defects of this size in the near future once more evidence is established [140, 199, 201, 205]. Larger defects of the knee with areas >2-3 cm^2 are treated with ACT/MACT or allograft transplantation [125, 174, 221]. The limit of chondrocyte transplantation is unknown, although there is evidence to suggest that massive lesions with areas >15 cm^2 are not treated adequately with ACT and warrant allograft transplantation [221]. Allografts are also used in the setting of uncontained defects, deep defects with bone loss and following failure of ACT/MACT [125]. Other procedures for knee malalignment, ligament insufficiency and meniscal injury are performed concomitantly or in a staged fashion with cartilage repair procedures [125].

In the treatment of defects of the ankle, primary repair is performed when fixable osteochondral pieces >1 cm^2 are present [126, 154]. Other modalities are considered if primary repair is not possible. For small defects with areas of <1.5 cm^2, marrow stimulation is the first-line treatment [154]. Larger defects of the ankle with areas >1.5 cm^2 are treated with cell or tissue transplantation. Specifically, OATS is limited to defects with areas of 1.5-3 cm^2, while ACT and allograft transplantation may be used for larger defects [134, 154]. Allograft

transplantation is particularly recommended for lesions with anatomic complexity, such defects of the talar shoulder, and for kissing lesions involving the talus and distal tibia [134, 192].

1.4.8 Limitations to current treatment algorithms

Although positive outcomes have been reported using this treatment algorithm, several issues exist with the established modalities of treatment. Marrow stimulation is not appropriate for large defects given that it results in resurfacing with fibrocartilage, which presumably does not adequately restore joint congruity and load distribution in joints with larger critical sized defects [98, 138-141]. OATS produces donor site morbidity and offers only short-term benefits as outcomes deteriorate with time [158, 159]. ACT requires a lengthy and costly protocol of two operative procedures and an *ex vivo* culture period that is limited by chondrocyte de-differentiation and senescence [244-253]. Allograft transplantation is logistically difficult given the need for donor-recipient size matching, testing for infectious diseases, sterilization, processing, and implantation within a short time frame following harvest to ensure chondrocyte viability [171].

1.5 Mesenchymal stem cell transplantation: an emerging strategy

Given the issues associated with current articular cartilage repair techniques, there has been a drive to develop novel tissue engineering techniques with the goal of resurfacing defects with bioengineered tissue that recapitulates the properties of

hyaline cartilage. MSC transplantation is a cell-based strategy in its early stages that has the potential to resurface articular cartilage defects while avoiding the downsides of ACT and MACT. MSCs have an enhanced proliferative capacity and may be reproducibly differentiated into chondrocytes [32]. Cell harvesting does not require an invasive procedure that destroys articular cartilage at another site [254]. Current evidence suggests that MSCs offer a promising alternative to present-day treatment modalities for articular cartilage defects [255].

Chapter 2

Mesenchymal Stem Cell Transplantation in the Treatment of Focal Articular Cartilage Defects: a Review of Current Concepts

Troy D. Bornes, Adetola B. Adesida and Nadr M. Jomha

This chapter has been published in part as:
Bornes TD, Adesida AB, Jomha NM: **Mesenchymal stem cells in the treatment of traumatic articular cartilage defects: a comprehensive review.** *Arthritis Res Ther* 2014, **16**(5):432.

2.1 Introduction to mesenchymal stem cells

Mesenchymal stem cells (MSCs) – also commonly referred to as mesenchymal stromal cells and mesenchymal stromal stem cells – are spindle-shaped cells capable of rapid proliferation and found within a number of tissues including bone marrow, synovial tissue, blood, adipose tissue, and periosteum [32, 256, 257]. There is evidence to suggest that MSCs reside in a perivascular location *in vivo* and differentiate based on local cues in order to repair injured mesenchymal tissues [258, 259]. Their multi-lineage potential has been illustrated *in vitro* with differentiation into chondrogenic, osteogenic, adipogenic, and myogenic pathways [32, 260]. Mediators capable of promoting MSC chondrogenesis, such

as transforming growth factor-beta (TGF-β) and dexamethasone, have been elucidated using simplified models [261].

In 2006, the Mesenchymal and Tissue Stem cell Committee of the International Society for Cellular Therapy (ISCT) proposed the minimal criteria required to define a cell as a human MSC [262]:

1. Adherence to tissue-culture plastic in standard culture conditions
2. Expression of cell surface antigens cluster of differentiation (CD)105, CD73 and CD90, and lack of expression of CD45, CD34, CD14 or CD11b, CD79α or CD19, and human leukocyte antigen (HLA)-DR
3. Multipotent differentiation to osteoblasts, adipocytes and chondroblasts *in vitro*

This set of criteria was produced to create consistency among scientists and to promote standardization of experimental practice. However, the definition of an MSC will likely change as our knowledge of MSCs grows. It is now apparent that heterogeneous subpopulations of cells demonstrating characteristics of MSCs exist with variability in plastic adherence, cell surface markers and differentiation capacity. Cells consistent with MSCs may be isolated by means other than conventional plastic adherence [263, 264]. Various cell surface antigens such as CD271, CD146, STRO-1, and SSEA-4 have been identified that are present within fractions of MSCs [265]. Differentiation capacity into chondrogenic,

osteogenic and adipogenic lineages varies between MSCs from different sources and MSCs isolated using different methods [256, 266].

2.2 Cartilage engineering from bench to bedside

2.2.1 *In vitro* studies

MSC chondrogenesis can be induced within simple *in vitro* models consisting of cell monolayers or cell aggregates, pellets, micromasses, or transwell cultures containing multiple layers of cells and matrix [32, 267-269]. High-density aggregation was achieved through the use of centrifugation and situates cells in a three-dimensional (3D) environment that fosters cellular interaction, mimicking cell condensation of mesenchymal cells during embryonic cartilage development and chondrogenic ECM formation [32, 261]. Alternatively, various biomaterials have been used as matrices on which MSCs are differentiated. MSCs embedded within collagen, agarose, alginate, chitosan and hyaluronic acid (HA) gels form aggregates of tissue that contain chondrocytes and cartilaginous ECM [270-274]. MSC-seeded porous scaffolds composed of collagen, HA, silk, decellularized cartilage ECM, polyglycolic acid (PGA), polylactic acid (PLA) and polylacticglycolic acid (PLGA) create tissue that histologically resembles hyaline cartilage [275-279].

2.2.2 *Ex vivo* explant studies

Chondral and osteochondral explant models allow for cartilage repair tissue formation to be assessed within simulated defects in controlled *in vitro*

environments. Porcine MSCs embedded in agarose gel implanted within chondral explants showed an abundance of type II collagen and glycosaminoglycan (GAG) matrix after 6 weeks of culture [271]. Similarly, human MSCs embedded in alginate gel and implanted within osteochondral explants for 4 weeks had collagen II gene expression and GAG production consistent with hyaline cartilage [270]. MSC-seeded gels displayed minimal integration with surrounding explant cartilage after 6 weeks of culture [271]. This may in part be due to the absence of sufficient remodeling time or *in vivo* factors, such as mechanical stimulation, required for integration to occur [280].

2.2.3 Preclinical animal studies

Animal models have provided preclinical *in vivo* assessment of MSCs in the treatment of articular cartilage defects. Starting with the work of Wakitani *et al.* in 1994 [29], MSC-based techniques have yielded positive outcomes in regenerating articular cartilage in several small-animal studies involving rabbits [281-298] and rats [299, 300]. Various MSC injection and transplantation protocols have been used to treat simulated, focal chondral and osteochondral defects in large animals such as sheep, goats, dogs, pigs, and horses [36, 274, 301-314]. These large-animal studies are summarized in Table 2.1.

Table 2.1 Large-animal studies assessing mesenchymal stem cells in the treatment of articular cartilage defects

Article	Model	Defect	Implanted construct	Follow-up	Key findings
Guo *et al*. (2004) [301]	28 sheep	Medial femoral condyle osteochondral defects; cylindrical (8-mm diameter)	Implantation of isolated BM-derived MSCs seeded on a TCP scaffold; compared to cell-free scaffolds and empty defects	6 months	Macroscopic: smooth, integrated tissue in MSC group; histological: proteoglycan and type II collagen consistent with hyaline cartilage in MSC group, compared with fibrocartilage in cell-free group; subchondral osseous regeneration; biochemical: GAG quantity in MSC group was 89% of native cartilage
Wayne *et al*. (2005) [36]	10 dogs	Medial and lateral femoral condyle osteochondral defects; cylindrical (6-mm diameter)	Implantation of isolated BM-derived MSCs suspended in alginate and seeded on a PLA scaffold; precultivated for 3 wk; compared to cell-free scaffolds	1.5 months	Macroscopic: improved coverage of defects in MSC group; histological: mixture of hyaline and fibrocartilage integrated with surrounding tissue; higher quality tissue in MSC group compared with cell-free group; no mineralization noted within osseous defects; mechanical: lower resistance to compression than native cartilage
Ando *et al.* (2007) [302]	9 piglets	Medial femoral condyle chondral defects; cylindrical (8.5-mm diameter)	Implantation of isolated, allogeneic synovial tissue MSCs derived from piglets and cultured in a 3D scaffold-free TEC; compared to empty defects	6 months	Macroscopic: greater defect coverage in TEC group; subchondral erosion in the empty defects; histological: smooth, integrated tissue containing proteoglycans and type II collagen in the TEC group; empty defects showed signs of OA; higher ICRS scores in the TEC group; mechanical: similar viscoelastic properties between TEC and native cartilage
Lee *et al.* (2007) [303]	27 mini-pigs	Medial femoral condyle chondral defects; cylindrical (8.5-mm diameter)	Injection of isolated BM-derived MSCs with HA (Synvisc) followed by HA weekly x2 wk; compared to HA alone	3 months	Macroscopic: greater defect coverage in the MSC+HA group; histological: hyaline-like cartilage noted in MSC+HA group; minimal defect filling in HA group; improvement in Wakitani histologic score with MSCs
Saw *et al.* (2009) [304]	15 goats	Femoral trochlea chondral defects; cylindrical (4 mm diameter)	Injection of BMDC collection with HA (Hyalgan) weekly for 3 wk starting 1 wk after subchondral drilling; compared to drilling with or without HA	6 months	Macroscopic: greater defect coverage in the BMDC+HA group; histological: HA group had some proteoglycans and type II collagen mixed with type I collagen; BMDC+HA group had superior proteoglycan and type II collagen content; cell morphology was improved in the BMDC+HA group
Zscharnack *et al.* (2010) [274]	10 sheep	Medial femoral condyle osteochondral defects; cylindrical (7-mm diameter)	Implantation of isolated BM-derived MSCs in type I (rat) collagen gel either immediately following seeding or after 2 wk of precultivation	6 months	Macroscopic: precultivation group produced more homogenous hyaline-like cartilage; histological: significantly better O'Driscoll and ICRS scores in the precultivation group compared with non-precultivated group, specifically with respect to surface features, integration, cell distribution, and mineralization; mechanical: precultivated tissue was firm

Table 2.1 Large-animal studies assessing mesenchymal stem cells in the treatment of articular cartilage defects (continued)

Article	Model	Defect	Implanted construct	Follow-up	Key findings
Shimomura *et al.* (2010) [305]	7 pigs 6 piglets	Medial femoral condyle chondral defects; cylindrical (8.5-mm diameter)	Implantation of isolated synovial tissue MSCs derived from piglets and cultured in a 3D scaffold-free TEC; compared to empty defects	6 months	Macroscopic: greater defect coverage in TEC group; histological: good integration of tissue that stained well for proteoglycans in the TEC group versus signs of OA in empty defects; higher ICRS scores in the TEC group; mechanical: similar properties between TEC and native tissue
Wegener *et al.* (2010) [306]	9 sheep	Medial femoral condyle chondral defects; cylindrical (8-mm diameter)	Implantation of BM cells in fibrin glue seeded on a PGA scaffold; secured to subchondral bone by PLGA darts; compared to no cells	3 months	Macroscopic: BM-seeded scaffolds had improved regeneration compared to cell-free scaffolds; histological: variation noted with fibrous tissue in some and hyaline-like cartilage in other BM cell-seeded scaffolds; O'Driscoll score was similar between cell-free and cell-seeded scaffolds
Fortier *et al*. (2010) [307]	12 horses	Lateral trochlear ridge chondral defects (15-mm diameter)	Implantation of BMDCs mixed with thrombin; compared to MFX	8 months	Macroscopic: BMDCs had improved regeneration compared to MFX; histological: ICRS scores were higher with BMDCs than MFX; good staining for proteoglycans and collagen II with BMDCs; MRI: T1p mapping showed increased GAG and T2 mapping showed improved collagen orientation with BMDCs
Marquass *et al.* (2011) [308]	9 sheep	Medial femoral condyle osteochondral defects; cylindrical (7-mm diameter)	Implantation of isolated BM-derived MSCs in type I (rat) collagen gel implanted either immediately following seeding or after 2 wk of precultivation; compared to MACT	12 months	Macroscopic/histological: significantly better O'Driscoll and ICRS scores with precultivated MSCs compared with both non-precultivated MSCs and MACT, specifically with respect to surface quality, matrix quality and integration; type II collagen content was superior in precultivated group; MRI: precultivated MSCs were similar to MACT but significantly better than non-precultivated MSCs on the MOCART score
McIlwraith *et al.* (2011) [309]	10 horses	Medial femoral condyle chondral defects (1 cm^2)	Injection of isolated BM-derived MSCs with HA (Hyvisc) into the knee joint 1 mo after MFX; compared to cell-free HA injection and MFX	12 months	Macroscopic: greater repair tissue area with MSCs, but no difference in volume; histological: no difference in surface, structure, integration, cellular architecture, and subchondral regeneration; contradictory proteoglycan and aggrecan staining; biochemical: equivalent GAG; mechanical: tissue derived from MSCs was firmer; MRI: no difference
Ando *et al.* (2012) [310]	6 piglets	Medial femoral condyle chondral defects; cylindrical (8.5-mm diameter)	Implantation of isolated, allogeneic synovial MSCs and cultured in a 3D scaffold-free TEC; compared to empty defects	6 months	Histological: tissue containing proteoglycans in the TEC group; empty defects were partially coverage with fibrous tissue and showed signs of OA; higher O'Driscoll scores in the TEC group; mechanical: similar properties between TEC and native cartilage

Table 2.1 Large-animal studies assessing mesenchymal stem cells in the treatment of articular cartilage defects (continued)

Article	Model	Defect	Implanted construct	Follow-up	Key findings
Zhang *et al.* (2012) [311]	20 mini-pigs	Femoral trochlea chondral defects; cylindrical (6-mm diameter)	Implantation of BMDCs or isolated, expanded BM-derived MSCs in type II collagen (porcine) hydrogel; compared to cell-free gels	2 months	Macroscopic: good defect filling with both MSCs and BMDCs; irregularity with cell-free gels; histological: hyaline-like cartilage with both MSCs and BMDCs; O'Driscoll score was greater in the MSC group at 4 wk, but equivalent between the BMDC and MSC groups at 8 wk
Bekkers *et al.* (2013) [312]	8 goats	Medial femoral condyle chondral defects; cylindrical (5-mm diameter)	Implantation of chondrons and BM-derived MSCs suspended in fibrin glue; compared to MFX	6 months	Macroscopic: improved defect filling with MSC+chondrons in comparison to MFX; histological: O'Driscoll score was significantly higher in the MSC+chondron group; biochemical: GAG content and GAG/DNA in the repair tissue was greater in the MSC+chondron group than the MF group
Kamei *et al.* (2013) [313]	16 mini-pigs	Patella chondral defects; cylindrical (6-mm diameter)	Magnetic accumulation of injected ferumoxide labeled MSCs; compared to gravity-focused MSCs	3 months	Arthroscopic: improved smoothness and integration with magnetic accumulation; histologic: superior integration and type II collagen content with magnetic accumulation; improved scoring on the Wakitani scale
Nam *et al.* (2013) [314]	18 goats	Medial femoral condyle chondral defects; cylindrical (5-mm diameter)	Injection of isolated BM-derived MSCs weekly (x 3wk) starting 2 wk after subchondral drilling; compared to drilling alone	6 months	Macroscopic: Smooth, integrated tissue with MSCs vs. partial, irregular filling with drilling alone; histological: O'Driscoll score was significantly higher in the MSC group; improved proteoglycan and type II collagen content with MSCs; biochemical: higher GAG quantity with MSCs

Table 2.1 abbreviations

3D, three-dimensional; BM, bone marrow; BMDC, bone marrow-derived cell; DNA, deoxyribonucleic acid; GAG, glycosaminoglycan; HA, hyaluronic acid; ICRS, International Cartilage Repair Society; MACT, matrix-associated autologous chondrocyte transplantation; MFX, microfracture; MOCART, Magnetic Resonance Observation of Cartilage Repair Tissue; MSC, mesenchymal stem cell; OA, osteoarthritis; PGA, polyglycolic acid; PLA, polylactic acid; PLGA, polylactide co-glycolide; TEC, tissue-engineered construct; wk, week(s); y, year(s)

Intra-articular injection of MSCs into rabbit knees containing femoral trochlea osteochondral defects led to resurfacing with fibrous tissue that

failed to remodel into hyaline cartilage over 24 weeks [288]. In contrast, MSCs implanted directly into the defect site produced cartilage-like tissue that remodeled with time to produce both cartilage and bone components similar to surrounding native osteochondral tissue. In another study, MSCs injected in conjunction with HA into porcine knees with partial-thickness chondral defects led to good defect coverage with hyaline-like cartilage at 12 weeks post-injection [303]. HA alone produced minimal defect filling in this time frame.

Other groups have performed MSC injection in association with subchondral drilling or microfracture [304, 309, 314]. Serial MSC injections performed weekly for three weeks after subchondral drilling for treatment of simulated chondral defects within the distal femur of goats produced integrated repair tissue consistent with hyaline cartilage after six months [314]. In a similar model, Saw *et al*. used bone marrow aspirate cell collections injected weekly with HA [304]. They found improved content of proteoglycan and type II collagen within femoral trochlea chondral defects that received cell injection in comparison to those that received only HA. In contrast to these findings, McIlwraith *et al*. found no difference between HA and an HA-MSC combination in several histologic parameters, MRI evaluation, and GAG quantity at one year in horses that received an injection and microfracture [309]. Possible reasons for inconsistent outcomes include variation in the number of injections, length of follow-up and species.

One potential drawback of intra-articular injection involves cell dispersion, associated lack of focus of injected contents into a defect site, and the potential for an insufficient amount of seeded cells required for regeneration. The use of magnetic labeling of cells and an external magnet has been proposed as a minimally invasive method to deliver injected MSCs to defects. In mini-pig knees, ferumoxide labeled MSCs were directed over patella chondral lesions by magnet for 10 minutes following injection and produced superior arthroscopic and histologic scores to an injection directed by gravity [313].

Various constructs for implantation have been proposed in the preclinical literature. A scaffold-free, 3D tissue-engineered construct derived from monolayers containing differentiated MSCs has been investigated [305, 310]. Over six months, constructs implanted within porcine femoral condyle chondral defects created repair tissue with a superficial fibrous layer and deep hyaline-like cartilaginous layer [305].

Transplantation of MSC-seeded matrices composed of collagen, PLA, PGA, PLGA, polycaprolactone (PCL), fibrin, chitosan, alginate, silk, demineralized bone matrix, and tricalcium phosphate (TCP) was successfully performed in several other small- and large-animal studies [29, 281-285, 287, 290, 292, 293, 295-297, 299, 306, 315]. Defect resurfacing with hyaline-like cartilaginous tissue was reported in the majority of cases at 1-6 months post-

implantation with more integrated, mature tissue found at later time points. Some groups also noted the presence of bone regeneration within the osseous component of osteochondral defects [283, 284, 293, 297, 301].

Implantation of matrices seeded with MSCs that were precultivated or predifferentiated *in vitro* for 2-3 weeks prior to implantation is an alternative protocol that has been assessed in three other studies [36, 274, 308]. Zscharnack *et al.* showed that precultivated MSC-seeded collagen gels implanted within sheep osteochondral defects produced superior repair tissue to non-precultivated MSC-seeded gels based on International Cartilage Repair Society (ICRS) histologic scoring at six months post-implantation [274]. Marquass *et al*. had similar findings after one year and also showed that precultivated MSCs had better histologic outcomes than matrix-associated chondrocyte transplantation (MACT) [308].

Bone marrow marrow-derived cell (BMDC) collections produced by centrifugation and made up of nucleated cell fractions that contain MSCs have been assessed by Fortier *et al.* and Zhang *et al.* [307, 311]. Fortier *et al.* mixed BMDCs with thrombin to create an implantable clot and compared this to microfracture in the treatment of equine trochlear ridge chondral defects [307]. Macroscopic and histological outcomes were superior with BMDC transplantation. Hyaline-like cartilaginous repair tissue containing proteoglycans and type II collagen was noted. Zhang *et al*. compared BMDCs to isolated,

expanded MSCs seeded with collagen II gels [311]. After two months, each cell type produced histologically and macroscopically equivalent hyaline-like cartilage repair tissue within porcine femoral trochlea chondral defects.

Co-transplantation of chondrons and MSCs suspended within fibrin glue into goat femoral condyle chondral defects was assessed in another study [312]. This technique showed superior defect filling, O'Driscoll histologic scoring and biochemical GAG quantity in comparison to microfracture. However, co-transplantation was not compared with MSC or chondrocyte transplantation alone.

Animal studies have yielding positive preclinical results that have provided support and direction for MSC-based therapies in humans. Specific techniques such as MSC injection, and transplantation of both isolated MSCs and BMDCs have been taken into a clinical realm. Other techniques such as scaffold-free tissue-engineered constructs, magnetically guided MSC injection, co-transplantation, and MSC precultivation have only been reported in the animal literature to date.

2.2.4 Clinical Studies

There is a growing body of clinical evidence supporting MSC transplantation as an effective treatment for traumatic articular cartilage injury (Table 2.2). Cells derived from autologous bone marrow aspirates from the iliac crest have been used for treatment of focal, traumatic chondral and osteochondral defects of the

femoral condyle [39, 254, 316-321], femoral trochlea [41, 43, 46, 317], talus [38, 40, 45, 322, 323], tibial plateau [41], and patella [41, 43, 46, 317]. Other studies have addressed the use of this technique in managing other defect types such as osteochondral lesions arising from osteochondritis dissecans [44, 324], septic arthritis [325] and unicompartmental OA [37]. One group has reported use of MSCS derived from synovium for treatment of femoral condyle defects for treatment of articular cartilage defects of the femoral condyle [326].

Following aspiration, MSCs were isolated and expanded within the laboratory for 2-3 weeks and implanted alone [317, 324, 326] or in association with biomaterial matrices [39, 43, 316, 318]. Alternatively, in other studies, BMDCs – also described as bone marrow concentrate (BMC) [319, 320] or bone marrow aspirate concentrate (BMAC) in the literature [41] – were separated using centrifugation systems [38, 40, 41, 45, 254, 319, 320]. Presumably, these collections contained a variety of cell types from the bone marrow space, some of which were MSCs. BMDCs were immediately implanted in conjunction with matrices into defects in the same operative period as the aspiration. Matrices used in these studies included platelet-rich fibrin gel [38, 40, 41, 46, 254, 316, 321], fibrin glue [319, 320], collagen gel and paste [38-40, 43, 45, 322], and scaffolds composed of collagen [39, 41, 43, 318, 319, 321], HA [38, 40, 45, 254, 321-323], and PGA-HA [320]. In most cases, MSCs or BMDCs were seeded onto scaffold or gel matrices for implantation. Combinations of scaffolds and cell-containing gels or glue were commonly described [38-40, 43-46, 150, 254, 319, 320, 322,

323]. Some protocols involved the implantation of cells within gel followed by coverage with biomaterial membranes [41, 46, 319, 320]. Cell-matrix constructs were implanted on the same day of scaffold seeding [38, 40, 44, 45, 150, 254] or following a few days of *in vitro* culture in an attempt to promote cell adherence to scaffolds prior to implantation [39, 43]. Some groups used fibrin glue [317] and overlying periosteal flaps [37, 39, 43, 316, 317, 324] or synovium [43] to stabilize implanted constructs.

Based on the available short-term and mid-term evidence, implantation of MSCs or BMDC collections containing MSCs appears to be a successful treatment for focal traumatic chondral and osteochondral defects (Table 2.2). Functional outcomes improved with time to 24-54 months of mean follow-up following implantation in the majority of patients with focal chondral and osteochondral lesions of the knee [41, 43, 46, 254, 317-321, 326]. With respect to lesions of the talus, functional outcomes improved post-operatively to a mean follow-up of 29-53 months [38, 40, 45, 322, 323]. Two studies reported a peak in the American Orthopaedic Foot and Ankle Society (AOFAS) score at 24 months from BMDC transplantation with a downward trend thereafter to final follow-up at 48-72 months [45, 322], while two other studies by this group demonstrated a peak at 36 months that remained stable to 48 months [40, 323]. Longer-term evidence is available from Wakitani *et al*. supporting the safety of MSC transplantation up to 137 months post-transplantation surgery, although other outcomes were not assessed [328].

Table 2.2 Clinical studies assessing mesenchymal stem cells in the treatment of traumatic articular cartilage defects

Article	Subjects	Defects	Implanted/ injected constructs	Follow -up	Key findings
Kuroda *et al*. (2007), case report (Level IV) [39]	1 M (age 31 y)	1 medial femoral condyle chondral defect (6.0 cm^2) from trauma	Implantation of isolated BM-derived MSCs within porcine type I collagen gel on a collagen scaffold; covered by a periosteal flap	12 months	Arthroscopic: firm, smooth repair tissue; histological: hyaline-like cartilage covered superficially by fibrous tissue; MRI: focal chondral and subchondral irregularities; clinical: return to previous level of activity
Wakitani *et al*. (2007), case series (Level IV) [43]	3: 2 M, 1 F (age 32-45 y)	5 femoral trochlea (0.7-4.2 cm^2) and 4 patella chondral defects (1.0-1.7 cm^2); defects in 2/3 participants from trauma	Implantation of isolated BM-derived MSCs within bovine type I collagen gel on a porcine collagen scaffold; covered by a periosteal flap or synovium; adjunctive subchondral drilling	18 months	Arthroscopic: firm, smooth tissue; histological: atypical cartilage; MRI: complete coverage of defects but quality unclear; clinical: improvement of symptoms and return to work; IKDC improvement
Giannini *et al*. (2009), case series (Level IV) [38]	48: 27 M, 21 F (mean age 28.5 ± 9.5 y)	48 talar dome osteochondral defects (2.07 ± 0.48 cm^2); 35 from trauma; previous MFX, debridement or ACT in 15	Implantation of BMDCs suspended within collagen/platelet paste or seeded on HA (HYAFF-11) scaffold	29 months	Arthroscopic: smooth tissue in some, hypertrophic in others; all integrated with firmness of native cartilage; histological: mixed with some hyaline quality; MRI: newly formed tissue in all lesions; clinical: improvement in AOFAS scores with time and return to sports with no difference between scaffold types; worse outcomes with previous surgery
Buda *et al*. (2010), case series (Level IV) [254]	20: 12 M, 8 F (mean age 28.5 ± 9.5 y)	16 medial femoral condyle and 6 lateral condyle osteochondral defects (no area provided); 18 traumatic and 2 OCD defects	Implantation of BMDCs seeded on a HA (HYAFF-11) scaffold supplemented with platelet-rich fibrin; adjunctive meniscus repair or debridement, ACL-R, or HTO	29 months	Histological: collagen II noted throughout repair tissue with focal proteoglycan content consistent with hyaline-like cartilage; MRI: variable signal intensity that correlated with KOOS score; clinical: improvement in IKDC and KOOS scores post-operatively
Giannini *et al*. (2010), Prospect-ive, compar-ative study (Level III) [40]	81: 47M, 34F (mean age 30 ± 8 y); 25 BMDC; 10ACT; 46 MACT	81 talar dome osteochondral defects (>1.5 cm^2) from trauma	Implantation of BMDCs seeded on a HA (HYAFF-11) scaffold supplemented with platelet-rich fibrin	39 months	Arthroscopic: good defect coverage; histological: hyaline-like cartilage noted; MRI: complete integration in 76% and homogenous tissue in 82% of all cases with hypertrophy in 3 BMDC and 2 ACT patients; clinical: improvement in AOFAS scores after surgery with no difference between BMDC-scaffold implants, ACT and MACT; lower overall cost for BMDC transplantation compared to ACT/MACT

Table 2.2 Clinical studies assessing mesenchymal stem cells in the treatment of traumatic articular cartilage defects (continued)

Article	Subjects	Defects	Implanted/ injected constructs	Follow-up	Key findings
Haleem *et al*. (2010), case series (Level IV) [316]	5: 4 M, 1 F (mean age 25.4 y)	5 femoral condyle chondral defects (3-12 cm^2); 2 traumatic, and 3 OCD defects (1 OA from neglected OCD)	Implantation of isolated BM-derived MSCs within platelet-rich fibrin glue; covered by a periosteal flap	12 months	Arthroscopic: smooth tissue; MRI: complete defect filling with good congruity in 3/5 patients; clinical: improvement in Lysholm and RHSSK scores with return to sports; worse outcomes in 1 patient with pre-operative OA
Nejadnik *et al*. (2010), prospect-ive study (Level III) [317]	72: 38 M, 34 F (mean age 44.0 ± 11.4 y) 36 MSCs; 36 ACT	13 patella, 4 femoral trochlea, 12 femoral condyle, and 7 multiple knee chondral defects (4.6 ± 3.5 cm^2) in MSC group; 14 traumatic, 20 OA and 2 other defects	Implantation of isolated BM-derived MSCs; covered by a periosteal flap; adjunctive partial meniscectomy, patellar realignment, ACL-R, or HTO	24 months	Arthroscopic: smooth tissue in most cases; histological: aggrecan and collagen II content consistent with hyaline cartilage; clinical: greater improvement in SF-36 Physical Role Functioning in MSCs vs. chondrocytes; equivalent IKDC, Tegner and Lysholm score improvement following both MSC and chondrocyte transplantation; superior outcomes in males vs. females
Gobbi *et al*. (2011), case series (Level IV) [41]	15: 10 M, 5 F (mean age 48 y, range 32-58 y)	7 patella, 6 femoral trochlea, 4 medial tibial plateau, 6 medial femoral condyle, and 1 lateral condyle chondral defects (9.2 ± 6.3 cm^2); all defects from trauma; 6 patients had multiple defects	Implantation of BMDCs mixed with batroxobin (Plateltex Act) to produce a clot; covered by a type I/III collagen matrix (Chondro-Gide); adjunctive ACL-R, HTO or patellar realignment	24 months	Arthroscopic: smooth, integrated tissue in all cases; no hypertrophy; histological: variability with properties of hyaline and fibrocartilage; MRI: complete defect filling in 80%, integration in 93%, and no hypertrophy in all patients; clinical: improvement in all scores (VAS, KOOS, Tegner, Marx, IKDC and Lysholm) following surgery; patients with single lesions and smaller lesions had better outcomes
Kasemkij wa-ttana *et al*. (2011), case series (Level IV) [318]	2 M (age 24-25 y)	2 lateral femoral condyle chondral (2.2-2.5 cm^2)	Implantation of isolated BM-derived MSCs seeded on a type I collagen scaffold supplemented with fibrin glue; covered by a periosteal flap; adjunctive ACL-R, meniscal repair	30 months	Arthroscopic: good defect fill, integration and firmness; clinical: significant improvement in IKDC score and KOOS post-operatively
Saw *et al.* (2011), case series (Level IV) [327]	5: 1 M, 4 F (mean age 39.4 y, range 19-52 y)	3 focal defects: 1 lateral femoral condyle (2 cm^2), 1 patella (8.8 cm^2), 1 femoral trochlea (0.5 cm^2); 2 OA defects	Injection of peripheral blood-derived MSCs with HA weekly (x5) starting 1 wk after subchondral drilling; adjunctive HTO or lateral patellar release; pre-injection GCSF	18 months	Arthroscopic: good filling in focal defects; range from devoid areas to smooth repair tissue in OA defects; histological: intense proteoglycan staining; type I collagen in superficial area with predominance to type II collagen in deep area; chondrocytes in subchondral drill holes

Table 2.2 Clinical studies assessing mesenchymal stem cells in the treatment of traumatic articular cartilage defects (continued)

Article	Subjects	Defects	Implanted/ injected constructs	Follow -up	Key findings
Gigante *et al.* (2012), case report (Level IV) [319]	1 M (age 37 y)	1 medial femoral condyle chondral defect (3 cm^2) from trauma	Implantation of BMDCs within fibrin glue (Tisseel) and coverage with a collagen membrane (MeRG) after arthroscopic MFX (CMBMC)	24 months	MRI: good defect filling with tissue that was isointense relative to native cartilage; no signs of bone edema; clinical: return to activity and asymptomatic
Enea *et al*. (2013), case series (Level IV) [320]	9: 5 M, 4 F (mean age 48 ± 9 y)	6 medial femoral condyle and 3 lateral condyle chondral defects (2.6 ± 0.5 cm^2); previous meniscectomy, debridement or ACL-R	Implantation of BMDCs within fibrin glue and coverage with a PGA-HA membrane (Chondro-tissue) after arthroscopic MFX (CMBMC); adjunctive meniscectomy, osteochondral fixation, or trochlea resurfacing	22 months	Arthroscopic: 1 normal, 3 nearly normal and 1 abnormal on ICRS CRA; histological: hyaline-like cartilage repair tissue; MRI: complete defect filling in all; mild subchondral irregularities in all; hypertrophy in 1 patient; clinical: improvement in IKDC and Lysholm scores compared to pre-operative scores; no change in Tegner score from pre-injury; one failure
Giannini *et al*. (2013), case series (Level IV) [45]	49: 27 M, 22 F (mean age 28.1 ± 9.5 y)	49 talar dome osteochondral defects (2.2 ± 1.2 cm^2); 36 traumatic defects with unknown etiology in others; previous debridement, MFX, ACT or BMDCs in 17	Implantation of BMDCs within collagen/platelet paste or seeded on HA (HYAFF-11) scaffold supplemented with platelet gel	48 months	MRI: complete defect filling in 45%, hypertrophy in 45%, integration in 65%, subchondral disruption in 65% of cases; 78% of repair area had hyaline quality; clinical: improvement in AOFAS scores with maximal value at 24 mo; decreased at 36-48 mo; decreased AOFAS associated with fibrocartilage quality; return to pre-injury sports in 78%
Saw *et al*. (2013), RCT (Level II) [257]	49: 17 M, 32 F (mean age 38 ± 7 y); 25 MSC+HA; 24 HA	49 chondral defects of the knee (57% patella, 29% trochlea, 12% femoral condyle, and 8% tibial plateau)	Injection of peripheral blood-derived MSCs and HA weekly (x5) starting 1 wk after subchondral drilling and then weekly (x3) at 6 months; pre-injection GCSF	24 months	Arthroscopic: smooth defect filling; histological: ICRS II score was significantly better in MSC+HA group; MRI: improved cartilage morphology, defect filling and integration in MSC+HA group; clinical: improvement in IKDC scores with no difference between MSC+HA and HA
Buda *et al*. (2013), case series (Level IV) [321]	20: 12 M, 8 F (mean age not reported)	14 medial femoral condyle, 4 lateral condyle and 2 both condyle osteochondral defects (no area provided); 18 traumatic and 2 OCD defects	Implantation of BMDCs seeded on a HA (HYAFF-11) or collagen (IOR-G1) scaffold supplemented with platelet-rich fibrin; adjunctive meniscus repair or debridement, ACL-R, or HTO	29 months	Histological: collagen II noted throughout repair tissue with proteoglycan content consistent with hyaline-like cartilage; MRI: MOCART correlated with KOOS score; clinical: improvement in IKDC and KOOS scores post-operatively

Table 2.2 Clinical studies assessing mesenchymal stem cells in the treatment of traumatic articular cartilage defects (continued)

Article	Subjects	Defects	Implanted/ injected constructs	Follow -up	Key findings
Buda *et al*. (2014), case series (Level IV) [322]	64: 34 M, 30 F (mean age 30.5 ± 10.5 y)	64 talar dome osteochondral defects (5.3 ± 0.7 cm^2); 50 traumatic defects with unknown etiology in others; previous debridement, MFX, or ACT in 17	Implantation of BMDCs within collagen/platelet paste (Spongostan1) or seeded on HA (HYAFF-11) scaffold supplemented with platelet gel	53 months	MRI: area of defect related to percentage of maximal possible improvement in AOFAS at each follow-up; clinical: improvement in AOFAS scores with maximal value at 24 mo; AOFAS scores decreased gradually at 36-72 mo (significance not established); return to high-impact sports in 77% at a mean of 12 mo; scaffold type did not impact AOFAS scores
Buda *et al*. (2015), retro-spective compar-ative study (Level III) [323]	80: 52 M, 28 F (mean age 30.2 ± 9.7 y) 40 BMDCs; 40 MACT	40 talar dome osteochondral defects (1.8 ± 0.6 cm^2) in BMDC group; 31 traumatic defects with unknown etiology in others	Implantation of BMDCs seeded on HA (HYAFF-11) scaffold supplemented with platelet gel	48 months	MRI: T2 values in range of hyaline cartilage in 85% with BMDCs and 75% with MACT; MOCART similar between groups; clinical: both groups had AOFAS increase and peak at 36 mo and remained stable to 48 mo with no difference between groups; rate of return to sports was slightly higher following BMDC transplantation
Gobbi *et al*. (2015), prospect-ive compar-ative study (Level III) [46]	37: 19 M, 18 F (mean age 43.1-45.5 y) 18 BMDCs; 19 MACT	18 patellofemoral chondral defects in BMDC group, 8 single and 10 multiple (10.5 ± 6.0 cm^2 total area per patient with 5.5 cm^2 per lesion); 13 traumatic and 5 degenerative defects	Implantation of BMDCs mixed with batroxobin (Plateltex Act) to produce a clot; covered by an HA (HYAFF-11) scaffold; adjunctive ACL-R, HTO or patellar realignment	54 months	Arthroscopic: smooth surface, stable graft with good integration at 13-14 mo; histological: proteoglycan and collagen II staining in the majority of BMDCs and MACT; MRI: >50% defect filling in 81% of patients with BMDCs and 76% with MACT; no deterioration between 2 y and final follow-up; clinical: improvement in IKDC, KOOS and VAS scores in both groups following surgery with no difference between groups other than IKDC subjective score that was better with BMDCs
Sekiya *et al*. (2015), case series (Level IV) [326]	10: 5 M, 5 F (median age 30.5 ± 10.5 y)	10 femoral condyle chondral and osteochondral defects (median 2 cm^2); all traumatic; previous meniscectomy in 2, ACL-R in 1	Implantation of synovium-derived MSCs; adjunctive removal of fragment or ACL-R during arthroscopy to harvest synovium	52 months	Arthroscopic: cartilage defect appeared improved in all; histological: proteoglycan staining in some tissue with fibrocartilage features in other tissue; MRI: filling scores improved after the procedure; clinical: Lysholm scores increased after the MSC transplantation

Table 2.2 abbreviations

ACT, autologous chondrocyte transplantation; ACL-R, ACL reconstruction; AOFAS, American Orthopaedic Foot and Ankle Society; BM, bone marrow; BMDC, bone marrow-derived cell; F, female; GCSF, granulocyte colony stimulating factor; CMBMC, covered microfracture and bone

marrow concentrate; HA, hyaluronic acid; HSS, Hospital for Special Surgery; HTO, high tibial osteotomy; ICRS, International Cartilage Repair Society; ICRS CRA, Cartilage Repair Assessment (arthroscopy); IKDC, International Knee Documentation Committee; KOOS, Knee Injury and Osteoarthritis Outcome Score; M, male; MACT, matrix-associated autologous chondrocyte transplantation; MFX, microfracture; MRI, magnetic resonance imaging; MSC, mesenchymal stem cell; OCD, osteochondral dissecans; PGA-HA, polyglycolic acid-hyaluronic acid; RCT, randomized controlled trial; RHSSK, Revised Hospital for Special Surgery knee; SF-36, Short Form 36; VAS, Visual Analogue Scale; y, year(s)

These positive outcomes contrast with those from patients with more advanced degenerative disease. In one study focusing on the management of unicompartmental OA of the knee, outcomes were equivalent between the MSC transplantation group and cell-free control group in 24 patients who underwent concomitant high tibial osteotomy [37]. Furthermore, one participant with OA in another case series had worse clinical scores post-operatively than others with focal defects [316].

MRI and arthroscopy have shown that repair tissue derived from MSC and BMDC transplantation contains hyaline-like cartilage and integrates within surrounding native tissue within 24 months of implantation [38, 45, 46, 254, 318-321, 326] (Table 2.2). Cartilage quality correlated with clinical outcomes [45, 254, 321] as did implant-defect congruity and the amount of defect filling [316]. In some cases, hypertrophic cartilage has been noted on arthroscopy, but healthy repair tissue was found upon arthroscopic debridement of this tissue [38]. Lack of complete filling and non-congruent resurfacing of defects have been reported in a minority of cases [316]. In osteochondral lesions, subchondral bone appears to

require longer periods of time than cartilage for remodeling. Giannini *et al*. found abnormal subchondral structure and separated osteochondral interfaces on MRI at 24 months following treatment of osteochondral lesions of the talus [45].

Histological analysis of repair tissue biopsies has been consistent with MRI and arthroscopic findings [38, 39, 41, 46, 254, 319-321, 326] (Table 2.2). A number of groups have reported intense proteoglycan staining surrounding differentiated chondrocytes [38, 41, 46, 254, 320, 321]. Furthermore, repair tissue often contained a moderate to large amount of collagen II with lesser amounts of collagen I on immunohistochemistry that supported the presence of hyaline-like cartilage phenotype [38, 39, 41, 46, 317, 322]. Fibrocartilage or mixed repair tissue has also been described, but in a relatively smaller number of patients [39, 43, 320, 326]. Periosteal flap coverage and subchondral drilling were used in these studies and are potential contributing factors.

Four clinical studies have compared MSC or BMDC transplantation to autologous chondrocyte transplantation (ACT) or matrix-associated ACT (MACT) [40, 46, 317, 323]. Similar positive outcomes were noted on most clinical scales, although differences were noted on certain parameters. Specifically, Nejadnik *et al*. reported better physical role functioning on the Short Form 36 (SF-36) scale with MSC transplantation relative to ACT for treatment of knee defects, while International Knee Documentation Committee (IKDC), Lysholm and Tegner scores were similar [317]. Giannini *et al.* reported no

differences in AOFAS score between ACT, MACT and BMDC transplantation for treatment of talus defects [40]. Buda *et al.* had similar findings of no difference on AOFAS scores between MACT and BMDC transplantation [323]. However, BMDC transplantation led to increased numbers of patients returning to sports and less retiring from sports. Gobbi *et al.* reported significantly better IKDC subjective scores with BMDC transplantation, although IKDC objective, Knee Injury and Osteoarthritis Outcome Score (KOOS) and visual analog scale (VAS) pain scores were not different between BMDC transplantation and MACT for treatment of patellofemoral defects [46].

In these studies, MRI, arthroscopic and histologic findings indicated that MSCs and chondrocytes were capable of resurfacing defects with hyaline-like cartilaginous repair tissue that integrated into surrounding cartilage [40, 46, 317, 323]. Buda *et al.* found a higher presence of features consistent with hyaline cartilage and a lower presence of features consistent with fibrocartilage following BMDC transplantation in comparison to MACT based on MRI T2 mapping [323]. Gobbi *et al.* reported >50% defect fill on MRI in 81% of patients treated with BMDC transplantation and 75% of patients treated with MACT [46]. Integration to native cartilage was 94% and 88% in these groups, respectively.

Although implantation of MSC-based constructs has been the focus of clinical literature to date, one group has reported outcomes following intra-articular injection of MSCs for the treatment of focal chondral defects [257, 327].

In a randomized controlled trial, autologous peripheral blood MSCs were injected with HA weekly for five weeks after subchondral drilling and subsequently for another three weeks at six months into the knees of patients with lesions of the femoral condyle, tibial plateau, patella, and femoral trochlea. Histologic assessment at 18 months showed the presence of hyaline-like cartilage in patients who received MSCs. Furthermore, ICRS II histologic scores were significantly better in participants who received MSCs and HA versus those who received HA. However, IKDC clinical scores were equivalent between these two groups at 24 months.

2.3 Tissue engineering and transplantation variables

The goal of MSC transplantation is to create repair tissue with properties of hyaline cartilage that integrates into surrounding native osteochondral tissue while limiting local and systemic adverse effects. Three general MSC transplantation protocols currently exist (Figure 2.1). The one-step BMDC transplantation protocol consists of bone marrow aspiration, separation of a nucleated cell population containing MSCs amongst other cells, seeding of these cells on a scaffold, and implantation all within a single operative period [38, 40, 41, 45, 254]. A second protocol involves isolation of MSCs within the laboratory, *in vitro* expansion, and scaffold seeding shortly before implantation [39, 43, 316-318]. The scaffold may be seeded at the time of implantation or a within a few days of implantation a short *in vitro* culture period to promote MSC adherence to the biomaterial [39]. The final protocol utilizes isolated, expanded MSCs that are

seeded onto a scaffold and precultivated – or predifferentiated – *in vitro* over 2-3 weeks to promote chondrogenesis prior to implantation [36, 274, 308].

BMDC transplantation and non-precultivated, isolated and expanded MSC transplantation have both resulted in the creation of hyaline-like cartilage based on arthroscopy, histology and imaging, and yielded positive outcomes in clinical studies [38-41, 43, 45, 316-318]. To our knowledge, implantation of precultivated MSC-matrix constructs has not been studied clinically to date, but was shown to produce hyaline-like cartilage tissue in large-animal *in vivo* studies [36, 274, 308]. Although successful resurfacing has been performed with all three transplantation protocols, each carries specific advantages and disadvantages that are described in Table 2.3.

At present, studies comparing these protocols in humans are lacking, but have been performed in animal models. Zhang *et al.* found no difference at two months between BMDCs and expanded MSCs seeded on collagen gels implanted within femoral trochlea chondral defects in mini-pigs [311]. Marquass *et al.* showed that precultivated MSC-seeded collagen gels produced superior repair tissue after one year to non-precultivated MSCs within distal femur osteochondral defects in sheep [274, 308].

Regardless of the specific transplantation protocol used, MSC-based therapies require a number of steps that may be optimized to improve MSC yield, chondrogenesis, repair tissue integration, and ultimately clinical outcome. These

steps may include cell collection, MSC isolation and expansion, matrix seeding, precultivation into cartilaginous tissue, and surgical implantation.

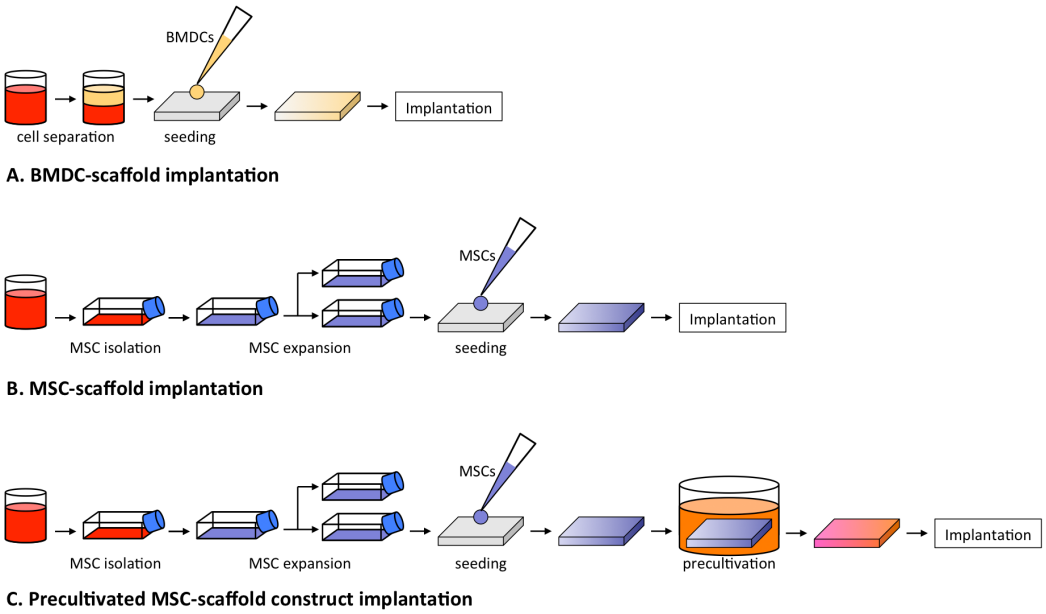

Figure 2.1 Mesenchymal stem cell transplantation constructs and protocols. (A) In bone marrow-derive cell (BMDC) transplantation, the bone marrow aspirate is centrifuged to create a BMDC concentrate that contains MSCs within a pool of other cells and chemical mediators. BMDCs are then seeded onto a scaffold and implanted within a cartilage defect. Mesenchymal stem cell (MSC) transplantation involves isolating MSCs from a bone marrow aspirate by plastic adherence and expansion in plastic tissue culture flasks. (B) MSCs are then seeded onto a scaffold and implanted or (C) precultivated *in vitro* to promote chondrogenesis prior to implantation.

2.3.1 Collection of tissue containing mesenchymal stem cells

MSCs are present within a number of tissues that may serve as potential harvest sites (Table 2.4). To date, needle aspiration of pelvic bone marrow has been the method of choice for MSC-based treatment of human articular defects [38, 40, 41, 43, 45, 254, 316-318, 320, 329]. The use of peripheral blood MSCs has also been

reported clinically [257, 327]. Synovial, periosteal and adipose tissues are other sources that have been assessed *in vivo* in the animal literature with relevance [29, 289, 305]. Synovial MSCs appear to have improved chondrogenic capacity relative to MSCs from bone marrow and periosteum based on *in vitro* assessment [256], although this advantage has not been reproduced *in vivo* in two rabbit studies [289, 292]. Adipose tissue offers the advantage of abundant availability, but adipose MSCs have a lower chondrogenic potential than MSCs from bone marrow, synovium and periosteum [256]. Bone marrow- and periosteum-derived MSCs have a heightened osteogenic potential [256]. Although this may be not ideal for cartilage engineering, it could be advantageous in osseous regeneration within osteochondral lesions. While present-day techniques utilize autologous MSCs in transplantation, MSC tissue banking and allogeneic transplantation could one day provide an alternative strategy [330]. However, further investigation is required to support allogeneic use of MSCs due to recent work suggesting that both undifferentiated and chondrogenic-differentiated MSCs cause immunoreaction [331].

2.3.2 Isolation and expansion of mesenchymal stem cells

Following the collection of bone marrow or other MSC-containing tissues, isolation and expansion of MSCs is performed under either two-dimensional (2D) or 3D conditions. In the conventional 2D method, tissue is placed in serum-containing medium within plastic tissue-culture flasks and incubated for a number of days [32]. Mononucleated cells (MNCs), some of which are MSCs, may be quantified and plated at 10,000-250,000 cells per cm^2 [32, 261, 317, 332]. MSC

isolation occurs through adherence of MSCs to plastic, as other cell types are non-adherent and discarded when culture medium is changed. Cell replication is monitored through the level of confluence observed by microscopy. Once confluence is achieved, trypsin and ethylenediaminetetraacetic acid (EDTA) are used to disrupt adherence, and MSCs are re-plated within a larger number of flasks [261]. This process is repeated through multiple passages to allow for expansion to occur. Although a greater number of passages yields a larger number of total MSCs available for implantation, long-term expansion should be avoided given that proliferation decreases and eventually stops with cellular senescence [333-338]. Furthermore, sustained 2D expansion on tissue-culture plastic leads to altered differentiation potential with reduced chondrogenic capacity and a propensity for cells enter an osteogenic pathway [333, 334, 339, 340]. Consequently, MSCs are usually expanded through a maximum of 2-3 passages in tissue-culture flasks.

Three-dimensional (3D) isolation and expansion of BMSCs has been proposed as a method of mimicking the natural bone marrow microenvironment and maintaining multipotency [266, 341]. Cell collections containing MNCs are seeded within 3D biomaterials for isolation and expansion [266, 342]. Although this method is in its early stages and currently under investigation, the available *in vitro* evidence suggests that MSCs derived from 3D isolation and expansion have superior chondrogenic differentiation capacity in comparison to 2D-isolated and expanded MSCs [266].

Given that only a small percentage of MNCs in bone marrow are MSCs (0.001-0.02%), expansion is necessary and must be optimized to ensure that an adequate yield of pure MSCs is available and the MSCs used for implantation are capable of chondrogenic differentiation [32, 343, 344]. Fibroblast growth factor-two (FGF-2) within culture medium increases MSC growth rate and maintains multipotency [345, 346]. Furthermore, FGF-2 has been shown to increase collagen and proteoglycan gene expression and GAG production [347, 348]. Hypoxic incubation during MSC expansion also augments chondrogenic potential [332]. GAG synthesis and gene expression of collagen II and sex determining region Y-box nine (SOX9) significantly increased in MSC pellet cultures expanded under 3% oxygen compared with those expanded under 21% oxygen [332]. Bioreactors may be used to improve yield as these provide efficient nutrient exchange and allow for increased cell densities during expansion [343]. Lastly, given that substrate stiffness has been shown to affect differentiation capacity of MSCs [349-351], there is a potential to optimize chondrogenesis by modulating substrate properties during MSC isolation and expansion.

2.3.3 Biomaterial matrix selection and seeding

Biomaterial matrices provide a framework for MSC proliferation and differentiation, and consolidate MSCs into 3D structures capable of filling defects. The majority of preclinical and clinical studies to date have used matrices (Tables 2.1 and 2.2). Gels or pastes composed of collagen or platelet-rich fibrin are moldable substances that hold the cells suspended [38, 39]. Porous scaffolds

made of materials such as collagen and HA serve as malleable, sponge-like structures that adhere MSCs at the time of seeding [36, 39]. Cell-seeded scaffolds with multiple layers engineered for osteochondral lesions have shown positive results in animal studies [283]. A tri-layer scaffold composed of collagen and hydroxyapatite has been tested in humans, but was used as a cell-free scaffold without co-implantation of MSCs [352]. There is potential for use of this product in conjunction with MSCs in the future. Combinations of MSC-embedded gels and scaffolds have been used in some *in vivo* studies [37, 38, 45, 320].

Table 2.3 Current mesenchymal stem cell transplantation protocols

Construct	Protocol	Advantages	Disadvantages
Bone marrow-derived cell (BMDC)-seeded scaffold [38, 40, 41, 45, 254, 311]	Bone marrow aspiration, separation of nucleated cell population (BMDC) by centrifugation, scaffold seeding, and implantation of BMDC-scaffold construct into the AC defect site	• Accessory cells/GFs create a natural microenvironment • One step procedure with aspiration and implantation in the same surgery	• Low number of MSCs • Cells other than MSCs could promote immunorejection in allogeneic transplantation
Mesenchymal stem cell (MSC)-seeded scaffold [39, 43, 274, 301, 308, 316-318]	Bone marrow aspiration, *in vitro* MSC isolation by adherence to plastic flasks, *in vitro* expansion of MSCs, scaffold seeding with MSCs, and implantation of MSC-scaffold construct into the AC defect site	• High MSC numbers are available due to expansion • Isolation allows for purification of MSCs and potentially reduced likelihood of rejection in allogeneic transplant • Mid-range time consumption	• *In vitro* expansion may increase the risk of contamination • MSCs have the capacity to become bone without *in vitro* cueing prior to implantation (bone may be beneficial in osteochondral lesions)
Precultivated MSC-seeded scaffold [36, 274, 308]	Bone marrow aspiration, MSC isolation by adherence to plastic flasks, expansion of MSCs *in vitro*, scaffold seeding with MSCs, *in vitro* precultivation in medium promoting chondrogenesis, and implantation of a cartilage tissue construct into the AC defect site	• High MSC numbers are available due to expansion • Chondrogenesis is stimulated • Increased mechanical stability of the implanted construct • Early neo-tissue remodeling occurs *in vitro* and may be accounted for at the time of implantation	• *In vitro* expansion and cultivation may increase the risk of contamination • Highest time and resource consumption • No clinical assessment to date

Table 2.3 abbreviations

BMDC: bone marrow-derived cell; GF: growth factor; MSC: mesenchymal stem cell

MSC seeding density has not been routinely reported to date in clinical studies. One reason for this is that some trials have used BMDCs, only a few of which are MSCs, rather than pure isolated MSCs [44]. In the *in vivo* animal literature, MSC densities of 10-48 million cells per cm^3 of scaffold have been used [36, 281, 283]. The optimal number of MSCs to be seeded per unit volume is currently unknown.

Table 2.4 Clinically relevant sources of mesenchymal stem cells for cartilage engineering

Source	*In vivo* assessment	Advantages	Disadvantages
Bone marrow	Clinical and preclinical [29, 36, 38-41, 43, 45, 254, 274, 281, 283, 284, 287, 289, 295, 296, 301, 303, 304, 306, 308, 309, 312-314, 316-318, 328]	• Most rigorous investigation and strongest supporting evidence • Ease of collection by needle • Long-term safety reported	• Propensity to form osseous tissue (could be beneficial for osseous regeneration in osteochondral lesions)
Peripheral blood	Clinical and preclinical [257, 297, 327]	• Ease of collection by needle	• Paucity of literature comparing this source to others • Paucity of clinical literature in comparison to bone marrow
Synovial tissue	Clinical and preclinical [286, 288-290, 292, 298, 300, 302, 305, 326]	• Greatest chondrogenic capacity noted based on *in vitro* study	• Paucity of clinical literature in comparison to bone marrow
Periosteum	Preclinical [29, 292]	• Equivalent chondrogenic capacity to bone marrow	• Propensity to form osseous tissue • Clinical assessment is lacking
Adipose tissue	Preclinical [282, 285, 292]	• Abundance of tissue • Widespread anatomic availability	• Reduced chondrogenic capacity • Clinical assessment is lacking

Table 2.4 abbreviations

BMDC: bone marrow-derived cell; MSC: mesenchymal stem cell

2.3.4 Cell-seeded biomaterial matrix implantation

Standard open or arthroscopic surgical approaches to the knee or ankle are used to access chondral and osteochondral defects during implantation procedures [38, 39, 44, 150]. Damaged articular cartilage is debrided down to subchondral bone and the edges are trimmed until a rim of healthy articular cartilage is evident [39, 317, 324]. In the setting of full-thickness chondral defects, microfracture or drilling of intact subchondral bone has been used by some groups in an attempt to stimulate the influx of cells and mediators into the repair zone [37, 43, 316, 319, 320], while other groups have left subchondral bone intact [39, 324, 353]. Subchondral bone is already disrupted in osteochondral lesions. Therefore careful debridement of malacic bone may be performed until healthy bone is reached [38].

At the time of implantation, matrices or cell-matrix constructs may be resized with punches or scalpels to fit within the margins of the defect [38]. Implantation orientation may be relevant in scaffolds engineered with separate porous and non-porous sides [37, 281].

Fibrin glue or autologous platelet-rich fibrin gel may be deposited within the defect and overlying the MSC-matrix construct to augment implant fixation [44, 281, 316, 317]. Sutures may be used to anchor cell-seeded scaffolds to surrounding native cartilage [353]. Autologous periosteal flaps or biomaterial membranes have also been used to prevent leakage of MSCs from cell collections

implanted alone [317, 324] or embedded within collagen or fibrin gel [37, 39, 316, 319, 320]. Periosteal flaps have been shown to form superficial fibrous caps that cover hyaline cartilage repair tissue [39]. In general, they are not recommended for use in scaffold-associated cell-based therapies, but may be used to contain implanted MSCs within defect areas when scaffolds are not used [317].

2.3.5 Precultivation of matrix-associated cells

Various *in vitro* culture techniques have been elucidated that may be used to promote the creation of bioengineered hyaline-like cartilage within precultivated MSC-scaffold constructs. Chemical mediators such as TGF-β and dexamethasone are placed with culture media for chondrogenic induction [261]. Several factors, including bone morphogenetic proteins (BMP-2, 4 and 6) and insulin-like growth factor (IGF-1) may be used in addition to TGF-β and dexamethasone to amplify chondrogenesis [278, 354]. Ascorbic acid serves as a cofactor in the hydroxylation of amino acids in collagen, and is also routinely used within chondrogenic culture medium [355].

Biomaterial properties such as stiffness and composition affect differentiation and may be used to drive chondrogenesis [349, 350]. Reduced stiffness of collagen-GAG scaffolds was shown to increase chondrogenesis-associated SOX9 gene expression, while increased stiffness was shown to increase osteogenesis-associated Runt-related transcription factor-two (RUNX2) expression in MSCs cultured *in vitro* in medium with no differentiation

supplements [350]. Furthermore, SOX9 gene expression was augmented in collagen-HA scaffolds relative to collagen-chondroitin sulphate scaffolds [350]. Incubator oxygen tension during precultivation may be used to modulate chondrogenesis. Hypoxic exposure was found to increase ECM deposition on scaffolds and gene expression of collagen II, aggrecan and SOX9 in pellet cultures [356]. Co-culture of MSCs with chondrocytes promotes the creation of cartilage through chondrocyte-enhanced MSC chondrogenesis [357]. Pellet co-culture of human MSCs and chondrocytes increased GAG deposition and expression of type II collagen while enhancing MSC-induced chondrocyte proliferation [357]. Cartilage formation may be augmented by mechanical stimulation during cultivation through either hydrostatic pressure or ultrasound. Hydrostatic pressure in constant and cyclic forms increased sulfated GAG matrix deposition by chondrocytes cultured on collagen scaffolds [358]. Furthermore, low-intensity ultrasound improved histological chondrogenic morphology, GAG and collagen II content, as well as gene expression of type II collagen, aggrecan and SOX9 [273, 359].

Bone marrow-derived MSCs have the propensity to enter an osteogenic pathway, a property that is not ideal for articular cartilage engineering [339]. During precultivation, osteogenesis may be dampened using a variety of methods. Parathyroid hormone-related protein (PTHrP) has been shown to reduce collagen X gene expression and alkaline phosphatase (ALP) activity [360]. Hypoxic culture of MSCs significantly suppressed expression of collagen X relative to

normoxic culture [332]. Lastly, co-culture of MSCs with chondrocytes reduced osteogenesis based on osteocalcin quantification, and Von Kossa and Alizarin Red staining [361].

2.4 Current recommendations and future directions

MSC-based therapy through injection or implantation is a promising treatment for traumatic chondral and osteochondral defects.

2.4.1 Injection protocol

MSC injection offers the advantage of minimal invasiveness, but dispersion of injected MSCs and lack of focus of these cells into defects make this method less appealing than direct implantation techniques. Several preclinical studies have been performed, but only one group has assessed MSC injection clinically to date [257]. The current literature supports performing microfracture or subchondral drilling in conjunction with weekly injections of MSCs and HA over the course of multiple weeks [257, 304, 314]. This protocol presumably increases the likelihood of defect seeding with MSCs from both injection and subchondral marrow sources.

2.4.2 Transplantation protocols

MSCs may be implanted alone or in conjunction with a biomaterial matrix. MSCs implanted and covered with a periosteal flap in a procedure analogous to ACT produced good outcomes based on one clinical study [317]. The majority of the

current clinical and preclinical literature has focused on matrix-associated transplantation of MSCs. Three general construct types have been implanted, including biomaterial scaffolds seeded with either BMDCs [38] or isolated and expanded MSCs [39], and precultivated constructs derived from MSCs cultured *in vitro* on scaffolds prior to implantation. [274]. All three protocols are capable of resurfacing focal articular cartilage defects with hyaline-like cartilage that integrates with surrounding tissue [39, 41, 274], while each has unique advantages and disadvantages. At present, all may be considered as potential treatment options. BMDC-scaffold implantation and non-precultivated isolated, expanded MSC-scaffold implantation have led to positive functional, arthroscopic, histologic and radiographic outcomes at 12-54 months in patients with traumatic, focal chondral and osteochondral defects of the knee and ankle [38, 39, 41, 43, 254, 316, 317]. No clinical studies have compared these two protocols, although one preclinical study found equivalent histologic outcomes [311]. The third protocol, precultivated MSC-scaffold construct implantation, has only been investigated in preclinical models but should be considered for clinical implementation given that it produced superior repair tissue in comparison to non-precultivated MSC-scaffold constructs over 6-12 months in two sheep studies [274, 308].

2.4.3 Articular cartilage defect characteristics

It is currently unclear whether defect characteristics should dictate the transplantation protocol used. Both full-thickness chondral and osteochondral

defects have been treated successfully with the current modalities, but several important differences exist between these defect types. In the setting of full-thickness chondral lesions, the subchondral bone is intact and there is no diffusion of subchondral marrow contents (MSCs, accessory cells and growth factors) into the defect site. Some groups have therefore recommended bone marrow stimulation techniques, such as microfracture and subchondral drilling, to be performed as an adjunct to MSC/BMDC-scaffold implantation [43, 329]. However, other groups have not used these techniques [38, 40, 45, 254, 317] possibly because the repair tissue derived from microfracture or subchondral drilling may produce fibrocartilage that is mechanically inferior to hyaline cartilage [98]. However, histologic assessment following combined arthroscopic microfracture and BMDC transplantation – described as the covered microfracture and bone marrow concentrate (CMBMC) technique by Gigante *et al*. – showed the presence of hyaline-like cartilage tissue [319, 320].

Osteochondral defects are deeper defects that involve subchondral plate disruption and diffusion of subchondral marrow contents into the defect site. These defects require more complex regeneration of separate layers of cartilage and bone. Tissue consistent with hyaline cartilage has been found following MSC transplantation [38, 45, 254]. Subchondral bone regeneration has also been reported, but restoration requires an extended period of time relative to cartilage. Specifically, 29 months following treatment of femoral condyle osteochondral defects, Buda *et al*. noted cartilage surface intactness in 70%, isointense cartilage

tissue in 65%, but subchondral lamina and bone intactness in only 30% of participants on MRI [254]. Similarly, at 24 months following treatment of talus osteochondral defects, Giannini *et al.* reported cartilage surface intactness in 40%, isointense cartilage tissue in 70%, but subchondral lamina and bone intactness in only 10% and 35%, respectively [45].

2.4.4 Mesenchymal stem cells versus chondrocytes

Detailed comparisons between MSC transplantation and other modalities of treatment for traumatic articular cartilage defects are lacking in the current literature. Chondrocyte transplantation (ACT/MACT), the current gold standard of cell-based treatment, has shown positive outcomes up at 10-20 years [227], while MSC/BMDC transplantation has only been assessed up to 12-54 months. In our review, one preclinical large-animal study and four clinical studies were found that directly compared MSC transplantation to chondrocyte transplantation [40, 308, 317]. Marquass *et al*. reported superior histologic findings in repair tissue derived from precultivated MSCs in comparison to ACT at one year post-implantation in sheep [308]. Clinically, Nejadnik *et al.* found similar positive functional outcomes on IKDC, Tegner and Lysholm scales between MSC implantation and ACT in the treatment of knee defects, but noted significantly higher physical role functioning on the SF-36 in patients treated with MSCs [317]. Gobbi *et al.* reported significantly better IKDC subjective scores with BMDC transplantation in comparison to MACT, although several other scores were not different following treatment of patellofemoral defects [46] Giannini *et*

al. noted similarly improved AOFAS scores with both BMDC and chondrocyte transplantation following treatment of talus defects, while Buda *et al.* found increased return to sports with BMDC [40, 323]. Further comparative evaluation is required to assess MSC transplantation relative to chondrocyte implantation.

MSC transplantation may reduce the likelihood of low chondrocyte yield and chondrocyte de-differentiation associated with chondrocyte transplantation [243, 246, 340]. Chondrocyte senescence is a concern with ACT and MACT [250, 251, 362], and although MSCs also undergo senescence over prolonged periods of proliferation, adequate MSC yields for transplantation may be attained at a stage during which there is still significant residual proliferative capacity [339]. Chondrocyte transplantation requires two invasive surgical procedures, one for cell collection and one for implantation [227]. In contrast, MSC transplantation only requires one surgical procedure at the time of implantation [43]. MSC collection may be performed through minimally invasive needle aspiration [39]. Consequently, MSC transplantation may be less expensive than ACT/MACT. Giannini *et al.* found that the total cost of arthroscopic matrix-associated BMDC transplantation was half of the cost of arthroscopic MACT and one-third of the cost of open ACT [40].

2.4.5 Guidelines

Based on the findings of *in vitro*, preclinical and clinical studies performed, several technical steps may be optimized in MSC transplantation to promote cell

numbers, chondrogenesis, repair tissue integration, and clinical outcome. With respect to cell collection, autologous bone marrow has been used in the majority of clinical studies to date and is the current preference [38-41, 43, 45, 254, 316-318]. However, synovial MSCs appear to have superior chondrogenic capacity and should be considered [256]. Furthermore, adipose tissue is abundantly available [285]. In MSC isolation, plastic adherence is used [261]. Expansion may be augmented using serum-containing medium supplemented with FGF-2 and incubation under hypoxic conditions [332, 345]. Several matrix types are appropriate for MSC transplantation. At present, 3D scaffolds composed of collagen or hyaluronic acid are the standard [39, 254]. Scaffolds composed of multiple layers are an option in the setting of osteochondral lesions [283]. Precultivation of MSC-scaffold constructs should be performed in serum-free medium containing TGF-β and dexamethasone supplemented with other mediators such as ascorbic acid, IGF-1 or BMPs [261, 278, 354]. Hypoxic incubation, co-culture with chondrocytes, mechanical stimulation with ultrasound, and dynamic culture within a bioreactor are other precultivation optimizing techniques that may be considered [273, 332, 343, 357]. Implantation is performed through either open or arthroscopic techniques. Fibrin glue or autologous platelet-rich fibrin gel may be used to stabilize implanted constructs [316, 318]. At present, there is insufficient evidence to support the use of marrow stimulation (i.e. subchondral drilling or microfracture) or periosteal flaps in MSC transplantation.

2.5 Thesis development and objectives

MSC transplantation is an emerging cell-based strategy for the treatment of traumatic chondral and osteochondral defects of the knee and ankle. Although there is currently no established consensus on protocol, multiple technical variations have successfully produced hyaline-like cartilaginous repair tissue. Clinical studies to date have reported good function in the majority of patients at 12-54 months following MSC implantation. Despite these positive findings, there is room for optimization of MSC transplantation with the goal of improving the quality of neo-cartilage developed.

In this thesis, several studies were performed to investigate variables of bone marrow-derived MSC (BMSC)-based cartilage engineering within *in vitro* and *in vivo* models. In Chapter 3, the impact of incubator oxygen tension during ovine BMSC isolation, expansion and differentiation on BMSC chondrogenesis within clinically approved porous scaffolds composed of type I collagen and esterified hyaluronic acid was investigated. Chapter 4 involved characterization of contraction during chondrogenesis of a porous collagen I scaffold seeded with human BMSCs that were isolated and expanded under different oxygen tensions. In Chapter 5, isolation and expansion environment and cell seeding density of a collagen I scaffold were assessed using ovine BMSCs in an *in vitro* model. Chapter 6 utilized an *in vivo* sheep model with full-thickness articular cartilage defects to assess a novel protocol for BMSC transplantation that involved BMSCs that were isolated, expanded, seeded within hyaluronic acid scaffolds, and

chondrogenically primed using a short culture period in chondrogenic medium prior to implantation. The impact of oxygen tension during pre-implantation culture on cartilaginous repair tissue formation was also investigated.

Chapter 3

Hypoxic Culture of Bone Marrow-Derived Mesenchymal Stromal Stem Cells Differentially Enhances *In Vitro* Chondrogenesis within Cell-Seeded Collagen and Hyaluronic Acid Porous Scaffolds

Troy D. Bornes, Nadr M. Jomha, Aillette Mulet-Sierra, and Adetola B. Adesida

This chapter has been published in part as:
Bornes TD, Jomha NM, Mulet-Sierra A, Adesida AB: **Hypoxic culture of bone marrow-derived mesenchymal stromal stem cells differentially enhances *in vitro* chondrogenesis within cell-seeded collagen and hyaluronic acid porous scaffolds.** *Stem Cell Res Ther* 2015, **6**(1):84.

3.1 Introduction

Bone marrow-derived mesenchymal stromal stem cells (BMSCs) are a promising cell-based option for treating articular cartilage defects [41, 43, 45, 254, 318, 320]. Clinical and preclinical studies have shown variable outcomes following BMSC transplantation for treatment of focal chondral and osteochondral defects [363]. Repair tissues consistent with hyaline cartilage, fibrocartilage and mixed tissue have been reported [41, 45, 254]. Clinical scores correlate with quality of

cartilaginous repair tissue based on magnetic resonance imaging (MRI) and histological analysis [45, 254, 320]. Therefore, culture conditions capable of improving cell and tissue phenotype are currently under investigation.

Incubator oxygen tension is a culture variable that has gained attention based on the posited role of oxygen in musculoskeletal tissue development and cellular microenvironments. There is evidence to suggest that hypoxia promotes chondrogenic differentiation of BMSCs during prenatal limb development [364]. Furthermore, BMSCs exist in hypoxic bone marrow spaces, while chondrocytes reside within avascular hyaline cartilage and are bathed in hypoxic synovial fluid [365, 366].

The positive impact of hypoxia on BMSC proliferation has been demonstrated based on cell count, nucleoside incorporation, and colony-forming capability [332, 367-370]. During prolonged expansion periods, stem cell characteristics such as rapid proliferation and multipotency are maintained with hypoxic incubation [367, 368], while senescence is delayed [253]. Hypoxic incubation during BMSC isolation and expansion [332, 369-372] and BMSC differentiation [332, 368-371, 373] have separately been associated with improved *in vitro* chondrogenesis within pellet, micromass and hydrogel models. Three studies have compared the impact of hypoxic isolation/expansion to hypoxic differentiation on chondrogenesis and variable improvements in gene

expression and cartilaginous extracellular matrix (ECM) formation were found with hypoxic exposure during each distinct culture period [332, 370, 373].

Although hypoxic enhancement of BMSC chondrogenesis has been studied extensively in pellet, micromass and hydrogel models, this effect has not been elucidated in detail in porous scaffolds. Porous scaffolds composed of natural and synthetic materials allow cells to permeate, adhere and organize within a three-dimensional environment, and deposit ECM to form tissue [374]. As a result, they serve as a suitable model for studying three-dimensional cartilage formation *in vitro.* [363]. Moreover, porous scaffolds composed of collagen or hyaluronic acid (HA) are commonly used in clinical BMSC transplantation [41, 45, 194, 254, 318]. At present, it is not known whether hypoxic culture improves chondrogenesis of BMSCs seeded on three-dimensional porous scaffolds. Accordingly, the first objective of this study was to assess the effect of oxygen tension during distinct isolation/expansion and differentiation culture periods on chondrogenesis within BMSC-seeded porous scaffolds. The impact of porous scaffold material on the modulation of chondrogenesis with oxygen tension has not been elucidated. Therefore, the second objective of this study was to investigate differences in chondrogenesis between BMSCs seeded and cultured on a collagen I porous scaffold and an esterified HA porous scaffold. It was hypothesized that hypoxic incubation during isolation/expansion and differentiation culture periods would improve BMSC chondrogenesis within each scaffold.

3.2 Methods

3.2.1 Bone marrow aspiration and mononucleated cell counting

Bone marrow-derived cell collections for this study were obtained from iliac crest aspirates from six skeletally mature, female Suffolk sheep (mean age ± standard error of the mean [SEM] of 3.3 ± 0.8 years). Characteristics of each sheep are summarized in Table 3.1. General anesthesia for the aspiration procedure was attained through sedation with intravenous dexmedetomidine (5 μg/kg) and ketamine (2 mg/kg) followed by endotracheal intubation and administration of gaseous isoflurane (2-4% in oxygen). The sheep were then positioned in lateral decubitus position and the posterolateral pelvic surgical site was clipped and prepared with 10% wt/vol povidone-iodine solution (Betadine, Purdue Pharma L.P., Stamford, USA). A small incision was made over the posterior ilium and an 11-gauge Jamshidi needle (Cardinal Health Canada, Vaughan, Canada) was inserted onto the iliac crest near the posterior superior iliac spine and through cortical bone into the marrow space. Bone marrow aspirate (mean volume ± SEM of 33 ± 2 ml) was collected and mixed immediately with 8 ml of heparin (10,000 units/10 ml; Pharmaceutical Partners of Canada, Richmond Hill, Canada). Aspirates were then filtered with a cell strainer (100-μm pore size; Becton Dickinson Canada, Mississauga, Canada). The number of mononucleated cells (MNCs) in each aspirate was determined by crystal violet nuclei staining and cell counting using a hemocytometer.

Table 3.1 Bone marrow donor information

Donor	Gender	Age (years)	Mass (kg)
Z28	Female	2.0	66
Z01	Female	2.2	71
Z33	Female	2.3	81
Y19	Female	3.2	63
Y08	Female	3.3	94
T10	Female	7.0	74

3.2.2 Isolation and expansion of bone marrow-derived mesenchymal stromal stem cells

Bone marrow aspirate collections containing 8×10^7 MNCs were seeded within each 150-cm^2 tissue culture flask. Culture medium composed of alpha-minimal essential medium (α-MEM) supplemented with 8.8% vol/vol heat-inactivated fetal bovine serum (FBS), penicillin-streptomycin-glutamine, 4-(2-hydroxyethyl)-1-piperazineethanesulfonic acid (HEPES), and sodium pyruvate (all from Life Technologies, Burlington, Canada) was pipetted into each flask (Appendix 1). Fibroblast growth factor-2 (FGF-2; Neuromics, Edina, USA) was added at a concentration of 5 ng/ml in order to maintain cell multipotency [346]. Nucleated cells were allowed to adhere and grow for 7 days before the first media change under normoxia (ambient 21% oxygen) or hypoxia (low 3% oxygen) at 37°C in a humidified incubator containing 5% carbon dioxide. Flasks from the hypoxic incubator experienced short periods (<5 minutes) of normoxic exposure during media changes. Thereafter, the media were changed twice per week until 80% cell

confluence was obtained. Adherent BMSCs were detached using 0.05% wt/vol trypsin-ethylenediaminetetraacetic acid (EDTA; Sigma-Aldrich, Oakville, Canada) and expanded under the same oxygen tension (normoxia or hypoxia) as during isolation until P2 prior to scaffold seeding. Hereafter for brevity, BMSCs described by expansion oxygen tension alone (normoxia-expanded and hypoxia-expanded BMSCs) will refer to BMSCs that were isolated and expanded under normoxia and hypoxia, respectively.

3.2.3 Colony-forming unit fibroblastic assay

A colony-forming unit fibroblastic (CFU-F) assay was conducted to determine the effect of oxygen tension on colony forming characteristics of BMSCs, and to calculate the proportion of plastic-adherent cells (BMSCs) derived from bone marrow aspirates containing a known number of MNCs. Bone marrow aspirates containing 1×10^5 MNCs from each donor were plated in triplicate within 100 mm-diameter sterile petri dishes (Becton Dickinson Canada Inc.) and cultured as described for expansion conditions under normoxia (21% oxygen) or hypoxia (3% oxygen) using α-MEM supplemented with 8.8% vol/vol heat-inactivated FBS, penicillin-streptomycin, HEPES, sodium pyruvate, and 5 ng/ml FGF-2. After the first week, the non-adherent cell population was removed by aspiration and culture media were replenished twice each week. During media changes, hypoxia cultivated cells experienced a short period (<5 minutes) of exposure to normoxia. The total duration of culture time used for each donor (mean ± SEM of 16.3 ± 0.5 days) was equivalent to the time required to attain 80% BMSC confluence at P0

and subsequent detachment and splitting to P1 for expansion in T150 flasks (see *Isolation and expansion of bone marrow-derived mesenchymal stromal stem cells*). For each donor, the culture times for petri dishes placed in hypoxic and normoxic conditions were identical. After the CFU-F culture period finished, the petri dishes were fixed with 10% wt/vol buffered formalin (3.8% wt/vol formaldehyde), washed using phosphate-buffered saline (PBS; Life Technologies) and stained with 0.25% wt/vol crystal violet solution (Sigma-Aldrich). During analysis, each stained cell collection was assessed and considered to be a colony only if: (1) the cell collection was stained strongly with crystal violet; (2) the periphery of the collection was circular and well defined with respect to the surrounding area of the plate that was not stained; and (3) the diameter of the stained cell collection was measured to be ≥2 mm. The number of BMSC colonies in each dish was recorded as well as the diameter of each colony.

3.2.4 Bone marrow-derived mesenchymal stromal stem cell proliferation

Total cell counts of trypsinized BMSCs at P0, P1 and P2 were calculated using trypan blue staining and hemocytometer counting of small aliquots of BMSCs in expansion medium. The number of colonies noted in each CFU-F assay was used to determine the number of BMSCs isolated per 1×10^5 MNCs plated for each donor, and this was extrapolated to calculate the number of BMSCs arising from 8×10^7 MNCs plated in each T150 culture flask during P0 expansion. Population doublings were determined using the method described by Solchaga *et al.* [346].

3.2.5 Trilineage differentiation potential of bone marrow-derived mesenchymal stromal stem cells

Osteogenic differentiation was performed by plating 5 $\times 10^3$ BMSCs/cm^2 within wells of a six-well plate (Becton Dickinson Canada Inc.) and culturing these in 2.5 ml of osteogenic medium for 21 days at 37°C in a humidified hypoxic incubator (3% oxygen and 5% oxygen). Osteogenic medium consisted of Dulbecco's modified Eagle's medium (DMEM) containing 4.5 mg/ml D-glucose, 110 μg/ml sodium pyruvate, 8.9 mM HEPES, 89 units/ml penicillin, 89 μg/ml streptomycin, 260 μg/ml L-glutamine (all from Life Technologies) supplemented with 8.8% vol/vol heat-inactivated FBS, 100 μM ascorbic acid 2-phosphate, 10 nM dexamethasone, and 10 mM beta (β)-glycerophosphate (Sigma-Aldrich). Media changes were performed twice per week. Following the culture period, the contents of each well were fixed with 10% wt/vol buffered formalin (3.8% wt/vol formaldehyde), stained for 30 minutes with 1% wt/vol Alizarin Red S (Sigma-Aldrich) with an adjusted pH of 4.2, washed with distilled water over 60 minutes, and stored at 4°C in 70% vol/vol glycerol (Fisher Scientific Chemical Division, Fair Lawn, USA). Images were captured using an Omano OM159T biological trinocular microscope (Microscope Store, Virginia, USA) fitted with an Optixcam Summit Series 5MP digital camera and Optixcam software, and assembled in Photoshop (Adobe Systems, San Jose, USA).

Adipogenic differentiation was performed on BMSCs plated at 5×10^3 BMSCs/cm^2 within wells of a six-well plate (Becton Dickinson Canada). Plated BMSCs were initially cultured in basic culture medium of 2.5 ml of DMEM containing 4.5 mg/ml D-glucose, 110 μg/ml sodium pyruvate, 8.9 mM HEPES, 89 units/ml penicillin, 89 μg/ml streptomycin, 260 μg/ml L-glutamine supplemented with 8.9% vol/vol heat-inactivated FBS (all from Life Technologies). Adipogenesis was then induced over 3 days in 2.5 ml of basic culture medium supplemented with 1 μM dexamethasone, 0.5 ml insulin-transferrin-selenium (ITS)+1, 100 μM indomethacin, and 500 μM isobutyl-1-methylxanthine (IBMX; Sigma-Aldrich Corp.), followed by 1 day of culture in 2.5 ml of basic culture medium supplemented with only 0.5 ml ITS+1. This 4-day cycle was then repeated three times, followed by culture for 7 days in 2.5 ml of basic culture medium supplemented with only 0.5 ml ITS+1. All culture was performed in a hypoxic humidified incubator (3% oxygen and 5% carbon dioxide). Following the culture period, the contents of each well were fixed with 10% wt/vol buffered formalin (3.8% wt/vol formaldehyde), stained for 60 minutes with 0.3% wt/vol Oil Red O (Sigma-Aldrich), washed with distilled water, and assessed immediately for staining. Oil Red O solution was prepared by creating a 0.5% wt/vol solution of Oil Red O (Sigma-Aldrich) in isopropanol (Fisher Scientific Chemical Division), and then diluting this to 0.3% wt/vol in an equivalent volume of distilled water. Microscopic images were captured in an identical fashion to osteogenic culture products.

Chondrogenic differentiation was verified using a pellet culture system. BMSCs were suspended in chondrogenic medium consisting of DMEM containing 4.5 mg/ml D-glucose, 110 μg/ml sodium pyruvate, 9.6 mM HEPES, 96 units/ml penicillin, 96 μg/ml streptomycin, 279 μg/ml L-glutamine (all from Life Technologies) supplemented with 365 μg/ml ascorbic acid 2-phosphate, 100 nM dexamethasone, 1× ITS+1 premix (Sigma-Aldrich), and 10 ng/ml transforming growth factor-beta three (TGF-β3; Neuromics; Appendix 1). A total of 5×10^5 BMSCs were spun within 1.5-ml sterile conical polypropylene microfuge tubes (Enzymax LLC, Kentucky, USA) at 1500 rpm for 5 minutes to form spherical cell pellets. Pellets were then submersed in 500 μl of chondrogenic medium and cultured in a hypoxic humidified incubator (3% oxygen and 5% carbon dioxide) for 21 days. Pellets experienced a short period (< 5 minutes) of exposure to normal oxygen tension during media changes. Following the culture period, BMSC pellets were processed and stained for histological analysis of cartilaginous proteoglycans (see *Histological and immunohistochemical analyses of extracellular matrix contents*).

3.2.6 Porous scaffold seeding and chondrogenic differentiation of bone marrow-derived mesenchymal stromal stem cell-seeded scaffolds

Cylindrical collagen scaffolds (3.5-mm thickness; 6-mm diameter) were created using a biopsy punch on sheets of porous, type I collagen sponge (125 × 100 × 3.5 mm^3 dimension; 115 ± 20 μm pore size; Integra LifeSciences, Plainsboro, USA). Cylindrical HA scaffolds (2-mm thickness; 6-mm diameter) were created using a

biopsy punch on sheets esterified HA (HYAFF) non-woven mesh (20 × 20 × 2 mm^3 dimensions; 10-20 μm-diameter fibers with varying inter-fiber spaces [202, 375]; Anika Therapeutics, Abano Terme, Italy). Scaffold seeding was performed at a consistent density of 1 $\times 10^7$ BMSCs/cm^3, which corresponded to 989,602 BMSCs seeded per collagen scaffold and 565,487 BMSCs seeded per HA scaffold. This seeding density was used given that health articular cartilage has been shown to contain around 1 $\times 10^7$ cells/cm^3 [57].

During seeding, BMSCs at P2 were re-suspended in chondrogenic culture medium (see *Trilineage differentiation potential of bone marrow-derived mesenchymal stromal stem cells*). Total cell counts were calculated from trypan blue staining and hemocytometer counting of small aliquots of BMSCs. BMSCs were micropipetted onto each scaffold within a 20-μl chondrogenic medium suspension. HA scaffolds were pre-soaked with 20 μl of chondrogenic medium to promote dispersion of the cell suspension over the scaffold during seeding. Seeded scaffolds were then incubated at 37°C for 15 minutes followed by addition of 100 μl of chondrogenic medium to the base of each scaffold. Thereafter, constructs were incubated for an additional 30 minutes to promote cell adhesion. All constructs, including cell-free scaffolds (control group) and those seeded with either normoxia- or hypoxia-expanded BMSCs, were subsequently immersed in 1 ml of chondrogenic medium and cultured statically at 37°C within humidified incubators containing 5% CO_2 and either 21% oxygen (normoxia) or 3% oxygen (hypoxia). Media were changed twice weekly thereafter.

3.2.7 Oxygen tension experimental groups

To determine the effect of oxygen tension during isolation/expansion and differentiation on *in vitro* chondrogenesis within BMSC-seeded scaffolds, BMSCs from five donors (Z28, Z01, Z33, Y19, and T10) with a mean age (± standard error of the mean [SEM]) of 3.3 ± 0.9 years were seeded onto collagen and HA scaffolds and cultured in chondrogenic medium for 14 days. The experimental set-up is illustrated in Figure 3.1. The treatment groups included: Hyp/Hyp (isolation and expansion under hypoxia, and differentiation under hypoxia), Hyp/Nrx (isolation and expansion under hypoxia, and differentiation under normoxia), Nrx/Hyp (isolation and expansion under normoxia, and differentiation under hypoxia), and Nrx/Nrx (isolation and expansion under normoxia, and differentiation under normoxia). Following culture, the tissue-engineered constructs were assessed with reverse-transcription quantitative polymerase chain reaction (RT-qPCR) for gene expression, histological staining of ECM proteoglycans, collagen II immunohistochemistry, and biochemical quantification of glycosaminoglycan (GAG) and deoxyribonucleic acid (DNA).

3.2.8 Reverse-transcription quantitative polymerase chain reaction analysis of chondrogenic genes

Total RNA was extracted from constructs using TRIzol Reagent (Life Technologies) after grinding with a pestle. In order to mitigate changes in gene expression, constructs under hypoxia and normoxia were immediately transferred

into TRIzol Reagent following removal from respective incubators. Total RNA (100 ng) in a 40-µl reaction was reverse transcribed to cDNA using GoScript Reverse Transcription System (Promega, Madison, USA) primed in the presence of oligo(dT) primers (1 µg). Quantitative PCR was performed with a DNA Engine Opticon II Continuous Fluorescence Detection System (Bio-Rad) using HotGoldStar Taq polymerase and SYBR Green detection (Eurogentec North America, San Diego, USA). Primer sequences (Table 3.2) were created using information from the National Center for Biotechnology Information (NCBI, Bethesda, USA) database and custom-designed using the Primer Express software (Applied Biosystems, Foster City, USA). All primers were obtained from Invitrogen (Life Technologies). Gene (messenger ribonucleic acid [mRNA]) expression levels for each primer set were normalized to the expression level of ovine beta-actin (β-actin) by the $2^{-\Delta\Delta C(T)}$ method [376].

RT-qPCR products were subsequently sequenced to confirm that expression levels were based on appropriate sequences for each gene. For sequencing, RT-qPCR products were purified using a QIAquick Gel Extraction Kit (Qiagen Canada, Toronto, Canada), combined with each primer – forward and reverse primers separately – and sequenced using the Sanger method (The Applied Genomics Centre, University of Alberta, Edmonton, Canada). The resulting traces were read using FinchTV Software Version 1.5 (Geospiza, Seattle, USA) and matched to corresponding regions within characterized gene

sequences using the nucleotide Basic Local Alignment Search Tool (BLAST, NCBI). Sequencing analysis is included within Appendix 1.

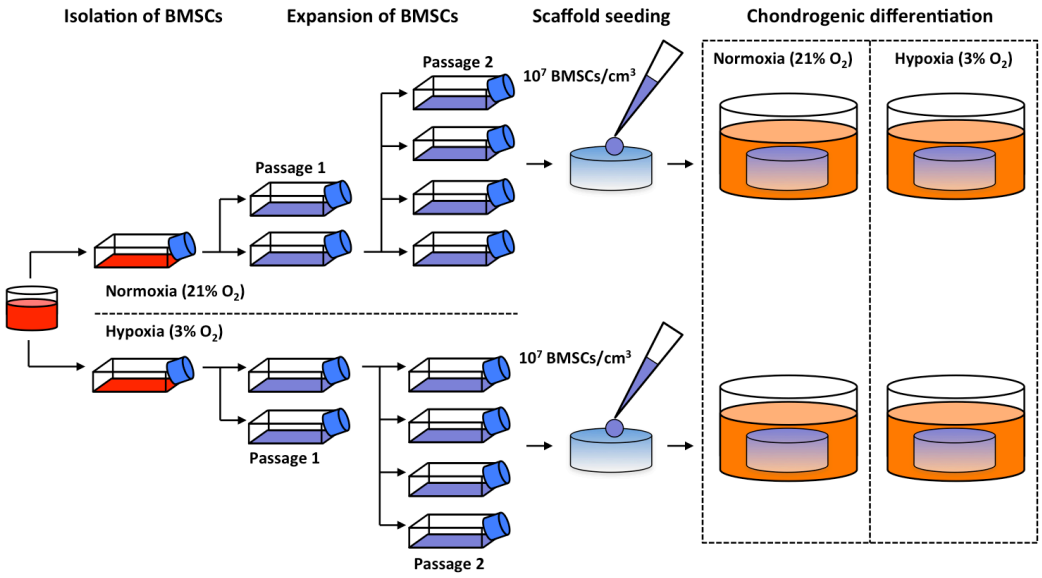

Figure 3.1 ***In vitro*** **cartilage engineering from bone marrow-derived mesenchymal stromal stem cell-seeded porous scaffolds.** Bone marrow-derived mesenchymal stromal stem cells (BMSCs) were isolated by plastic adherence from bone marrow aspirates and expanded in tissue culture flasks to passage two within defined expansion medium containing fetal bovine serum and fibroblast growth factor-two under either normoxic (21% oxygen) or hypoxic (3% oxygen) incubator conditions. Thereafter, BMSCs were seeded at 10 million cells/cm^3 onto clinically approved, cylindrical, porous scaffolds composed of collagen or hyaluronic acid. BMSC-scaffold constructs were subsequently cultured under either normoxia or hypoxia for 14 days within serum-free chondrogenic medium containing transforming growth factor-beta three and dexamethasone.

3.2.9 Histological and immunohistochemical analyses of extracellular matrix contents

Pellets and scaffold-based constructs were removed from media, fixed in 10% wt/vol buffered formalin (3.8% wt/vol formaldehyde), processed into paraffin wax, and sectioned at a thickness of 5 μm. Sections were stained with 0.1%

wt/vol safranin O to reveal proteoglycan matrix depositions, and counterstained with 1% wt/vol fast green. Other sections from scaffold-based constructs were treated with chondroitinase (Sigma-Aldrich Corp.) at 0.2 units per section and incubated with an antibody against collagen II (II-II6B3 from Developmental Studies Hybridoma Bank at University of Iowa, Iowa City, USA; 1:50 dilution).

Table 3.2 Ovine primer sequences used in reverse-transcription polymerase chain reaction analysis

Gene	Primer sequences		NCBI Reference
β-actin (*ACTB*)	5'-CGGCGGGACCACCAT-3'	Forward	NM_001009784.1
	5'-GCAGTGATCTCTTTCTGCATCCT-3'	Reverse	
Aggrecan (*ACAN*)	5'-TGGAATGATGTCCCATGCAA-3'	Forward	XM_004018048.1
	5'-GCCACTGTGCCCTTTTTACAG-3'	Reverse	
COMP (*COMP*)	5'-CCTAACTGGGTGGTGCTCAAC-3'	Forward	XM_004009150.1
	5'-CTGGGTCGCTGTTCATCGT-3'	Reverse	
Collagen I (*COL1A1*)	5'-CGCCCCAGACCAGGAATT-3'	Forward	XM_004012773.1
	5'-GTGGAAGGAGTTTACAGGAAGCA-3'	Reverse	
Collagen II (*COL2A1*)	5'-ACCTCACGTCTCCCCATCA-3'	Forward	XM_004006408.1
	5'-CTGCTCGGGCCCTCCTAT-3'	Reverse	
Collagen X (*COL10A1*)	5'-CAGGCTCGAATGGGCTGTAC-3'	Forward	XM_004011185.1
	5'-CCACCAAGAATCCTGAGAAAGAG-3'	Reverse	
SRY-Box 9 (*SOX9*)	5'-GCTGCTGGCCGTGATGA-3'	Forward	XM_004013527.1
	5'-GGGTCGCGCGTTTGTTT-3'	Reverse	

Immune-localized antigens were visualized with horse anti-mouse IgG biotinylated secondary antibody (Vectastain, Vector Laboratories Inc., Burlingame, USA) and an aminoethylcarbazole (AEC)-based peroxidase labeling kit (Enzo Life Sciences, Farmingdale, USA). Images were captured using an

Eclipse Ti-S microscope (Nikon Canada, Mississauga, Canada) fitted with NIS Elements Basic Research Imaging Software Version 4.20 (Nikon Canada, Inc.) and assembled in Photoshop (Adobe Systems, San Jose, USA).

3.2.10 Biochemical analysis of glycosaminoglycan and deoxyribonucleic acid quantity

In vitro cultured BMSC-scaffold constructs were rinsed in PBS and digested in proteinase K (1 mg/ml in 50 mM Tris with 1 mM EDTA, 1 mM iodoacetamide and 10 mg/ml pepstatin A; all from Sigma-Aldrich Corp.) for 16 hours at 56°C. Sulfated glycosaminoglycan (GAG) content was measured by 1,9-dimethylmethylene blue binding (Sigma-Aldrich Corp.) using chondroitin sulfate (Sigma-Aldrich Corp.) as the standard. Deoxyribonucleic acid (DNA) content was determined using the CyQUANT Cell Proliferation Assay Kit (Life Technologies) with supplied bacteriophage λ DNA as the standard.

3.2.11 Analysis of cell-scaffold construct size

To characterize changes in diameter with culture time, BMSC-seeded scaffolds (five per donor) were photographed with a high-quality digital camera after 7 and 14 days of *in vitro* chondrogenic culture. Each image was evaluated for diameter changes as previously described [377, 378]. The diameter of each scaffold was measured in four separate planes with ImageJ software (National Institutes of Health, Bethesda, USA), and the resulting mean diameter was expressed as a percentage change from the initial diameter at the time of seeding [377].

3.2.12 Statistical analysis

Analyses were performed using SPSS Statistics 22 (IBM, Armonk, USA) and significance was concluded when $p<0.05$. Proliferation analyses utilized a repeated measures analysis of variance (ANOVA) for BMSC count and doublings over time, while a t-test was used for assessment of these parameters on specific culture days. CFU-F analysis involved a Mann-Whitney U test for assessment of colony count and diameter. For analyses of gene expression and biochemical quantities, a Kruskal-Wallis one-way ANOVA was used to determine differences between the four experimental groups with pairwise (post-hoc) comparisons, while a Mann-Whitney U test was used for pooled analyses. For analysis of construct diameter, a repeated measures ANOVA was used to determine differences between the four experimental groups over time, whereas a t-test was used for pooled analysis at each time point.

3.2.13 Ethical considerations

All experiments were implemented with BMSCs isolated from bone marrow aspirates taken from adult sheep following ethical approval from the University of Alberta's Animal Care and Use Committee.

3.3 Results

3.3.1 Hypoxic isolation and expansion may enhance bone marrow-derived mesenchymal stromal stem cell proliferation

Similar cell counts were found for hypoxia- and normoxia-expanded BMSCs throughout the expansion period ($p=0.60$, Figure 3.2A). At the end of P2, there were 26.5 ± 3.6 million BMSCs and 23.2 ± 4.7 million BMSCs yielded from each T150 flask plated at P0 and expanded under hypoxia and normoxia, respectively. Five of six donors had higher BMSC counts under hypoxia (Figure 3.2A inset). However, mean values were not statistically different ($p=0.74$). Population doublings per day were highest at P0 and decreased significantly with subsequent passages ($p=0.02$; Figure 3.2B). Hypoxia-expanded BMSCs had higher population doublings per day than normoxia-expanded BMSCs throughout the expansion period ($p<0.05$). Cumulative population doublings were not different between groups ($p=0.67$; Figure 3.2C). Values of mean time (± SEM) between plating at P0 and 80% BMSC confluence at the end of P2 was 23.4 ± 0.8 days for normoxia-expanded BMSCs and 25.3 ± 1.5 days for hypoxia-expanded BMSCs ($p=0.38$).

A CFU-F assay was performed to determine the effect of oxygen tension on colony forming characteristics of adherent BMSCs isolated from plated MNCs and cultured in expansion medium under normoxia and hypoxia. Colony counts and diameters were assessed at the end of P0 when corresponding BMSCs undergoing expansion in T150 flasks had reached 80% confluence (16.3 ± 0.5

days of culture). Seeded petri dishes from one donor (Z01) lacked colony formation over this period. Hypoxic isolation/expansion augmented BMSC colony counts in petri dishes seeded with cells from four of the remaining five donors (Figures 3.3A-J), although there was not a significant difference in mean colony counts between the groups (p=0.30 for triplicate dishes and p=0.22 for best-growth dishes; Figures 3.3K-L).

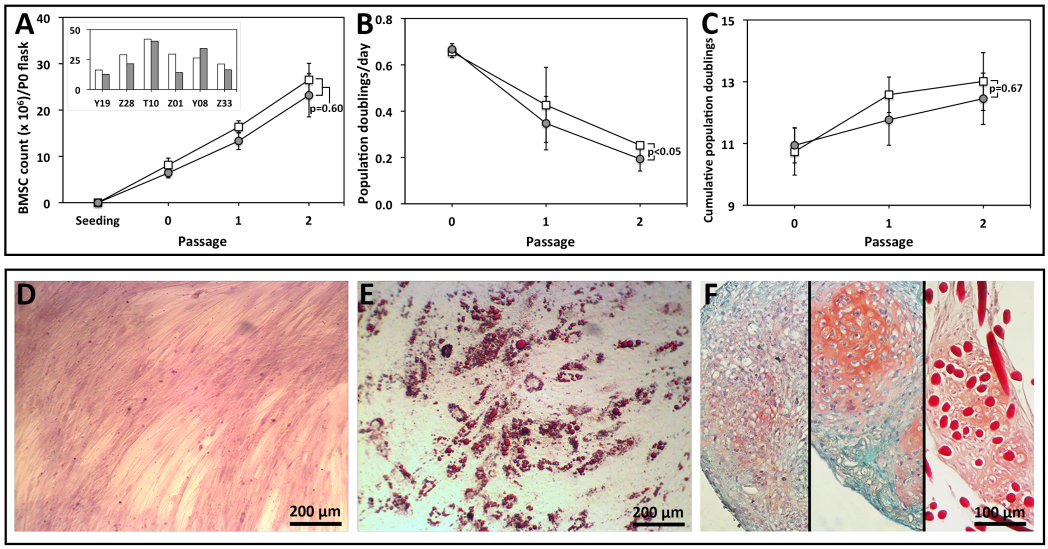

Figure 3.2 Proliferation and trilineage differentiation of bone marrow-derived mesenchymal stromal stem cells. (A) Cell counts, (B) population doublings per day, and (C) cumulative population doublings at each passage during expansion of bone marrow-derived mesenchymal stromal stem cells (BMSCs) under normoxia and or hypoxia. Data points represent mean ± standard error of the mean of cells from six donors, with p-values listed. (D) Osteogenic differentiation of BMSCs verified with Alizarin Red S staining following expansion under hypoxia and monolayer culture within medium containing beta-glycerophosphate, dexamethasone and fetal bovine serum (FBS; 5× combined magnification of objective and camera lenses). (E) Adipogenic differentiation of BMSCs verified with Oil Red O staining following expansion under hypoxia and monolayer culture within medium containing 3-isobutyl-1-methylxanthine, indomethacin, dexamethasone, and FBS (5× magnification). (F) Chondrogenic differentiation of BMSCs verified by safranin O staining following expansion under hypoxia and culture performed in pellets (left) or scaffolds composed of collagen (middle) or hyaluronic acid (right) submersed in a defined serum-free chondrogenic medium (10× magnification).

Crystal violet staining of adherent cells in hypoxia- and normoxia-cultured dishes showed the presence of a spectrum of cell morphologies ranging from long, spindle-shaped cells to circular and cuboidal cells (Figures 3.3M-N). No difference was noted in colony diameter between culture groups (p=0.36; Figure 3.3L).

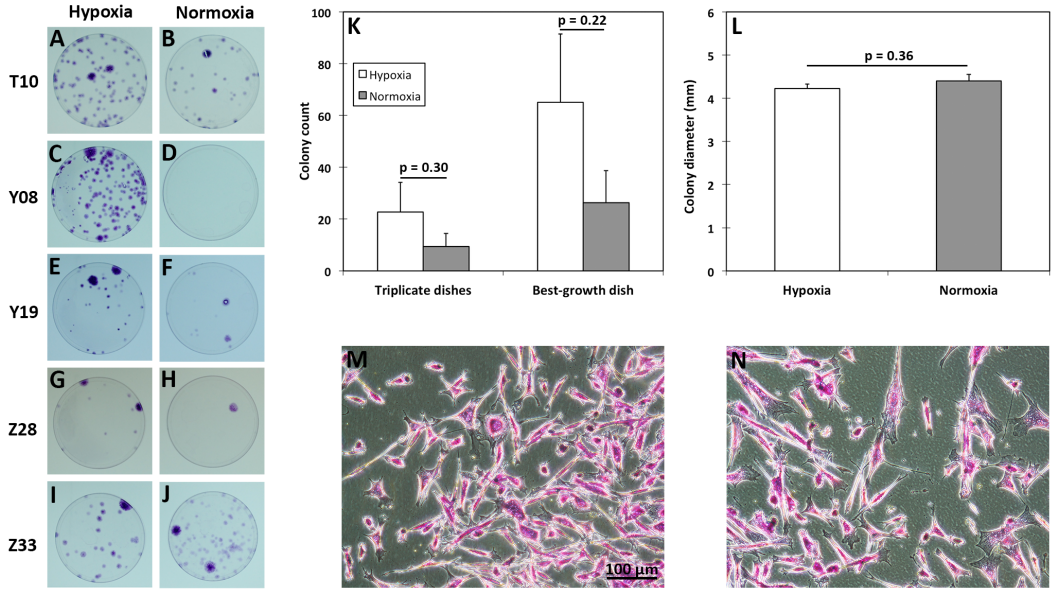

Figure 3.3 Colony-forming unit fibroblastic assay of bone marrow-derived mesenchymal stromal stem cells isolated and expanded under normoxia or hypoxia. (A-J) Plastic-adherent bone marrow-derived mesenchymal stromal stem cells (BMSCs) were isolated and expanded under hypoxia or normoxia, and formed colonies that were stained with crystal violet for visualization. Dishes seeded with cells from donor Z01 were excluded due to lack of colony formation. (K-L) Colony counts and diameters were measured and are reported as mean ± standard error of the mean, with p-values listed. Representative photomicrographs of adherent cells from donor Y19 formed under (M) hypoxic and (N) normoxic culture (14× combined magnification of objective and camera lenses).

3.3.2 Trilineage differentiation of adherent bone marrow-derived mesenchymal stromal stem cells

Plastic-adherent BMSCs were expanded to P2 and differentiated *in vitro* toward bone, adipose and cartilage tissue lineages to confirm multilineage potential [262]. Tissues derived from BMSCs stained extensively with Alizarin Red S (Figure 3.2D) and Oil Red O (Figure 3.2E), which confirmed the presence of bone and adipose matrix following culture in defined osteogenic and adipogenic media, respectively. Positive safranin O staining of sections from BMSC pellets and cell-seeded scaffolds following culture in chondrogenic medium supported the chondrogenic capacity of the adherent cells (Figure 3.2F).

3.3.3 Hypoxic isolation/expansion and differentiation augment chondrogenic gene expression differentially within bone marrow-derived mesenchymal stromal stem cell-seeded collagen and hyaluronic acid scaffolds

The impact of oxygen tension during isolation/expansion and differentiation on BMSC chondrogenic gene expression within collagen and HA scaffolds was assessed with RT-qPCR after 14 days of chondrogenic culture. For BMSC-seeded collagen scaffolds, Hyp/Hyp constructs had significantly higher aggrecan and collagen II mRNA expressions than Nrx/Nrx constructs ($p<0.05$; Figures 3.4A and D), while a trend was seen for cartilage oligomeric matrix protein (COMP) and collagen II/I ratio ($p=0.06$ and 0.09, respectively; Figure 3.4B). Collagen I, collagen X and sex determining region Y (SRY)-box 9 (SOX9) expressions and

the ratio of collagen II/X were not significantly different between oxygen tension groups ($p=0.20$, 0.31, 0.22, and 0.40 respectively; Figures 3.4C, E and F). Within HA scaffolds, Hyp/Hyp BMSCs had significantly higher aggrecan mRNA expression than Nrx/Nrx BMSCs ($p=0.009$; Figure 3.4A). COMP, collagen I, collagen II, collagen X, and SOX9 gene expressions, and the ratios of collagen II/I and collagen II/X were not significantly different between oxygen tension groups ($p=0.72$, 0.60, 0.13, 0.32, 0.99, 0.17, and 0.40 respectively; Figures 3.4B-F).

To further characterize the impact of oxygen tension on gene expression, data were pooled based on expansion oxygen tension and differentiation oxygen tension. BMSCs expanded under hypoxic conditions and seeded within collagen scaffolds produced significantly higher mRNA expression of collagen II and increased ratios of collagen II/I and collagen II/X than BMSCs expanded under normoxic conditions ($p<0.01$; Figure 3.4H). However, aggrecan expression was not significantly different between groups ($p=0.19$; Figure 3.4G). HA scaffolds seeded with BMSCs expanded under hypoxia produced significantly higher mRNA expression of aggrecan than BMSCs expanded under normoxia ($p=0.02$; Figure 3.4G). Collagen II mRNA expression and ratios of collagen II/I and collagen II/X were not significantly different ($p=0.31$ and 0.74, respectively; Figure 3.4H). Within both collagen- and HA-based constructs, oxygen tension during expansion did not significantly impact collagen I, collagen X, COMP, or SOX9 mRNA expression ($p\geq0.29$, 0.52, 0.14, and 0.16, respectively).

Pooling of data based on differentiation condition indicated that hypoxic differentiation also augmented chondrogenic gene expression. Collagen scaffolds seeded with BMSCs and differentiated under hypoxia had significantly higher aggrecan and collagen I mRNA expressions ($p=0.008$ and 0.03; Figure 3.4G), and approached statistically significant higher degrees of collagen II expression ($p=0.09$; Figure 3.4H). Collagen X mRNA expression was marginally lower with hypoxic differentiation ($p=0.06$). SOX9 and COMP mRNA expressions, and the ratios of collagen II/I and collagen II/X were not significantly different between groups ($p=0.20$, 0.02, 0.28 and 0.13, respectively). HA scaffolds seeded with BMSCs and differentiated under hypoxia had significantly higher mRNA expressions of aggrecan and collagen II ($p<0.05$; Figures 3.4G and H), and an increased collagen II/I ratio that approached significance ($p=0.09$). SOX9, COMP, collagen I, and collagen X mRNA expressions and the ratio of collagen II/X were not significantly different between hypoxic and normoxic differentiation ($p=0.62$, 0.28, 0.99, 0.31, and 0.13, respectively).

Scaffold composition modulated chondrogenic gene expression of BMSCs. BMSC-seeded collagen scaffolds had notably higher expressions of aggrecan, collagen II and SOX9 genes than BMSC-seeded HA scaffolds in the majority of oxygen tension groups ($p<0.05$; Figures 3.4A, D and F).

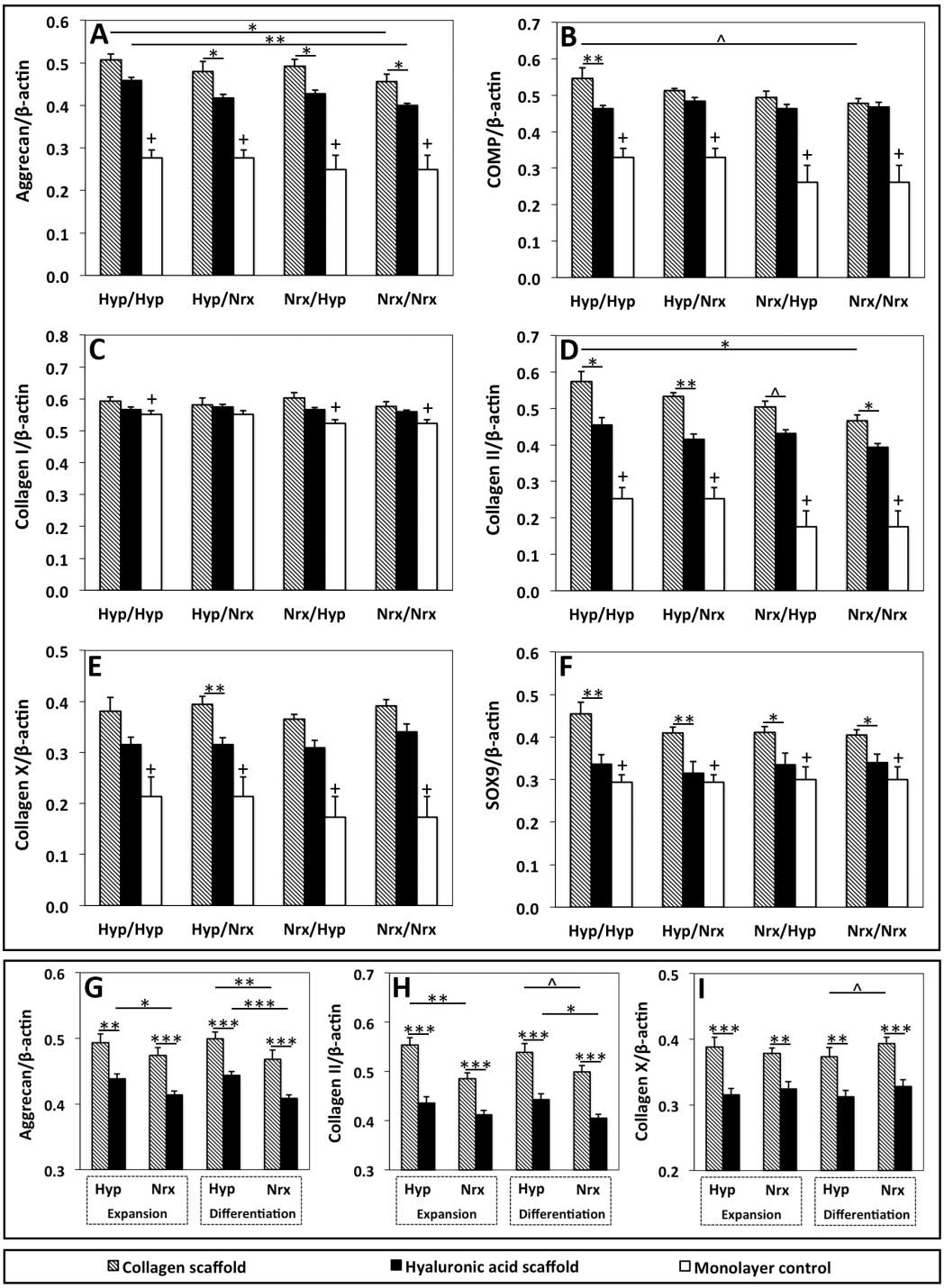

Figure 3.4 Gene expression within collagen and hyaluronic acid scaffolds seeded with hypoxia- and normoxia-cultured bone marrow-derived mesenchymal stromal stem cells. Bone marrow-derived mesenchymal stromal stem cells (BMSCs) were isolated/expanded under normoxia or hypoxia, seeded within collagen or hyaluronic acid scaffolds, and subsequently differentiated under normoxia or hypoxia for 14 days in chondrogenic medium. Reverse

transcription quantitative polymerase chain reaction (RT-qPCR) was performed using SYBR Green detection. (A-F) Data represent the mean ± standard error of mean (SEM) of constructs in doublets based on oxygen tension group. (G-I) Data represent mean ± SEM of constructs from the same donors pooled based on oxygen tension during isolation/expansion or differentiation. Statistical analysis is represented by unlabeled: not significant; ^: approaching significance p=0.05-0.10; *: significant p<0.05; **: significant p<0.01; ***: significant p<0.001; +: monolayer control value that is significantly different than BMSC-seeded scaffolds (p<0.05).

Within pooled data, BMSCs seeded within collagen scaffolds had augmented aggrecan, collagen II, SOX9, and collagen X gene expressions relative to BMSCs seeded within HA scaffolds regardless of expansion or differentiation oxygen tension ($p<0.01$; Figures 3.4G, H and I). Collagen I gene expression was not significantly different between scaffolds under hypoxic expansion, normoxic expansion or normoxic differentiation ($p\geq0.18$). However, under hypoxic differentiation, collagen I expression was significantly higher in BMSCs seeded within collagen scaffolds relative to HA scaffolds ($p=0.03$). COMP gene expression was significantly increased in BMSCs seeded on collagen scaffolds only when expansion and differentiation were performed under hypoxia ($p<0.01$).

3.3.4 Hypoxic isolation/expansion and differentiation enhance chondrogenic extracellular matrix deposition differentially within bone marrow-derived mesenchymal stromal stem cell-seeded collagen and hyaluronic acid scaffolds

Safranin O staining was used to assess ECM proteoglycan content within BMSC-seeded collagen and HA scaffolds after 14 days of chondrogenic differentiation (Figure 3.5). Within collagen scaffolds, ECM was deposited throughout areas of

the scaffold with portions containing intense proteoglycan staining noted in constructs that were exposed to hypoxia during the culture period. Widespread staining with safranin O was particularly seen in collagen scaffolds seeded with BMSCs that underwent hypoxic isolation/expansion prior to seeding (Hyp/Hyp and Hyp/Nrx). Hypoxic differentiation also appeared to promote proteoglycan deposition in constructs containing normoxia-expanded BMSCs (Nrx/Hyp). Immunohistochemistry verified the presence of collagen II within constructs that were exposed to hypoxia during isolation/expansion or differentiation (Figure 3.6). Collagen II content appeared to be most pronounced in constructs exposed to hypoxia throughout the culture period (Hyp/Hyp).

Within HA scaffolds, pockets of ECM were found around HA fibers, which led to the creation of patchy tissue after 14 days of culture (Figure 3.5). BMSCs that were isolated and expanded under hypoxia demonstrated the most pronounced safranin O staining (Hyp/Hyp and Hyp/Nrx). Although ECM was also noted within HA scaffolds seeded with BMSCs that underwent isolation/expansion under normoxia (Nrx/Hyp and Nrx/Nrx), these constructs lacked safranin O staining. Hypoxic differentiation appeared to augment proteoglycan content in hypoxia-expanded BMSC-seeded HA scaffolds (Hyp/Hyp) but not normoxia-expanded BMSC-seeded HA scaffolds (Nrx/Hyp). Immunohistochemistry revealed the presence of collagen II within ECM in constructs that were exposed to hypoxia during the culture period (Figure 3.6).

Quantitative GAG and GAG/DNA values were consistent with histological staining of ECM proteoglycans (Figures 3.7A and C). DNA quantities were not significantly different between oxygen tension conditions ($p=0.23$; Figure 3.7B). GAG production and GAG/DNA in Hyp/Hyp constructs were significantly higher than Nrx/Nrx constructs for BMSCs seeded on both collagen and HA scaffolds ($p<0.05$ and $p<0.01$, respectively; Figures 3.7A and C). GAG/DNA was also significantly higher in the Hyp/Nrx group than the Nrx/Nrx group regardless of scaffold type ($p<0.05$; Figure 3.7C). Data pooled based on expansion oxygen showed that hypoxic expansion improved GAG and GAG/DNA regardless of scaffold type ($p<0.01$; Figures 3.7D and F). Data pooled based on differentiation oxygen tension indicated no significant difference in GAG between hypoxic differentiation and normoxic differentiation for collagen- and HA-based constructs ($p=0.12$ and 0.45, respectively; Figure 3.7D). There was a trend for higher GAG/DNA in BSMC-seeded collagen scaffolds differentiated under hypoxia ($p=0.09$), and this effect was not seen in BMSC-seeded HA scaffolds ($p=0.59$; Figure 3.7F).

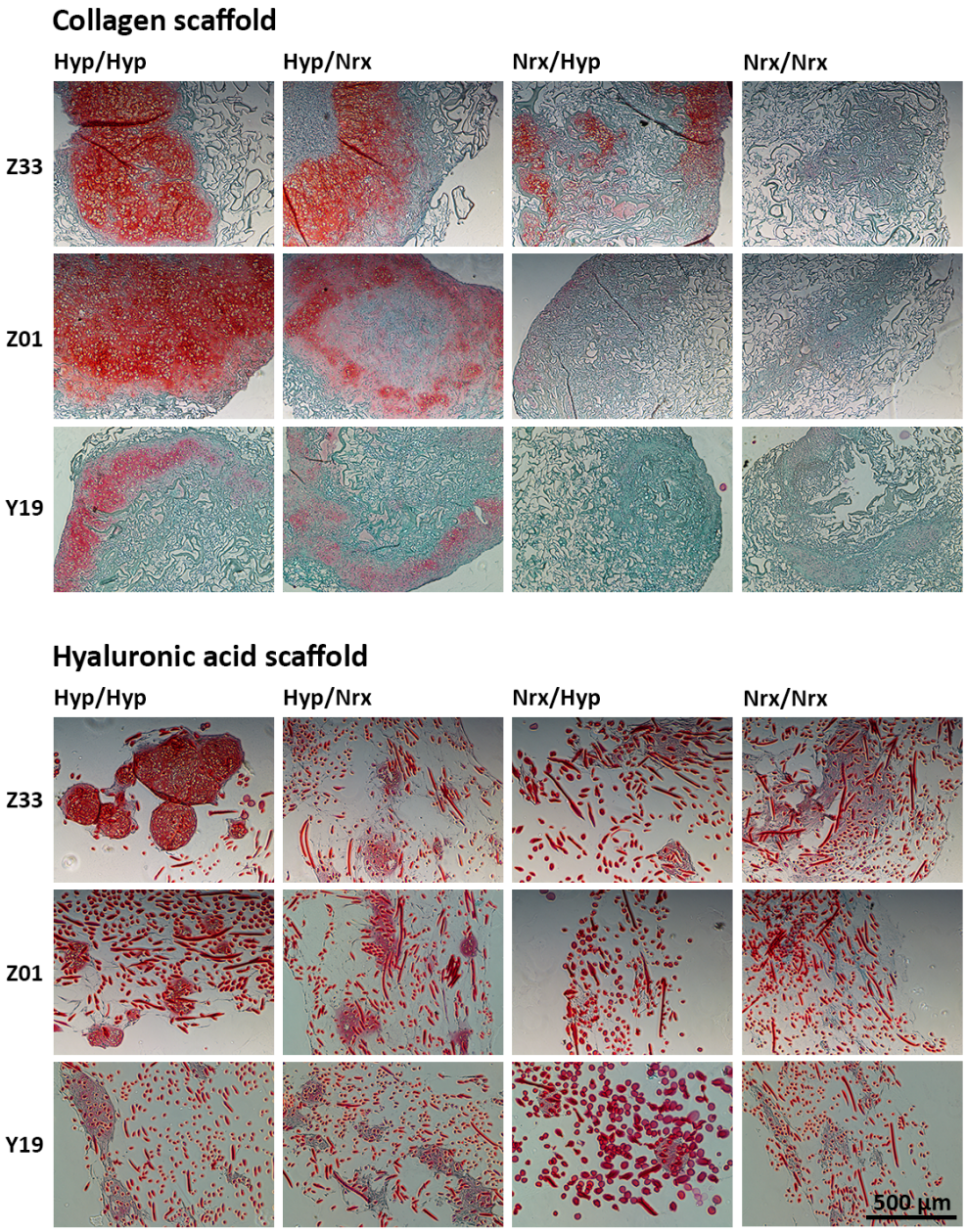

Figure 3.5 Histological analysis of chondrogenic proteoglycan content within collagen and hyaluronic acid scaffolds seeded with hypoxia- and normoxia-cultured bone marrow-derived mesenchymal stromal stem cells. Bone marrow-derived mesenchymal stromal stem cells (BMSCs) were isolated/expanded under normoxia or hypoxia, seeded within collagen or hyaluronic acid (HA) scaffolds, and subsequently differentiated under normoxia or hypoxia for 14 days in chondrogenic medium. Thereafter, constructs were sectioned at 5-µm thickness and stained with safranin O and fast green. Presented photomicrographs represent collagen and HA

acid scaffolds seeded with BMSCs from three donors (7× combined magnification of objective and camera lenses).

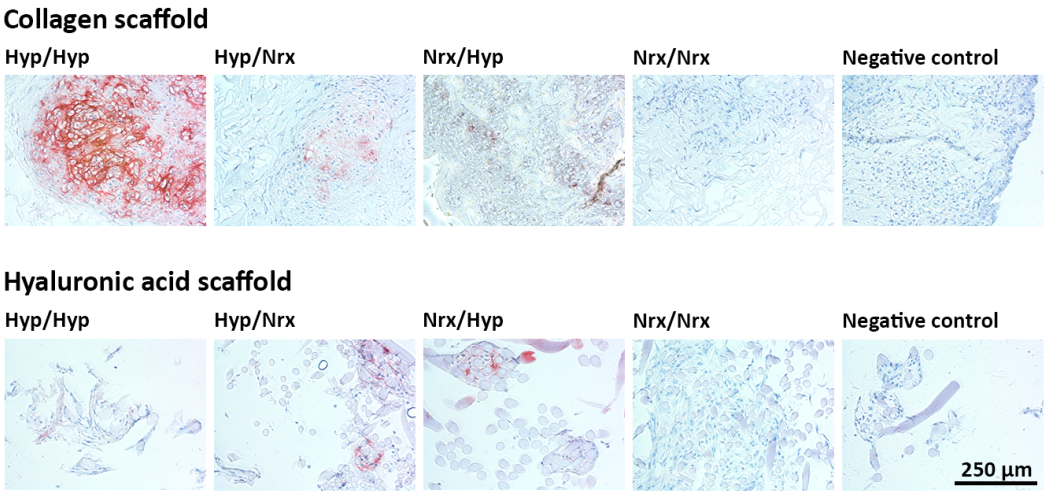

Figure 3.6 Immunohistochemical analysis of collagen II content within collagen and hyaluronic acid scaffolds seeded with hypoxia- and normoxia-cultured bone marrow-derived mesenchymal stromal stem cells. Bone marrow-derived mesenchymal stromal stem cells (BMSCs) were isolated/expanded under normoxia or hypoxia, seeded within collagen or hyaluronic acid (HA) scaffolds, and subsequently differentiated under normoxia or hypoxia for 14 days in chondrogenic medium. Thereafter, constructs were sectioned at 5-µm thickness and collagen II immunostaining was performed using an aminoethylcarbazole-based peroxidase labeling kit. Presented photomicrographs represent collagen and HA scaffolds seeded with BMSCs from donor Z33 (14× combined magnification of objective and camera lenses).

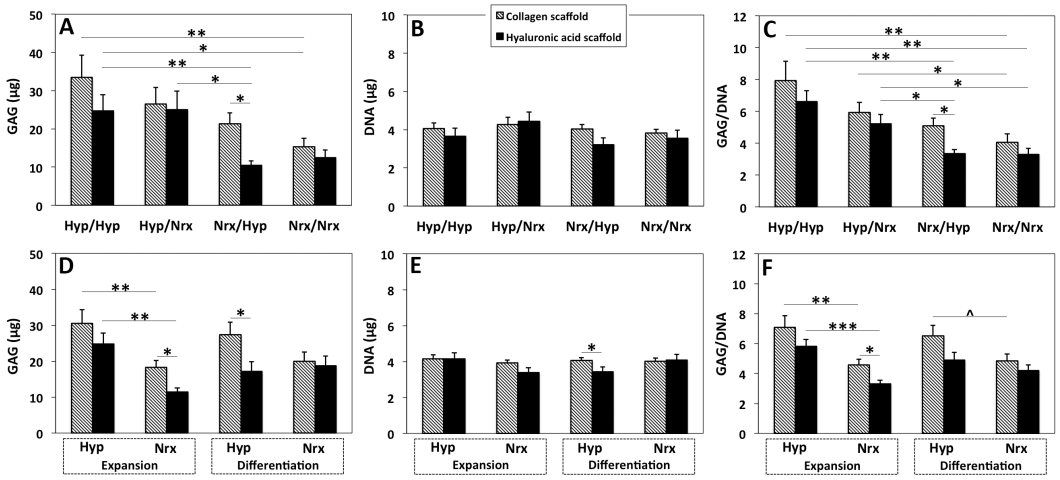

Figure 3.7 Glycosaminoglycan and deoxyribonucleic acid quantification of collagen and hyaluronic acid scaffolds seeded with hypoxia- and normoxia-cultured bone marrow-derived mesenchymal stromal stem cells. Bone marrow-derived mesenchymal stromal stem cells (BMSCs) were isolated/expanded under normoxia or hypoxia, seeded within collagen or hyaluronic acid (HA) scaffolds, and subsequently differentiated under normoxia or hypoxia for 14 days in chondrogenic medium. (A-C) Data represent the mean ± standard error of the mean (SEM) of glycosaminoglycan (GAG) quantity, deoxyribonucleic acid (DNA) quantity and GAG/DNA within constructs from five donors in doublets based on oxygen tension group. (D-F) Data represent mean ± SEM of constructs from the same donors pooled based on oxygen tension during expansion or differentiation. Statistical analysis is represented by unlabeled: not significant; ^: approaching significance p=0.05-0.10; *: significant p<0.05; **: significant p<0.01; ***: significant p<0.001.

Scaffold composition had a notable effect on ECM proteoglycan deposition. In a comparison of collagen and HA scaffold-based constructs within each oxygen tension group, a significant difference was seen only in the Nrx/Hyp group in which BMSC-seeded collagen scaffolds had higher GAG and GAG/DNA than BMSC-seeded HA scaffolds (p<0.05; Figures 3.7A and C). Collagen scaffolds that were seeded with normoxia-expanded BMSCs but switched to hypoxic conditions for differentiation (Nrx/Hyp) appeared to have

improved GAG/DNA relative to BMSCs that were exposed to sustained normoxic conditions (Nrx/Nrx; p=0.18; Figure 3.7C). This finding was supported by proteoglycans stained within BMSC-seeded collagen scaffolds (Figure 3.5). This effect was not seen in BMSC-seeded HA scaffolds, as Nrx/Hyp constructs had stunted GAG/DNA values that were statistically equivalent to Nrx/Nrx constructs (p=0.97), and significantly lower than Hyp/Hyp and Hyp/Nrx constructs (p<0.05; Figure 3.7C). Pooled data showed higher proteoglycan deposition by cells seeded on collagen scaffolds in comparison to HA scaffolds only when expansion was performed under normoxia (p=0.03 and 0.04 for GAG and GAG/DNA, respectively; Figures 3.7D and F), and when differentiation was performed under hypoxia (p=0.02 for GAG; Figure 3.7D).

3.3.5 Oxygen tension and scaffold composition modulate cell-scaffold construct size during chondrogenesis

Collagen scaffolds seeded with BMSCs displayed significant diameter contraction with time during chondrogenic culture (p<0.001) to 60.1 ± 8.8% of the initial diameter (Figure 3.8A). A significant difference was noted between oxygen tension groups at day 7 of culture for BMSC-seeded collagen scaffolds (p=0.004), but not at day 14 (p=0.64). Based on pooled analysis, collagen scaffolds seeded with BMSCs expanded under hypoxia had diameters that approached significantly larger values (mean ± SEM of 68.2 ± 1.0%) at day 7 than those seeded with BMSCs expanded under normoxia (65.0 ± 1.6%; p=0.09), This difference was abolished by day 14 with diameters of 60.3 ± 1.5% and 60.0 ±1.7, respectively (p=0.88; Figure 3.8C). BMSC-seeded collagen scaffolds that were differentiated

under hypoxia were more contracted (64.6 ± 1.3%) than BMSC-seeded scaffolds differentiated under normoxia at day 7 (68.5 ± 1.4%; p=0.04), but a significant difference was not present by day 14 (61.2 ± 1.7% and 59.1 ± 1.6%; p=0.36).

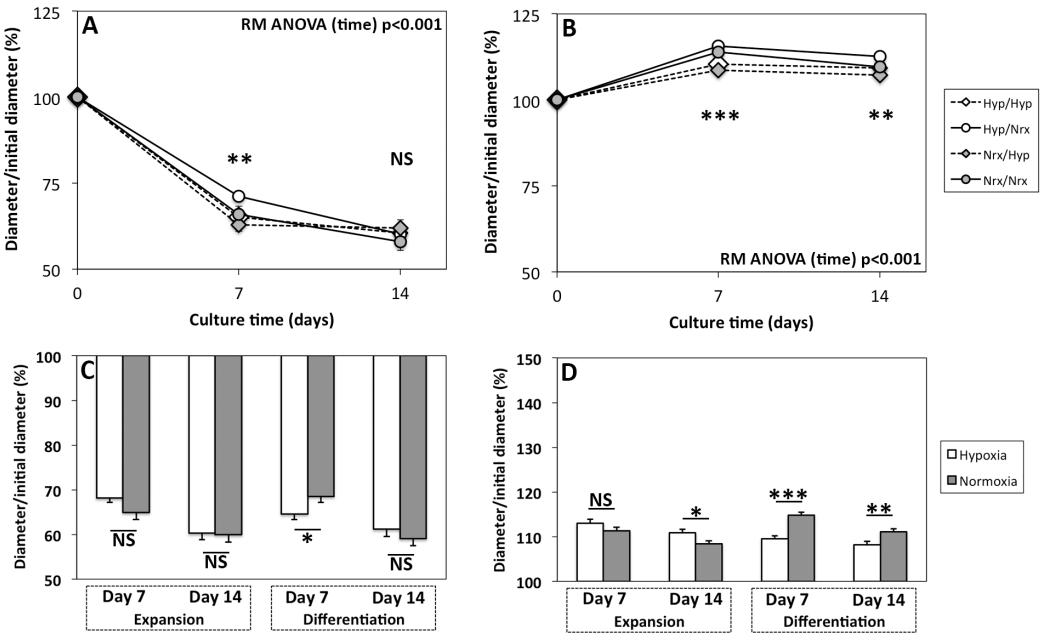

Figure 3.8 Cell-seeded scaffold diameter during chondrogenesis. Bone marrow-derived mesenchymal stromal stem cells (BMSCs) were isolated/expanded under normoxia or hypoxia, seeded within collagen or hyaluronic acid (HA) scaffolds, and subsequently differentiated under normoxia or hypoxia for 14 days in chondrogenic medium. Construct diameter was assessed using high-quality digital photography and ImageJ software. Data represent the mean ± standard error of the mean (SEM) of constructs containing (A) collagen scaffolds or (B) HA scaffolds seeded with BMSCs from three donors (five constructs per donor) based on oxygen tension group. Data were pooled based on oxygen tension during expansion or differentiation for (C) collagen scaffolds and (D) HA scaffold seeded with BMSCs. Statistical analysis is represented by NS: not significant; *: significant $p<0.05$; **: significant $p<0.01$; ***: significant $p<0.001$.

In contrast to collagen scaffold-based constructs, HA scaffold-based constructs increased in size to 109.7 ± 4.2% of the initial diameter ($p<0.001$; Figure 3.8B). A significant difference was noted between oxygen tension groups at day 7 and day 14 ($p\leq0.003$). Based on pooled analysis, expansion oxygen tension affected HA scaffolds similarly to collagen scaffolds (Figure 3.8D). Although there was not a significant difference between hypoxia- and normoxia-expanded BMSC-seeded scaffolds at day 7 (113.0 ± 0.8% and 111.3 ± 0.9%, respectively; $p=0.15$), an effect became statistically significant by day 14 in which hypoxic expansion led to increased diameters relative to normoxic expansion (110.9 ± 0.7% and 108.4 ± 0.8, respectively; $p=0.02$). Like BMSC-seeded collagen scaffolds, BMSC-seeded HA scaffolds that were differentiated under hypoxia were more contracted (109.5 ± 0.7%) than BMSC scaffold differentiated under normoxia at day 7 (114.8 ± 0.7%; $p<0.001$). This effect was also seen at day 14 (108.2 ± 0.7% vs. 111.1 ± 0.7%; $p=0.006$).

3.4 Discussion

The major findings of this study are incubation of ovine BMSCs under hypoxia (3% oxygen) during isolation/expansion and differentiation enhanced *in vitro* chondrogenesis within clinically approved porous collagen I and esterified HA scaffolds, and porous scaffold composition impacted the effect of oxygen tension on chondrogenesis in this *in vitro* model.

Enhancement of chondrogenesis by hypoxic culture was elucidated in BMSC-seeded porous scaffolds, which is an important finding given that cell-seeded scaffolds are used routinely as three-dimensional models of *in vitro* chondrogenesis and clinically in cell transplantation protocols for treatment of cartilage defects [194, 363]. It was shown that chondrogenesis could be promoted with hypoxic exposure during distinct isolation/expansion and differentiation conditions. Although oxygen tension during distinct isolation/expansion and differentiation periods was previously studied in detail within pellet and hydrogel models in three studies, the results were inconsistent and warranted further investigation [332, 370, 373]. In the study at hand, hyaline chondrogenic gene expression of BMSC-seeded porous scaffolds was enhanced with hypoxic exposure during both isolation/expansion and differentiation. This is consistent with our previous findings in a human BMSC pellet model [332]. ECM proteoglycan and collagen II deposition was significantly improved with hypoxic isolation/expansion based on histological and biochemical analyses, whereas the impact of hypoxic differentiation appeared to be less pronounced in this study. Although this finding was also demonstrated previously in human BMSC pellets [332], others have reported highly significant findings following hypoxic differentiation in human BMSC pellet [373] and porcine BMSC pellet and hydrogel models [370]. Differences in the effect of hypoxic differentiation between studies could relate to variations in species, duration of incubation, and/or culture protocols.

BMSC proliferation was also examined and it was found that hypoxic isolation and expansion to P2 only modestly improve BMSC proliferation. Increased population doublings per day were noted with hypoxic exposure. However, BMSC counts at each passage, cumulative population doublings and CFU-F colony counts were not significantly different between oxygen tension groups. These results are consistent with previous work that showed non-significant differences during early passages and enhanced proliferation under hypoxia only with prolonged expansion beyond P2 [367, 368].

Collagen and HA porous scaffolds were assessed in this study given that these biomaterials are commonly used in cartilage engineering applications and clinical BMSC transplantation [43, 45, 254, 318]. Both scaffolds were capable of fostering gene expression and ECM formation consistent with hyaline-like cartilage from BMSCs cultured *in vitro*. Chondrogenesis on collagen and HA scaffolds was responsive to oxygen tension. However, differences were noted between scaffolds in BMSC gene expression, ECM deposition and construct size during differentiation. BMSCs seeded and cultured within collagen scaffolds had higher expressions of aggrecan, collagen II and SOX9 mRNA than BMSCs within HA scaffolds regardless of oxygen tension, which suggests that BMSC differentiation on collagen increases the expression of genes associated with hyaline cartilage relative to the HA. However, BMSCs within collagen scaffolds also had higher mRNA expression of collagen X regardless oxygen tension, and higher expression of collagen I under hypoxic differentiation. These findings

suggest that culture on an HA scaffold could modulate gene expression more favourably for hyaline cartilage regeneration by reducing the expression of collagens I and X, which are associated with fibrocartilage and hypertrophic cartilage [379, 380], while maintaining the expression of genes associated with hyaline cartilage. Differences between scaffolds were not as pronounced for ECM deposition as gene expression. In most oxygen tension groups, proteoglycan content was not significantly different between collagen- and HA-based constructs. BMSC-seeded collagen scaffolds had higher proteoglycan deposition specifically when expansion was performed under normoxia and differentiation was performed under hypoxia. Hypoxic differentiation appeared to partially reverse dampening of chondrogenesis by normoxic isolation/expansion on BMSC-seeded collagen scaffolds but not on BMSC-seeded HA scaffolds.

The underlying mechanisms for modulation of chondrogenic gene expression and tissue formation by scaffold type were not elucidated in this study but warrant further investigation. BMSCs interact with collagen scaffolds via integrins, and HA scaffolds through CD44 [381, 382]. Scaffold characteristics such as stiffness, biomaterial topography and pore dimension presumably alter intracellular signaling and subsequent processes related to chondrogenesis through these cell-surface proteins [380]. Matrix stiffness was found previously to regulate BMSC differentiation and tissue formation [349]. Topographical factors such as scaffold fiber alignment and nanoscale surface features have been shown to influence cell lineage commitment [383, 384]. Furthermore, content, size and

orientation of scaffold pores appear to affect BMSC differentiation [385, 386]. Porosity alters oxygen diffusion through scaffolds, which could also modulate chondrogenesis through the creation of oxygen gradients [387].

BMSC-scaffold construct diameter was investigated during culture given that fluctuations in construct size occur with tissue formation and remodeling, and ultimately impact the suitability for constructs for implantation *in vivo*. Size was maintained during culture in BMSC-seeded HA scaffolds, while BMSC-seeded collagen scaffolds exhibited progressive contraction with time. Variation in size presumably involves a balance of cell-scaffold interactions, biomaterial chemistry, scaffold degradation, and ECM formation. Cell-mediated contraction that occurs through smooth muscle actin has been described in detail within collagen-based constructs [388]. HA is hydrophilic and may promote increased scaffold swelling through water absorption relative to collagen I[375]. Biomaterial degradation, hydrolysis or fragmentation may reduce the size of a construct if an adequate amount of ECM has not been deposited by the time that these processes occur [375, 389, 390]. In the study at hand, it is not known how scaffold size affected chondrogenesis, although collagen scaffold contraction presumably led to increased cell density per volume of scaffold, which could have modulated cell-cell interactions and increased chondrogenesis [391]. It is also possible that contraction inhibited chondrogenesis, as it was shown previously that contraction may promote differentiation to a fibroblastic lineage [392, 393]. Given that esterified HA scaffold size was maintained, the findings of this study

suggest that, in a clinical setting, implantation of BMSCs on an esterified HA scaffold could promote better early cartilage defect filling than on a collagen scaffold.

Construct size was also affected by incubator oxygen tension. Both collagen and HA scaffold seeded with BMSCs had increased diameters when BMSC isolation and expansion were performed under hypoxia, and differentiation was performed under normoxia. Various mechanisms could be involved including modulation of cell-mediated contraction through smooth muscle actin and cytoskeletal alteration [388], ECM proteoglycan formation [332, 394], crosslinking via lysyl oxidase [395], or degradation through matrix metalloproteinases [396].

This study has some limitations. Although two defining criteria of mesenchymal stem cells – plastic adherence and multipotential differentiation – were confirmed, determination of cell surface antigens was not performed to fulfill the third criterion of the Mesenchymal and Tissue Stem Cell Committee [262]. This third criterion was omitted because the study at hand involved an identical method of BMSC isolation and expansion described in our previous work, which included flow cytometric analysis of cell surface markers [332]. Secondly, the findings of this study demonstrate enhanced *in vitro* chondrogenesis with hypoxic culture, although it is still not clear whether *in vitro* hypoxic culture improves chondrogenesis following implantation within cartilage defects and

prolonged *in vivo* exposure to joint elements. Joints have been shown to be hypoxic, and it is possible that this characteristic could promote *in vivo* chondrogenesis regardless of the *in vitro* culture conditions prior to construct implantation [366]. Lastly, ovine rather than human BMSCs were utilized in this study. Although sheep are routinely used as animal models in cartilage engineering studies [100, 274, 369], differences between species could impact the clinical applicability of our findings.

3.5 Conclusion

BMSCs seeded on clinically relevant collagen I and esterified HA porous scaffolds displayed enhanced *in vitro* chondrogenesis with hypoxic incubation during distinct isolation/expansion and differentiation culture periods. Hypoxic culture of BMSCs may therefore play a role in improving cartilaginous tissue formation following transplantation of BMSC-seeded scaffolds. Both collagen I and esterified HA scaffold supported the creation of hyaline-like engineered cartilage. However, differences were noted in chondrogenic gene expression, ECM deposition, and cell-scaffold construct size during differentiation that could impact the choice of biomaterial for use in BMSC transplantation protocols.

Chapter 4

Hypoxic Expansion of Bone Marrow-Derived Mesenchymal Stem Cells: a Novel Method of Offsetting Cell-Mediated Collagen Scaffold Contraction in Cartilage Engineering

Troy D. Bornes, Nadr M. Jomha, Aillette Mulet-Sierra, Leila Laouar, Lauren A. Beaupre and Adetola B. Adesida

This chapter has been submitted for publication.

4.1 Introduction

Mesenchymal stem cell (MSC) transplantation is a promising cell-based option for treating cartilage defects given the high proliferative capacity of MSCs and their ability to differentiate into chondrocytes without requiring major surgical intervention for harvesting [32-34]. MSCs are commonly seeded within biomaterial porous scaffolds or hydrogels that aid cell delivery during transplantation and support chondrogenic differentiation, extracellular matrix formation and three-dimensional (3D) neo-tissue development [35]. Collagen-based scaffolds are in widespread clinical use due to the natural occurrence of collagen in articular cartilage, propensity for cellular attachment, minimal

immunoreactivity, and success of this construct in producing hyaline-like cartilage *in vivo* in animals and humans[39, 41, 43, 56, 274, 318, 397].

A major drawback of collagen-based biomaterials is cell-mediated contraction [377, 378, 388, 398] that presumably precludes integration of neo-tissue constructs within adjacent native cartilage and promotes construct delamination. Seeded scaffolds that maintain their implantation position within defects but contract may remain separated from native cartilage leading to the formation of gaps and uneven articular surfaces. Lack of complete defect filling and integration, some of which could be related to scaffold contraction, has been noted on post-operative magnetic resonance imaging (MRI) [41]. Gaps between implants and native cartilage may also fill with fibrocartilage in a similar fashion to the spaces between cylindrical osteochondral autografts in mosaicplasty [158]. Repair tissue containing varying amounts of fibrocartilage has been noted on histologic assessment following implantation of MSC-seeded collagen scaffolds [41, 43]. This may be problematic given that fibrocartilage possesses inferior mechanical properties to hyaline cartilage [1]. Delamination of cell-seeded biomaterial scaffolds from cartilage defects has been reported in both animal and human studies [233, 399].

Various techniques to offset cell-mediated contraction of collagen scaffolds have been proposed and tested using *in vitro* models. They involve either scaffold alteration or cellular modulation. Scaffold clamping, biomaterial

crosslinking with various techniques and inhibition of cellular smooth muscle actin (SMA) have all been shown to reduce cell-mediated contraction [377, 378, 398, 400, 401]. Although these modalities have successfully reduced contraction *in vitro*, a number of adverse effects have been reported. Clamping decreases glycosaminoglycan (GAG) production [378]. Crosslinking with DHT and UV are associated with increased susceptibility of matrices to degradation by certain proteases [402]. Carbodiimide inhibits adhesion of cells to scaffolds and chondrogenesis [398]. Glutaraldehyde is cytotoxic and may bind to scaffold materials and release into bioengineered tissue during scaffold degradation [403, 404]. The negative impact of decreased SMA expression on cytoskeleton function, cellular processes and articular cartilage are unclear [401]. Consequently, the development of a contraction-reducing technique that minimizes these adverse effects and is compatible with *in vivo* implantation is quite relevant to the optimization of MSC transplantation.

The first objective of this study was to characterize contraction of bone marrow-derived MSC-seeded porous collagen scaffolds in detail during *in vitro* culture over 30 days. The effect of oxygen tension during MSC expansion on collagen scaffold contraction was investigated with the aim of developing a novel technique of reducing cell-mediated contraction. It was previously demonstrated by our group that human and ovine MSCs isolated and expanded under hypoxic conditions exhibited improved chondrogenesis and produced an augmented level of extracellular proteoglycans relative to MSCs isolated and expanded under

normoxia during *in vitro* culture (Chapter 3) [332, 405]. Given that enhanced proteoglycan content following hypoxic isolation and expansion of MSCs presumably increases water absorption and swelling pressure [394], it was hypothesized that MSC-seeded collagen scaffolds would display reduced contraction when BMSCs were isolated and expanded under hypoxic conditions.

The second objective of this study was to evaluate cartilage tissue formation, defect filling and integration of hypoxia-expanded MSC-seeded collagen scaffolds that were inserted within full-thickness cartilage defects in an osteochondral explant model. MSC-seeded scaffolds were inserted either immediately following seeding or after 21 days of *in vitro* precultivation. Precultivation allows for chondrogenic differentiation of MSCs to occur in an *in vitro* setting with the formation of neo-tissue containing functionally relevant extracellular matrix (ECM) prior to insertion [406]. Previously, precultivated MSC-seeded collagen gels were found to produce superior cartilage repair tissue after 6 months compared to scaffolds implanted immediately following seeding in the knee joint of sheep [274, 308]. Consequently, we hypothesized that precultivation of constructs seeded with hypoxia-expanded MSCs would support the creation of higher quality hyaline-like cartilaginous neo-tissue over a 21-day post-insertion *ex vivo* culture period than constructs inserted immediately following scaffold seeding. It was also proposed that improved integration with explant cartilage would be noted with precultivated scaffolds that were oversized at the time of seeding to account for contraction during the precultivation period.

4.2 Methods

4.2.1 Isolation and expansion of mesenchymal stem cells

Bone marrow-derived cell collections for our study were obtained from surgically discarded material from the iliac crest of nine male human donors (mean age ± standard error of the mean [SEM] of 41.0 ± 4.6 years, range of 20-56 years). The number of nucleated cells in the aspirates was determined by crystal violet nuclei staining and cell counting using a hemocytometer. Fifteen million mononucleated cells (MNCs) were seeded within each 150-cm^2 tissue-culture flask. Culture medium composed of alpha-minimal essential medium (α-MEM) supplemented with 8.8% heat-inactivated fetal bovine serum, penicillin-streptomycin-glutamine, 4-(2-hydroxyethyl)-1-piperazineethanesulfonic acid (HEPES), and sodium pyruvate (all from Life Technologies, Burlington, Canada) was pipetted into each flask (Appendix 1). Fibroblast growth factor-2 (FGF-2; Neuromics, Edina, USA) was added at a concentration of 5 ng/ml in order to maintain cell multipotency.

MNCs were allowed to adhere and grow for seven days before the first media change under normoxia (ambient oxygen tension of 21%) or hypoxia (low oxygen tension of 3%) at 37°C in a humidified incubator with 5% carbon dioxide. Flasks from the hypoxic incubator experienced short periods (<5 minutes) of re-oxygenation during media changes. Thereafter, the media were changed twice per week until 80% cell confluence was obtained. Adherent bone marrow-derived MSCs were detached using 0.05% trypsin-ethylenediaminetetraacetic acid

(EDTA; Sigma-Aldrich, Oakville, Canada) and expanded under the same oxygen tension (normoxia or hypoxia) as during isolation until passage two (P2) prior to experimental use. The time taken from plating of nucleated cells (P0) to reach approximately 80% confluence at P2, before experimental use, varied from three to four weeks. The experimental set-up for MSC isolation, expansion and chondrogenic differentiation is illustrated in Figure 4.1.

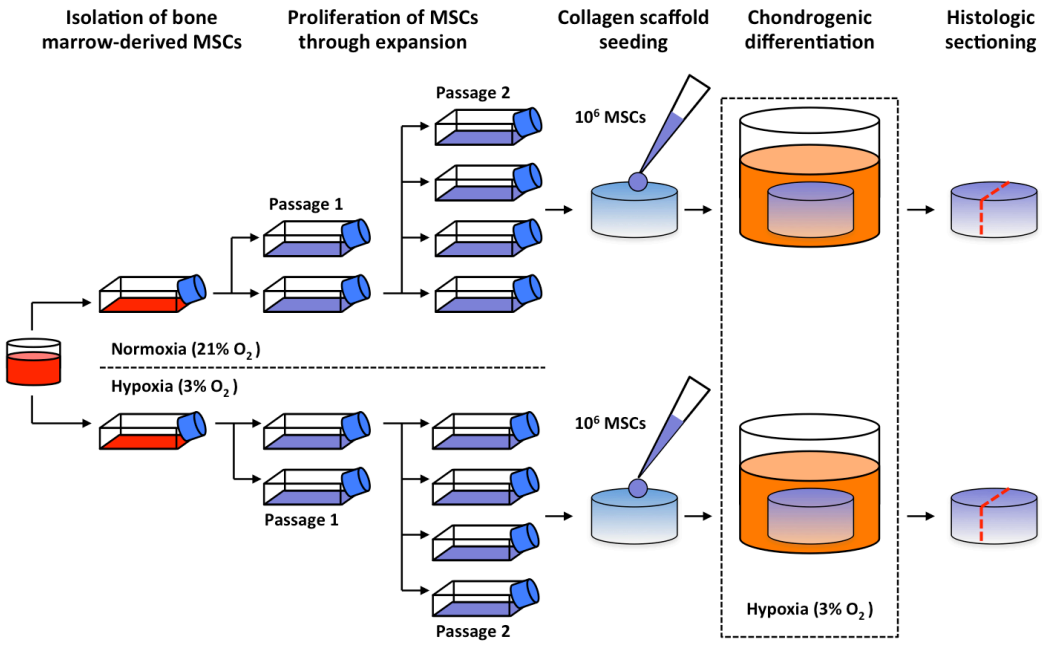

Figure 4.1 Cartilage engineering from mesenchymal stem cells and collagen scaffolds. Mesenchymal stem cells (MSCs) were isolated by plastic adherence from bone marrow aspirates and expanded in tissue-culture flasks to passage two within defined medium containing serum and fibroblast growth factor-two under either normoxic (21% oxygen) or hypoxic (3% oxygen) incubator conditions. Thereafter, one million MSCs were seeded onto cylindrical, porous, type I collagen scaffolds with diameters of 6-12 mm. MSC-scaffold constructs were subsequently cultured under hypoxia within serum-free chondrogenic medium containing transforming growth factor-beta three. After 21 days of culture, some scaffolds were processed and sectioned longitudinally for histologic analysis.

4.2.2 Collagen scaffold seeding and culture of mesenchymal stem cells

Cylindrical scaffolds were created using biopsy punches of varying sizes on a clinically approved collagen type I matrix sheet (3.5 mm thickness and 115 ± 20 μm pore size; Integra LifeSciences, Plainsboro, USA). Scaffolds with diameters of 6, 8, 10, and 12 mm were seeded statically with one million MSCs per scaffold. Seeding densities were calculated to be 10.1, 5.7, 3.6, and 2.5 million MSCs/cm^3, respectively.

During seeding, MSCs at P2 were re-suspended in chondrogenic medium consisting of consisting of Dulbecco's modified Eagle's medium (DMEM) containing 4.5 mg/ml D-glucose, 110 μg/ml sodium pyruvate, 9.6 mM HEPES, 96 units/ml penicillin, 96 μg/ml streptomycin, 279 μg/ml L-glutamine (all from Life Technologies) supplemented with 365 μg/ml ascorbic acid 2-phosphate, 100 nM dexamethasone, 1× insulin-transferrin-selenium (ITS)+1 premix (Sigma-Aldrich), and 10 ng/ml transforming growth factor-beta three (TGF-β3; Neuromics; Appendix 1). Total cell counts were calculated from trypan blue staining and hemocytometer counting of small aliquots of MSCs. One million MSCs were micropipetted onto each scaffold within a 20-μl chondrogenic medium suspension. Seeded scaffolds were then incubated at 37°C for 15 minutes, followed by addition of 100 μl of chondrogenic medium to the base of each scaffold, and re-incubation for 30 minutes. All scaffolds, including cell-free scaffolds (control group) and those seeded with either normoxia- and hypoxia-expanded MSCs, were subsequently immersed in 1 ml of chondrogenic medium

and cultured statically within a humidified incubator at 37°C with 5% carbon dioxide and 3% oxygen (hypoxia). Thereafter, the media were changed twice per week.

4.2.3 Characterization of scaffold diameter contraction and chondrogenesis

To characterize changes in diameter with culture time, scaffolds with diameters of 6 mm, 8 mm, 10 mm, and 12 mm were seeded with normoxia-expanded MSCs, hypoxia-expanded MSCs, or left empty as cell-free controls (Figure 4.1). Eight scaffolds were created for each group with MSCs derived from pelvic aspirates from four male human donors (two scaffolds per donor), three of which were paired in groups. MSCs from the fourth group were taken from similarly aged donors. Consequently, the mean ages (± SEM) of the normoxia- and hypoxia-expanded MSC-seeded scaffold groups were 34.8 ± 4.8 years (range of 25-48 years) and 34.5 ± 4.6 years (range of 25-47 years), respectively.

Scaffolds were photographed with a high-quality digital camera every 3 days over the course of a 30-day *in vitro* culture period. Each image was evaluated with ImageJ software (National Institutes of Health, Bethesda, USA). The diameter of each scaffold was measured in four separate planes to account for non-concentric contraction, and the resulting mean diameter was expressed as a percentage change from the initial diameter at the time of seeding. Scaffold-specific effects on diameter change were studied using cell-free scaffolds. Cell-

specific effects were calculated by subtracting diameter measurements of cell-free scaffolds from diameter measurements of cell-seeded scaffolds. After 30 days of *in vitro* culture, MSC-scaffold constructs from the diameter contraction experiments were subjected to histologic and immunohistochemical analyses to assess the quality of cartilaginous ECM in each group.

Quantitative GAG and deoxyribonucleic acid (DNA) biochemical assays were performed on a separate set of 6 mm-diameter scaffolds that were seeded with either hypoxia-expanded or normoxia-expanded MSCs derived from five male human donors with a mean (± SEM) age of 45.8 ± 5.4 years (range of 33-58 years). These constructs were cultured *in vitro* in chondrogenic medium for either 15 or 30 days prior to biochemical assessment.

4.2.4 Osteochondral explant creation, insertion, *ex vivo* culture, and assessment

Cylindrical osteochondral explants with a 10-mm diameter were trephined from the fresh cadaveric knee of a 20-year-old male (Figure 4.2D). Circular, 6-mm diameter full-thickness cartilage defects were created in the center of each explant. Hypoxia-expanded MSCs from a male donor (20 years of age) were seeded onto six collagen scaffolds and inserted within osteochondral explant cartilage defects either immediately following seeding (Figure 4.2A) or after 21 days of *in vitro* chondrogenic precultivation (Figure 4.2B). Scaffolds with an initial diameter of 8 mm were used for the precultivation group as it was

anticipated that these scaffolds would contract over the 21 days of *in vitro* culture and fit within the 6-mm diameter defects at the time of insertion (Figure 4.2B). Scaffolds that were inserted immediately following seeding had an initial diameter of 6 mm. Tisseel Fibrin Sealant (Baxter, Mississauga, Canada) was used to secure the scaffolds. Following insertion, the constructs were subsequently cultured *ex vivo* in chondrogenic medium containing TGF-β3 for 7, 14 or 21 days, and subjected to histologic and immunohistochemical analyses to assess the quality of cartilaginous ECM in each group.

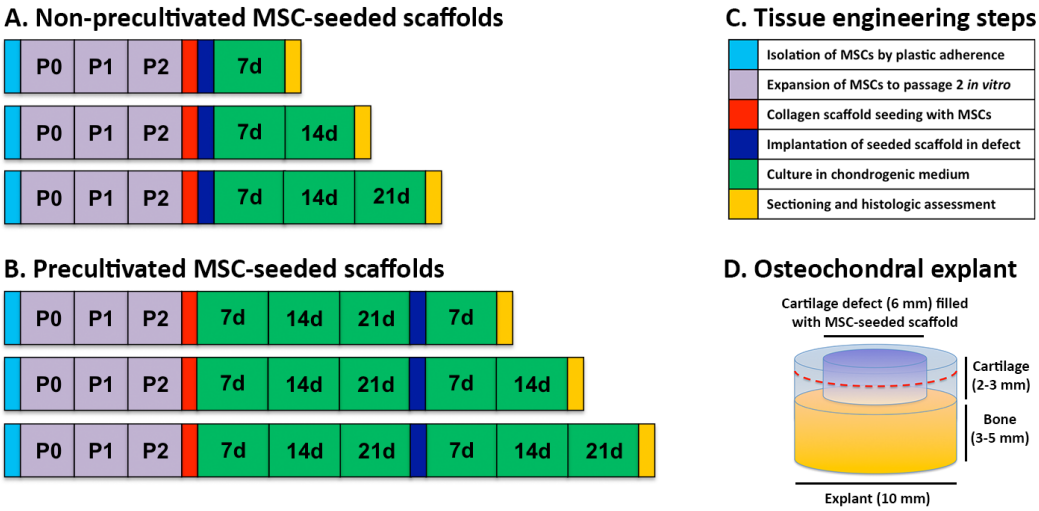

Figure 4.2 Osteochondral explant model and experimental groups. Mesenchymal stem cells (MSCs) were isolated and expanded under hypoxic (3% oxygen) conditions, and then seeded on collagen scaffolds and implanted within explant cartilage defects either (A) immediately or (B) following 21 days of *in vitro* precultivation in a defined chondrogenic medium containing transforming growth factor-beta three and dexamethasone (legend shown in C). An initial scaffold diameter of 6 mm was used in scaffolds implanted immediately following seeding, while 8 mm was used in precultivated scaffolds in an attempt to account for contraction during precultivation. Constructs were cultured *ex vivo* for 7-21 days post-implantation. (D) Osteochondral explants were 10 mm in diameter and each contained a 6-mm diameter full thickness cartilage defect.

4.2.5 Histology and immunohistochemistry

Tissue engineered constructs and explants were removed from media, fixed in 4% phosphate-buffered formalin (10% vol/vol), processed into paraffin wax, and sectioned at 5 μm. Scaffolds were sectioned longitudinally (Figure 4.1), while explants were sectioned in a transverse orientation through the explant cartilage and tissue-engineered scaffold (Figure 4.2D). Sections were then stained with 0.1% safranin O to reveal proteoglycan matrix depositions, and counterstained with 1% fast green. Other sections were probed with antibodies raised against type II collagen (II-II6B3; Developmental Studies Hybridoma Bank at University of Iowa, USA). Immune-localized antigens were visualized with horse anti-mouse biotinylated secondary antibody and an aminoethylcarbazole (AEC)-based peroxidase labeling kit (Enzo Life Sciences, Farmingdale, USA). Images were captured using an Eclipse Ti-S microscope (Nikon Canada, Mississauga, Canada) fitted with NIS Elements Basic Research Imaging Software Version 4.20 (Nikon Canada, Inc.) and assembled in Photoshop (Adobe Systems, San Jose, USA).

4.2.6 Biochemical glycosaminoglycan and deoxyribonucleic acid quantification

In vitro cultured MSC-scaffold constructs were rinsed in phosphate buffered saline (PBS; Life Technologies) and digested in proteinase K (1 mg/ml in 50 mM Tris with 1 mM EDTA, 1 mM iodoacetamide and 10 mg/ml pepstatin A; all from Sigma-Aldrich) for 16 hours at 56°C. Sulfated GAG content was measured by 1,9-dimethymethylene blue binding (Sigma-Aldrich) using chondroitin sulfate

(Sigma-Aldrich) as the standard. DNA content was determined using the CyQuant cell proliferation assay kit (Life Technologies) with supplied bacteriophage λ DNA as the standard.

4.2.7 Statistical analysis

Scaffold diameter data was analyzed using three-way repeated measures analysis of variance (ANOVA) in SPSS Statistics 22 (IBM, Armonk, USA) to determine the effects of cell seeding and initial scaffold diameter (and cell seeding density) on scaffold diameter with time over the course of the 30-day culture period. Two-way ANOVA was utilized to further assess the effects of cell seeding and initial scaffold diameter (and cell seeding density) at each culture time interval. Post-hoc tests on significant data were performed using the Bonferroni method. GAG/DNA data was analyzed using Kruskal-Wallis one-way ANOVA. Statistical significance was concluded when $p<0.05$.

4.2.8 Ethical considerations

All experiments were implemented with MSCs propagated from bone marrow aspirates taken from surgical discards of patients undergoing routine orthopaedic procedures after ethical approval and a waiver of informed consent of the University of Alberta's Health Research Ethics Board – Biomedical Panel. Osteochondral explants were derived from cadaveric tissue that was obtained following ethical approval.

4.3 Results

4.3.1 Contraction of mesenchymal stem cell-seeded collagen scaffolds

All collagen scaffolds exhibited a biphasic change in diameter with time over 30 days of *in vitro* culture (Figure 4.3). Scaffolds enlarged over the first 3-6 days, returned to their original diameters by day 9, and then progressively contracted thereafter. Three-way repeated measures ANOVA confirmed the presence of significant differences in scaffold diameter between all adjacent time points ($p<0.001$) other than between days 3 and 6 ($p=0.05$).

A significant difference in scaffold diameter was noted between normoxia-expanded MSC-seeded scaffolds, hypoxia-expanded MSC-seeded scaffolds and cell-free scaffolds ($p<0.001$; Figure 4.3). Differences between seeding groups were dependent on culture time. On day 3, normoxia- and hypoxia-expanded MSC-seeded scaffolds were not significantly different in size, although both were significantly smaller than cell-free scaffolds ($p<0.001$). Between days 6 and 24, all groups were significantly different in size ($p\leq0.03$). During this period, cell-free scaffolds were the largest and scaffolds seeded with hypoxia-expanded MSCs were mid-sized, while scaffolds seeded with normoxia-expanded MSCs were the smallest. The difference between hypoxia-expanded MSC-seeded scaffolds and normoxia-expanded MSC-seeded scaffolds was most pronounced from day 18 onward ($p<0.001$). Near the end of the culture period (days 27 and 30), cell-free scaffolds and scaffolds seeded with hypoxia-expanded cells were equivalent in size and both significantly larger than normoxia-

expanded MSC-seeded scaffolds ($p<0.001$). The effect of seeding group on scaffold size was pronounced in scaffolds with initial diameters of 6 mm, 8 mm and 10 mm ($p<0.001$; Figure 4.3). A less significant difference was noted between cell-seeded scaffolds and empty scaffolds with an initial diameter of 12 mm ($p=0.047$).

At the completion of the 30-day *in vitro* culture period, normoxia-expanded MSC-seeded scaffolds with initial diameters of 6, 8, 10, and 12 mm had reduced in size by 23.9 ± 1.8, 26.6 ± 1.7, 21.1 ± 1.4, and 19.5 ± 1.3% compared to their initial diameters, respectively (Figure 4.3). Corresponding scaffolds seeded with hypoxia-expanded MSCs contracted significantly less by 18.0 ± 2.0, 15.5 ± 2.0, 18.6 ± 1.7, and 17.5 ± 2.6% ($p<0.001$). Hypoxia-expanded MSC-seeded scaffolds were not significantly different in size from control scaffolds at this time point ($p=0.674$). Diameter reductions of cell-free scaffolds were measured at 13.5 ± 1.3, 12.9 ± 2.3, 18.1 ± 1.5, and 19.5 ± 1.0% on day 30.

Isolated cell-mediated effects on scaffold size were then characterized. A cell-mediated decrease in diameter to a maximal point of contraction between days 6 and 21, followed by a progressive increase in diameter was elucidated in all MSC-seeded scaffolds (Figure 4.4). The contraction effect was most pronounced in scaffolds with a higher seeding density and was significantly dampened in scaffolds with a lower seeding density ($p<0.001$), although post-hoc analysis revealed no significant difference between 3.6 and 5.7 million MSCs/cm^3

densities (p=0.114). Scaffolds seeded with hypoxia-expanded MSCs displayed significantly less cell-mediated contraction than scaffolds seeded with normoxia-expanded MSCs (p<0.001).

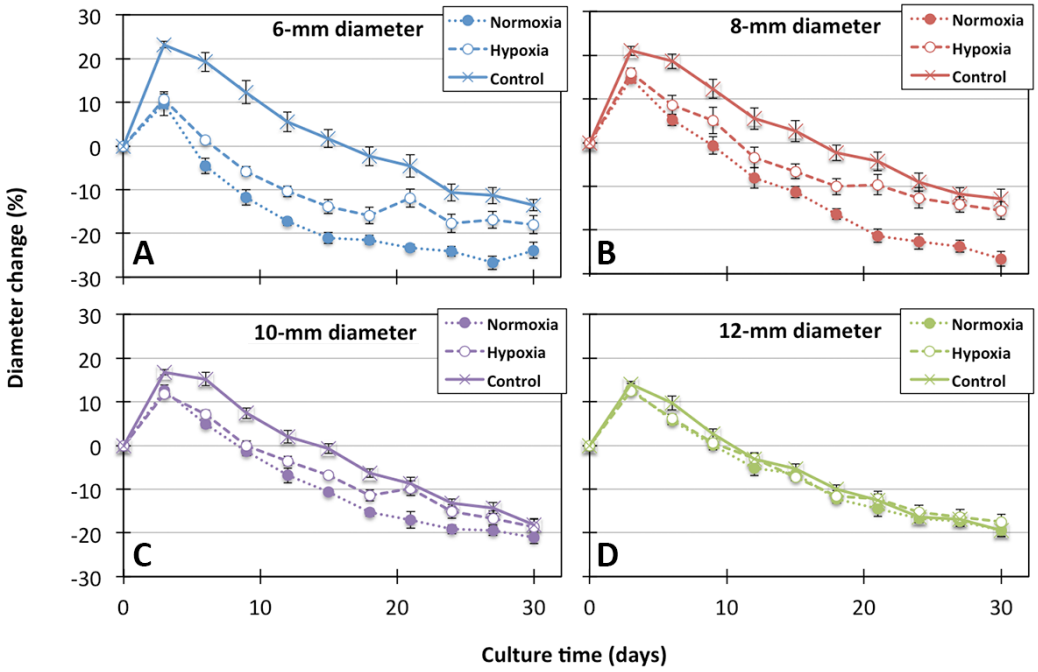

Figure 4.3 Contraction of mesenchymal stem cell-seeded and cell-free collagen scaffolds. Scaffolds seeded with one million normoxia (21% oxygen)- or hypoxia (3% oxygen)-expanded mesenchymal stem cells (MSCs) were plotted based on initial diameters of (A) 6 mm, (B) 8 mm, (C) 10 mm, and (D) 12 mm. Change in diameter was measured using photography and ImageJ software. Each point represents the mean ± standard error of the mean of eight scaffolds seeded in doublet with cells from four male donors. All scaffolds exhibited a biphasic pattern of expansion to a maximal point at 3-6 days, followed by progressive contraction. On repeated measures analysis of variance, there was a significant difference in diameter between normoxia (21% oxygen)-expanded MSC-seeded scaffolds, hypoxia (3% oxygen)-expanded MSC-seeded scaffolds, and cell-free scaffolds in scaffolds with diameters of 6, 8 and 10 mm (p<0.001). This difference was less pronounced in 12-mm-diameter scaffolds (p=0.047).

Scaffold-specific diameter changes followed a biphasic pattern with an increase in size to a maximal point at day 3 of the culture period (Figure 4.3). After that point, scaffolds significantly decreased in size with time ($p \leq 0.005$). Initial scaffold diameter had a significant effect on scaffold-specific changes ($p < 0.001$). Diameter reductions were less pronounced in smaller scaffolds and more pronounced in larger scaffolds. Scaffolds with initial diameters of 6 mm and 8 mm were similar in size ($p = 1.0$) and significantly larger than scaffolds with an initial diameter of 12-mm ($p < 0.001$).

4.3.2 Proteoglycan deposition within constructs undergoing contraction

Collagen scaffolds seeded with one million MSCs underwent chondrogenic differentiation during *in vitro* culture. Tissue consistent with hyaline cartilage was noted in longitudinal sections (Figure 4.1) based on safranin O staining of proteoglycans (Figures 4.5A and B) and type II collagen immunobinding (Figures 4.5C and D). The quality of proteoglycan staining was enhanced in scaffolds seeded with hypoxia-expanded MSC in comparison to those seeded with normoxia-expanded MSCs (Figure 4.5). Accordingly, after 15 days of chondrogenic culture there were significantly higher absolute sulfated GAG quantity and GAG/DNA in hypoxia-expanded MSC- seeded scaffolds relative to those seeded with normoxia-expanded MSCs ($p < 0.05$; Figures 4.6A and C). After 30 days, a similar relationship was evident although the difference lacked statistical significance for both GAG and GAG/DNA. At this time point, four of

five donors showed higher GAG and GAG/DNA with hypoxic expansion (insets in Figures 4.6A and C). Within each oxygen tension group, GAG production and GAG/DNA were higher after 30 days of culture than 15 days ($p<0.05$; Figures 4.6A and C). DNA content was not significantly different between the culture groups ($p=0.111$; Figure 4.6B).

4.3.3 Chondrogenic differentiation, defect filling and integration of hypoxia-expanded mesenchymal stem cell-seeded collagen scaffolds inserted into osteochondral explant cartilage defects

Collagen scaffolds seeded with MSCs and inserted immediately into cartilage defects within osteochondral explants failed to produce obvious ECM proteoglycans based on safranin O staining following 7-21 days of *ex vivo* culture (Figure 4.7A). In contrast, cell-seeded collagen scaffolds that were precultivated *in vitro* for 21 days, inserted, and then cultured *ex vivo* produced hyaline-like cartilage tissue that was supported during 7-21 days of subsequent *ex vivo* culture (Figure 4.7B-D). Lack of integration with surrounding explant cartilage was evident in all cell-scaffold constructs.

4.4 Discussion

In this study, we characterized diameter changes of a clinically approved type I porous scaffold seeded with MSCs over 30 days of *in vitro* chondrogenic culture. All scaffolds showed a biphasic change in diameter with expansion to a maximal

diameter over 3-6 days and contraction thereafter. These findings are consistent with the progressive diameter contraction noted in three other studies in which contraction of porous collagen-GAG scaffolds seeded with MSCs or chondrocytes was followed during 14-21 days of *in vitro* culture, although these studies did not show an initial increase in diameter [378, 388, 407].

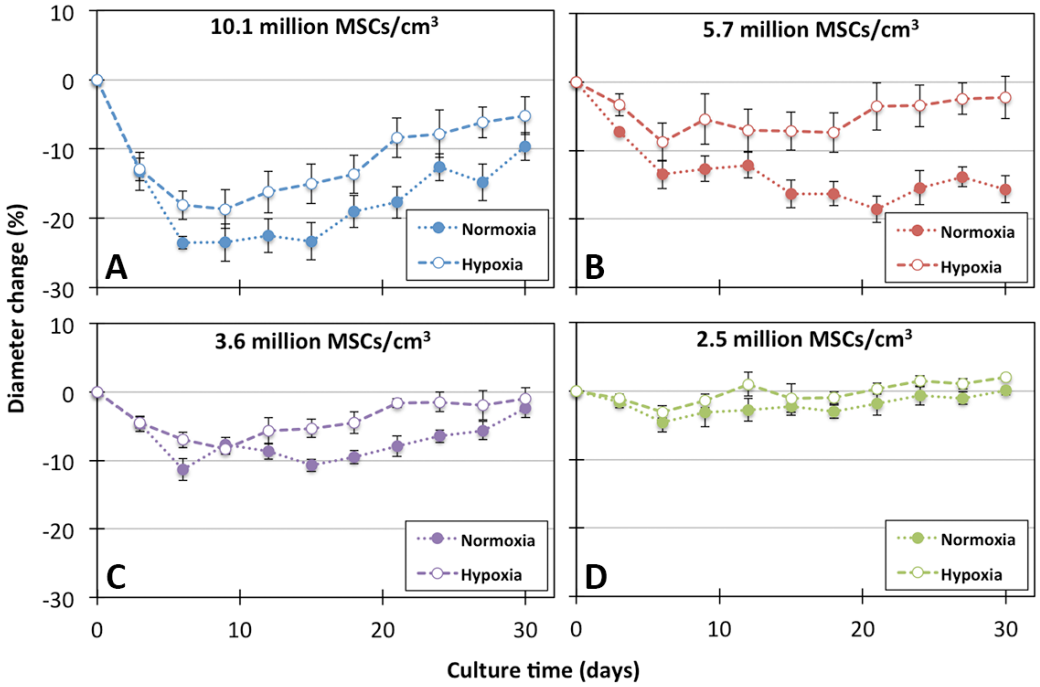

Figure 4.4 Cell-specific effects on diameter of cell-scaffold constructs. Cell-mediated effects were calculated by subtracting diameter changes of cell-free scaffolds from cell-seeded scaffolds. Each point represents the mean ± standard error of the mean of eight scaffolds seeded in doublet with cells from four donors. Contraction was significantly greater in scaffolds seeded at higher densities ($p<0.001$). Scaffolds seeded with hypoxia (3% oxygen)-expanded mesenchymal stem cells (MSCs) contracted significantly less than those seeded with normoxia (21% oxygen)-expanded MSCs ($p<0.001$) based on three-way repeated measures analysis of variance.

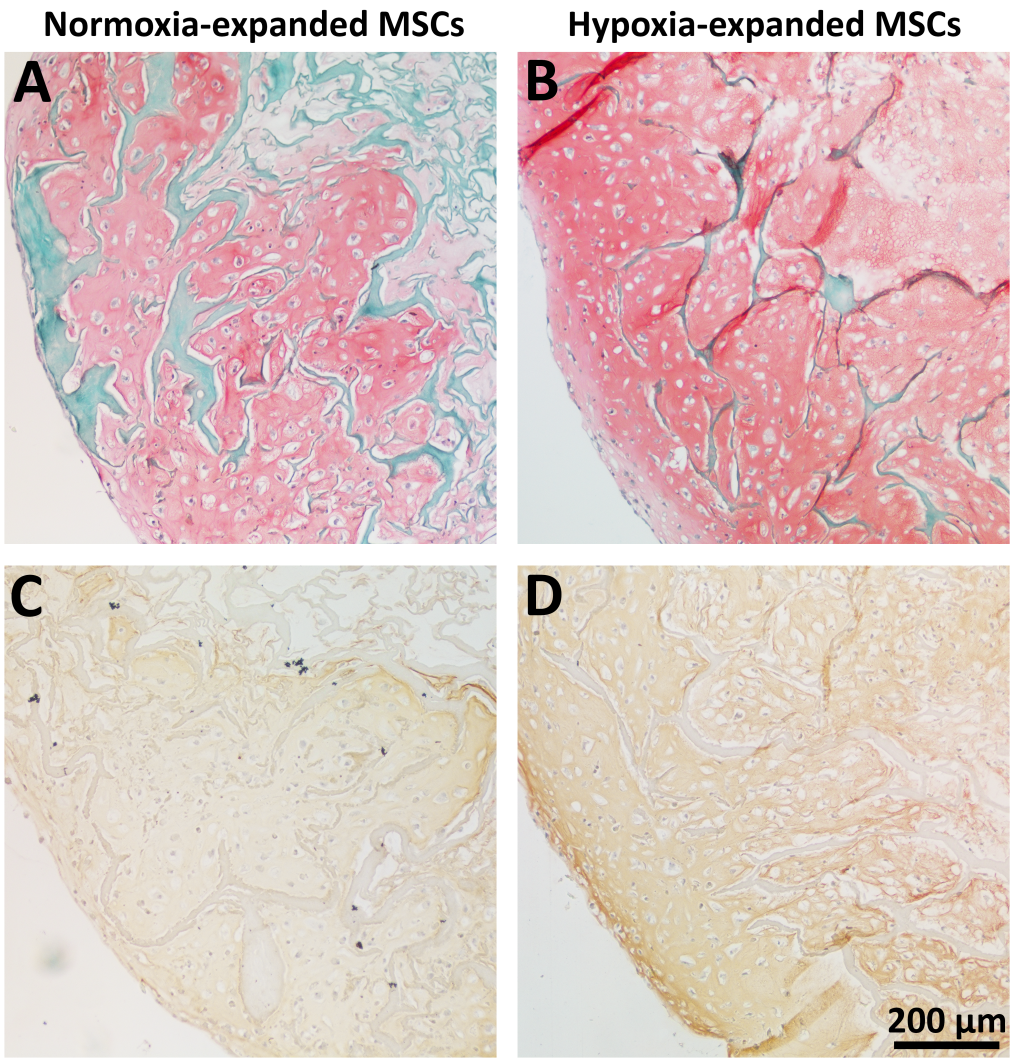

Figure 4.5 Chondrogenesis in mesenchymal stem cell-seeded collagen scaffolds. Safranin O staining showed more abundant proteoglycan content after 30 days of culture in scaffolds seeded with (B) hypoxia-expanded mesenchymal stem cells (MSCs) in comparison to those seeded with (A) normoxia-expanded MSCs. (C and D) Immunohistochemistry of corresponding scaffolds verified the presence of type II collagen in both groups (7× combined magnification of objective and camera lenses).

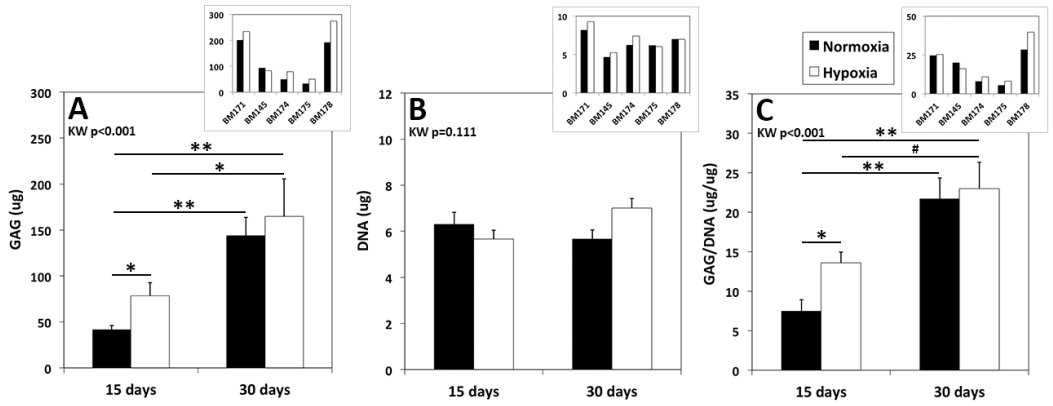

Figure 4.6 Glycosaminoglycan and deoxyribonucleic acid quantification. Scaffolds were seeded with mesenchymal stem cells (MSCs) from four donors expanded under either normoxic (21% oxygen) or hypoxic (3% oxygen) conditions, cultured in a defined chondrogenic medium for 15 or 30 days, and then assessed for (A) sulfated glycosaminoglycan (GAG), (B) deoxyribonucleic acid (DNA) and (C) GAG/DNA. Data represents mean ± standard error of the mean (SEM). Insets convey GAG, DNA and GAG/DNA of hypoxia- and normoxia-expanded MSC seeded scaffolds from each donor. Kruskal-Wallis one-way analysis of variance (ANOVA) was performed for statistical analysis. There appeared to be higher absolute sulfated GAG quantity (A) and GAG/DNA (C) in hypoxia-expanded MSCs relative to normoxia-expanded MSC seeded scaffolds after both 15 and 30 days of chondrogenic culture, although a significant difference was noted only after 15 days. GAG quantity increased with time regardless of culture group. There was not a significant difference in DNA between culture groups. Statistical analysis is represented by: #, approaching significance $p=0.06$; *, significant $p<0.05$; **, significant $p<0.001$.

It was demonstrated that oxygen tension during MSC expansion had a significant effect on cell-mediated scaffold contraction. From days 6-30, hypoxia-expanded MSC-seeded scaffolds contracted significantly less than normoxia-expanded MSC-seeded scaffolds. These finding indicate that expanding MSCs under hypoxic conditions may substantially reduce cell-mediated contraction of tissue-engineered constructs.

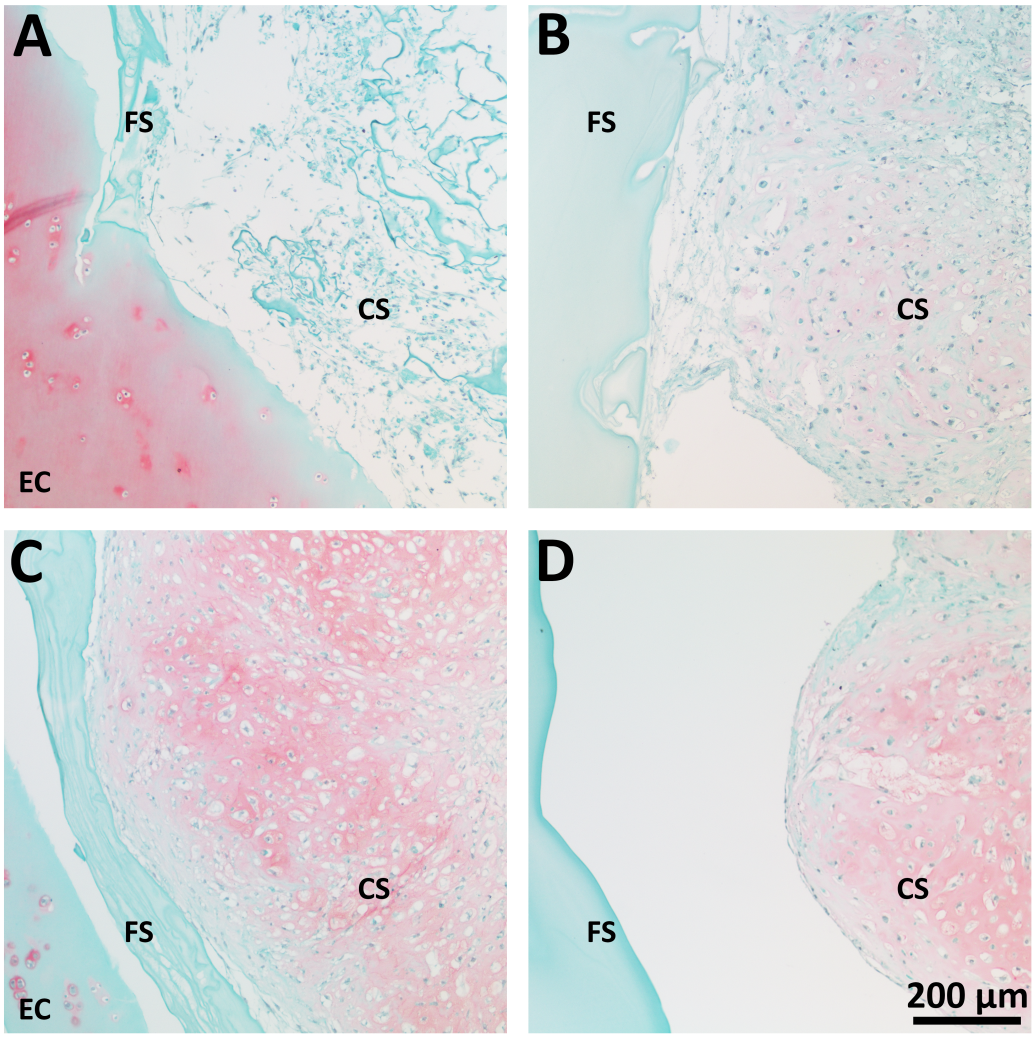

Figure 4.7 Histologic assessment of cell-scaffold constructs within osteochondral explants cartilage defects. Histologic sections were made in a transverse orientation through osteochondral explant cartilage and hypoxia-expanded mesenchymal stem cell (MSC)-seeded scaffolds. (A) Collagen scaffolds seeded with MSCs and implanted immediately without *in vitro* precultivation were stained with safranin O. Although cells were noted within areas of each scaffold, the constructs lacked proteoglycan content, regardless of *ex vivo* culture time (7-21 days); a representative MSC-scaffold construct implanted and cultured *ex vivo* for 14 days is shown. MSCs seeded within scaffolds, precultivated *in vitro* for 21 days prior to implantation, and cultured *ex vivo* for (B) 7, (C) 14 or (D) 21 days produced tissue containing abundant proteoglycans. However, all scaffolds lacked integration with surrounding osteochondral explant cartilage over this time period. CS, cell-seeded scaffolds; EC, explant articular cartilage; FS, Tisseel fibrin sealant.

Scaffold-specific and cell-mediated diameter changes were elucidated. Cell-free scaffolds were used to determine scaffold-specific effects that displayed a pattern of expansion followed by contraction. This biphasic effect presumably resulted from scaffold engorgement with water followed by progressive degradation (or fragmentation specifically) of scaffold contents with time[389, 390, 408]. Cell-specific effects showed a contraction that peaked early to midway through the culture period and then reduced with time.

Consistent with previous studies using MSCs, the scaffold group seeded with highest density of cells (6-mm diameter group) underwent the most pronounced cell-mediated contraction [392, 409, 410]. The seeding density for this group was 10 million cells/cm^3, a density that has been utilized routinely in our laboratory and *in vivo* in animal studies [36, 281]. The dampened cell-mediated contraction noted with time may have been secondary to an expansive force generated by increased proteoglycan production given that both hypoxia- and normoxia-expanded MSCs produced increasing amounts of sulfated GAG with culture time.

Reduced cell-mediated contraction in the hypoxia-expanded MSC-seeded scaffolds corresponded with improved proteoglycan content in comparison to normoxia-expanded scaffolds. This difference was most prominent after 15 days of culture. After 30 days, the GAG quantity in hypoxia-expanded MSC-seeded

scaffolds was larger but the difference lacked statistical significance in the Kruskal-Wallis ANOVA. Out of five donors, improved GAG quantity and GAG/DNA was noted with hypoxic expansion in four. However, variability in the magnitudes of these parameters between donors was noted, as in previous reports, and may be contributing factor to the lack of statistical significance [332]. The improved chondrogenesis noted in this study is consistent with previous work by our group and others that showed enhanced proteoglycan and sulfated GAG content with hypoxic expansion of MSCs cultured in pellets and scaffolds for 14-21 days [332, 369, 411].

Hypoxia-expanded MSC-seeded scaffolds were inserted within full-thickness cartilage defects created in osteochondral explants to assess if this contraction-reducing technique could promote defect filling and integration in this model. Precultivated scaffolds displayed a phenotype consistent with hyaline-like cartilage that was supported following insertion within explant defects. Although hypoxic expansion promoted defect filling based on our *in vitro* findings, neo-tissue constructs lacked integration during 7-21 days of post-insertion *ex vivo* culture. It is possible that longer periods of time are required for integration to occur. Furthermore, factors other than cell-mediated contraction may have promoted enhanced diameter reduction and lack of integration in this model. Scaffold degradation secondary to enzymes or other mediators released from the osteochondral explants may have promoted this effect [390]. Moreover, formalin fixation and staining during histologic processing could have caused scaffold fragmentation or dehydration.

Collagen scaffolds that were seeded and inserted immediately following seeding within explant cartilage defects lacked cartilaginous ECM production over 21 days of *ex vivo* culture even though cells were noted in various areas of each scaffold. The contrast noted between non-precultivated and precultivated MSC-seeded scaffolds is consistent with the *in vivo* sheep study of Zscharnack *et al.* [274]. They showed that precultivated MSC-seeded collagen hydrogels implanted within full-thickness cartilage defects produced histologically superior repair tissue to non-precultivated constructs at 6 months post-implantation. Although non-precultivated constructs produced some cartilaginous repair tissue in that study, their histologic scores did not differ significantly from cell-free gels and empty defects.

Despite the improved outcomes with precultivation noted in previous work and in our study, this technique has not been routinely adopted in clinical trials to date. Non-precultivated scaffolds implanted shortly following seeding with MSCs or bone marrow-derived cell (BMDC) collections have been shown to produce hyaline-like repair tissue in based on magnetic resonance imaging, second-look arthroscopy and histologic assessment performed months after implantation [38, 39, 41]. Further investigation is required to determine if *in vitro* precultivation improves tissue characteristics in humans as it does in animals and *ex vivo* models.

This study had some limitations. Firstly, contraction of cylindrical scaffolds was assessed in the transverse plane with diameter recordings, but not in the longitudinal plane with thickness recordings. Characterization of thickness contraction would offer important information related to defect filling and the creation of a smooth articular surface following implantation of constructs. Secondly, due to the use of a static culture system, MSCs might not have distributed uniformly throughout each scaffold, especially in the larger scaffolds. This could have impacted cell-mediated contraction. Lastly, other limitations were present that relate specifically to the use of an osteochondral explant model. This model afforded the creation of cartilage defects and simulation of MSC-scaffold construct insertion within an *in vitro* setting. However, it is currently unclear whether explant tissue remains viable beyond 3-6 weeks of *ex vivo* culture [270, 271]. We limited our explant culture time to 3 weeks in an attempt to avoid extensive explant death. Preliminary experiments were performed that verified the presence of predominantly live cells within explants over this time period. It is possible that this relatively short culture period contributed to lack of integration of cell-scaffold constructs. *In vivo* factors such as mechanical loading are absent although these factors could play a critical role in tissue remodeling and integration of neo-tissue *in vivo* [280]. Other factors, such as soluble mediators and enzymes that could impact cellular physiology, may be present extracellularly due to release during explant devitalization.

4.5 Conclusion

Collagen scaffolds contracted progressively during *in vitro* culture as a result of cellular and non-cellular effects. Cell-mediated contraction was reduced significantly when MSCs were isolated and expanded under hypoxic conditions, potentially as a result of increased proteoglycan production and hydrostatic swelling. Hypoxia-expanded MSC may be used in cartilage engineering to reduce construct contraction. Secondly, hypoxia-expanded MSC-seeded scaffolds that were precultivated *in vitro* in chondrogenic medium containing TGF-β3 for 21 days prior to insertion into osteochondral explant cartilage defects produced tissue consistent with hyaline cartilage, while scaffolds inserted immediately after seeding did not. Accordingly, precultivation may serve as a method of improving the quality of articular cartilage repair tissue in MSC transplantation.

Chapter 5

Optimal Seeding Densities for *In Vitro* Chondrogenesis of Two- and Three-Dimensional-Isolated and Expanded Bone Marrow-Derived Mesenchymal Stromal Stem Cells within a Porous Collagen Scaffold

Troy D. Bornes, Nadr M. Jomha, Aillette Mulet-Sierra, and Adetola B. Adesida

This chapter has been published in part in Tissue Engineering Part C: Methods. Bornes TD, Jomha NM, Mulet-Sierra A, Adesida AB: **Optimal Seeding Densities for In Vitro Chondrogenesis of Two- and Three-Dimensional-Isolated and -Expanded Bone Marrow-Derived Mesenchymal Stromal Stem Cells Within a Porous Collagen Scaffold.** *Tissue Eng Part C Methods* 2016, **22**(3):208-20.

5.1 Introduction

Bone marrow-derived mesenchymal stromal stem cells (BMSCs) are a promising cell source for treating articular cartilage defects [29]. BMSCs seeded within biomaterial scaffolds and implanted into focal chondral defects are capable of resurfacing cartilage in animal and human joints, although inconsistent outcomes have been reported based on macroscopic assessment, histological analysis, magnetic resonance imaging, and clinical scoring [39, 41, 43, 45, 254, 363].

Repair tissue quality has been shown to correlate with functional outcome [45, 254, 320]. Therefore, tissue engineering variables, such as cell expansion environment and seeding density of scaffolds, are currently under investigation with the goal of improving neo-cartilage quality.

BMSCs have conventionally been isolated by plastic adherence and expanded in a two-dimensional (2D) environment within tissue-culture flasks [31, 32]. Although this method has been shown to produce cells capable of chondrogenic differentiation [274, 332, 369, 405], major drawbacks include loss of multipotent differentiation, inability to produce cartilaginous extracellular matrix (ECM) proteins and cellular senescence during prolonged expansion periods [333, 334, 339, 368]. Three-dimensional (3D) isolation and expansion of BMSCs has been proposed as a method of mimicking the natural bone marrow microenvironment and maintaining multipotency and chondrogenic capacity [266, 341]. Cell collections containing bone marrow-derived mononucleated cells (BMNCs) – a small fraction of which are BMSCs – are seeded within biomaterials for 3D isolation, expansion and subsequent differentiation [266, 342].

Cell seeding density is a transplantation variable that has not been evaluated in detail to date for either 2D- or 3D-expanded BMSCs. Healthy articular cartilage naturally contains 9.6×10^6 chondrocytes/cm^3 [57]. The optimal BMSC seeding density required for cell organization, chondrogenic

differentiation and ECM production to create engineered tissue that resembles native cartilage is currently unknown. For implantation purposes *in vivo*, BMSC seeding densities of 1-50 $\times 10^6$ cells/cm^3 of biomaterial matrix have been used in preclinical animal studies [29, 36, 274, 281, 283, 285, 287, 291, 293, 297, 315, 412]. In clinical studies, a density of 5 $\times 10^6$ cells/cm^3 has been reported although the rationale for adopting this seeding density was not described [39, 43].

The objective of this study was to assess the impact of cell seeding density within a clinically relevant, collagen I scaffold on *in vitro* BMSC chondrogenesis following 2D and 3D isolation and expansion. Two-dimensional isolation was performed by seeding whole bone marrow aspirate into tissue-culture flasks, while 3D isolation involved seeding whole bone marrow aspirate within collagen scaffolds. Collagen was used as a biomaterial given that it is used routinely in preclinical animal and human studies [39, 41, 43, 274]. Ovine cells were studied as sheep are emerging as a useful animal model for the study of cell transplantation techniques for cartilage repair [274]. It was hypothesized that hyaline-like cartilage would be produced within collagen scaffolds by 2D- and 3D-expanded BMSCs with an optimal seeding density of 10 $\times 10^6$ cells/cm^3.

5.2 Methods

5.2.1 Bone marrow aspiration and mononucleated cell counting

Bone marrow aspirates (BMAs) were obtained from the iliac crest of six female Suffolk sheep (mean age ± standard error of the mean [SEM] of 3.3 ± 0.8 years)

as previously described following ethical approval from the University of Alberta's Animal Care and Use Committee (Table 5.1) [405]. Staining with crystal violet (Sigma-Aldrich, Oakville, Canada) and hemocytometer counting were used to determine the number of BMNCs in each BMA.

Table 5.1 Bone marrow donor information

Donor	Gender	Age (years)	Mass (kg)
Z28	Female	2.0	66
Z01	Female	2.2	71
Z33	Female	2.3	81
Y19	Female	3.2	63
Y08	Female	3.3	94
T10	Female	7.0	74

5.2.2 Culture of two-dimensional-expanded bone marrow-derived mesenchymal stromal stem cells

BMSCs were isolated in a 2D environment by plastic adherence from BMAs and expanded in tissue-culture flasks to passage two (P2) within expansion medium (Figure 5.1). Expanded BMSCs were then seeded onto porous collagen scaffolds at 50, 10, 5, 1, or 0.5 $\times 10^6$ BMSCs/cm^3. Thereafter, BMSC-scaffold constructs were differentiated within chondrogenic medium for 21 days.

Table 5.2 Cell seeding density

Density ($x10^6$ cells/cm^3)	Number of cells seeded
50	4,948,000
10	989,600
5	494,800
1	98,960
0.5	49,480

Two-dimensional isolation and expansion involved seeding whole BMA collections containing 8×10^7 BMNCs within each 150-cm^2 tissue culture flask and submersing each BMA collection in expansion medium containing alpha-minimal essential medium (α-MEM; Corning-Mediatech, Manassas, USA) supplemented with 8.8% vol/vol heat-inactivated fetal bovine serum (FBS), 88.5 units/ml penicillin, 88.5 μg/ml streptomycin, 258.4 μg/ml L-glutamine, 8.8 mM 4-(2-hydroxyethyl)-1-piperazineethanesulfonic acid (HEPES), 885.0 μM sodium pyruvate (all from Life Technologies, Burlington, Canada), and 5 ng/ml fibroblast growth factor-2 (FGF-2; Neuromics, Edina, USA). Cells were allowed to adhere and grow statically for 7 days in a humidified incubator. The humidified incubator used throughout the entirety of the study for cell and tissue culture contained air with 3% oxygen and 5% carbon dioxide heated to 37°C. After seven days, the media were changed twice per week. Once 80% cell confluence was attained, adherent BMSCs were washed with phosphate-buffered saline (PBS), detached

using 0.05% wt/vol trypsin-ethylenediaminetetraacetic acid (EDTA; Corning-Mediatech) and expanded to P2.

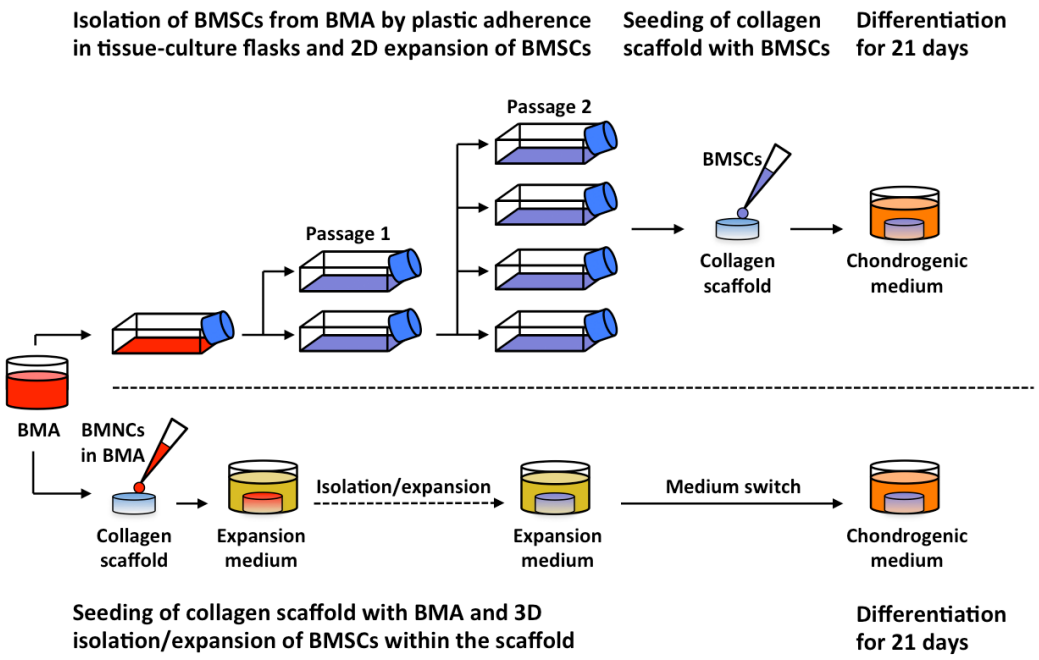

Figure 5.1 ***In vitro*** **cartilage engineering from two-dimensional- and three-dimensional-expanded bone marrow-derived mesenchymal stromal stem cells.** Bone marrow-derived mesenchymal stromal stem cells (BMSCs) were isolated in a two-dimensional (2D) environment by plastic adherence from bone marrow aspirates (BMAs) and expanded in tissue-culture flasks to passage two within expansion medium. BMSCs were then seeded onto porous collagen scaffolds at 50, 10, 5, 1, or 0.5 $\times 10^6$ BMSCs/cm^3. For three-dimensional (3D) isolation and expansion, BMAs containing known numbers of bone marrow-derived mononucleated cells (BMNCs) were seeded onto porous collagen scaffolds at densities of 50, 10, 5, 1, or 0.5 $\times 10^6$ BMNCs/cm^3, and cultured in expansion medium. Thereafter, all constructs were differentiated within chondrogenic medium for 21 days.

For chondrogenic differentiation, 2D-expanded BMSCs were suspended in chondrogenic medium consisting of Dulbecco's modified Eagle's medium

(DMEM) containing 4.5 mg/ml D-glucose, 110 μg/ml sodium pyruvate and L-glutamine (Sigma-Aldrich) supplemented with 9.6 mM HEPES, 95.6 units/ml penicillin, 95.6 μg/ml streptomycin, 279.2 μg/ml L-glutamine (all from Life Technologies), 1× insulin-transferrin-selenium (ITS)+ premix (BD Biosciences, Mississauga, Canada), 365 μg/ml ascorbic acid 2-phosphate, 40 μg/ml L-proline, 100 nM dexamethasone, 125 μg/ml human serum albumin (all from Sigma-Aldrich), and 10 ng/ml transforming growth factor-beta three (TGF-β3; ProSpec, East Brunswick, USA). Cylindrical collagen scaffolds (3.5-mm thickness; 6-mm diameter) were created using a biopsy punch on sheets of type I collagen sponge (125 x 100 × 3.5 mm^3 dimension; 115 ± 20 μm pore size; Integra LifeSciences, Plainsboro, USA). Cell counts were calculated using trypan blue staining and hemocytometer counting, and BMSCs were micropipetted onto each scaffold within a 20-μl chondrogenic medium suspension. Scaffold seeding was performed at five BMSC densities (Table 5.2). Seeded scaffolds were incubated for 15 minutes followed by addition of 100 μl of chondrogenic medium to the base of each scaffold. Thereafter, constructs were incubated for an additional 30 minutes to promote cell adhesion and then submersed in 1 ml of chondrogenic medium. Constructs were cultured statically for 21 days within a humidified incubator. Media were changed twice per week.

5.2.3 Culture of three dimensional-expanded bone marrow-derived mesenchymal stromal stem cells

Bone marrow aspirates containing known numbers of BMNCs were seeded onto collagen scaffolds at densities of 50, 10, 5, 1, or 0.5 $\times 10^6$ BMNCs/cm^3, and cultured in expansion medium to foster 3D isolation and expansion of BMSCs. Following the expansion period, all constructs were differentiated within chondrogenic medium for 21 days (Figure 5.1).

For 3D isolation and expansion, scaffolds were prepared in an identical fashion to the protocol used for seeding of 2D-expanded BMSCs. During seeding, BMAs containing known numbers of BMNCs were centrifuged and suspended within expansion medium to create 20-µl seeding collections that were micropipetted onto scaffolds. Scaffold seeding was performed at five BMNC densities (Table 5.2). Seeded scaffolds were incubated at for 15 minutes followed by addition of 100 µl of expansion medium to the base of each scaffold. Constructs were incubated for an additional 30 minutes to promote cell adhesion and were subsequently immersed in 1 ml of expansion medium and cultured within a humidified incubator. In an identical fashion to the 2D expansion group, BMA-seeded scaffolds were cultured statically for 7 days undisturbed. Media were changed twice weekly thereafter. For each donor, 3D expansion was carried out for the equivalent amount of time as 2D expansion.

To induce chondrogenic differentiation, the medium used for culture of 3D-expanded BMSC-seeded scaffolds was switched from 1 ml of expansion medium to 1 ml of chondrogenic medium at the same time point as chondrogenic culture commenced for 2D-expanded BMSC-seeded scaffolds. Constructs were cultured statically for 21 days within a humidified incubator. Media were changed twice per week.

5.2.4 Cell count and population doubling during isolation and expansion

A colony-forming unit fibroblastic (CFU-F) assay of P0 BMSCs was performed as previously described (Chapter 3) [405]. Each colony was considered to have derived from a single isolated BMSC, which enabled calculation of the number of BMSCs isolated from 1 $\times 10^5$ BMNCs that were seeded. The ratio of isolated BMSCs to seeded BMNCs was used to calculate the number of BMSCs arising from 8 $\times 10^7$ BMNCs plated in each tissue-culture flask at P0. At the end of P0, P1 and P2, cell counts of BMSCs were determined using trypan blue staining and hemocytometer counting. In the 3D expansion group, crystal violet staining and hemocytometer counting were used to calculate the quantity of BMNCs per volume of BMA. Known numbers of BMNCs were seeded within BMA collections onto scaffolds prior to expansion. The number of seeded BMSCs was estimated using the BMSC-to-BMNC ratio calculated from the CFU-F assay. Post-expansion cell counts were calculated from a standard curve (Figure 5.2) based on deoxyribonucleic acid (DNA) content derived from a CyQUANT Cell

Proliferation Assay (Life Technologies). Population doublings were determined using the method described by Solchaga *et al.* [346].

5.2.5 Trilineage differentiation potential of bone marrow-derived mesenchymal stromal stem cells

To confirm the presence of cells with properties of mesenchymal stem cells within the BMAs, plastic adherent P2 BMSCs were cultured in osteogenic, adipogenic and chondrogenic media and trilineage differentiation potential was demonstrated as previously described (Chapter 3) [405].

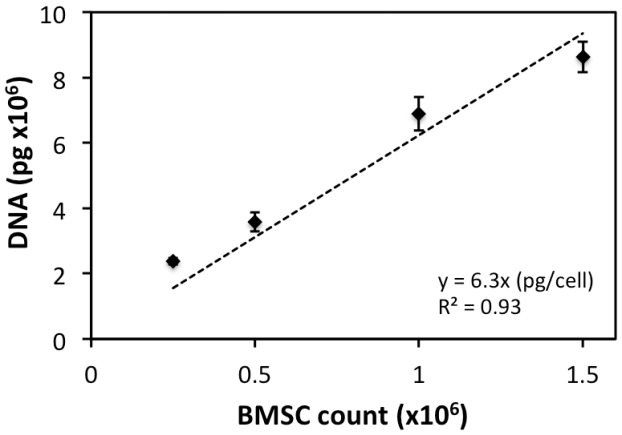

Figure 5.2 Deoxyribonucleic acid versus bone marrow-derived mesenchymal stromal stem cell count. Deoxyribonucleic acid (DNA) quantification was performed on constructs containing known numbers of bone marrow-derived mesenchymal stromal stem cell (BMSCs) to produce a standard curve.

5.2.6 Assessment of chondrogenesis

Tissue-engineered constructs were assessed with reverse-transcription quantitative polymerase chain reaction (RT-qPCR) for gene expression (primers are shown in Table 5.3), safranin O staining of ECM proteoglycans and biochemical quantification of glycosaminoglycan (GAG) and DNA as described previously (Chapter 3) [405]. Histological scoring was also performed, and depositions of collagens I and II were assessed with immunofluorescence.

Table 5.3 Ovine primer sequences used in reverse-transcription polymerase chain reaction analysis

Gene	Primer sequences		NCBI Reference
β-actin (*ACTB*)	5'-CGGCGGGACCACCAT-3'	Forward	NM_001009784.1
	5'-GCAGTGATCTCTTTCTGCATCCT-3'	Reverse	
Aggrecan (*ACAN*)	5'-TGGAATGATGTCCCATGCAA-3'	Forward	XM_004018048.1
	5'-GCCACTGTGCCCTTTTTACAG-3'	Reverse	
Collagen I (*COL1A1*)	5'-CGCCCCAGACCAGGAATT-3'	Forward	XM_004012773.1
	5'-GTGGAAGGAGTTTACAGGAAGCA-3'	Reverse	
Collagen II (*COL2A1*)	5'-ACCTCACGTCTCCCCATCA-3'	Forward	XM_004006408.1
	5'-CTGCTCGGGCCCTCCTAT-3'	Reverse	
Collagen X (*COL10A1*)	5'-CAGGCTCGAATGGGCTGTAC-3'	Forward	XM_004011185.1
	5'-CCACCAAGAATCCTGAGAAAGAG-3'	Reverse	
SRY-Box 9 (*SOX9*)	5'-GCTGCTGGCCGTGATGA-3'	Forward	XM_004013527.1
	5'-GGGTCGCGCGTTTGTTT-3'	Reverse	

5.2.7 Histological scoring using the Bern score

Constructs containing BMSCs from five donors were fixed in 10% wt/vol buffered formalin, processed into paraffin wax, and sectioned at a thickness of 5

μm. Sections were stained with safranin O and fast green as previously described[405], and graded using the Bern score based on ECM staining, intercellular distance and ECM accumulation, and cell morphology [413]. Each category was scored out of three with a combined maximal Bern score of nine. Non-homogeneous constructs were evaluated through assessing distinct regions and combining scores based on the percentage area represented as described by Grogan *et al*. [413].

5.2.8 Immunofluorescence

Sections with a thickness of 5 μm were treated with Protease XXV (Fisher Scientific, Ottawa, Canada) and hyaluronidase (Sigma-Aldrich) and incubated with rabbit anti-collagen I (NBP1-30054, Novus Biologicals, Oakville, Canada; 1:250 dilution) and mouse anti-collagen II (II-II6B3, Developmental Studies Hybridoma Bank, Iowa City, USA; 1:200 dilution). Immune-localized antigens were visualized with Texas Red anti-rabbit IgG (Vector Laboratories, Burlington, Canada) and fluorescein isothiocyanate (FITC) goat anti-mouse Ig (BD Biosciences). Sections were mounted using Biotium EverBrite Mounting Medium with DAPI (4',6-diamidino-2-phenylindole; Cedarlane Laboratories, Burlington, Canada). Images were captured using an Eclipse Ti-S microscope (Nikon Canada, Mississauga, Canada) fitted with NIS Elements (version 4.20; Nikon Canada) and assembled in Photoshop (Adobe Systems, San Jose, USA).

5.2.9 Statistical analysis

Analyses were performed using SPSS Statistics 22 (IBM, Armonk, USA) and significance was concluded when $p<0.05$. Repeated measures analysis of variance (ANOVA) was used for assessment of cell count and doubling over time during expansion and differentiation. For assessment of cell count over time within specific seeding density groups, a paired t-test was used. When different constructs were used at different time points, as in the analysis of peri-differentiation cell count of 3D-expanded BMSC-seeded scaffolds, a t-test was used given that pairing was not possible. Comparison of gene expressions, biochemical quantities, cell counts, and histological scores following chondrogenic differentiation between seeding groups required a Kruskal-Wallis ANOVA with pairwise comparisons. A Mann-Whitney U test was used to compare pre-differentiation to post-differentiation gene expressions.

5.3 Results

5.3.1 Isolation and expansion within two- and three-dimensional environments

The duration of time from plating of BMNCs to reach 80% confluence at P2 during 2D expansion was 23.8 ± 0.8 days. The mean number (± SEM) of BMSCs present per flask at the completion of P0 was $7.9 \pm 1.4 \times 10^6$ and this number increased to $16.1 \pm 1.6 \times 10^6$ and $27.6 \pm 4.4 \times 10^6$ at the completion of P1 and P2, respectively ($p<0.001$; Figure 5.3A). BMSC count following 2D expansion was 34.2 ± 4.5% of the BMNC count initially seeded. There were 12.3 ± 1.0

cumulative BMSC population doublings during expansion (Figure 5.3B). Based on the CFU-F assay (Figure 5.3C), 18.0 ± 8.5 BMSCs were isolated from 1 $\times 10^5$ seeded BMNCs. Therefore, 0.018 ± 0.009% of all seeded BMNCs were BMSCs.

Following 3D expansion, the number of BMSCs present was significantly lower than the initial number of BMNCs seeded in scaffolds at densities of 50, 10 and 5 $\times 10^6$ BMNCs/cm^3 ($p<0.001$), while there was not a significant difference noted for densities of 1 and 0.5 $\times 10^6$ BMNCs/cm^3 ($p=0.87$ and 1.0, respectively; Figure 5.3D). For seeding densities of 50, 10, 5, 1, and 0.5 BMNCs/cm^3, BMSC counts following 3D expansion were 0.29 ± 0.05, 0.15 ± 0.06, 0.12 ± 0.05, 0.09 ± 0.06, and 0.05 ± 0.05 $\times 10^6$ BMSCs. These BMSC counts equated to 5.8 ± 0.9%, 14.9 ± 6.2%, 24.2 ± 9.9%, 89.5 ± 59.2%, and 100.3 ± 92.2% of initial BMNC counts, respectively. Following expansion, cell densities were calculated to be 2.9 ± 0.5, 1.5 ± 0.6, 1.2 ± 0.5, 0.9 ± 0.6, and 0.5 ± 0.5 BMSCs/cm^3, respectively. Cumulative BMSC population doublings were 9.3 ± 1.1, 9.7 ± 1.4, 10.2 ± 1.2, 11.1 ± 1.2, and 10.7 ± 1.2, respectively.

5.3.2 Trilineage differentiation of bone marrow-derived mesenchymal stromal stem cells

Spindle-shaped BMSCs demonstrated plastic adherence and were differentiated into cells capable of producing cartilaginous proteoglycans, adipose droplets and calcified bone matrix (Figure 5.3E).

5.3.3 Seeding density of two- and three-dimensional-expanded bone marrow-derived mesenchymal stromal stem cells affected chondrogenic gene expression

Constructs containing 2D- and 3D-expanded BMSCs had varying levels of cartilage-related genes that were dependent on seeding density following chondrogenic culture. In 2D-expanded BMSC-seeded scaffolds, mRNA expressions of hyaline cartilage-related collagen II and aggrecan were highest in scaffolds seeded at 5-10 $\times 10^6$ BMSCs/cm^3 (Figures 5.4A and E). For aggrecan mRNA expression, constructs containing 10 and 5 $\times 10^6$ BMSCs/cm^3 had significantly enhanced aggrecan mRNA expression in comparison to scaffolds seeded with more cells (50 $\times 10^6$ BMSCs/cm^3; $p<0.001$) and less cells (0.5 $\times 10^6$ BMSCs/cm^3; $p<0.01$; Figure 5.4A). Seeding at 5 $\times 10^6$ BMSCs/cm^3 also resulted in improved aggrecan mRNA expression relative to 1 $\times 10^6$ BMSCs/cm^3 ($p<0.01$). Densities of 10 and 5 $\times 10^6$ BMSCs/cm^3 corresponded to greater collagen II mRNA expression than densities of 50, 1 and 0.5 $\times 10^6$ BMSCs/cm^3 ($p<0.01$; Figure 5.4E). Ratios of collagen II/I and collagen II/X also followed this pattern ($p<0.05$). Expression of transcription factor SOX9 was not different between scaffolds seeded at 50, 10 and 5 $\times 10^6$ BMSCs/cm^3 ($p\geq0.29$), but these densities led to increased expression relative to 0.5 $\times 10^6$ BMSCs/cm^3 ($p<0.05$; Figure 5.4I).

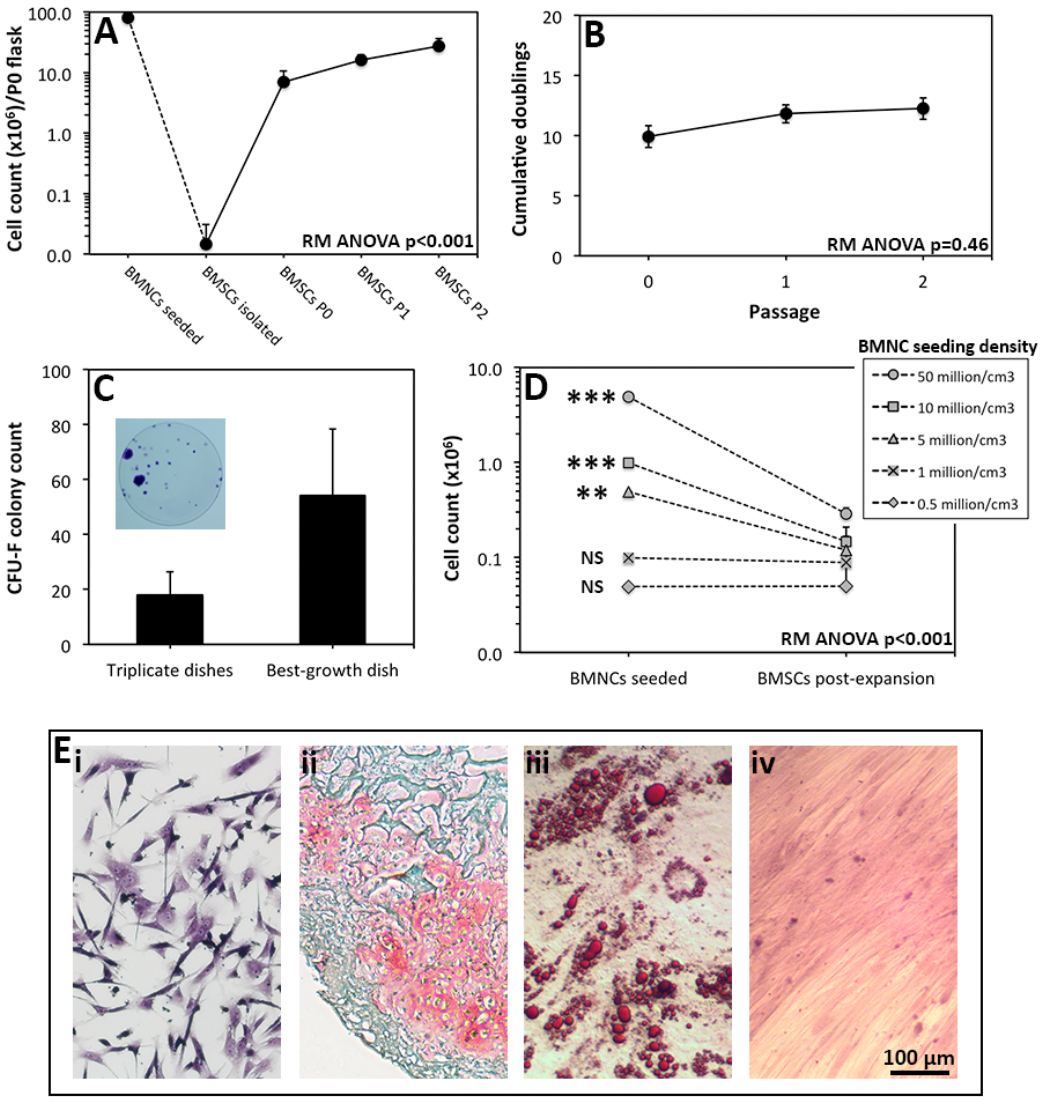

Figure 5.3 Expansion and trilineage differentiation of bone marrow-derived mesenchymal stromal stem cells. (A) Cell counts and (B) cumulative doublings of bone marrow-derived mesenchymal stromal stem cells (BMSCs) during two-dimensional (2D) isolation and expansion. (C) A colony-forming unit fibroblastic (CFU-F) assay was performed to determine the number of BMSCs present in each bone marrow aspirate (BMA) containing 1×10^5 bone marrow-derived mononucleated cells (BMNCs). Colonies were stained with crystal violet. (D) Cell counts during three-dimensional (3D) isolation and expansion. (E) [i] Plastic adherent BMSCs stained with crystal violet. BMSCs differentiated into [ii] chondrogenic, [iii] adipogenic and [iv] osteogenic lineages and stained with safranin O, Oil Red O and Alizarin Red S, respectively (5× combined magnification of objective and camera lenses).

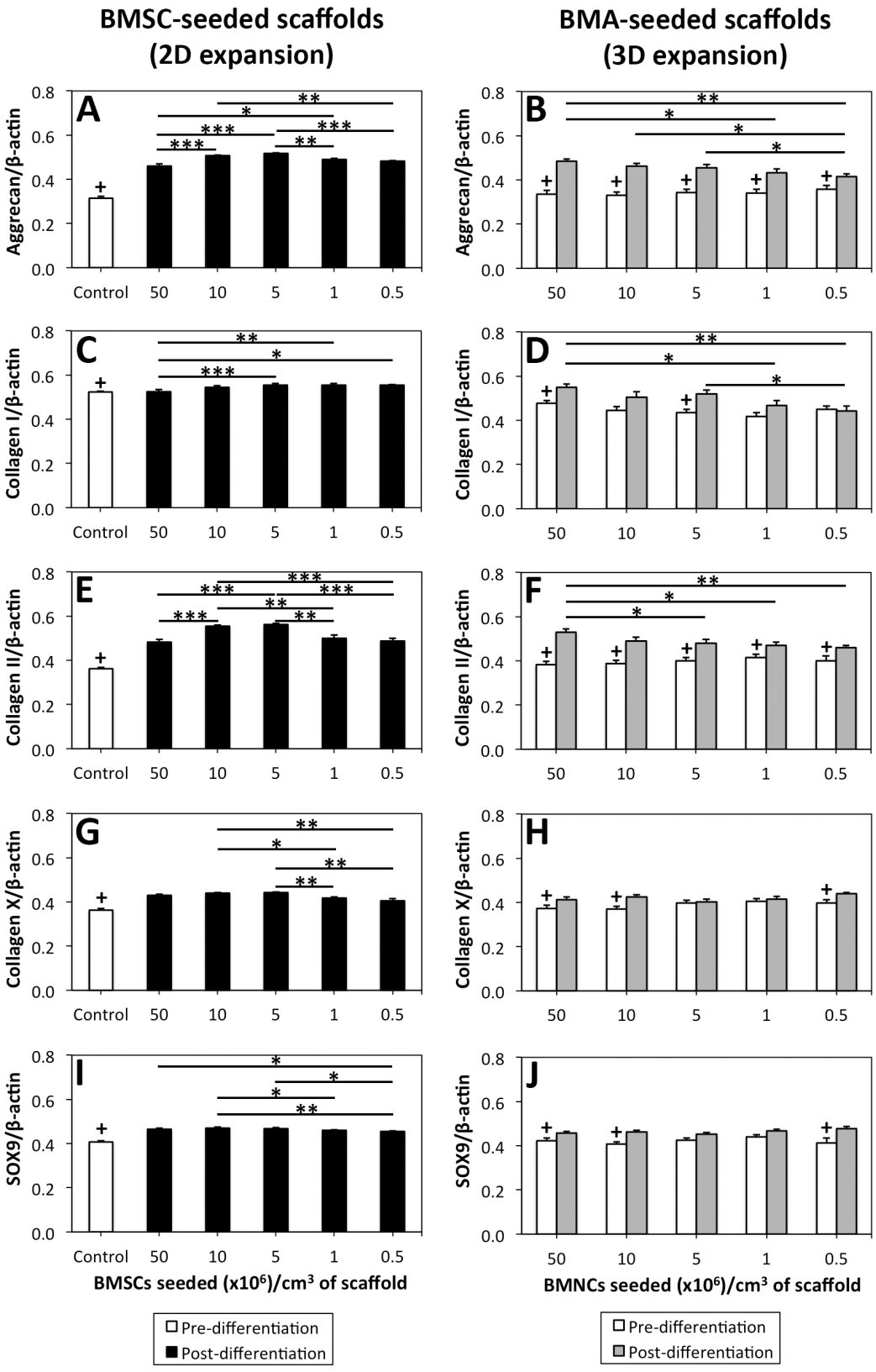
BMSC-seeded scaffolds
(2D expansion)
BMA-seeded scaffolds
(3D expansion)
A
B
C
D
E
F
G
H
I
J
Aggrecan/β-actin
Collagen I/β-actin
Collagen II/β-actin
Collagen X/β-actin
SOX9/β-actin
0.0
0.2
0.4
0.6
0.8
Control
50
10
5
1
0.5
BMSCs seeded (x10⁶)/cm³ of scaffold
BMNCs seeded (x10⁶)/cm³ of scaffold
Pre-differentiation
Post-differentiation

Figure 5.4 Gene expression analysis of two- and three-dimensional-expanded bone marrow-derived mesenchymal stromal stem cells seeded within collagen scaffolds. Bone marrow-derived mesenchymal stromal stem cells (BMSCs) were isolated and expanded within two-dimensional (2D) and three-dimensional (3D) environments, differentiated within collagen scaffolds for 21 days and assessed with reverse-transcription polymerase chain reaction (RT-qPCR) using SYBR Green detection. (A, C, E, G, I) Data represent the mean ± standard error of the mean (SEM) of 2D-expanded BMSCs in doublets based on seeding density group. (B, D, F, H, J) Data represent the mean ± SEM of 3D-expanded BMSCs in doublets based on seeding density group. Statistical analysis is represented by unlabeled, not significant; *, significant $p<0.05$; **, significant $p<0.01$; ***, significant $p<0.001$; +, pre-differentiation control value that is significantly different than differentiated BMSC-seeded scaffold ($p<0.05$).

With respect to fibrocartilage-related collagen I mRNA expression, constructs seeded at 5, 1 and 0.5 $\times 10^6$ BMSCs/cm^3 had greater collagen I mRNA expression than 50 $\times 10^6$ BMSCs/cm^3 ($p<0.05$; Figure 5.4C). Expression of hypertrophic cartilage-associated collagen X was greater in constructs containing 10 and 5 BMSCs/cm^3 than those containing 1 and 0.5 $\times 10^6$ BMSCs/cm^3 ($p<0.05$; Figure 5.4G).

In 3D-expanded BMSC-seeded scaffolds, aggrecan and collagen II mRNA expressions were highest in scaffolds seeded with BMA collections containing 50 $\times 10^6$ BMNCs/cm^3 (Figures 5.4B and F). Significantly higher aggrecan mRNA expression was found in scaffolds seeded at 50, 10 and 5 $\times 10^6$ BMNCs/cm^3 than 0.5 $\times 10^6$ BMNCs/cm^3 ($p<0.05$), although the difference was most significant between 50 and 0.5 $\times 10^6$ BMNCs/cm^3 ($p<0.01$; Figure 5.4B). Hyaline cartilage-related collagen II mRNA expression was significantly higher in scaffolds seeded at 50 $\times 10^6$ BMNCs/cm^3 than 5, 1 or 0.5 $\times 10^6$ BMNCs/cm^3 ($p<0.05$), and approached a significantly higher level in scaffolds seeded at 50 $\times 10^6$

BMNCs/cm^3 relative to 10 $\times 10^6$ BMNCs/cm^3 ($p=0.07$; Figure 5.4F). Post-differentiation collagen II mRNA was significantly greater than pre-differentiation collagen II mRNA in all seeding density groups ($p<0.05$). For fibrocartilage-related collagen I, mRNA expression was more pronounced in constructs containing 50 $\times 10^6$ BMNCs/cm^3 than 1 or 0.5 $\times 10^6$ BMNCs/cm^3 ($p<0.05$; Figure 5.4D). Significant differences were not noted between seeding density groups for collagen X and SOX9 mRNA expressions ($p=0.13$ and 0.25; respectively; Figures 5.4H and J). The collagen II/X ratio was higher in scaffolds seeded at 50 $\times 10^6$ BMNCs/cm^3 than 10, 1 and 0.5 $\times 10^6$ BMNCs/cm^3 ($p<0.05$). The collagen II/I ratio was higher in scaffolds seeded at 0.5 $\times 10^6$ BMNCs/cm^3 than 50 and 5 $\times 10^6$ BMNCs/cm^3 ($p<0.05$).

To determine whether BMNC seeding density during 3D isolation and expansion primed chondrogenic gene expression before onset of differentiation, 3D-expanded BMSC-seeded scaffolds were also assessed for gene expression directly following expansion. Seeding density did not significantly impact mRNA expressions of aggrecan, collagen I, collagen II, collagen X, or SOX9 ($p=0.82$, 0.09, 0.64, 0.40, 0.40, respectively; Figure 5.4 right column).

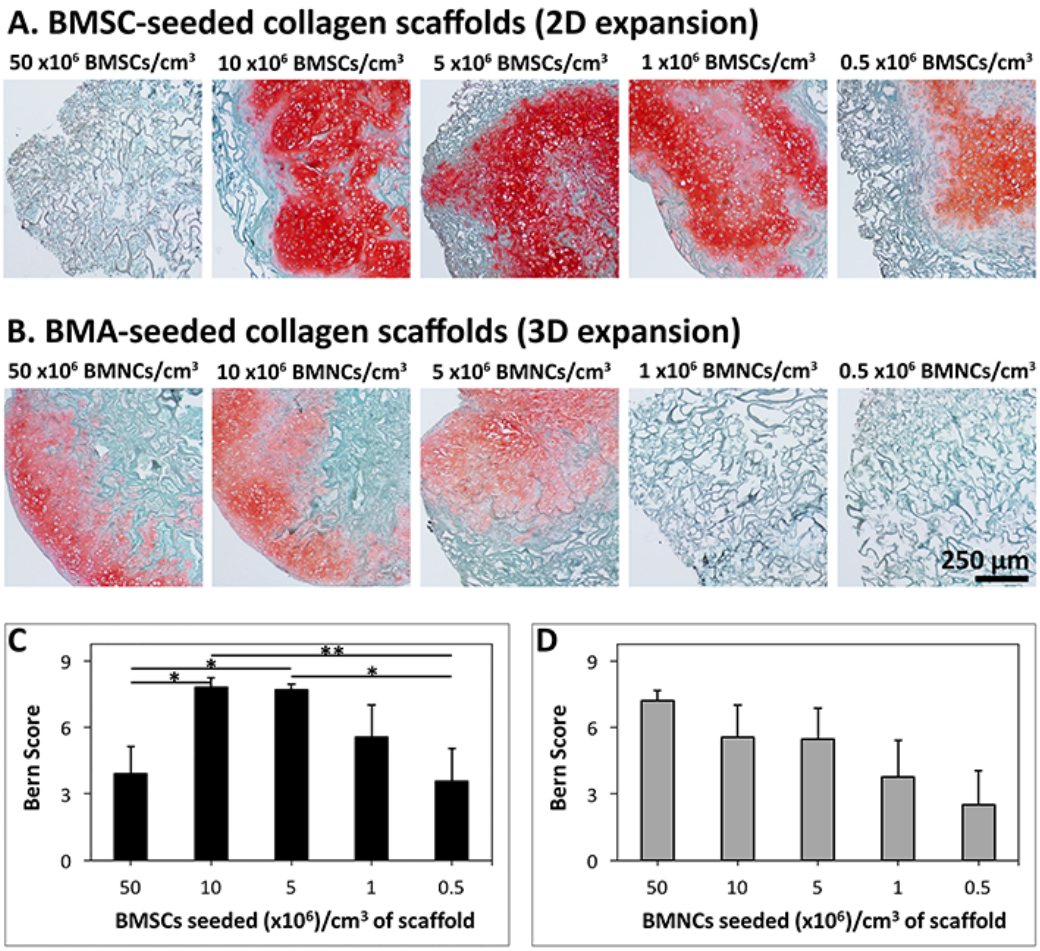

Figure 5.5 Histological analysis and scoring of two- and three-dimensional-expanded bone marrow-derived mesenchymal stromal stem cell-seeded collagen scaffolds. Bone marrow-derived mesenchymal stromal stem cells (BMSCs) were isolated and expanded within two-dimensional (2D) and three-dimensional (3D) environments, and differentiated within collagen scaffolds for 21 days. Thereafter, constructs were fixed, sectioned at 5-µm thickness and stained with safranin O and fast green. Presented photomicrographs represent cell-scaffold constructs derived from (A) 2D-expanded BMSCs seeded at 50, 10, 5, 1, or 0.5 $\times 10^6$ BMSCs/cm^3, and (B) 3D-expanded BMSCs seeded at 50, 10, 5, 1, or 0.5 $\times 10^6$ BMNCs/cm^3 (cells from donor Z28; 7× combined magnification of objective and camera lenses). (C) Mean (± standard error of the mean [SEM]) Bern score of 2D-expanded BMSCs from five donors based on seeding density group. (D) Mean (± SEM) Bern score of 3D-expanded BMSCs from five donors based on seeding density group. Statistical analysis is represented by unlabeled, not significant; *, significant $p<0.05$; **, significant $p<0.01$.

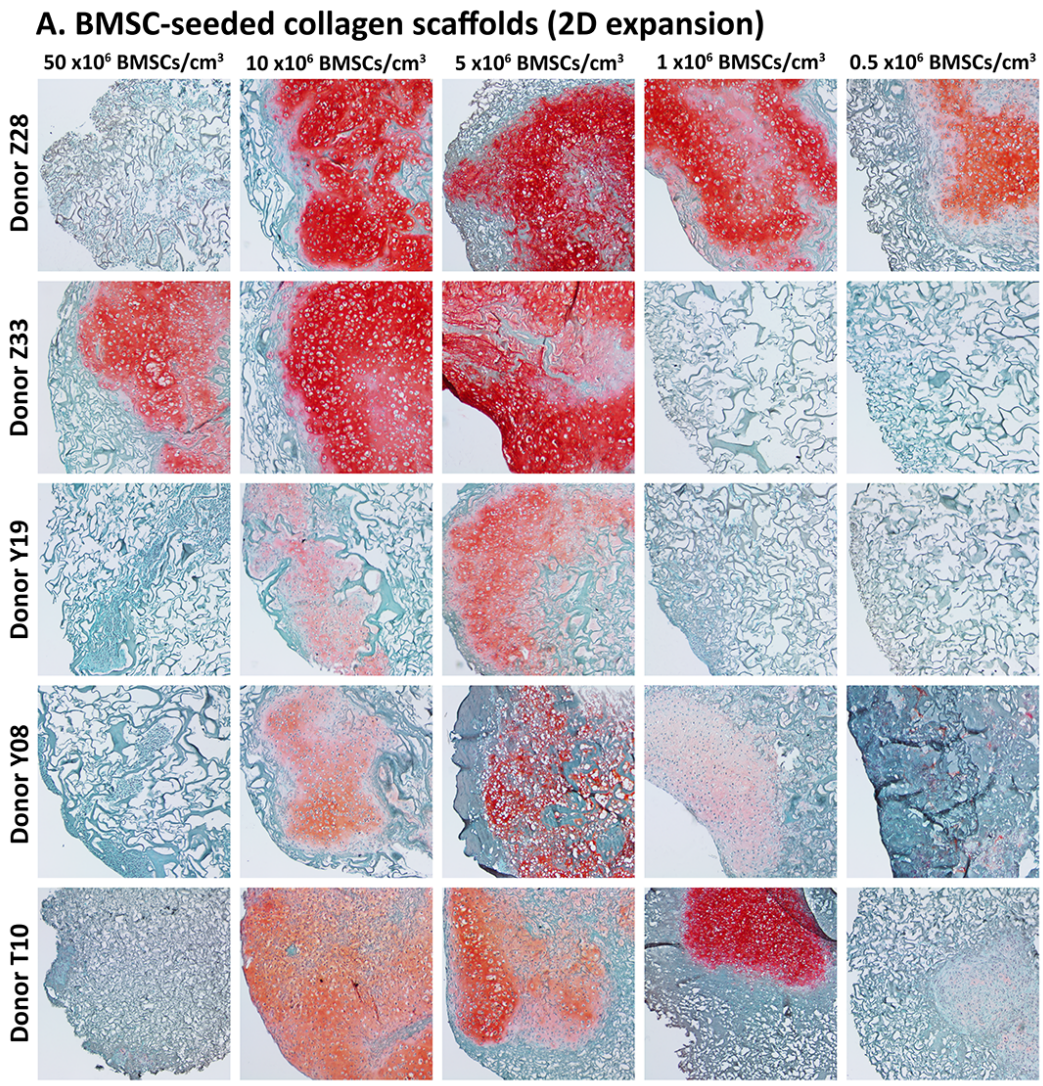

Figure 5.6A Histological analysis of chondrogenic proteoglycan content within two-dimensional expanded bone marrow-derived mesenchymal stromal stem cell-seeded collagen scaffolds. Bone marrow-derived mesenchymal stromal stem cells (BMSCs) were isolated and expanded within a two-dimensional (2D) environment and differentiated within collagen scaffolds for 21 days. Thereafter, constructs were fixed, sectioned at 5-µm thickness and stained with safranin O and fast green. Presented photomicrographs represent cell-scaffold constructs derived from 2D-expanded BMSCs seeded at 50, 10, 5, 1, or 0.5 $\times 10^6$ BMSCs/cm^3 from five donors (7× combined magnification of objective and camera lenses).

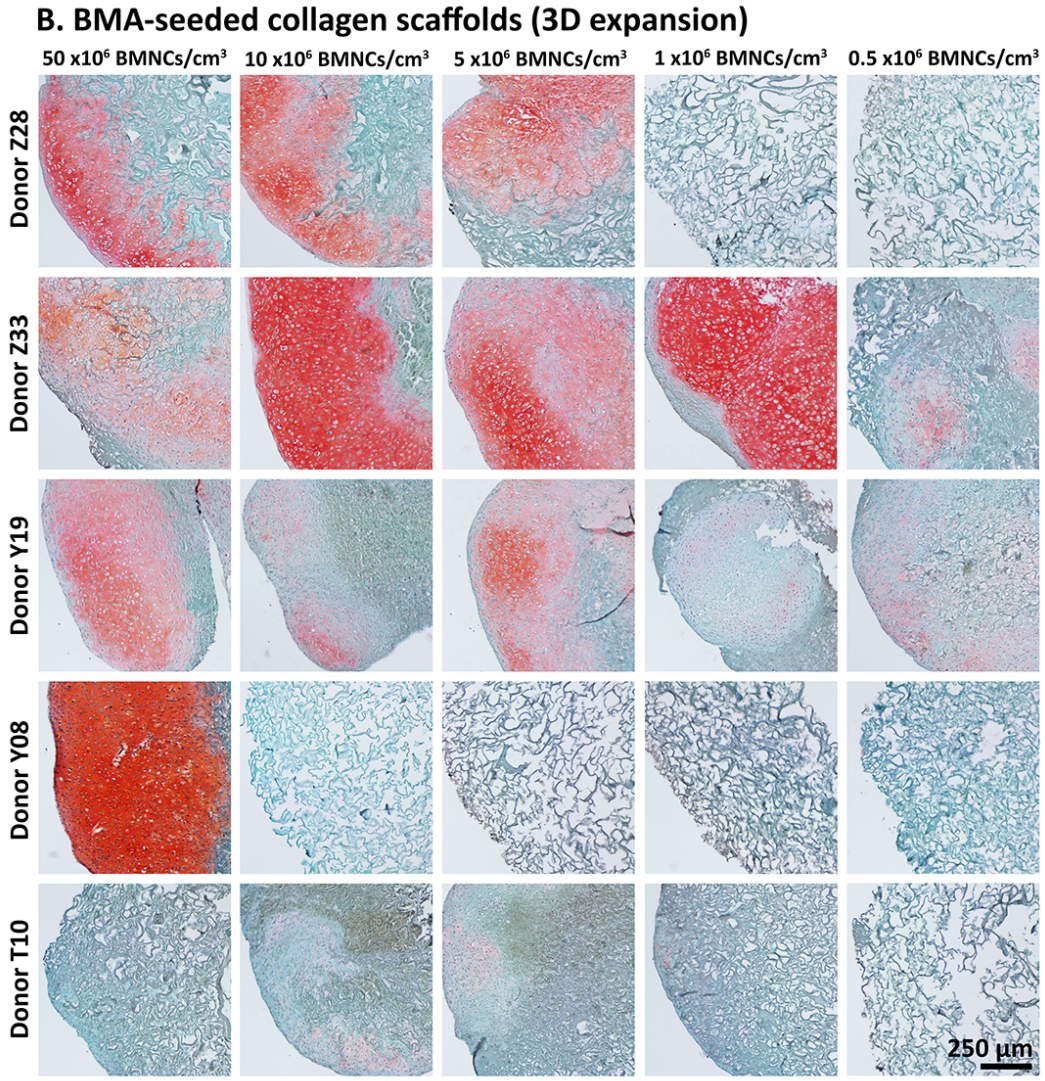

Figure 5.6B Histological analysis of chondrogenic proteoglycan content within three-dimensional-expanded bone marrow-derived mesenchymal stromal stem cell-seeded collagen scaffolds. Bone marrow-derived mesenchymal stromal stem cells (BMSCs) were isolated and expanded within a three-dimensional (3D) environment and differentiated within collagen scaffolds for 21 days. Thereafter, constructs were fixed, sectioned at 5-µm thickness and stained with safranin O and fast green. Presented photomicrographs represent cell-scaffold constructs derived from 3D-expanded BMSCs seeded at 50, 10, 5, 1, or 0.5 $\times 10^6$ bone marrow-derived mononucleated cells (BMNCs)/cm^3 from five donors (7× combined magnification of objective and camera lenses).

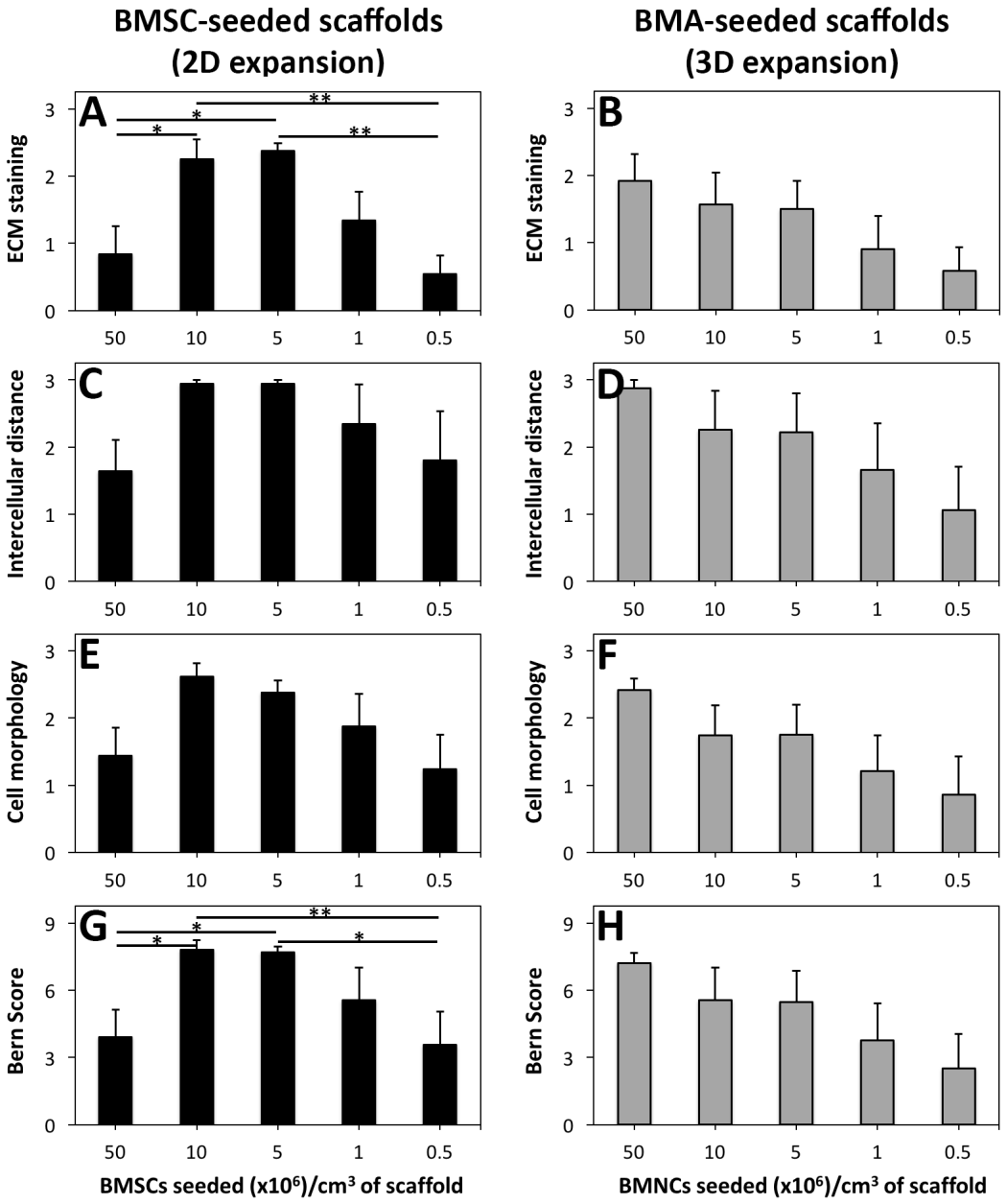

Figure 5.7 Histological scoring of two- and three-dimensional-expanded bone marrow-derived mesenchymal stromal stem cell-seeded collagen scaffolds. Stained sections from two-dimensional (2D)- and three-dimensional (3D)-expanded BMSC-seeded scaffolds were assessed using the Bern score. (A, C, E, G). Data represent the mean ± standard error of the mean (SEM) of extracellular matrix (ECM) staining, intercellular distance, cell morphology, and Bern score of sections containing 2D-expanded BMSC-seeded scaffolds from five donors. (B, D, F, H) Data represent the corresponding subscores and Bern score of sections containing 3D-expanded BMSC-

seeded scaffolds from the same five donors. Statistical analysis is represented by unlabeled, not significant; *, significant $p<0.05$; **, significant $p<0.01$.

5.3.4 Seeding density of two- and three-dimensional-expanded bone marrow-derived mesenchymal stromal stem cells affected chondrogenic extracellular matrix deposition

In 2D-expanded BMSC-seeded scaffolds, safranin O staining of proteoglycans appeared to be most pronounced in scaffolds seeded at 10 and 5 $\times 10^6$ BMSCs/cm^3, although abundant staining was also apparent in scaffolds seeded at other densities (Figures 5.5A and 5.6A). Accordingly, Bern scores were highest in scaffolds seeded at 10 and 5 $\times 10^6$ BMSCs/cm^3 (7.8 ± 0.4 and 7.7 ± 0.3, respectively; Figures 5.5C and 5.7). Scores for these densities were significantly larger than those for 50 and 0.5 $\times 10^6$ BMSCs/cm^3 ($p<0.05$).

Analysis of proteoglycan quantity demonstrated that total GAG, GAG/DNA and GAG/cell were highest in scaffolds seeded at 10 and 5 $\times 10^6$ BMSCs/cm^3 (Figures 5.8A, E and G). There was not a significant difference between 10 and 5 $\times 10^6$ BMSCs/cm^3 for these parameters ($p=0.72$, 0.18 and 0.21, respectively). Constructs containing 5 $\times 10^6$ BMSCs/cm^3 had significantly higher GAG/DNA than constructs containing 50, 1 and 0.5 $\times 10^6$ BMSCs/cm^3 ($p<0.01$; Figure 5.8E). Constructs containing 10 $\times 10^6$ BMSCs/cm^3 had significantly higher GAG/DNA than scaffolds seeded with 50 and 0.5 $\times 10^6$ BMSCs/cm^3 ($p<0.01$), but were marginally different than 1 $\times 10^6$ BMSCs/cm^3 ($p=0.50$; Figure 5.8E). Collagen II deposition was pronounced in scaffolds seeded at 10, 5, 1, and 0.5

$\times 10^6$ BMSCs/cm^3, while scaffolds seeded at all densities appeared to lack abundant collagen I deposition (Figure 5.9A).

During chondrogenic differentiation of 2D-expanded BMSCs, cell counts decreased in scaffolds that were seeded at densities of 50 and 10 $\times 10^6$ BMSCs/cm^3 ($p<0.05$), while cell counts increased in scaffolds that were seeded at densities of 5, 1 and 0.5 $\times 10^6$ BMSCs/cm^3 ($p<0.05$; Figure 5.10A). At the end of the differentiation period, cell counts were not significantly different between scaffolds seeded at 10 and 5 $\times 10^6$ BMSCs/cm^3 ($p=0.19$). There was also not a significant difference between 1 and 0.5 $\times 10^6$ BMSCs/cm^3 ($p=0.27$). Cell counts between other seeding groups were notably different ($p<0.05$).

Scaffolds seeded with 3D-expanded BMSCs contained cartilaginous proteoglycans following differentiation. Proteoglycan staining appeared to be most pronounced in scaffolds seeded at 50, 10 and 5 $\times 10^6$ BMNCs/cm^3 (Figure 5.5), although variability was noted between donors and cells from one donor (Z33) produced large depositions of proteoglycans at 1 $\times 10^6$ BMNCs/cm^3 (Figure 5.6B). Bern scores were highest in scaffolds seeded at 50 $\times 10^6$ BMNCs/cm^3 (7.2 ± 0.5; Figures 5.5D and 5.7). However, a significant difference in scores between seeding densities was not present based on Kruskal-Wallis ANOVA ($p=0.16$).

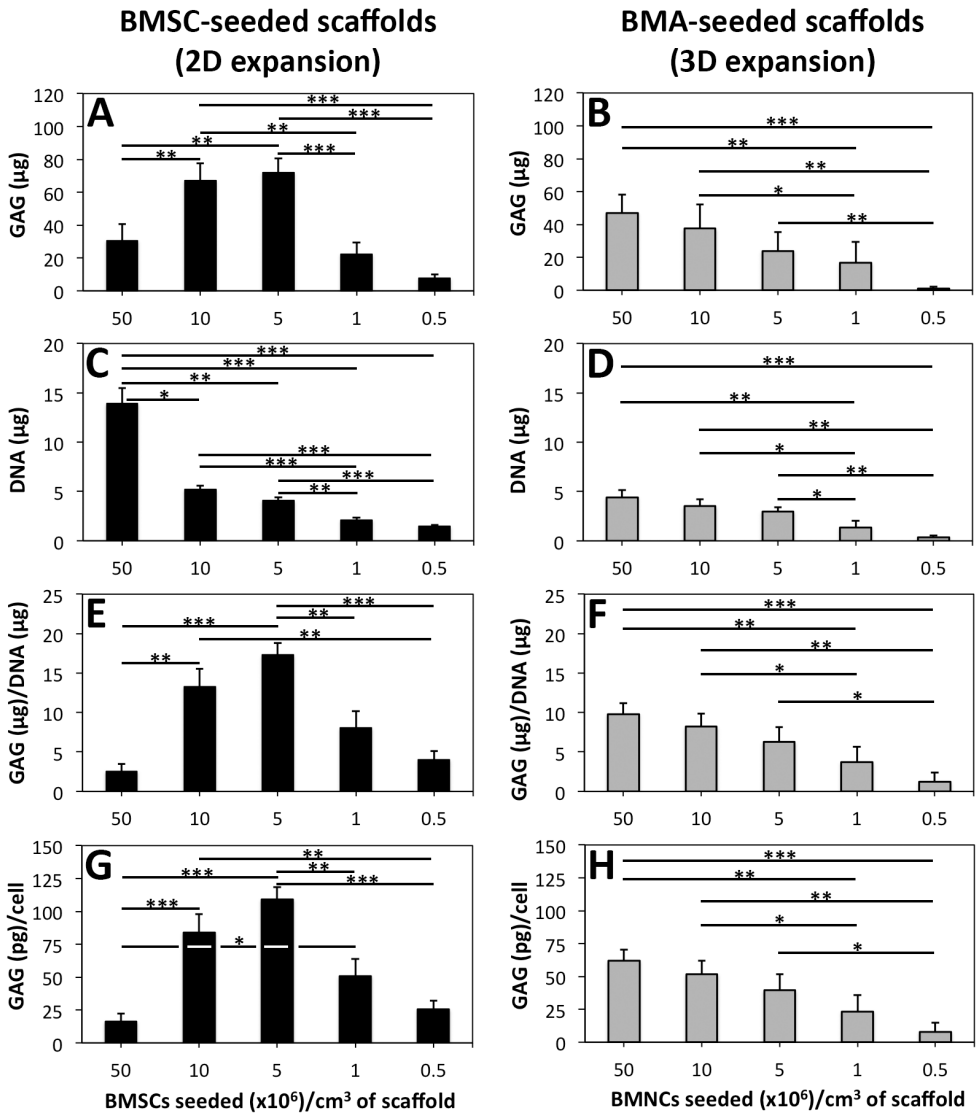

Figure 5.8 Glycosaminoglycan and deoxyribonucleic acid quantification of two- and three-dimensional-expanded bone marrow-derived mesenchymal stromal stem cell-seeded collagen scaffolds. (A, C, E, G) Data represent the mean ± standard error of the mean (SEM) of glycosaminoglycan (GAG), deoxyribonucleic acid (DNA), GAG/DNA, and GAG/cell within constructs from six donors in doublets based on bone marrow-derived mesenchymal stromal stem cell (BMSC) seeding density in two-dimensional (2D)-expanded BMSC-seeded scaffolds. (B, D, F, H) Data represent the mean ± SEM of GAG, DNA, GAG/DNA, and GAG/cell within constructs from six donors in doublets based on bone marrow-derived mononucleated cell (BMNC) seeding density in three-dimensional (3D)-expanded BMSC-seeded scaffolds. Statistical analysis is represented by unlabeled, not significant; *, significant $p<0.05$; **, significant $p<0.01$; ***, significant $p<0.001$.

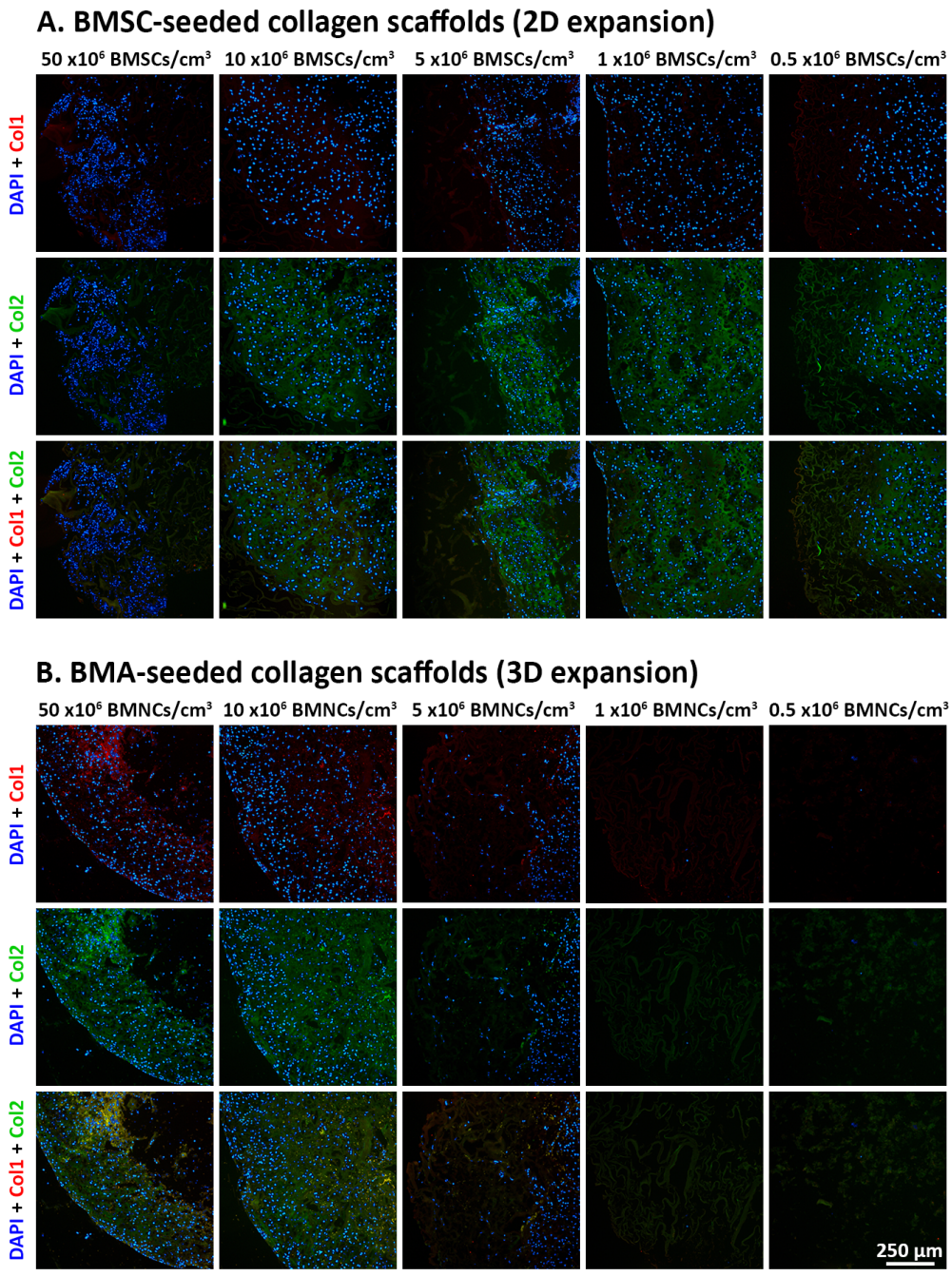

Figure 5.9 Immunofluorescence analysis of collagen I and collagen II content within two- and three-dimensional-expanded bone marrow-derived mesenchymal stromal stem cell-seeded collagen scaffolds. Bone marrow-derived mesenchymal stromal stem cells (BMSCs) were isolated and expanded within two-dimensional (2D) and three-dimensional (3D) environments and differentiated within collagen scaffolds for 21 days in chondrogenic medium. Thereafter, constructs were fixed, sectioned at 5-µm thickness and processed for visualization of cells with

4',6-diamidino-2-phenylindole (DAPI; blue), collagen I (Col I; red) and collagen II (Col II; green). Presented photomicrographs represent cell-scaffold constructs derived from (A) 2D-expanded BMSCs seeded at 50, 10, 5, 1, or 0.5 $\times 10^6$ BMSCs/cm^3, and (B) 3D-expanded BMSCs seeded at 50, 10, 5, 1, or 0.5 $\times 10^6$ bone-marrow-derived mononucleated cells (BMNCs)/cm^3 (cells from donor Z28; 7× combined magnification of objective and camera lenses).

Immunofluorescence controls (see below). From left to right, presented photomicrographs represent three positive controls consisting of hyaline cartilage and subchondral bone, inner third meniscus, and outer third meniscus from the stifle joint of sheep, and a negative control consisting of a BMSC-seeded scaffold processed with a secondary antibody and DAPI but no primary antibody (7× combined magnification of objective and camera lenses).

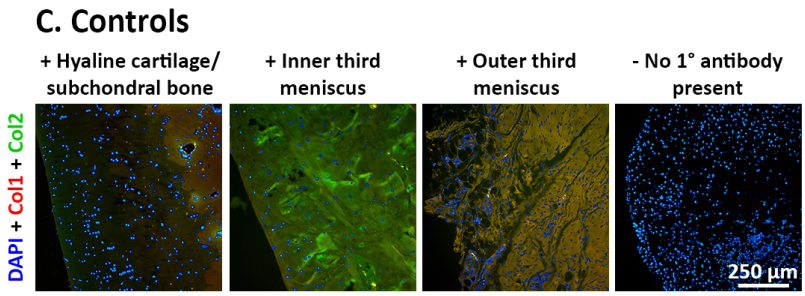

Quantitative analysis of proteoglycan deposition demonstrated that seeding at 50 $\times 10^6$ BMNCs/cm^3 led to higher total GAG, GAG/DNA and GAG/cell than scaffolds seeding at 1 $\times 10^6$ BMNCs/cm^3 ($p<0.01$) and 0.5 $\times 10^6$ BMNCs/cm^3 ($p<0.001$; Figures 5.8B, F and H). For these parameters, less significant differences were noted between 10 $\times 10^6$ BMNCs/cm^3 and lower densities of 1 $\times 10^6$ BMNCs/cm^3 ($p<0.05$) and 0.5 $\times 10^6$ BMNCs/cm^3 ($p<0.01$). Scaffolds seeded at 5 $\times 10^6$ BMNCs/cm^3 also had higher total GAG, GAG/DNA and GAG/cell than scaffolds seeded at 0.5 $\times 10^6$ BMNCs/cm^3 ($p<0.05$). Immunofluorescence indicated deposition of both collagens I and II, particularly in scaffolds seeded at 50 and 10 $\times 10^6$ BMNCs/cm^3 (Figure 5.9B).

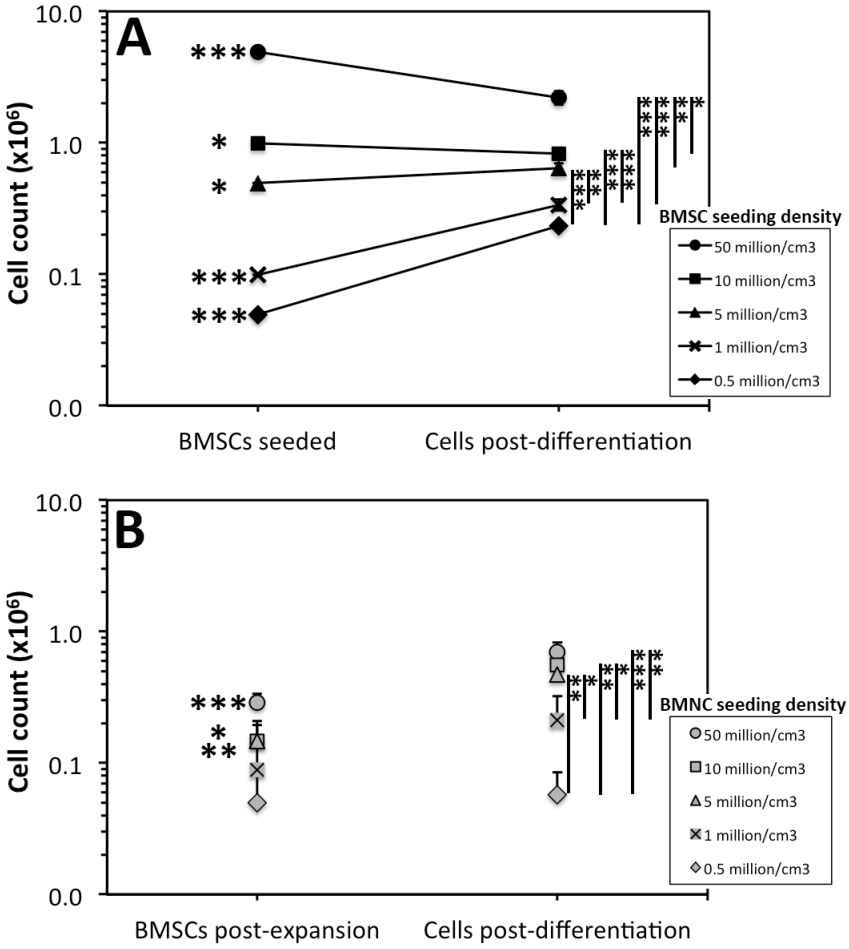

Figure 5.10 Peri-differentiation cell counts of two- and three-dimensional-expanded bone marrow-derived mesenchymal stromal stem cell-seeded collagen scaffolds. (A) Bone marrow-derived mesenchymal stromal stem cells (BMSCs) were isolated and expanded within a two-dimensional (2D) environment in tissue-culture flasks containing expansion medium, seeded at specific cell counts within collagen scaffolds to create five seeding densities and differentiated for 21 days in chondrogenic medium. Deoxyribonucleic acid (DNA) levels were then quantified and used to calculate cell count following differentiation. (B) Bone marrow aspirates (BMAs) were seeded within a three-dimensional environment in collagen scaffolds to create five bone marrow-derived mononucleated cell (BMNC) densities, cultured in expansion medium, and subsequently differentiated within chondrogenic medium for 21 days. DNA levels were quantified in one group of scaffolds after expansion and another group of scaffolds after differentiation. Data represent the mean ± standard error of the mean of cell counts from six donors. Statistical analysis is represented by unlabeled, not significant; *, significant $p<0.05$; **, significant $p<0.01$; ***, significant $p<0.001$.

Following chondrogenic culture of 3D-expanded BMSC-seeded scaffolds, cell counts were not significantly different between scaffolds seeded at 50 and 10 $\times 10^6$ BMNCs/cm^3, or between scaffolds seeded at 1 and 0.5 $\times 10^6$ BMNCs/cm^3 ($p \geq 0.22$; Figure 5.10B). Seeding at 1 and 0.5 $\times 10^6$ BMNCs/cm^3 resulted in post-differentiation BMSC counts of 0.21 ± 0.11 and $0.06 \pm 0.03 \times 10^6$. Considerable variation in BMSC counts between donors were noted at these lowest BMNC seeding densities as some scaffolds appeared to have very low cell numbers present following differentiation, while others contained sufficient cell numbers to produce significant levels of cartilaginous ECM (and Figures 5.6B and 5.9B).

5.4 Discussion

The major finding of this study is that isolation and expansion of ovine BMSCs under 2D and 3D conditions yielded cell populations capable of producing hyaline-like neo-cartilage *in vitro*, and chondrogenic differentiation of these cells was dependent on seeding density within collagen I scaffolds. Optimal seeding densities were identified for 2D- and 3D-expanded BMSCs.

Two-dimensional isolation and expansion were performed using a conventional protocol within tissue-culture flasks [31, 32]. Whole BMA was seeded into flasks containing expansion medium in an attempt to maintain the natural bone marrow microenvironment on the 2D surface of the tissue-culture flask during isolation and the first week of expansion [261, 332, 405], while avoiding the loss of cells and mediators that could be discarded through the use of

cell separation techniques [31, 32]. An extended expansion period beyond P2 was not used in this study as it was previously shown that prolonged expansion leads to de-differentiation, senescence and loss of multipotential capacity of BMSCs [334, 368].

Three-dimensional isolation and expansion were performed by seeding BMA collections containing defined numbers of BMNCs within scaffolds followed by culture in expansion medium. The goal of this technique was to maintain BMSCs within a 3D environment and to avoid subjecting cells to the artificial environment within tissue-culture flasks. Presumably, BMSCs adhered to the scaffold through integrin-mediated binding to type I collagen [414], while other cellular and chemical components of bone marrow[258, 415-417] were entrapped within scaffold pores but washed away over the course of the expansion period with media changes. Bone marrow aspirate collections were seeded within scaffolds to create seeding densities of 50, 10, 5, 1 and 0.5 $\times 10^6$ BMNCs/cm^3. The total number of BMSCs present following isolation and expansion was 5.8% of the initial BMNC count in the scaffolds seeded at 50 $\times 10^6$ BMNCs/cm^3. The percentage of post-expansion BMSCs increased as BMNC seeding density decreased, and was measured to be 100.3% in scaffolds seeded at the lowest density of 0.5 $\times 10^6$ BMNCs/cm^3. Increased proliferation may have played a role in this effect, as population doublings were higher in constructs seeded at lower densities. Augmented proliferation at lower density was reported previously during both 2D and 3D expansion [418-421], and could involve reduced contact

inhibition and increased nutrient availability per cell [33]. Higher probability of attachment at the time of seeding due to a relatively increased availability of scaffold binding sites could also increase BMSC count at lower BMNC seeding densities.

The impact of seeding density on chondrogenesis was evaluated after 21 days of *in vitro* culture. To date, multiple parameters have been used in the literature to assess hyaline-like chondrogenic capacity including proteoglycan content, histological scoring, GAG/DNA, collagen II quantity, and collagen II/I ratio [31, 32, 346, 369, 405, 413]. These parameters involve either gene expression or measurement of macromolecule deposition in the ECM. A number of assays were employed in the study at hand to provide a rigorous and multimodal evaluation of engineered tissue. Neo-cartilage was considered hyaline-like if: (1) collagen II was present based on collagen II mRNA expression, collagen II/I mRNA ratio and collagen II immunofluorescence; and (2) proteoglycan was abundant as measured through aggrecan mRNA expression, safranin O staining, Bern score, total GAG, and GAG/DNA. Neo-cartilage was considered to be superior if these parameters were more pronounced in one construct relative to another construct.

Following 2D expansion, BMSCs seeded at all densities were shown to be capable of hyaline-like cartilaginous tissue formation based on increased collagen II and aggrecan mRNA expressions relative to controls, and proteoglycan

deposition. Collagen scaffolds seeded at 10 and 5 $\times 10^6$ BMSCs/cm^3 had the highest mRNA expressions of hyaline cartilage-related collagen II, aggrecan and SOX9, although expressions of collagens I and X that relate to fibrocartilage and hypertrophic cartilage, respectively, were also highest in these constructs. Scaffolds seeded at 10 and 5 $\times 10^6$ BMSCs/cm^3 produced the highest levels of ECM proteoglycan deposition and were found to be superior based on histological scoring. Collagen II deposition was apparent in scaffolds seeded at 0.5-10 $\times 10^6$ BMSCs/cm^3, while collagen I was lacking. Constructs containing 50 $\times 10^6$ BMSCs/cm^3 at the time of seeding displayed stunted chondrogenesis in comparison to 10 and 5 $\times 10^6$ BMSCs/cm^3, which could relate to cell crowding, nutrient limitation and relatively less volume available for ECM deposition [33, 422]. These findings suggest that the optimal seeding density for chondrogenesis of 2D-expanded BMSCs within collagen scaffolds is 5-10 $\times 10^6$ BMSCs/cm^3.

In 3D-expanded BMSC-seeded scaffolds, constructs seeded at all densities produced increased collagen II and aggrecan mRNA expressions relative to controls, and proteoglycan deposition. Constructs seeded at 50 $\times 10^6$ BMNCs/cm^3 had the highest levels of aggrecan mRNA expression and ECM proteoglycan deposition, although scaffolds seeded at 10 and 5 $\times 10^6$ BMNCs/cm^3 also had higher levels of proteoglycans in comparison to lower seeding densities. The Bern score was highest in scaffolds seeded at 50 $\times 10^6$ BMNCs/cm^3, but a significant difference was not demonstrated between seeding groups. Collagen II mRNA expression was highest in scaffolds seeded at 50 $\times 10^6$ BMNCs/cm^3. Based on

immunofluorescence, deposition of collagen II was particularly notable within scaffolds seeded at both 50 and 10 $\times 10^6$ BMNCs/cm^3. Collagen I mRNA expressions was highest in scaffolds seeded at 50, 10 and 5 $\times 10^6$ BMNCs/cm^3, while immunofluorescence showed significant deposition in scaffolds seeded at 50 and 10 $\times 10^6$ BMNCs/cm^3. The results of this study suggest that a seeding density of 50 $\times 10^6$ BMNCs/cm^3 leads to the highest level of hyaline-like chondrogenesis, although it is possible that higher densities that were not assessed in this study could further augment chondrogenesis.

At present, there is a paucity of literature examining the impact of BMSC seeding density on chondrogenesis. Several *in vitro* studies have assessed the impact of mature chondrocyte density on chondrogenesis. Hansen *et al.* demonstrated that seeding at 1.2 $\times 10^6$ chondrocytes/cm^3 augmented chondrogenesis within a porous methoxypolyethylene glycol-polylactic-co-glycolic acid scaffold relative to higher densities of 4-20 $\times 10^6$ chondrocytes/cm^3 [412]. Mahmoudifar *et al.* and Vunjak-Novakovic *et al.* showed superior chondrogenesis within polyglycolic acid scaffolds seeded with 25-27 $\times 10^6$ chondrocytes/cm^3 in comparison to lower densities of 5-15 $\times 10^6$ chondrocytes/cm^3 [423, 424]. Francioli *et al.* reported that chondrogenesis improved by increasing cell density within porous collagen II scaffolds from 25 to 66 $\times 10^6$ chondrocytes/cm^3 [393]. In agarose hydrogels, Huang *et al.* demonstrated that a density of 9 $\times 10^6$ chondrocytes/cm^3 was superior to 3-6 $\times 10^6$

chondrocytes/cm^3, while Mauck *et al.* found that 60 $\times 10^6$ chondrocytes/cm^3 augmented chondrogenesis relative to 20 $\times 10^6$ chondrocytes/cm^3 [425, 426].

Cell density analysis in this study was based on the number of cells and volume of scaffold present during seeding, as this is the time point at which these parameters would be known in a clinical setting [39]. It was demonstrated that cell count following differentiation varied in comparison to pre-differentiation cell count, and this could have involved a balance between multiple factors including cell loss during scaffold seeding and culture, and ongoing proliferation during the differentiation period [427]. With the assumption that construct volume was maintained during chondrogenesis, final cell densities at the end of *in vitro* chondrogenesis were 22.3, 8.4, 6.5, 3.4, and 2.4 $\times 10^6$ BMSCs/cm^3 for 2D-expanded BMSCs seeded at 50, 10, 5, 1, and 0.5 $\times 10^6$ BMSCs/cm^3, respectively, and 7.1, 5.6, 4.8, 2.1, and 0.6 $\times 10^6$ BMSCs/cm^3 for 3D-expanded BMSCs seeded at 50, 10, 5, 1, and 0.5 $\times 10^6$ BMNCs/cm^3 respectively. Cell-seeded collagen scaffolds have been shown previously to decrease in volume during chondrogenesis as a result of cell-mediated contraction and degradation of scaffold biomaterials [428]. Therefore, cell densities at the end of chondrogenic culture were potentially higher than calculated.

Although both 2D- and 3D-expanded BMSC-seeded collagen scaffolds were assessed and shown to produce bioengineered tissue with properties of hyaline cartilage, a direct comparison of these methods was not performed given

that the properties of the cells populating scaffolds at the time of isolation and following culture may have differed. Two dimensional-expanded BMSCs were shown to have qualities of plastic adherence and trilineage differentiation. Previously, our group characterized cell surface markers of BMSCs isolated and expanded using this isolation method [332]. Although 3D-expanded BMSCs were derived from the same BMA collections as 2D-expanded BMSCs, the cells that adhered to the collagen scaffold during 3D isolation were not characterized and may have derived from a different subpopulation of BMSCs than those that adhered to plastic during 2D isolation. It was shown previously that different subpopulations of BMSCs are present based on adherence and cell surface markers [264, 266]. Future study is required to characterize cells derived from 3D isolation and to compare these cells to those derived from 2D methods utilizing whole BMA and cell fractions (BMNCs).

This study has some limitations. Static culture conditions were used, which may have led to less uniform densities throughout scaffolds relative to dynamic conditions. Secondly, ovine rather than human BMSCs were used. Sheep are routinely involved as animal models in cartilage engineering studies [100, 274, 308]. However, differences between species could impact the clinical applicability of our findings. Aspirates were derived from sheep at an age that is consistent with skeletal maturity and cartilage maturity based on zonal architecture, presence of a continuous calcified cartilage layer and lack of spontaneous cartilage repair [429]. Given that sheep have a life expectancy of 10-

12 years, the sheep in this study (mean age of 3.3 years) could correspond to an adult human population that would be amenable to cell-based cartilage restoration techniques. Only female sheep were included as donors. A difference in *in vitro* chondrogenesis between cells from male and female animals and humans has been demonstrated previously with a higher chondrogenic capacity demonstrated in males [430, 431]. Although the use of female sheep potentially reduced variability that may have been caused through the use of a mixed sample of animals, the impact of seeding density on chondrogenesis could be different in male animals. Thirdly, an *in vitro* model was used, and the applicability of the conclusions to clinical use is unclear. It is possible that remodeling that occurs *in vivo* over time could offset differences that are apparent within this *in vitro* model [412, 432]. Fourthly, seeding of cells within biomaterial scaffolds was considered to be an effective process in this study and the number of cells that did not adhere was not determined. Lastly, during the calculation of population doublings during 3D expansion, the initial number of BMSCs present following isolation required the use of a ratio derived from the CFU-F assay. Given that the CFU-F involved plastic adherence, it is possible that the fraction of BMSCs present from the BMNC pool following 3D isolation was different than that calculated from the CFU-F assay.

5.5 Conclusion

BMSCs isolated and expanded in 2D and 3D environments are capable of producing hyaline-like cartilaginous tissue within a porous collagen I scaffold.

Chondrogenesis appeared to be most pronounced with seeding densities of 5-10 $\times 10^6$ BMSCs/cm^3 and 50 $\times 10^6$ BMNCs/cm^3 for 2D and 3D expansion protocols, respectively. Accordingly, these densities could be considered when seeding collagen I scaffolds in BMSC transplantation protocols.

Chapter 6

Articular Cartilage Repair with Mesenchymal Stromal Stem Cells following Isolation, Expansion and Chondrogenic Priming in Normoxic and Hypoxic Conditions: a Preclinical Pilot Study

Troy D. Bornes, Adetola B. Adesida* and Nadr M. Jomha*

***Co-senior authors**

6.1 Introduction

Bone marrow-derived mesenchymal stromal stem cells (BMSCs) are a promising cell source for treating articular cartilage defects [363]. Collection of bone marrow containing BMSCs is performed by needle aspiration with minimal invasiveness and adequate cell numbers for transplantation may be attained with relative ease given the rapid proliferation profile of these cells [34, 333, 433]. BMSCs are capable of differentiation into chondrocytes and production of extracellular matrix (ECM) that is consistent with hyaline cartilage [31, 32, 434]. Several studies have demonstrated resurfacing of focal chondral defects in animal and human joints with BMSCs, although inconsistent outcomes have been reported based on macroscopic assessment, histological analysis, magnetic

resonance imaging (MRI), and clinical scores [29, 38, 39, 41, 43, 45, 46, 254, 317]. Cartilaginous repair tissue quality has been shown to correlate with post-operative function in clinical studies [45, 254, 320]. Therefore, tissue engineering and transplantation variables are currently under investigation with the goal of improving neo-cartilage quality and outcome.

Several BMSC transplantation protocols have been proposed to date with no clear consensus on technique established [363]. One protocol involves implantation of bone marrow aspirate concentrate, which contains a heterogeneous cell collection that includes BMSCs, on a biomaterial scaffold into a cartilage defect [38, 41, 254]. This protocol allows for aspiration, processing and implantation to occur during the same operative period and avoids the need for *ex vivo* cell culture [254]. However, the number of BMSCs present in each concentrate is not known at the time of implantation. Furthermore, there is evidence to suggest that the BMSC content of concentrates varies between donors and depends on the processing system used [307, 435]. It is therefore unclear whether the implanted concentrate contains an adequate number of BMSCs to differentiate and populate the defect site with cells capable of undergoing chondrogenesis. A second protocol entails isolation and expansion of BMSCs in the laboratory and implantation on scaffolds [39, 43]. Although the BMSCs in this protocol are purified during the isolation process, they are undifferentiated and there is only limited evidence to suggest that they are capable of producing ECM consistent with hyaline cartilage rather than fibrocartilage or bone [43, 256, 316,

339]. A third protocol involves creation of a tissue-engineered construct developed through *ex vivo* culture of BMSC-seeded scaffolds for several weeks to allow for differentiation and ECM production prior to implantation [36, 274, 287, 308]. Although the transplanted construct contains cells that may be inclined to continue down a chondrogenic lineage, this protocol is time consuming and presumably more expensive than shorter protocols [274].

Tissue engineering strategies have been employed within transplantation protocols with the goal of promoting BMSC chondrogenesis and hyaline-like cartilaginous ECM formation. Incubator oxygen tension is a culture variable that has gained attention given the posited role of oxygen in guiding BMSC differentiation in musculoskeletal development [364]. Our group and others have established extensive *in vitro* support for the use of hypoxic incubation to drive BMSC chondrogenesis [332, 369-371, 405]. Hypoxic culture has been shown to augment chondrogenesis following subcutaneous implantation in mouse models [368, 372]. However, pre-implantation hypoxic culture has not been investigated in BMSCs implanted within joints in animals or humans to date.

The first objective of this pilot study was to assess a novel protocol for BMSC transplantation that involved BMSCs that were isolated, expanded, seeded within esterified hyaluronic acid (HYAFF) scaffolds, and chondrogenically primed using a short (4-day) culture period in chondrogenic medium prior to implantation in an ovine model. The rationale of this protocol was to expose

BMSCs to chondrogenic factors with the goal of predisposing them to the chondrogenic lineage while avoiding a time- and resource-intensive differentiation period. Scaffolds composed of HYAFF have been shown to support BMSC chondrogenesis and the formation of hyaline-like cartilaginous tissues *in vitro* in several studies, and have been used clinically in BMSC transplantation protocols involving bone marrow aspirate concentrate [38, 40, 45, 46, 254, 315, 405]. Sheep are routinely used as large-animal models in cartilage research [100, 274, 301, 306, 308]. The second objective of this study was to assess the impact of oxygen tension during pre-implantation culture of BMSCs on neo-cartilage formation *in vivo* within full-thickness cartilage defects. It was hypothesized that chondrogenically primed BMSC-seeded HYAFF scaffolds implanted into full-thickness cartilage defects would produce superior cartilaginous repair tissue to control defects. Secondly, it was hypothesized that BMSC isolation, expansion and chondrogenic priming under hypoxia would yield improved cartilaginous repair tissue in comparison to normoxia.

6.2 Methods

6.2.1 Bone marrow aspiration and processing

The Animal Care and Use Committee at the University of Alberta provided ethical approval for this study. Bone marrow aspirates were obtained from the iliac crest of five female Suffolk sheep with mean age ± standard error of the mean (SEM) of 2.6 ± 0.3 years and mean mass ± SEM of 75.0 ± 5.6 kg (Table 6.1). General anesthesia for the aspiration procedure was attained through

intravenous sedation with 5 μg/kg dexmedetomidine and 2 mg/kg ketamine followed by endotracheal intubation and administration of 2-4% gaseous isoflurane (all from Western Drug Distribution Center, Edmonton, Canada). The sheep were then positioned in lateral decubitus position using a positioning device (Hug-U-Vac, Salem, USA) and the posterolateral pelvic surgical site was clipped and prepared with 10% wt/vol povidone-iodine solution (Betadine, Purdue Pharma, Stamford, USA). A small incision was made over the posterior ilium and an 11-gauge Jamshidi needle (Cardinal Health Canada, Vaughan, Canada) was inserted onto the iliac crest near the posterior superior iliac spine and through cortical bone into the marrow space. Bone marrow aspirate was collected and mixed with 8 ml of heparin (10,000 units/10 ml; Pharmaceutical Partners of Canada, Richmond Hill, Canada). Each aspirate was then filtered with a cell strainer (100-μm pore size; Becton Dickinson Canada, Mississauga, Canada). Staining with crystal violet (Sigma-Aldrich, Oakville, Canada) and hemocytometer counting were used to determine the number of bone marrow mononucleated cells (BMNCs) within an aspirate.

6.2.2 Isolation and expansion of bone marrow-derived mesenchymal stromal stem cells

Bone marrow aspirates containing 8×10^7 BMNCs were seeded within each 150-cm^2 tissue culture flask and submersed in expansion medium containing alpha-minimal essential medium (α-MEM; Corning-Mediatech, Manassas, USA) supplemented with 8.8% vol/vol heat-inactivated fetal bovine serum (FBS), 88.5

units/ml penicillin, 88.5 μg/ml streptomycin, 258.4 μg/ml L-glutamine, 8.8 mM 4-(2-hydroxyethyl)-1-piperazineethanesulfonic acid (HEPES), 885.0 μM sodium pyruvate (all from Life Technologies, Burlington, Canada), and 5 ng/ml fibroblast growth factor-2 (FGF-2; Neuromics, Edina, USA; Appendix 1). Cells were allowed to adhere and grow statically for 7 days under normoxia (21% oxygen) or hypoxia (3% oxygen) at 37°C in a humidified incubator containing 5% carbon dioxide. Flasks from the hypoxic incubator experienced short periods (<5 minutes) of normoxic exposure during media changes. After 7 days, the media were changed twice per week. Once 80% cell confluence was attained, adherent BMSCs were washed with phosphate-buffered saline (PBS), detached using 0.05% wt/vol trypsin-ethylenediaminetetraacetic acid (EDTA; Corning-Mediatech) and expanded to passage two (P2).

Table 6.1 Sheep involved in autologous bone marrow-derived mesenchymal stromal stem cell transplantation

Sheep	Gender	Age (years)	Mass (kg)
Z28	Female	2.0	66
Z01	Female	2.2	71
Z33	Female	2.3	81
Y19	Female	3.2	63
Y08	Female	3.3	94

Proliferation during expansion was assessed via cell counts. Total cell counts of trypsinized BMSCs at P0, P1 and P2 were calculated using trypan blue staining and hemocytometer counting of small aliquots of BMSCs in expansion medium. The number of BMSCs isolated in each flask containing 8×10^7 BMNCs was extrapolated from a colony-forming unit fibroblastic assay previously described [405]. Population doublings were determined using the method described by Solchaga *et al.* [346].

6.2.3 Scaffold seeding and chondrogenic priming

Expanded BMSCs were suspended in chondrogenic medium consisting of Dulbecco's modified Eagle's medium (DMEM) containing 4.5 mg/ml D-glucose, 110 μg/ml sodium pyruvate and L-glutamine (Sigma-Aldrich) supplemented with 9.6 mM HEPES, 95.6 units/ml penicillin, 95.6 μg/ml streptomycin, 279.2 μg/ml L-glutamine (all from Life Technologies), 1x insulin-transferrin-selenium (ITS)+ premix (BD Biosciences, Mississauga, Canada), 365 μg/ml ascorbic acid 2-phosphate, 40 μg/ml L-proline, 100 nM dexamethasone, 125 μg/ml human serum albumin (all from Sigma-Aldrich), and 10 ng/ml transforming growth factor-beta three (TGF-β3; ProSpec, East Brunswick, USA).

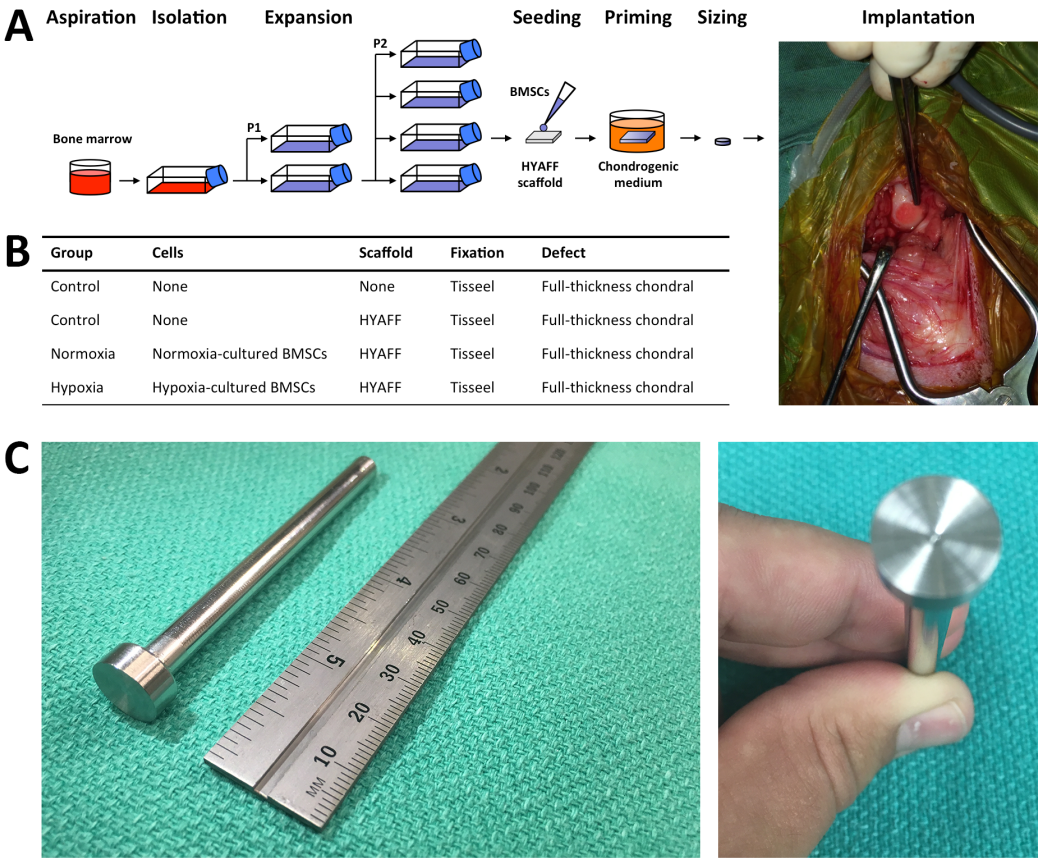

B

Group	Cells	Scaffold	Fixation	Defect
Control	None	None	Tisseel	Full-thickness chondral
Control	None	HYAFF	Tisseel	Full-thickness chondral
Normoxia	Normoxia-cultured BMSCs	HYAFF	Tisseel	Full-thickness chondral
Hypoxia	Hypoxia-cultured BMSCs	HYAFF	Tisseel	Full-thickness chondral

Figure 6.1 Bone marrow-derived mesenchymal stromal stem cell *ex vivo* culture and transplantation. (A) Bone marrow-derived mesenchymal stromal stem cells (BMSCs) were isolated by plastic adherence from a sheep bone marrow aspirate and expanded to passage two in tissue-culture flasks containing expansion medium. Expanded bone marrow-derived mesenchymal stromal stem cells (BMSCs) were seeded onto a porous esterified hyaluronic acid (HYAFF) scaffold at 10 $\times 10^6$ BMSCs/cm^3. The BMSC-seeded scaffold was then chondrogenically primed with culture in chondrogenic medium for four days. Thereafter, a 7 mm-diameter implant was created from the cell-seeded scaffold and transplanted autologously into a full-thickness cartilage defect on the femoral condyle of the stifle joint. The implant was reinforced with Tisseel fibrin sealant. (B) Each full-thickness cartilage defect was treated with either a cell-free control, normoxia-cultured BMSC-seeded HYAFF scaffold or hypoxia-cultured BMSC-seeded scaffold. (C) Custom, stainless steel, 1.2 cm-diameter device with slight concavity used for compression of the implant following transplantation while the fibrin sealant solidified.

BMSCs were seeded at a consistent density of 1×10^7 BMSCs/cm^3 onto scaffolds composed of non-woven, 10-20 μm-diameter HYAFF fibers (varying inter-fiber spaces) with dimensions of 2-cm length, 2-cm width and 0.2-cm thickness (Anika Therapeutics, Abano Terme, Italy) [202, 375]. Under sterile conditions, scaffolds were placed into the wells of a six-well plate and were moistened with 320 μl of chondrogenic medium micropipetted in 20-μl aliquots to 16 points on the top surface of each scaffold. Thereafter, 8×10^6 BMSCs were re-suspended in 320 μl of chondrogenic medium and micropipetted in 20-μl aliquots over the same points. Cell-free chondrogenic medium was used for cell-free, control scaffolds. Seeded scaffolds were then incubated for one hour at 37°C in a humidified incubator to allow for cell adhesion to occur. Five milliliters of chondrogenic medium was then slowly added to each well to submerse each scaffold.

BMSC-seeded scaffolds were cultured statically for 4 days in chondrogenic medium within a humidified incubator with an oxygen tension consistent with the oxygen tension used for isolation and expansion (21% or 3% oxygen). Media were changed daily during this chondrogenic priming period.

6.2.4 Assessment of chondrogenic priming

BMSC-seeded scaffolds that were cultured for 4 days in chondrogenic medium were assessed with reverse-transcription quantitative polymerase chain reaction (RT-qPCR) to quantify gene expressions of aggrecan, collagen II and sex

determining region Y-box nine (SOX9) that are related to hyaline cartilage. These gene expressions were compared to unprimed BMSCs that were not exposed to chondrogenic medium and BMSCs that were seeded at 1×10^7 BMSCs/cm^3 onto HYAFF scaffolds and cultured in chondrogenic medium for 14 days.

To perform gene expression analysis, total ribonucleic acid (RNA) was extracted from constructs using TRIzol Reagent (Life Technologies) after grinding with a pestle. Total RNA (100 ng) in a 40-µl reaction was reverse transcribed to complementary deoxyribonucleic acid (cDNA) using GoScript Reverse Transcription System (Promega, Madison, USA) primed in the presence of oligo(dT) primers (1 µg). Quantitative PCR was performed with a DNA Engine Opticon II Continuous Fluorescence Detection System (Bio-Rad) using HotGoldStar Taq polymerase and SYBR Green detection (Eurogentec North America, San Diego, USA). Primers (Table 6.2) were obtained from Invitrogen (Life Technologies). Gene (messenger RNA [mRNA]) expression levels for each primer set were normalized to the expression level of ovine beta-actin (β-actin) by the $2^{-\Delta\Delta C(T)}$ method [376].

BMSC-seeded scaffolds that were cultured for 4 days in chondrogenic medium were also assessed for proteoglycan production through the quantification of sulfated glycosaminoglycan (GAG) per DNA (GAG/DNA). These gene expressions were compared to unprimed BMSCs that were not exposed to chondrogenic medium and BMSCs that were seeded at 1×10^7

BMSCs/cm^3 onto HYAFF scaffolds and cultured in chondrogenic medium for 14 days.

Table 6.2 Ovine primer sequences used in reverse-transcription polymerase chain reaction analysis

Gene	Primer sequences		NCBI Reference
β-actin (*ACTB*)	5'-CGGCGGGACCACCAT-3'	Forward	NM_001009784.1
	5'-GCAGTGATCTCTTTCTGCATCCT-3'	Reverse	
Aggrecan (*ACAN*)	5'-TGGAATGATGTCCCATGCAA-3'	Forward	XM_004018048.1
	5'-GCCACTGTGCCCTTTTTACAG-3'	Reverse	
Collagen II (*COL2A1*)	5'-ACCTCACGTCTCCCCATCA-3'	Forward	XM_004006408.1
	5'-CTGCTCGGGCCCTCCTAT-3'	Reverse	
SRY-Box 9 (*SOX9*)	5'-GCTGCTGGCCGTGATGA-3'	Forward	XM_004013527.1
	5'-GGGTCGCGCGTTTGTTT-3'	Reverse	

To perform this biochemical analysis, constructs were rinsed in PBS and digested in proteinase K (1 mg/ml in 50 mM Tris with 1 mM EDTA, 1 mM iodoacetamide and 10 mg/ml pepstatin A; all from Sigma-Aldrich) for 16 hours at 56°C. Sulfated GAG content was measured by 1,9-dimethylmethylene blue binding (Sigma-Aldrich) using chondroitin sulfate as the standard (Sigma-Aldrich). *De novo* sulfated GAG production was determined by subtracting GAG quantities of BMSCs that were not exposed to chondrogenic medium from GAG quantities in constructs that were primed for 4 days or differentiated for 14 days in chondrogenic medium. DNA content was determined using the CyQUANT Cell Proliferation Assay Kit (Life Technologies) with supplied bacteriophage λ DNA as the standard.

6.2.5 Joint surgery for defect creation and transplantation

In preparation for surgery, sheep were fasted for 24 hours and an indwelling jugular catheter was placed. Ceftiofur was administered at 2 mg/kg IV prior to the procedure (Western Drug Distribution Center). General anesthesia was performed as described for the aspiration procedure. Sheep were positioned in a supine position on a positioning device (Hug-U-Vac). Each hind limb was clipped around the stifle joint, prepared with 10% wt/vol povidone-iodine solution (Purdue Pharma), and draped to create a sterile field centered over the stifle joint using an impervious stockinette (Spectrum Laboratories, Rancho Dominguez, USA) and surgical drapes.

A 6-cm midline incision through skin was made over each stifle joint from the patella to the tibial tuberosity in order to expose the patellar tendon. Medial and lateral parapatellar approaches were then utilized to access the medial and lateral femoral condyles. Specifically, 3-cm longitudinal incisions were made medial and lateral to the inferior patella and patellar tendon and deepened to enter the stifle joint. The femoral condyle on each side was visualized with the stifle joint in full flexion. The patella was not dislocated with either approach. During exposure of the lateral femoral condyle, care was taken to identify, isolate, protect, and retract the tendon of the extensor digitorum longus muscle that originates from the lateral femoral condyle [436]. The weight-bearing area of each femoral condyle was determined to be midway between the medial and lateral

aspects of each condyle with the stifle joint in full flexion. A full-thickness cartilage defect was created on each condyle using a 6.95 mm-diameter custom punch to create a circular defect boundary and a curette to excise cartilage. The subchondral bone was left intact and no bleeding was seen from this bone.

During implantation, an autologous cell-seeded scaffold or cell-free scaffold was cut with a biopsy punch to create a 7 mm-diameter circular implant (Figure 6.1A). Tisseel fibrin sealant was applied to fill the cartilage defect (Baxter, Mississauga, Canada) to help secure the implant that was subsequently inserted into the cartilage defect. A custom, stainless steel, 1.2 cm-diameter compression device with slight concavity (Argyll Innovations, Edmonton, Canada) was then applied to the implant and surrounding native cartilage and held in place for 3 minutes (Figure 6.1C). The implant was then inspected for adequate placement and to ensure that a smooth transition point between native cartilage and implant was present. If the defect was serving as an empty-defect control, it was filled with fibrin sealant only. Thereafter, the same implantation procedure was performed on the defect of the other femoral condyle of the same stifle joint. The joint was then ranged multiple times from flexion to extension and both implants were inspected to ensure that they were adequately positioned at each defect.

Medial and lateral windows to the distal femur and skin were then closed with 2-0 Vicryl suture (Ethicon, Somerville, USA). Skin was closed

subcutaneously with 2-0 Vicryl suture and superficially using 2-0 PDS suture (Ethicon). Incision sites were dressed. Post-operatively, sheep received a five-day course of ceftiofur 2 mg/kg IV daily for infection prophylaxis (Western Drug Distribution Center). Flunixin and buprenorphine were used for anti-inflammatory and analgesic purposes (Western Drug Distribution Center). Vital signs, incision sites and activity were monitored closely for one week. The animals returned to full activity and weight bearing as tolerated shortly following surgery. They were assessed routinely for signs of lameness until explantation.

6.2.6 Treatment groups

The treatment groups in this study included cell-free controls, normoxia-cultured BMSC-seeded scaffolds and hypoxia-cultured BMSC-seeded scaffolds (Figure 6.1B). Four defects in two stifle joints were treated as cell-free controls by leaving defects empty or implanting cell-free scaffolds. Eight defects in four stifle joints were treated with normoxia-cultured BMSC-seeded scaffolds. The BMSCs in this group were isolated, expanded and chondrogenically primed under normoxic conditions. Eight defects in four other stifle joints were treated with hypoxia-cultured BMSC-seeded scaffolds. The BMSCs in this group were isolated, expanded and chondrogenically primed under hypoxic conditions. Both defects in each joint received the same cell condition of no cells (control), normoxia-cultured BMSCs or hypoxia-cultured BMSCs to avoid interaction of one treatment group with another.

6.2.7 *In vivo* reassessment of implants

To ensure that the BMSC-seeded scaffolds were capable of remaining in the defect site following implantation, sheep Z01 was reassessed in a second-look procedure one week after the initial surgery. During this procedure, anesthesia, surgical approach and closure were identical to the implantation procedure. The femoral condyles of each stifle joint were visualized.

6.2.8 Explantation

Six months after the transplantation surgery, sheep were sacrificed using sodium pentobarbital (Western Drug Distribution Center). The stifle joint was extracted from each animal. High-quality photography was performed on the distal femur of each hind limb.

6.2.9 Histological processing and assessment

Processing for histological analysis involved reducing each condyle to osteochondral blocks centered on the defect site with 5-10 mm of native articular cartilage surrounding the defect on all sides. Each specimen was fixed using 10% wt/vol buffered formalin for 7 days (Sigma-Aldrich). Thereafter, decalcification was performed for 4 months in a solution containing 10% wt/vol ethylenediaminetetraacetic acid (EDTA) tetrasodium salt dehydrate and 0.1% wt/vol formalin followed by 2 months in a solution containing 10% wt/vol EDTA tetrasodium salt dehydrate and 0.1% wt/vol formalin (Sigma-Aldrich). Specimens were then dehydrated, processed into paraffin wax and sectioned at a thickness of

8 μm in a longitudinal plane. Sections were stained with 0.1% wt/vol safranin O to reveal proteoglycan matrix depositions and counterstained with 1% wt/vol fast green. Microphotographs of each section were captured using an Eclipse Ti-S microscope (Nikon Canada, Mississauga, Canada) fitted with NIS Elements Basic Research Imaging Software Version 4.20 (Nikon Canada). The microscope automatically stitched magnified photomicrographs into larger images containing the entire defect site, repair tissues and native tissues. Images were subsequently assembled in Photoshop (Adobe Systems, San Jose, USA).

For histological assessment, each defect site was divided into five equivalent radial zones from the center to the outer border of each defect site. Microphotographs of sections from the inner four zones of all defect sites were coded, placed in random order and assessed by a blinded observer using a modified version of the O'Driscoll histological scoring system derived from the version of Frenkel *et al*. (Table 6.3 and Appendix 3) [437-439]. In our modification of the O'Driscoll scoring system, hyaline-like cartilaginous tissue and safranin O staining parameters were normalized to area of repair tissue / area of defect site. Thickness of repair tissue was normalized to the width of the defect site containing repair tissue / total width of defect site.

Table 6.3 Modified O'Driscoll histological scoring system

Nature of repair tissue		
Hyaline-like cartilaginous repair tissue*:	80 – 100% of all repair tissue	8
	60 – 79% of all repair tissue	6
	40 – 59% of all repair tissue	4
	20 – 39% of all repair tissue	2
	0 – 19% of all repair tissue	0
Safranin O staining*:	80 – 100% of all repair tissue	2
	40 – 79% of all repair tissue	1
	0 – 39% of all repair tissue	0
Structural characteristics of repair tissue		
Surface regularity:	Smooth and intact	2
	Fissures present	1
	Severe disruption and/or fibrillation	0
Structural integrity:	Normal	2
	Slight disruption and/or including cysts	1
	Severe lack of integrity	0
Thickness[&]:	100% of adjacent native cartilage	2
	50 – 99% of adjacent native cartilage	1
	0 – 49% of adjacent native cartilage	0
Bonding to adjacent cartilage:	Both ends bonded fully	2
	Bonded at one end or partially at both ends	1
	Not bonded	0
Bonding to subchondral bone:	100% of repair tissue bonded	2
	50 – 99% of repair tissue bonded	1
	0 – 49% of repair tissue bonded	0
Freedom from degeneration		
Changes in repair tissue:	Normal cellularity, no clusters	2
	Slight hypocellularity, <25% clusters	1
	Moderate hypocellularity/hypercellularity, ≥25% clusters	0
Changes in adjacent native cartilage:	Normal cellularity, no clusters, and normal staining	3
	Normal cellularity, mild clusters, moderate staining	2
	Mild-moderate hypocellularity, slight staining	1
	Severe hypocellularity, poor or no staining	0
Intactness of subchondral bone plate:	100% of defect width intact	2
	50 – 99% of defect width intact	1
	0 – 49% of defect width intact	0

* Normalized to the area of repair tissue / area of defect site

[&] Normalized to the width of repair tissue / width of defect site

Hyaline-like cartilaginous repair tissue was defined as repair tissue that contained predominantly circular cells (≥75% of cells present within the area of tissue) within lacunae surrounded by extracellular matrix that stained positively with safranin O [437]. Superficial repair tissue was also considered to be hyaline-

like if it contained flattened, non-circular cells, lacked lacunae and safranin O staining, and was adjacent to deeper tissue containing predominantly circular cells within lacunae and positive safranin O staining given that this phenotype resembles the structural organization of native hyaline articular cartilage [440].

Microphotographs of sections from the inner four zones of all defect sites were also assessed in a blinded fashion for quantitative measures using ImageJ software (National Institutes of Health, Bethesda, USA). Areas of the defect site, repair tissue within the defect site, and hyaline-like cartilaginous repair tissue within the defect site were measured. Defect fill was calculated using: repair tissue area / defect site area × 100%.

6.2.10 Macroscopic assessment

Photographs of each defect site were coded, placed in random order and assessed by a blinded observer using a modified Goebel macroscopic scoring system (Table 6.4 and Appendix 4) [441]. In our modification of the Goebel system, the point scale was numbered inversely relative to the original scale. The defect fill parameter was assessed based on percentage of defect filled to the level of the adjacent native cartilage and did not involve an assessment of depth.

6.2.11 Statistical analysis

Analyses were performed using SPSS Statistics 23 (IBM, Armonk, USA) and significance was concluded when $p<0.05$. Repeated measures analysis of variance

(ANOVA) was used for assessment of cell count and doubling over time during isolation and expansion. Gene expressions of BMSCs cultured for 0, 4 or 14 days were compared using a Kruskal-Wallis one-way ANOVA with pairwise comparison, while oxygen tension groups were compared using a Mann-Whitney U test. For assessment of modified O'Driscoll scores, dimensions of defect site and repair tissue, and modified Goebel scores between controls, normoxia-cultured BMSC-seeded scaffolds and hypoxia-cultured, BMSC seeded scaffolds, a Kruskal-Wallis one-way ANOVA with pairwise comparison was used. A Mann-Whitney U test was used for assessment of these parameters between cell-free controls and cell-seeded scaffolds. Paired comparison of defects between joints within the same animal was performed using a Wilcoxon test. A Fisher's exact test was employed to assess subchondral bone intactness and reaction.

6.3 Results

6.3.1 Bone marrow-derived mesenchymal stromal stem cell isolation and expansion

Bone marrow aspirates with a mean volume ± SEM of 32 ± 2 ml were collected from five ovine donors. BMSCs were isolated by plastic adherence and expanded in tissue-culture flasks under normoxic and hypoxic conditions (Figure 6.1A). Cell count, cell population doublings per day and cumulative population doublings were not significantly different between oxygen tension groups over the course of the expansion period ($p=0.11$, 0.40 and 0.79; Figures 6.2A-C). Cell count increased progressively with each passage ($p<0.001$; Figure 6.2A). Once

80% confluence was reached at P2, there were 16.1 ± 2.7 $\times 10^6$ BMSCs derived from each flask seeded and cultured under normoxia and 18.7 ± 4.3 $\times 10^6$ BMSCs derived from each flask seeded and cultured under hypoxia (p=0.10). Population doublings per day were fastest at P0 and decreased significantly with passage thereafter (p=0.03; Figure 6.2B). Cumulative population doublings by the end of the expansion period were 13.1 ± 0.5 doublings for normoxia-expanded BMSCs and 13.0 ± 1.1 doublings for hypoxia expanded BMSCs (p=1.0; Figure 6.2C).

6.3.2 Chondrogenic priming of bone marrow-derived mesenchymal stromal stem cells

BMSCs were isolated, expanded to P2, seeded onto HYAFF scaffolds, and cultured for 4 days *ex vivo* in chondrogenic medium containing TGF-β3 and dexamethasone to induce chondrogenic priming. This 4-day culture period resulted in significantly increased hyaline cartilage-related aggrecan, collagen II and SOX9 mRNA expressions of BMSCs relative to unprimed controls ($p<0.01$; Figures 6.3A-C). Expressions of these genes after chondrogenic priming were increased to levels similar to expressions after a 14-day period of chondrogenic differentiation (p=0.35, 1.0 and 0.33, respectively). Although chondrogenic priming augmented cartilaginous gene expression, proteoglycan production was not yet established given that GAG/DNA after 4 days of chondrogenic culture was negligible and similar to BMSCs not exposed to chondrogenic medium (p=1.0; Figure 6.3D).

Table 6.4 Modified Goebel macroscopic scoring system

Characteristics of repair tissue		
Color of repair tissue:	Hyaline or white (100%)	4
	Predominantly white (50 – 99%)	3
	Predominantly translucent or empty (50 – 99%)	2
	Translucent (100%)	1
	Empty	0
Presence of blood vessels:	0% of tissue	4
	0 – 24% of tissue	3
	25 – 49% of tissue	2
	50 – 74% of tissue	1
	75 – 100% of tissue	0
Surface quality:	Full resurfacing with smooth, homogeneous tissue	4
	Full resurfacing with smooth, heterogeneous tissue	3
	Full resurfacing with presence of fibrillated tissue	2
	Incomplete repair tissue with subchondral bone exposed	1
	No repair tissue with exposure of subchondral bone	0
Defect filling with repair tissue		
Defect fill:	100% of defect filled to level of adjacent cartilage	4
	50 – 99% of defect filled to level of adjacent cartilage	3
	<50% of defect filled to level of adjacent cartilage	2
	Empty defect	1
	Subchondral bone damage in at least part of the defect site	0
Characteristics of native cartilage		
Degeneration of adjacent cartilage:	No changes in normal cartilage	4
	Cracks or fibrillations in integration zone	3
	Diffuse degenerative changes	2
	Extension of defect into adjacent cartilage	1
	Subchondral bone damage	0

Oxygen tension during culture modulated gene expressions of BMSCs seeded within HYAFF scaffolds after 4 days of chondrogenic priming. The increase in collagen II mRNA expression between 0 and 4 days of culture in chondrogenic medium was more significant in hypoxia-cultured BMSCs ($p=0.002$) than normoxia cultured BMSCs ($p=0.01$; Figure 6.3B). Collagen II mRNA in hypoxia-cultured BMSCs approached significantly higher levels than normoxia-cultured BMSCs after 4 days of chondrogenic priming ($p=0.095$; Figure 6.3B). With respect to aggrecan, the increase in mRNA expression between 0 and 4 days of chondrogenic culture was highly significant in both

hypoxia-cultured BMSCs (p=0.001) and normoxia-cultured BMSCs p=0.004), and there was not a significant difference between hypoxia- and normoxia-cultured BMSCs established after 4 days of culture (p=0.15; Figure 6.3A). SOX9 mRNA expression was higher following hypoxic isolation and expansion than normoxic isolation and expansion in unprimed BMSCs (p=0.05, Figure 6.3C). This difference was no longer evident after BMSCs were exposed to chondrogenic medium for 4 days (p=0.31; Figure 6.3C).

6.3.3 Post-operative course

Following joint surgery for simulated defect creation and transplantation, sheep returned to full activity. One week from the time of surgery, a second-look procedure was performed on sheep Z01 to assess the position of each implant. BMSC-seeded scaffolds were noted to be in place within the femoral condyle cartilage defects. None of the sheep displayed signs of post-operative infection or lameness during the 6-month post-transplantation period.

6.3.4 Histological assessment of repair tissue

Defect sites were assessed histologically 6 months from the time of joint surgery. Variation was seen in the quality of repair tissue within each treatment group as some defect sites contained hyaline-like cartilaginous tissue that strongly stained with safranin O, while others either lacked the presence of tissue or contained tissue more consistent with fibrocartilage (Figures 6.4A-I). Cartilaginous repair

tissue appeared to be derived from either the implant (Figure 6.4C) or adjacent native cartilage creeping into the defect site (Figure 6.4G).

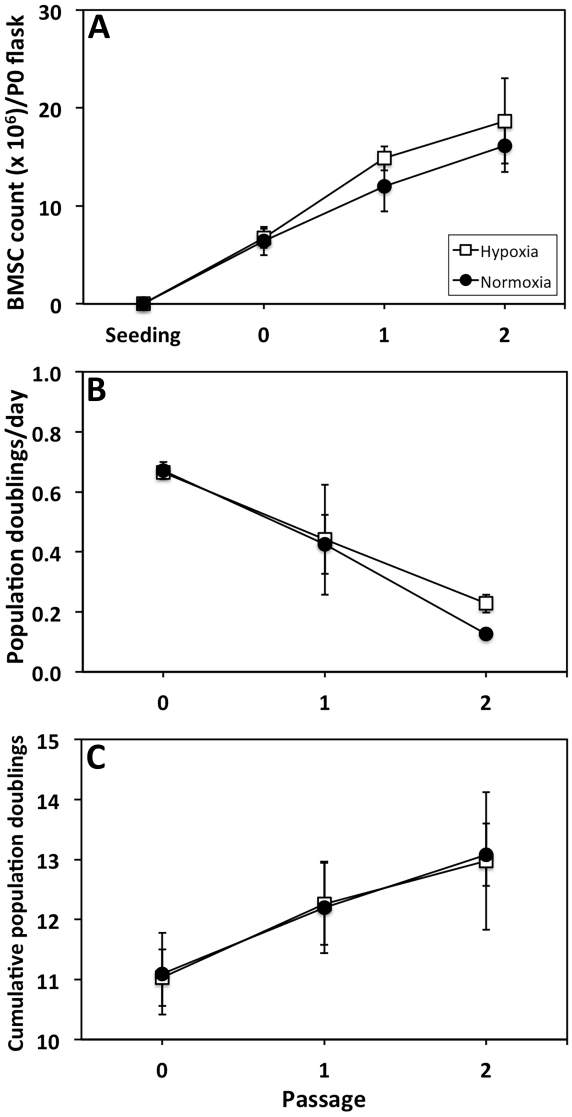

Figure 6.2 Expansion of bone marrow-derived mesenchymal stromal stem cells. (A) Cell counts, (B) population doublings per day, and (C) cumulative population doublings at each passage during expansion of bone marrow-derived mesenchymal stromal stem cells (BMSCs) under normoxic and hypoxic conditions. Data points represent mean ± standard error of the mean (SEM) of cells from five donors.

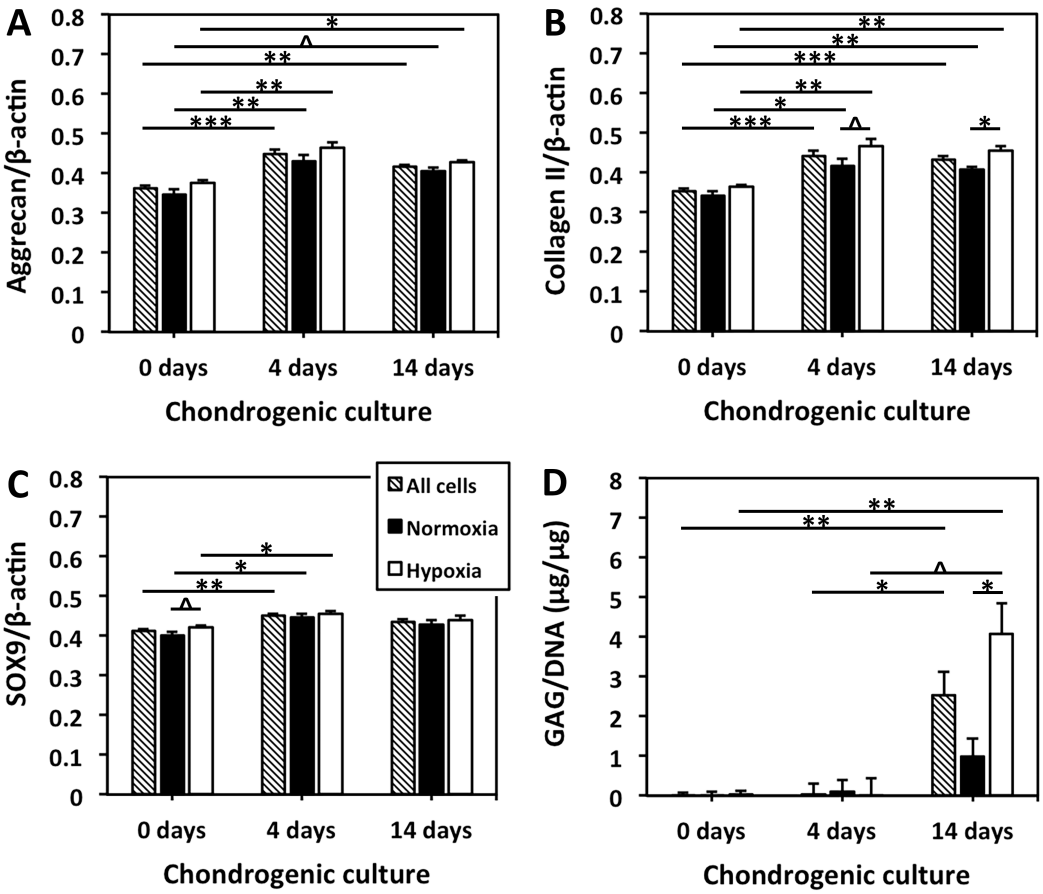

Figure 6.3 Chondrogenic priming of bone marrow-derived mesenchymal stromal stem cell-seeded scaffolds. Bone marrow-derived mesenchymal stromal stem cells (BMSCs) were isolated and expanded under either normoxia or hypoxia and subsequently not exposed to chondrogenic medium (0 days) or seeded onto hyaluronic acid (HYAFF) scaffolds and either primed in chondrogenic medium for 4 days or differentiated in chondrogenic medium for 14 days within the same oxygen condition as isolation and expansion. Thereafter, (A) aggrecan, (B) collagen II and (C) SOX9 mRNA expressions were quantified relative to beta-actin using reverse-transcription quantitative polymerase chain reaction (RT-qPCR). (D) Glycosaminoglycan (GAG) per deoxyribonucleic acid (DNA) was determined in another set of constructs using biochemical assays. Data points represent mean ± standard error of the mean (SEM) of BMSCs from five sheep. Statistical analysis is represented by unlabeled, not significant; ^ approaching significance $p \leq 0.10$; *, significant $p < 0.05$; ** significant $p < 0.01$; *** significant $p < 0.001$.

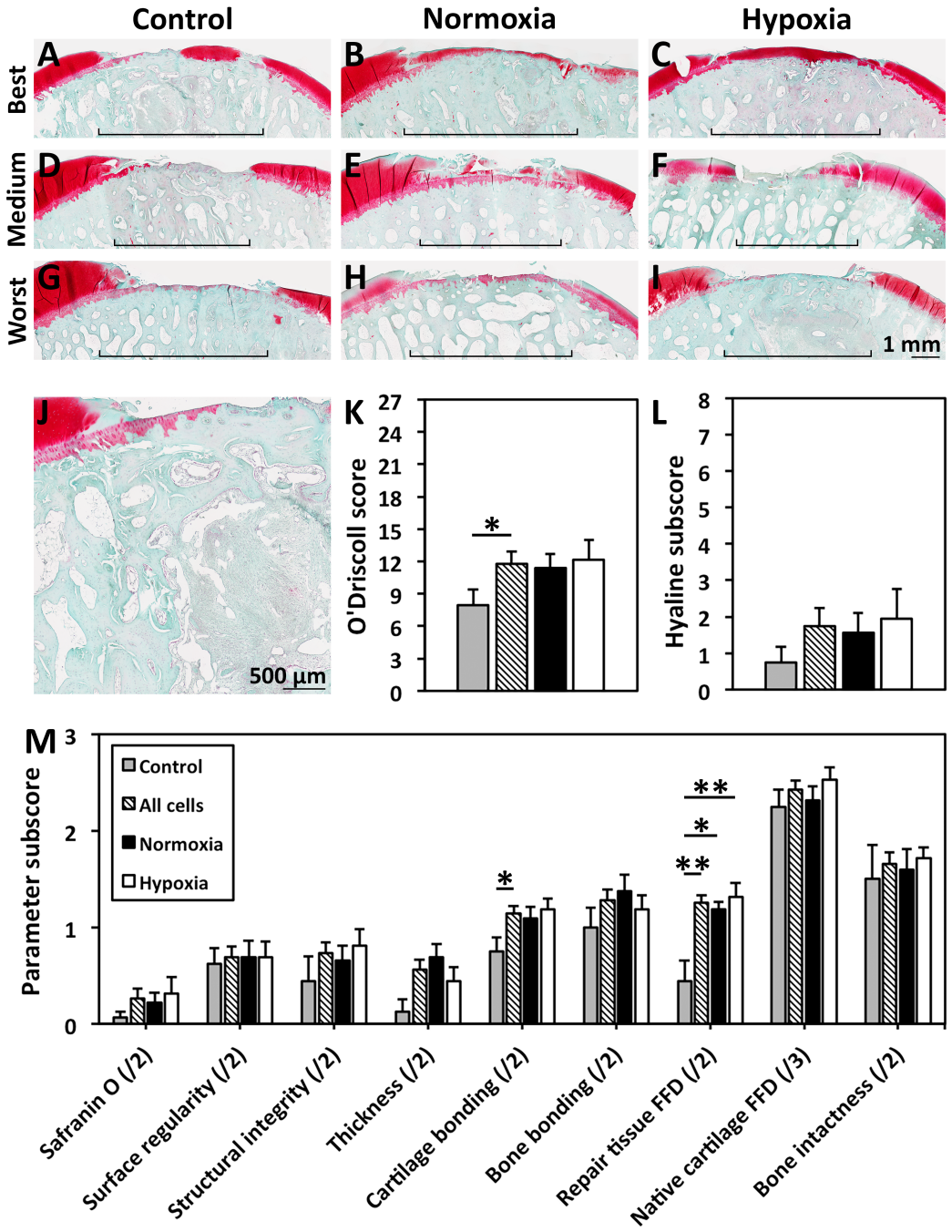

Figure 6.4 Histological staining and scoring of cartilaginous repair tissue. Six months following transplantation, femoral condyles were explanted, processed, sectioned at 8-µm thickness, and stained with safranin O and fast green. (A-I) Histological sections of defect sites (brackets) containing cartilaginous repair tissue, adjacent native articular cartilage and subchondral bone for cell-free controls and defects treated with normoxia- and hypoxia-cultured BMSC-seeded scaffolds (7× combine magnification of objective and camera lenses; stitching of images performed by the microscope). Sections awarded the best, medium (mean) and worst modified

O'Driscoll scores for each group are displayed. (J) Extensive reaction was noted in the subchondral bone of some sections (7× magnification). (K) Modified O'Driscoll score, (L) O'Driscoll subscore for percentage of hyaline-like cartilaginous tissue, and (M) other O'Driscoll subscores for repair tissues from 20 defects in five sheep based on transplantation group. Data points represent mean ± standard error of the mean. Statistical analysis is represented by unlabeled, not significant; *, significant $p<0.05$; **, highly significant $p<0.01$.

The subchondral bone plate was fully intact in 50% of defect sites. Half of defect sites treated with cell-free controls, normoxia-cultured BMSC-seeded scaffolds and hypoxia-cultured BMSC-seeded scaffolds had at least some subchondral plate compromise ($p=1.0$). In some sections, an extensive subchondral reaction characterized by infiltration of cells and altered structural microanatomy was noted in the subchondral bone (Figure 6.4J). An extensive subchondral reaction was present in 50% of control defect sites, 25% of defect sites implanted with normoxia-cultured BMSC-seeded scaffolds and 12.5% of defect sites implanted with hypoxia-cultured BMSC-seeded scaffolds. There was not a significant difference in the presence of extensive subchondral reaction based on oxygen tension or cell implantation ($p=1.0$ and 0.25, respectively).

Modified O'Driscoll scores were similar for defects implanted with hypoxia-cultured BMSC-seeded scaffolds (12.1 ± 1.8) and normoxia-cultured BMSC-seeded scaffolds (11.4 ± 1.0; $p=0.80$). These scores were higher than control defects (7.9 ± 0.7) in a comparison that approached a statistically significant difference ($p=0.10$; Figure 6.4K). Statistical significance was noted in the subscore analysis for freedom from degeneration in repair tissue ($p=0.02$;

Figure 6.4M). For this parameter, pairwise comparison demonstrated that defects implanted with either normoxia- and hypoxia-cultured BMSC-seeded scaffolds had significantly higher scores than control defects ($p=0.02$ and 0.008), although subscores for normoxia- versus hypoxia-cultured BMSC-seeded scaffolds were similar ($p=1.0$). Subscores for other parameters were not significantly different between groups ($p\geq0.11$; Figures 6.4L and M).

In a comparison of cell-seeded scaffolds – which included a pooled group of all scaffolds containing either hypoxia- or normoxia-cultured BMSCs – and cell-free controls, defects implanted with cell-seeded scaffolds had significantly higher modified O'Driscoll scores (11.8 ± 1.0) than cell-free controls (7.9 ± 0.7, $p=0.04$; Figure 6.4K). Subscores for freedom from degeneration in repair tissue were significantly higher ($p=0.005$), and subscores for bonding of repair tissue to native cartilage and repair tissue thickness approached significantly higher levels in defects filled with cell-seeded scaffolds ($p=0.05$ and 0.08; Figure 6.4M).

Quantitative analysis of repair tissue and defect site dimensions demonstrated that the area of all forms of repair tissue – including hyaline-like cartilaginous and fibrocartilaginous repair tissues – localized to the defect site in each section was significantly higher in defects implanted with cell-seeded scaffolds than cell-free controls ($p=0.02$; Figure 6.5A). Pairwise comparison demonstrated that normoxia-cultured BMSC-seeded scaffolds produced significantly larger areas of repair tissue than controls ($p=0.01$; Figure 6.5A).

Hypoxia-cultured BMSC-seeded scaffolds also appeared to produce larger areas of repair tissue than controls that approached significance ($p=0.09$; Figure 6.5A). Percentages of defect fill with repair tissue were not significantly different between cell-seeded and cell-free controls ($p=0.18$; Figure 6.5B). For normoxia-cultured BMSC-seeded scaffolds, hypoxia-cultured BMSC-seeded scaffolds and controls, percentages of defect fill were 50.4% ± 6.5%, 44.4% ± 8.0% and 35.0% ± 2.1%, respectively ($p=0.17$; Figure 6.5B). Percentages of defect fill with hyaline-like cartilaginous tissue and percentages of repair tissue with features of hyaline-like cartilage were not significantly different between groups ($p=0.92$ and $p=1.0$, respectively; Figures 6.5B and C).

To more closely investigate the impact of oxygen tension during pre-implantation culture and identify variability between sheep, histological scoring and tissue dimension analyses were performed within each animal by comparing sections derived from contralateral defects (Figure 6.6). Three sheep were treated with normoxia-cultured BMSC-seeded scaffolds in one joint and hypoxia-cultured BMSC-seeded scaffolds in the contralateral joint (Y08, Z01 and Z33). For sheep Y08, there was not a significant difference between groups for the modified O'Driscoll score ($p=0.31$; Figure 6.6K). Subscores for structural integrity approached significantly higher levels in defects implanted with hypoxia-cultured BMSC-seeded scaffolds ($p=0.08$), but all other subscores were not significantly different between groups ($p\geq0.16$). Repair tissue area was significantly larger in hypoxia-cultured BMSC-seeded scaffolds than normoxia-cultured BMSC seeded

scaffolds ($p=0.02$; Figure 6.6M). Defect fill with all forms of repair tissue and hyaline-like cartilaginous tissue was not different between groups ($p\geq0.58$; Figures 6.6L and N). For sheep Z01, hypoxia-cultured BMSC-seeded scaffolds from donor Z01 had significantly higher modified O'Driscoll scores and subscores for percentage of hyaline-like repair tissue, safranin O staining and bone intactness ($p<0.05$; Figure 6.6K). However, repair tissue area and defect fill were not significantly different between groups ($p\geq0.40$; Figures 6.6L-N). In contrast to this relationship, normoxia-cultured BMSC-seeded scaffolds from sheep Z33 led to significantly higher modified O'Driscoll scores and subscores for percentage of hyaline-like repair tissue and repair tissue thickness ($p<0.05$; Figure 6.6K). Repair tissue area, defect fill with all forms of repair tissue and hyaline-like cartilaginous tissue were significantly higher in defects implanted with normoxia-cultured BMSC-seeded scaffolds ($p<0.05$; Figures 6.6L-N).

6.3.5 Macroscopic assessment of repair tissue

Defect sites were assessed macroscopically at the time of explantation. Variation was seen in the quality of repair tissue within each treatment group as some defect sites were resurfaced with tissue while other defect sites were relatively unfilled (Figures 7A-C). Analysis using a modified Goebel scoring system demonstrated that scores between controls (13.5 ± 0.7) and defects implanted with normoxia-cultured BMSC-seeded scaffolds (13.3 ± 1.2) and hypoxia-cultured BMSC-seeded scaffolds (14.6 ± 0.9) were not significantly different ($p=0.76$; Figure 6.7D).

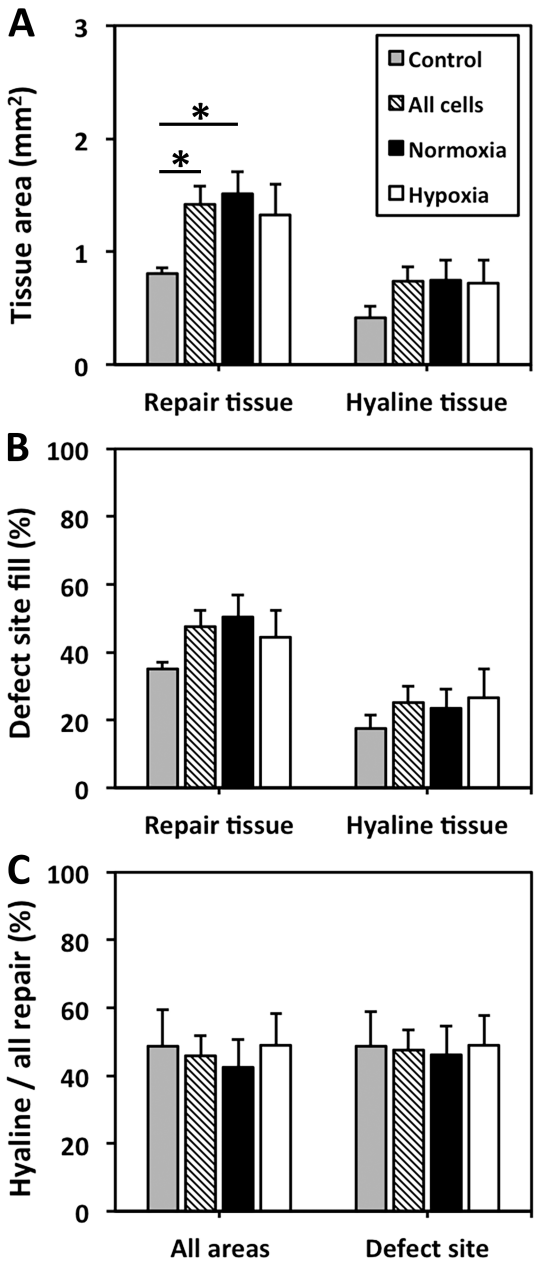

Figure 6.5 Quantitative analysis of repair tissue and defect site dimensions. Histological sections were assessed for (A) area of all forms of repair tissue and hyaline-like cartilaginous repair tissue, (B) percentage of defect site fill with all forms of repair tissue and hyaline-like cartilaginous repair tissue, and (C) percentage of hyaline-like cartilaginous tissue within all forms of repair tissue located specifically in the defect site and outside the defect site. Data points represent mean ± standard error of the mean of 20 defects in five sheep based on transplantation group. Statistical analysis is represented by unlabeled, not significant; *, significant $p<0.05$.

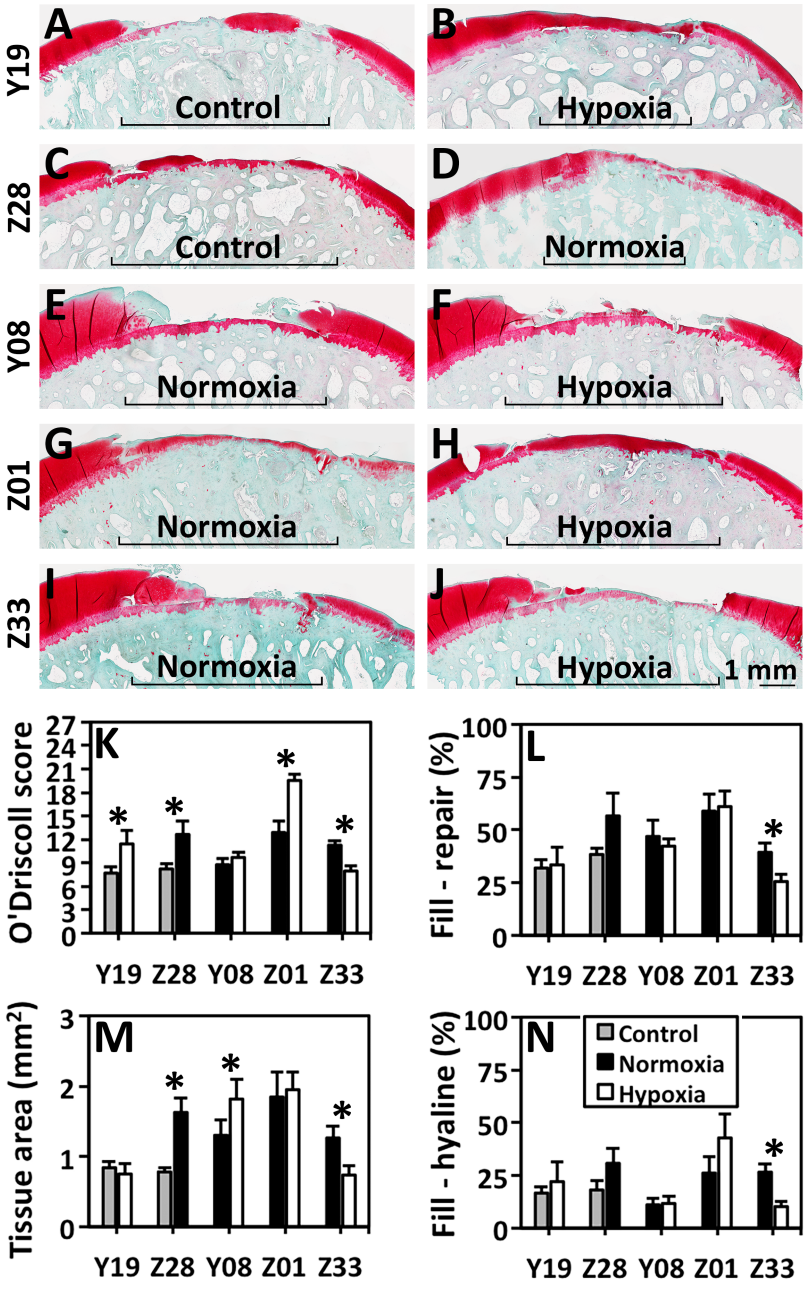

Figure 6.6 Histological staining, scoring and defect site dimension analysis per sheep. Six months following transplantation, femoral condyles were explanted, processed, sectioned at 8-µm thickness, and stained with safranin O and fast green. (A-J) Histological sections of defect sites (brackets) containing cartilaginous repair tissue, adjacent native articular cartilage and subchondral bone for cell-free controls and defects treated with normoxia- and hypoxia-cultured BMSC-seeded scaffolds. Sections awarded the best modified O'Driscoll scores for each animal are displayed (7× combine magnification of objective and camera lenses; stitching of images performed by the microscope). Sections were assessed for (K) modified O'Driscoll score, (L)

percentage of defect site fill with all forms of repair tissue, (M) area of all forms of repair tissue within the defect site, and (N) percentage of defect site fill with hyaline-like cartilaginous repair tissue. Data points represent mean ± standard error of the mean of four zones within two defects per sheep. Statistical analysis is represented by unlabeled, not significant; *, significant $p<0.05$.

Modified Goebel scores were not different between cell-free controls and cell-seeded scaffolds ($p=0.96$; Figure 6.7D). Subscores based on repair tissue color, blood vessel formation in repair tissue, surface quality of repair tissue, and native cartilage degeneration were similar between groups ($p\geq0.55$).

6.4 Discussion

The main finding of this pilot study is that BMSCs that were isolated, expanded, seeded within HYAFF scaffolds, and chondrogenically primed prior to implantation were capable of producing hyaline-like cartilaginous repair tissue that was superior to controls within full-thickness, ovine articular cartilage defects. In addition to this, it was shown that incubator oxygen tension during *ex vivo* culture of BMSCs modulated the quality of repair tissue, although this effect was variable between animals.

The proposed pre-implantation protocol of BMSC isolation, expansion and chondrogenic priming is a hybrid of BMSC transplantation protocols that have been assessed in preclinical and clinical studies [29, 38, 43, 254, 274]. In the clinical setting, undifferentiated BMSCs have been transplanted as part of heterogeneous bone marrow aspirate concentrates or following *ex vivo* isolation and expansion [38, 39, 41, 43, 254]. Repair tissues may lack the qualities of

hyaline cartilage. Specifically, tissue consistent with fibrocartilage has been found in some defects on histological analysis and MRI in preclinical and clinical studies following transplantation of undifferentiated BMSCs [43, 45, 46, 254, 307, 320]. Moreover, there is evidence to suggest that undifferentiated BMSCs are predisposed to entering an osteogenic pathway following sustained expansion [339]. Predifferentiation of BMSCs with *ex vivo* chondrogenic culture for 2-3 weeks prior to implantation has been proposed previously and shown to improve repair tissue quality in animal models [36, 274, 287]. One downside of this technique is that chondrogenic predifferentiation prolongs the culture period and may be time and resource intensive relative to other protocols [274]. Furthermore, there is *in vitro* evidence to suggest that prolonged predifferentiation periods may not be required to induce chondrogenesis [442].

The goal of the protocol proposed in this study is to reduce the duration of the *ex vivo* culture period while providing chondrogenic priming to undifferentiated BMSCs prior to implantation. Four days of culture in chondrogenic medium was shown to enhance collagen II, aggrecan and SOX9 gene expressions of ovine BMSCs within HYAFF scaffolds. This finding was consistent with the literature available prior to this study that assessed chondrogenic priming of BMSCs in serum-free medium containing TGF-β3 and dexamethasone for less than 7 days within *in vitro* culture systems. Oldershaw *et al.* demonstrated that mRNA expression of Notch ligand Jagged-1 – which is involved in chondrogenesis and precedes collagen II expression – by human

BMSCs in pellets increased after 1 day and peaked after 2 days of chondrogenic culture with a subsequent decline [443]. Increased expression followed by shut down of Jagged-1 was required for full chondrogenesis demonstrated by increased SOX9 mRNA expression after 1 day and augmented collagen II and aggrecan mRNA expressions after 7 days. Murdoch *et al.* reported augmented collagen II mRNA expression by human BMSCs in scaffold-free transwell culture after 1-6 days of culture [269]. After 3 days of culture, Chung *et al.* noted enhanced mRNA expressions of collagen II, aggrecan and SOX9 in BMSCs seeded within methacrylated hyaluronic acid hydrogels [444]. Xu *et al.* found increased mRNA expressions of aggrecan and collagen II after 6 days of culture of human BMSC-seeded alginate gels [445].

BMSCs that were isolated, expanded, seeded within HYAFF scaffolds, chondrogenically primed, and implanted within full-thickness cartilage defects led to superior cartilaginous repair tissue formation and quality based on modified O'Driscoll scores and repair tissue area measurements than cell-free controls. This finding provides preliminary evidence that this protocol is promising and may serve as an option for treatment of full-thickness cartilage defects. Furthermore, this finding indicates that the HYAFF scaffold is suitable for use in this BMSC transplantation protocol as it has been with other protocols involving undifferentiated BMSCs, bone marrow aspirate concentrates and differentiated chondrocytes [38, 46, 254, 315, 446]. More rigorous study of the proposed protocol is warranted to establish that it is capable of consistently fostering

chondrogenesis. Furthermore, future investigation is required to compare BMSCs that are chondrogenically primed to undifferentiated BMSCs and BMSCs that have been predifferentiated for multiple weeks prior to transplantation.

The effect of incubator oxygen tension on quality of cartilaginous repair tissue developed *in vivo* within large-animal joint cartilage defects was assessed for the first time in this study. Hypoxic exposure during isolation, expansion and differentiation was shown previously to improve chondrogenic gene expression and ECM formation within *in vitro* pellet, micromass, hydrogel, and scaffold culture systems [332, 368-372, 405]. Our group demonstrated that hypoxic culture during distinct periods of isolation/expansion and differentiation augmented *in vitro* BMSC chondrogenesis within a HYAFF scaffold [405]. In this study, culture in hypoxic conditions appeared to enhance collagen II gene expression measured in pre-implantation constructs at the end of the priming period. *In vivo* study to date has been limited to subcutaneous implantation in a mouse model [368, 372]. In two mouse studies, pre-implantation hypoxic culture appeared to improve the development of post-implantation cartilaginous tissue that was assessed after 4-5 weeks [368, 372]. The longer-term results of the current large-animal study do not demonstrate a consistent effect of oxygen tension during *ex vivo* culture on cartilaginous repair tissue formation after transplantation into articular cartilage defects.

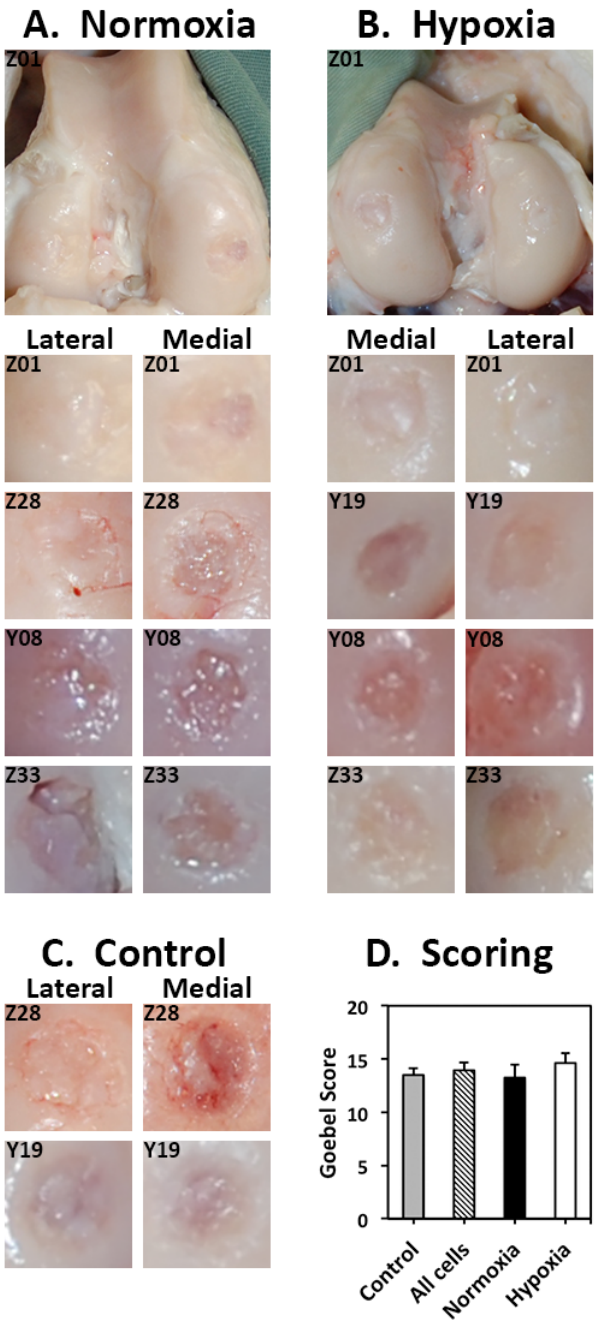

Figure 6.7 Macroscopic images and scoring of cartilaginous repair tissue. Six months following transplantation, distal femora were explanted and photographed. (A-C) Photographs of defect sites for defects treated with normoxia- and hypoxia-cultured bone marrow-derived mesenchymal stem cell-seeded scaffolds, and cell-free controls. (D) Modified Goebel score for repair tissues from twenty defects in five sheep based on transplantation group. Data points represent mean ± standard error of the mean. Statistical analysis is represented by unlabeled, not significant; *, significant $p<0.05$.

Significant differences between pre-implantation normoxic and hypoxic culture across all donors on histological scoring, repair tissue dimensions and macroscopic scoring were not found. In the paired assessment of these parameters within each of three donors that were implanted with normoxia-cultured BMSC-seeded scaffolds in one stifle joint and hypoxia-cultured BMSC-seeded scaffolds in the contralateral stifle joint, variability between donors was apparent. In sheep Y08, there was no difference in modified O'Driscoll scores between oxygen tension groups, although repair tissue area was higher in defects implanted with hypoxia-cultured BMSC-seeded scaffolds. In sheep Z01 that had the highest histological scores and repair tissue dimensions across all donors, repair tissue derived from BMSCs cultured under hypoxia had the highest modified O'Driscoll scores. Conversely, in sheep Z33, repair tissue derived from BMSCs cultured under normoxia had the highest modified O'Driscoll scores, repair tissue areas and defect fills.

Lack of a consistent difference between oxygen tension groups could relate to a number of factors. First, the duration of exposure of differentiating cells to specific oxygen tensions within *ex vivo* and *in vivo* environments could modulate chondrogenesis. *In vitro* experiments involve sustained control of oxygen tension during BMSC culture periods of isolation, expansion and differentiation [332, 370, 405]. *In vivo* experiments that utilize subcutaneous implantation of BMSC-seeded biomaterials into mice allow for control of oxygen tension during *ex vivo* culture periods that are similar in duration to *in vivo*

periods during which oxygen tension is not controlled [368, 372]. However, *in vivo* experiments like those performed in this study involve *ex vivo* culture periods that are much shorter than *in vivo* periods. The effects induced during *ex vivo* culture periods may become less relevant to modulation of cellular activity and quality of remodeling repair tissue as the duration of *in vivo* period is lengthened. Since joints have been shown to be naturally hypoxic [366], it is possible that sustained exposure of implanted cells to hypoxic joint environments could modulate chondrogenesis and reduce differences between groups. Similar to this proposed effect but within a shorter time frame, it was previously shown *in vitro* that hypoxic exposure during differentiation offsets the differences established between hypoxia and normoxia during isolation and expansion [332, 405]. In addition to the effects of oxygen tension, other modulatory factors that are present within joints, such as mechanical loading, could become more prominent in affecting tissue formation as time between implantation and joint assessment is lengthened for *in vivo* studies [447].

A second factor that could be involved in absence of a consistent difference between oxygen tension groups in this study is the involvement of a donor-specific impact of oxygen tension on tissue quality. Although hypoxic culture has been shown to augment chondrogenesis in BMSCs derived from the majority of donors in the studies published to date, our group has reported evidence that human and ovine BMSCs have varying *in vitro* chondrogenic responses to oxygen tension with BMSCs from some donors demonstrating

pronounced chondrogenesis under normoxia [332, 405]. Another group has reported superior chondrogenesis of BMSCs following a protocol of normoxic preconditioning and hypoxic differentiation, but noted variability between donors in the positive impact of hypoxia on chondrogenesis [373]. To fully appreciate the general effect and variability of effect of oxygen tension during pre-implantation culture on *in vivo* cartilaginous tissue formation, a study involving a larger number of animals would be required.

The impact of incubator oxygen tension on BMSC proliferation during expansion was also assessed. Cell counts following expansion under hypoxia approached significantly higher levels than those following expansion under normoxia. Population doublings per day and cumulative population doublings were similar under normoxia and hypoxia. These results are consistent with previous studies reporting non-significant differences during early passages and enhanced expansion under hypoxia with prolonged expansion periods beyond P2 [367, 368].

Repair and native tissues were investigated with multiple parameters in this study. Histological assessment was performed using a modified O'Driscoll scoring system given that the original system and previously modified versions have been used routinely in the assessment of cartilage injury and treatment modalities in animal models [274, 301, 306, 308, 315, 438, 439, 448, 449]. The amount of repair tissue formed and defect fill varied in the study at hand.

Parameters that have not previously accounted for such variability include percentage of hyaline-like cartilage and percentage of safranin O staining [439]. These parameters were normalized to area of repair tissue / area of defect site with the goal of preventing over-scoring of repair tissues that are relatively high in quality but fill only small fractions of the defect site, and under-scoring of repair tissues that are relatively poor in quality but fill large fractions of the defect site. Similarly, thickness of repair tissue was normalized to the width of the defect site containing repair tissue / total width of defect site.

Macroscopic assessment was performed using a modified Goebel scoring system [441]. The Goebel scoring system was created for assessment of experimental cartilage repair in large-animal models and shown to display strong reliability and good correlation with magnetic resonance imaging [441]. The parameter for defect fill was modified to assess percentage of tissue in the defect site that existed at the level of the adjacent native cartilage. The point system of the original score was inverted to award the highest score to the best tissue, which was consistent with the histological scoring system used in this study and other macroscopic scoring system used in a clinical setting [450].

During histological assessment of subchondral bone, an extensive reaction was noted within some sections from control defects and defects treated with cell-seeded scaffolds. Subchondral reactions were characterized by cell infiltration and altered structural microanatomy within an area that involved areas of subarticular

spongiosa and sinusoids [394, 451]. There was not a significant difference between groups with respect to the presence of extensive reactions. Histological findings consistent with these reactions have been seen reported previously in cartilage studies employing a sheep model [274]. In a clinical setting, they could represent the same process as bone marrow edema described in patients with cartilage defects visualized with MRI [45, 320, 452]. Bone marrow edema-like lesions have been associated with osteoarthritis and could be the result of inflammatory reactions to injured cartilage or micro-traumatic changes related to changes in biomechanics [453].

The specific injury and transplantation model used in this study allows for preclinical investigation of BMSC transplantation principles, although a number of limitations of this model exist. Sheep were used given that this species is commonly utilized in the assessment of cell-based treatment modalities for cartilage restoration [274, 301, 306, 308]. Simulated defects were created during the same surgical procedure and just prior to construct transplantation. This protocol has been described previously and allows for minimization of surgical insult to each stifle joint given that separate surgical procedures are not required for defect creation and treatment [36, 301, 307]. However it fails to represent the time period between cartilage injury and surgical intervention that chronic models account for [274]. The defect diameter of 7 mm used is consistent with previous literature and considered to be a critical-sized defect [100, 274]. Each defect was created to involve the full thickness of cartilage without compromising the

subchondral bone plate in order to prevent the involvement of a subchondral source of cells. The downside of this technique is that the cartilage of the ovine femoral condyle is quite thin, which leads to relatively shallow defects that potentially increase the likelihood of implant delamination in comparison to osteochondral defects. Two defects were situated in each stifle joint with one on the medial condyle and another on the lateral condyle, which allowed for defects to be situated within different microenvironments within each joint. Exposure and visualization of the lateral condyle was more difficult than the medial condyle given the origin of the extensor digitorum longus [436]. Both defects within each stifle joint were treated with the same cell condition of no cells (with or without scaffold), normoxia-cultured BMSC-seeded scaffolds or hypoxia-cultured BMSC-seeded scaffolds to avoid interaction [454].

Other possible limitations of the sheep model used in this study relate to implant fixation and post-operative activity. Fixation of cell-seeded scaffolds is controversial [363]. Construct implantation was supplemented with Tisseel fibrin sealant. This technique is consistent with multiple clinical studies that have used fibrin sealant or platelet-rich fibrin gel to promote implant fixation [38, 40, 45, 46, 254, 320]. However, the use of suture to augment fixation has also been reported [46]. It is unclear whether suture augmentation is required for the model used in this study. Damage to adjacent native cartilage by sutures has been described previously in a sheep study that utilized full-thickness cartilage defects [455]. Post-operatively, animals were allowed to perform weight bearing as tolerated. In

contrast to clinical studies in which guarded weight bearing is used in the post-operative setting [38], sheep returned to full weight bearing immediately following surgery.

6.5 Conclusion

BMSCs that were isolated, expanded, seeded within HYAFF scaffolds, and chondrogenically primed for four days in chondrogenic medium prior to implantation were capable of producing hyaline-like cartilaginous repair tissue within full-thickness cartilage defects. This repair tissue had improved quality relative to cell-free controls. These findings provide preliminary evidence that this protocol may serve as an option for treatment of full-thickness cartilage defects. Incubator oxygen tension during *ex vivo* culture modulated the quality of repair tissue variably between animals. It is currently unclear whether pre-implantation culture of BMSCs in hypoxic conditions improves cartilaginous tissue formation following transplantation. Therefore, further study is required to assess the use of oxygen tension modulation in the optimization of BMSC transplantation.

Chapter 7

General Discussion and Conclusions

Troy D. Bornes

7.1 General discussion

Articular cartilage defects progress to osteoarthritis (OA), a condition that results in significant patient morbidity and substantial cost to our healthcare system [1, 2, 4-6, 12, 107, 109]. At present, effective surgical treatment options for focal chondral and osteochondral defects are limited.

Marrow stimulation using microfracture, osteochondral autograft transplantation (OATS), cell-free scaffolds, and autologous matrix-induced chondrogenesis (AMIC) are treatment options for small-to-midsized defects of the knee and ankle [125, 140, 154, 199, 201, 203]. Larger defects are treated with autologous chondrocyte transplantation (ACT), matrix-associated autologous chondrocyte transplantation (MACT) or osteochondral allograft transplantation (OCA) [125, 154].

Although positive outcomes have been reported to date in the surgical management of articular cartilage defects, significant downsides exist with each modality of treatment. Marrow stimulation is not appropriate for large defects given that it results in resurfacing with fibrocartilaginous repair tissue that does

not recapitulate the properties of hyaline cartilage [98, 138-141]. OATS produces donor site morbidity and offers only short-term benefit as outcomes deteriorate with time [158, 159]. ACT requires a lengthy and costly protocol of two operative procedures and an *ex vivo* culture period that is limited by chondrocyte de-differentiation and senescence [244-253]. Allograft transplantation is logistically difficult given the need for donor-recipient size matching, testing for infectious diseases, sterilization, processing, and implantation within a short time frame following harvest to ensure chondrocyte viability [171].

Mesenchymal stem cell (MSC) transplantation is a cell-based strategy devised to resurface defects with bioengineered cartilage that recapitulates the properties of hyaline cartilage while avoiding or reducing the downsides associated with the current modalities of treatment. Based on the available literature, a number of specific bone marrow-derived mesenchymal stromal stem cell (BMSC) transplantation protocols have successfully resurfaced articular cartilage in animals and humans [29, 36-38]. Several studies have reported the creation of repair tissue consistent with hyaline cartilage based on arthroscopic, histologic and imaging assessment [38-44]. However, inconsistencies in tissue quality and clinical scores have been described [29, 38, 39, 41, 43, 45, 46, 254, 317]. Therefore, it is apparent that there is room for improvement of current tissue engineering and transplantation protocols related to articular cartilage regeneration.

The objective of this thesis was to investigate variables of BMSC-based cartilage engineering including BMSC isolation and expansion environment, biomaterial matrix composition and seeding density, and chondrogenic differentiation conditions using *in vitro* and *in vivo* models. The goal of the studies was to optimize the quality of cartilaginous neo-tissue formed from BMSCs.

The first original research article of this thesis described in Chapter 3 involved an assessment of incubator oxygen tension during ovine BMSC isolation, expansion and differentiation on *in vitro* BMSC chondrogenesis within clinically approved porous scaffolds composed of type I collagen and esterified hyaluronic acid (HA). It was shown that collagen and HA scaffolds seeded with BMSCs that were isolated, expanded and differentiated under hypoxia (3% oxygen) exhibited superior aggrecan and collagen II mRNA expressions, GAG quantity and proteoglycan staining in comparison to normoxia (21% oxygen). GAG/DNA was augmented with hypoxic isolation/expansion in all constructs. Comparison by scaffold composition indicated increased mRNA expression of hyaline cartilage-associated collagen II, aggrecan and SOX9 on the collagen scaffold, although expression of collagen X, which is related to hypertrophic cartilage, was also elevated. Proteoglycan deposition was similar between BMSCs seeded on collagen and HA scaffolds for conditions of sustained hypoxia and sustained normoxia in which isolation, expansion and differentiation were performed under the same oxygen tension. Proteoglycan deposition was

significantly improved within the collagen scaffold over the HA scaffold when culture specifically involved normoxic isolation/expansion followed by hypoxic differentiation. During chondrogenesis, collagen-based constructs progressively contracted to 60% of the initial diameter after 14 days, while HA-based construct size was maintained at 110%.

The findings of this study are important given that hypoxic enhancement of BMSC chondrogenesis had been previously studied extensively in pellet, micromass and hydrogel models [332, 368-372], but not in porous scaffolds that are commonly used to study three-dimensional (3D) cartilage formation *in vitro* and in clinical BMSC transplantation protocols [41, 45, 194, 254, 318, 363]. The results further support hypoxic incubation as a tool that may be used during BMSC isolation, expansion or precultivation to improve cartilaginous tissue in BMSC transplantation protocols. To date, normoxic incubation has been the standard in a clinical realm [363]. Scaffolds composed of type I collagen and HA porous were assessed in this study given that these biomaterials are commonly used in cartilage engineering applications and clinical BMSC transplantation [43, 45, 254, 318]. Each scaffold was shown to be capable of fostering gene expression and ECM formation consistent with hyaline-like cartilage from BMSCs. The collagen I scaffold demonstrated increased expressions of genes related to hyaline, fibrous, and hypertrophic cartilage. However, ECM deposition was similar between scaffolds in most oxygen tension groups. Therefore both collagen I and HA scaffolds are suitable for use in BMSC transplantation

protocols. The HA scaffold was able to maintain size during chondrogenesis, which could be beneficial for defect filling in a clinical setting.

Chapter 4 involved a study that characterized the contraction during chondrogenesis of a porous collagen I scaffold seeded with human BMSCs that were isolated and expanded under different oxygen tensions. It was noted in Chapter 3 that BMSC-seeded collagen scaffolds contracted significantly during the 14-day differentiation period and that hypoxic isolation and expansion reduced the contraction. In Chapter 4, the goal was to characterize contraction of human BMSC-seeded collagen scaffolds over 30 days with a detailed assessment of diameter in 3-day increments. During chondrogenesis, the diameter of scaffolds was found to increase to a peak at 3-6 days, return to the original size by 9 days and then decrease thereafter to the end of the 30-day culture period. Scaffold-specific diameter changes and cell-mediated diameter changes were elucidated. Hypoxic isolation and expansion were found to reduce contraction at a statistically significant level in comparison to normoxia. After 15 days, scaffold diameter contractions were measured at 14% and 21% in scaffolds that were seeded with hypoxia- and normoxia-expanded BMSCs. After 30 days, diameter contractions were 18% and 24%, respectively. Cell-mediated contraction was more pronounced in scaffolds seeded at higher densities. It was noted that proteoglycan production during contraction was higher in hypoxia-cultured BMSCs than normoxia-cultured BMSCs, particularly after 15 days.

The results of this study are relevant to BMSC transplantation given that collagen scaffolds are routinely used in a clinical setting and contraction is an issue that presumably reduces defect filling and promotes implant delamination [39, 41, 43]. This study provides evidence that *in vitro* differentiation of BMSCs on collagen I scaffolds should be limited to a time period that reduces contraction but allows for cartilaginous ECM formation prior to implantation. Hypoxic isolation and expansion may be used to reduce contraction as an adjunct to other previously developed techniques, such as dehydrothermal treatment (DHT) and ultraviolet (UV) crosslinking, given that this novel technique did not fully prevent contraction [48, 49].

In Chapter 5, isolation and expansion environment and cell seeding density of a collagen I scaffold were assessed using ovine BMSCs in an *in vitro* model. BMSCs that were isolated and expanded by a conventional two-dimensional (2D) technique in tissue-culture flasks were seeded at densities of 50, 10, 5, 1, and 0.5 $x10^6$ BMSCs/cm^3 within collagen scaffolds. BMSCs seeded at all densities were capable of proteoglycan production and displayed increased expressions of aggrecan and collagen II mRNA relative to pre-differentiation controls. Collagen II deposition was apparent in scaffolds seeded at 0.5-10 $x10^6$ BMSCs/cm^3. Chondrogenesis of 2D-expanded BMSCs was most pronounced in scaffolds seeded at 5-10 $x10^6$ BMSCs/cm^3 based on aggrecan and collagen II mRNA, safranin O staining, Bern histological score, total GAG, and GAG/DNA.

For three-dimensional (3D) isolation and expansion, bone marrow aspirates containing known quantities of mononucleated cells (BMNCs) were seeded on scaffolds at 50, 10, 5, 1, and 0.5 x10^6 BMNCs/cm^3 and cultured in expansion medium for an equivalent duration to 2D expansion, and then differentiated in chondrogenic medium. All densities of BMSCs had increased aggrecan and collagen II mRNA expressions relative to controls. Proteoglycan deposition was present in scaffolds seeded at 0.5-50 x10^6 BMNCs/cm^3, while collagen II deposition occurred in scaffolds seeded at 10-50 x10^6 BMNCs/cm^3. The highest levels of aggrecan and collagen II mRNA, Bern score, total GAG, and GAG/DNA occurred with seeding at 50 x10^6 BMNCs/cm^3.

This study further supports the previous work showing that a 3D environment is a viable option for isolation and expansion of BMSCs [266]. The results related to cell seeding density provide information that was previously lacking in the field of BMSC-based cartilage engineering. Chondrogenesis appeared to be most pronounced with seeding densities of 5-10 x10^6 BMSCs/cm^3 and 50 x10^6 BMNCs/cm^3 for 2D and 3D expansion protocols, respectively. These densities could be considered when seeding collagen I scaffolds in BMSC transplantation protocols in future *in vitro* and *in vivo* studies.

The final study of this thesis described in Chapter 6 utilized an *in vivo* sheep model with full-thickness articular cartilage defects to assess a novel protocol for BMSC transplantation that involved BMSCs that were isolated,

expanded, seeded within HYAFF scaffolds, and chondrogenically primed using a short (four-day) culture period in chondrogenic medium prior to implantation. The impact of oxygen tension during pre-implantation culture on cartilaginous tissue formation was also investigated. Implantation of BMSC-seeded scaffolds yielded repair tissues that varied in quality and were consistent with hyaline cartilage and fibrocartilage. Defects implanted with cell-seeded scaffolds had significantly higher histological scores and repair tissue areas than cell-free controls. Analysis per donor demonstrated that histological scores were significantly higher with cell-seeded scaffolds than cell-free controls in two sheep. Normoxia- and hypoxia-cultured BMSC-seeded scaffolds were compared in three other sheep and outcomes were variable. Two sheep had histological findings that suggested improved repair tissue formation following hypoxic culture of BMSCs, while histological scores and defect fill were superior in a third sheep following normoxic culture. Macroscopic scoring was not significantly different between groups.

This finding provided preliminary evidence that a protocol of BMSC isolation, expansion, scaffold seeding, chondrogenic priming, and implantation is promising and may serve as an option for treatment of full-thickness cartilage defects. This benefit of this protocol is that BMSCs may be predisposed to enter the chondrogenic lineage while avoiding a time- and resource-intensive differentiation period that is required by precultivation protocols [36, 274, 308]. This study provided the first investigation of the effect of incubator oxygen

tension during *ex vivo* culture on the quality of cartilaginous repair tissue developed *in vivo* within large-animal joint cartilage defects. However, a consistent effect of oxygen tension was not established across donors.

The studies performed as part of this thesis have furthered our knowledge of particular aspects of BMSC chondrogenesis and generated questions to be answered in future research. Although culture in hypoxic conditions during BMSC isolation, expansion and differentiation has been shown to improve chondrogenesis *in vitro* in pellet, micromass, hydrogel, and porous scaffold models (Chapters 3 and 4), and *in vivo* in subcutaneous mouse models, it is still unclear whether hypoxic culture is relevant to BMSC transplantation protocols [332, 368-372]. Although we have started this assessment with a pilot study in sheep (Chapter 6), further investigation is required in large-animal studies with larger sample sizes before this technique becomes relevant to consider in a clinical realm.

Isolation and expansion under 3D conditions has been proposed as a method of mimicking the natural bone marrow microenvironment and maintaining multipotency and chondrogenic capacity [266, 341]. The results of Chapter 5 indicate that both 2D and 3D isolation and expansion lead to BMSCs that differentiate into cells the create hyaline-like cartilage that is rich in proteoglycans and type II collagen. Future investigation is required to compare the quality of cartilaginous tissue derived from cells isolated and expanded within

each environment. Whole bone marrow and bone marrow-derived cell (BMDC) collections created from centrifugation and separation systems have been seeded into tissue-culture flasks and on scaffolds for 2D and 3D isolation protocols [31, 32, 261, 332, 405, 435]. Components of bone marrow and cell collections have been elucidated and compared recently by Fortier *et al*. [417, 435]. However, characterization of the properties of cells – including cell surface markers, adherence capability and differentiation capacity – derived using each method should be performed.

Several BMSC transplantation protocols have been proposed with no clear consensus on technique established. Clinically, BMDC collections, also known as bone marrow aspirate concentrates (BMACs) or bone marrow concentrates (BMCs), and isolated and expanded BMSCs have been implanted on biomaterial matrices [38, 39, 41, 43, 254, 328]. Precultivated BMSCs on matrices have been implanted within large-animal joints but not used clinically to date [36, 274, 308]. In Chapter 6, a hybrid method was proposed that consisted of BMSC isolation, expansion, priming with a short differentiation period, scaffold seeding, and implantation. Although some comparison of protocols has been performed in animal models [274, 308, 311], more rigorous study is required to compare different protocols available to each other and to chondrocyte transplantation (MACT). Furthermore, the use of tissue engineering strategies such as hypoxic incubation, cell co-culture and mechanical stimulation using bioreactors within

each protocol should be considered during protocol comparison and optimization [332, 357, 447].

7.2 Conclusions

This research investigated tissue engineering variables associated with the bioengineering of articular cartilage from BMSCs. Hypoxic incubation of BMSCs during isolation, expansion and differentiation within collagen I and hyaluronic acid scaffolds improved the quality of cartilaginous repair tissue formed *in vitro*. BMSCs that were isolated and expanded within 2D and 3D environments were shown to be capable of producing hyaline-like cartilage *in vitro*. Within a collagen I scaffold, the optimal seeding densities of 2D- and 3D-expanded BMSCs was 5-10 $x10^6$ BMSCs/cm^3 and 50 $x10^6$ BMNCs/cm^3, respectively. BMSCs that were isolated, expanded, seeded within hyaluronic acid scaffolds, and chondrogenically primed prior to implantation were capable of producing hyaline-like cartilaginous repair tissue that was superior to controls within full-thickness, distal femoral articular cartilage defects in sheep. Incubator oxygen tension during *ex vivo* culture modulated the quality of repair tissue variably between animals.

References

1. Buckwalter JA, Brown TD: **Joint injury, repair, and remodeling: roles in post-traumatic osteoarthritis.** *Clin Orthop Relat Res* 2004, **(423)**(423)**:**7-16.

2. Brown TD, Johnston RC, Saltzman CL, Marsh JL, Buckwalter JA: **Posttraumatic osteoarthritis: a first estimate of incidence, prevalence, and burden of disease.** *J Orthop Trauma* 2006, **20**(10)**:**739-744.

3. Maletius W, Messner K: **The effect of partial meniscectomy on the long-term prognosis of knees with localized, severe chondral damage. A twelve- to fifteen-year followup.** *Am J Sports Med* 1996, **24**(3)**:**258-262.

4. Stufkens SA, Knupp M, Horisberger M, Lampert C, Hintermann B: **Cartilage lesions and the development of osteoarthritis after internal fixation of ankle fractures: a prospective study.** *J Bone Joint Surg Am* 2010, **92**(2)**:**279-286.

5. Messner K, Maletius W: **The long-term prognosis for severe damage to weight-bearing cartilage in the knee: a 14-year clinical and radiographic follow-up in 28 young athletes.** *Acta Orthop Scand* 1996, **67**(2)**:**165-168.

6. Shelbourne KD, Jari S, Gray T: **Outcome of untreated traumatic articular cartilage defects of the knee: a natural history study.** *J Bone Joint Surg Am* 2003, **85-A**(Suppl 2)**:**8-16.

7. Cross M, Smith E, Hoy D, Nolte S, Ackerman I, Fransen M, Bridgett L, Williams S, Guillemin F, Hill CL, Laslett LL, Jones G, Cicuttini F, Osborne R, Vos T, Buchbinder R, Woolf A, March L: **The global burden of hip and knee osteoarthritis: estimates from the global burden of disease 2010 study.** *Ann Rheum Dis* 2014, **73**(7)**:**1323-1330.

8. O'Donnell S, Lagace C, McRae L, Bancej C: **Life with arthritis in Canada: a personal and public health challenge.** *Chronic Dis Inj Can* 2011, **31**(3)**:**135-136.

9. Public Health Agency of Canada: **Life with Arthritis in Canada: A personal and public health challenge.** 2010, **1:**1-128.

10. Buckwalter JA, Saltzman C, Brown T: **The impact of osteoarthritis: implications for research.** *Clin Orthop Relat Res* 2004, **427**(Suppl)**:**S6-15.

11. Centers for Disease Control and Prevention (CDC): **Prevalence of doctor-diagnosed arthritis and arthritis-attributable activity limitation - United States, 2010-2012.** *MMWR Morb Mortal Wkly Rep* 2013, **62**(44)**:**869-873.

12. Centers for Disease Control and Prevention (CDC): **National and state medical expenditures and lost earnings attributable to arthritis and other rheumatic conditions--United States, 2003.** *MMWR Morb Mortal Wkly Rep* 2007, **56**(1)**:**4-7.

13. Centers for Disease Control and Prevention (CDC): **Arthritis: At A Glance 2015.** 2015, **1:**1-4.

14. Chen A, Gupte C, Akhtar K, Smith P, Cobb J: **The Global Economic Cost of Osteoarthritis: How the UK Compares.** *Arthritis* 2012, **2012:**698709.

15. March LM, Bachmeier CJ: **Economics of osteoarthritis: a global perspective.** *Baillieres Clin Rheumatol* 1997, **11**(4)**:**817-834.

16. Gupta S, Hawker GA, Laporte A, Croxford R, Coyte PC: **The economic burden of disabling hip and knee osteoarthritis (OA) from the perspective of individuals living with this condition.** *Rheumatology (Oxford)* 2005, **44**(12)**:**1531-1537.

17. Le Pen C, Reygrobellet C, Gerentes I: **Financial cost of osteoarthritis in France. The "COART" France study.** *Joint Bone Spine* 2005, **72**(6)**:**567-570.

18. Leardini G, Salaffi F, Caporali R, Canesi B, Rovati L, Montanelli R, Italian Group for Study of the Costs of Arthritis: **Direct and indirect costs of osteoarthritis of the knee.** *Clin Exp Rheumatol* 2004, **22**(6)**:**699-706.

19. Loza E, Lopez-Gomez JM, Abasolo L, Maese J, Carmona L, Batlle-Gualda E, Artrocad Study Group: **Economic burden of knee and hip osteoarthritis in Spain.** *Arthritis Rheum* 2009, **61**(2)**:**158-165.

20. World Health Organization Scientific Group: **The Burden of Musculoskeletal Conditions at the Start of the New Millennium.** *WHO Technical Report Series* 2003, **919:**24-27.

21. Andersen RE, Crespo CJ, Ling SM, Bathon JM, Bartlett SJ: **Prevalence of significant knee pain among older Americans: results from the Third National Health and Nutrition Examination Survey.** *J Am Geriatr Soc* 1999, **47**(12)**:**1435-1438.

22. Lawrence RC, Felson DT, Helmick CG, Arnold LM, Choi H, Deyo RA, Gabriel S, Hirsch R, Hochberg MC, Hunder GG, Jordan JM, Katz JN, Kremers HM, Wolfe F, National Arthritis Data Workgroup: **Estimates of the prevalence of arthritis and other rheumatic conditions in the United States. Part II.** *Arthritis Rheum* 2008, **58**(1)**:**26-35.

23. Richmond JC: **Surgery for osteoarthritis of the knee.** *Rheum Dis Clin North Am* 2013, **39**(1)**:**203-211.

24. Pivec R, Johnson AJ, Mears SC, Mont MA: **Hip arthroplasty.** *Lancet* 2012, **380**(9855)**:**1768-1777.

25. Pailhe R, Sharma A, Reina N, Cavaignac E, Chiron P, Laffosse JM: **Hip resurfacing: a systematic review of literature.** *Int Orthop* 2012, **36**(12)**:**2399-2410.

26. Zaidi R, Cro S, Gurusamy K, Siva N, Macgregor A, Henricson A, Goldberg A: **The outcome of total ankle replacement: a systematic review and meta-analysis.** *Bone Joint J* 2013, **95-B**(11)**:**1500-1507.

27. DePalma AF, McKeever CD, Subin DK: **Process of repair of articular cartilage demonstrated by histology and autoradiography with tritiated thymidine.** *Clin Orthop Relat Res* 1966, **48:**229-242.

28. Brittberg M, Lindahl A, Nilsson A, Ohlsson C, Isaksson O, Peterson L: **Treatment of deep cartilage defects in the knee with autologous chondrocyte transplantation.** *N Engl J Med* 1994, **331**(14)**:**889-895.

29. Wakitani S, Goto T, Pineda SJ, Young RG, Mansour JM, Caplan AI, Goldberg VM: **Mesenchymal cell-based repair of large, full-thickness defects of articular cartilage.** *J Bone Joint Surg Am* 1994, **76**(4)**:**579-592.

30. Benthien JP, Behrens P: **Autologous matrix-induced chondrogenesis (AMIC). A one-step procedure for retropatellar articular resurfacing.** *Acta Orthop Belg* 2010, **76**(2)**:**260-263.

31. Mackay AM, Beck SC, Murphy JM, Barry FP, Chichester CO, Pittenger MF: **Chondrogenic differentiation of cultured human mesenchymal stem cells from marrow.** *Tissue Eng* 1998, **4**(4)**:**415-428.

32. Pittenger MF, Mackay AM, Beck SC, Jaiswal RK, Douglas R, Mosca JD, Moorman MA, Simonetti DW, Craig S, Marshak DR: **Multilineage potential of adult human mesenchymal stem cells.** *Science* 1999, **284**(5411)**:**143-147.

33. Fossett E, Khan WS: **Optimising human mesenchymal stem cell numbers for clinical application: a literature review.** *Stem Cells Int* 2012, **2012:**465259.

34. Mafi R, Hindocha S, Mafi P, Griffin M, Khan WS: **Sources of adult mesenchymal stem cells applicable for musculoskeletal applications - a systematic review of the literature.** *Open Orthop J* 2011, **5**(Suppl 2)**:**242-248.

35. Vannini F, Filardo G, Kon E, Roffi A, Marcacci M, Giannini S: **Scaffolds for cartilage repair of the ankle joint: The impact on surgical practice.** *Foot Ankle Surg* 2013, **19**(1)**:**2-8.

36. Wayne JS, McDowell CL, Shields KJ, Tuan RS: **In vivo response of polylactic acid-alginate scaffolds and bone marrow-derived cells for cartilage tissue engineering.** *Tissue Eng* 2005, **11**(5-6)**:**953-963.

37. Wakitani S, Imoto K, Yamamoto T, Saito M, Murata N, Yoneda M: **Human autologous culture expanded bone marrow mesenchymal cell transplantation for repair of cartilage defects in osteoarthritic knees.** *Osteoarthritis Cartilage* 2002, **10**(3)**:**199-206.

38. Giannini S, Buda R, Vannini F, Cavallo M, Grigolo B: **One-step bone marrow-derived cell transplantation in talar osteochondral lesions.** *Clin Orthop Relat Res* 2009, **467**(12)**:**3307-3320.

39. Kuroda R, Ishida K, Matsumoto T, Akisue T, Fujioka H, Mizuno K, Ohgushi H, Wakitani S, Kurosaka M: **Treatment of a full-thickness articular cartilage defect in the femoral condyle of an athlete with autologous bone-marrow stromal cells.** *Osteoarthritis Cartilage* 2007, **15**(2)**:**226-231.

40. Giannini S, Buda R, Cavallo M, Ruffilli A, Cenacchi A, Cavallo C, Vannini F: **Cartilage repair evolution in post-traumatic osteochondral lesions of the talus: from open field autologous chondrocyte to bone-marrow-derived cells transplantation.** *Injury* 2010, **41**(11)**:**1196-1203.

41. Gobbi A, Karnatzikos G, Scotti C, Mahajan M, Mazzucco L, Grigolo B: **One-Step Cartilage Repair with Bone Marrow Aspirate Concentrated Cells and Collagen Matrix in Full-Thickness Knee Cartilage Lesions: Results at 2-Year Follow-up.** *Cartilage* 2011, **2**(286)**:**286-299.

42. Wakitani S, Kawaguchi A, Tokuhara Y, Takaoka K: **Present status of and future direction for articular cartilage repair.** *J Bone Miner Metab* 2008, **26**(2)**:**115-122.

43. Wakitani S, Nawata M, Tensho K, Okabe T, Machida H, Ohgushi H: **Repair of articular cartilage defects in the patello-femoral joint with autologous**

bone marrow mesenchymal cell transplantation: three case reports involving nine defects in five knees. *J Tissue Eng Regen Med* 2007, **1**(1)**:**74-79.

44. Kon E, Vannini F, Buda R, Filardo G, Cavallo M, Ruffilli A, Nanni M, Di Martino A, Marcacci M, Giannini S: **How to treat osteochondritis dissecans of the knee: surgical techniques and new trends: AAOS exhibit selection.** *J Bone Joint Surg Am* 2012, **94**(1)**:**e1(1-8).

45. Giannini S, Buda R, Battaglia M, Cavallo M, Ruffilli A, Ramponi L, Pagliazzi G, Vannini F: **One-step repair in talar osteochondral lesions: 4-year clinical results and t2-mapping capability in outcome prediction.** *Am J Sports Med* 2013, **41**(3)**:**511-518.

46. Gobbi A, Chaurasia S, Karnatzikos G, Nakamura N: **Matrix-Induced Autologous Chondrocyte Implantation versus Multipotent Stem Cells for the Treatment of Large Patellofemoral Chondral Lesions: A Nonrandomized Prospective Trial.** *Cartilage* 2015, **6**(2)**:**82-97.

47. Buckwalter JA, Mankin HJ, Grodzinsky AJ: **Articular cartilage and osteoarthritis.** *Instr Course Lect* 2005, **54:**465-480.

48. Mankin HJ, Grodzinsky AJ, Buckwalter JA: **Articular Cartilage and Osteoarthritis.** In *Orthopaedic Basic Science: Foundations of Clinical Practice. Volume Third Edition*. Edited by Einhorn TA, O'Keefe RJ, Buckwalter JA. 2007:161-174.

49. Martel-Pelletier J, Boileau C, Pelletier JP, Roughley PJ: **Cartilage in normal and osteoarthritis conditions.** *Best Pract Res Clin Rheumatol* 2008, **22**(2)**:**351-384.

50. Kheir E, Shaw D: **Hyaline articular cartilage.** *Orthopaedics and Trauma* 2009, **23**(6)**:**450-455.

51. Kuettner KE: **Biochemistry of articular cartilage in health and disease.** *Clin Biochem* 1992, **25**(3)**:**155-163.

52. Shepherd DE, Seedhom BB: **Thickness of human articular cartilage in joints of the lower limb.** *Ann Rheum Dis* 1999, **58**(1)**:**27-34.

53. Buckwalter JA, Mow VC, Ratcliffe A: **Restoration of Injured or Degenerated Articular Cartilage.** *J Am Acad Orthop Surg* 1994, **2**(4)**:**192-201.

54. Muir H: **The chondrocyte, architect of cartilage. Biomechanics, structure, function and molecular biology of cartilage matrix macromolecules.** *Bioessays* 1995, **17**(12)**:**1039-1048.

55. O'Conor CJ, Leddy HA, Benefield HC, Liedtke WB, Guilak F: **TRPV4-mediated mechanotransduction regulates the metabolic response of chondrocytes to dynamic loading.** *Proc Natl Acad Sci U S A* 2014, **111**(4)**:**1316-1321.

56. Huber M, Trattnig S, Lintner F: **Anatomy, biochemistry, and physiology of articular cartilage.** *Invest Radiol* 2000, **35**(10)**:**573-580.

57. Hunziker EB, Quinn TM, Hauselmann HJ: **Quantitative structural organization of normal adult human articular cartilage.** *Osteoarthritis Cartilage* 2002, **10**(7)**:**564-572.

58. Stockwell RA: **The cell density of human articular and costal cartilage.** *J Anat* 1967, **101**(Pt 4)**:**753-763.

59. Alsalameh S, Amin R, Gemba T, Lotz M: **Identification of mesenchymal progenitor cells in normal and osteoarthritic human articular cartilage.** *Arthritis Rheum* 2004, **50**(5)**:**1522-1532.

60. Dowthwaite GP, Bishop JC, Redman SN, Khan IM, Rooney P, Evans DJ, Haughton L, Bayram Z, Boyer S, Thomson B, Wolfe MS, Archer CW: **The surface of articular cartilage contains a progenitor cell population.** *J Cell Sci* 2004, **117**(Pt 6)**:**889-897.

61. Grogan SP, Miyaki S, Asahara H, D'Lima DD, Lotz MK: **Mesenchymal progenitor cell markers in human articular cartilage: normal distribution and changes in osteoarthritis.** *Arthritis Res Ther* 2009, **11**(3)**:**R85.

62. Williams R, Khan IM, Richardson K, Nelson L, McCarthy HE, Analbelsi T, Singhrao SK, Dowthwaite GP, Jones RE, Baird DM, Lewis H, Roberts S, Shaw HM, Dudhia J, Fairclough J, Briggs T, Archer CW: **Identification and clonal characterisation of a progenitor cell sub-population in normal human articular cartilage.** *PLoS One* 2010, **5**(10)**:**e13246.

63. Seol D, McCabe DJ, Choe H, Zheng H, Yu Y, Jang K, Walter MW, Lehman AD, Ding L, Buckwalter JA, Martin JA: **Chondrogenic progenitor cells respond to cartilage injury.** *Arthritis Rheum* 2012, **64**(11)**:**3626-3637.

64. Koelling S, Kruegel J, Irmer M, Path JR, Sadowski B, Miro X, Miosge N: **Migratory chondrogenic progenitor cells from repair tissue during the later stages of human osteoarthritis.** *Cell Stem Cell* 2009, **4**(4)**:**324-335.

65. Gerter R, Kruegel J, Miosge N: **New insights into cartilage repair - the role of migratory progenitor cells in osteoarthritis.** *Matrix Biol* 2012, **31**(3)**:**206-213.

66. Lemperg RK, Larsson SE, Hjertquist SO: **Distribution of water and glycosaminoglycans in different layers of cattle articular cartilage.** *Isr J Med Sci* 1971, **7**(3)**:**419-421.

67. Wotton SF, Duance VC: **Type III collagen in normal human articular cartilage.** *Histochem J* 1994, **26**(5)**:**412-416.

68. Poole CA, Ayad S, Schofield JR: **Chondrons from articular cartilage: I. Immunolocalization of type VI collagen in the pericellular capsule of isolated canine tibial chondrons.** *J Cell Sci* 1988, **90**(4)**:**635-643.

69. Schmid TM, Linsenmayer TF: **Immunohistochemical localization of short chain cartilage collagen (type X) in avian tissues.** *J Cell Biol* 1985, **100**(2)**:**598-605.

70. Boos N, Nerlich AG, Wiest I, von der Mark K, Ganz R, Aebi M: **Immunohistochemical analysis of type-X-collagen expression in osteoarthritis of the hip joint.** *J Orthop Res* 1999, **17**(4)**:**495-502.

71. Roughley PJ: **The structure and function of cartilage proteoglycans.** *Eur Cell Mater* 2006, **12:**92-101.

72. Morgelin M, Paulsson M, Hardingham TE, Heinegard D, Engel J: **Cartilage proteoglycans. Assembly with hyaluronate and link protein as studied by electron microscopy.** *Biochem J* 1988, **253**(1)**:**175-185.

73. Sun DD, Guo XE, Likhitpanichkul M, Lai WM, Mow VC: **The influence of the fixed negative charges on mechanical and electrical behaviors of articular cartilage under unconfined compression.** *J Biomech Eng* 2004, **126**(1)**:**6-16.

74. Clarke IC: **Articular cartilage: a review and scanning electron microscope study. 1. The interterritorial fibrillar architecture.** *J Bone Joint Surg Br* 1971, **53**(4)**:**732-750.

75. Lotz MK, Kraus VB: **New developments in osteoarthritis. Posttraumatic osteoarthritis: pathogenesis and pharmacological treatment options.** *Arthritis Res Ther* 2010, **12**(3)**:**211.

76. Quinn TM, Grodzinsky AJ, Hunziker EB, Sandy JD: **Effects of injurious compression on matrix turnover around individual cells in calf articular cartilage explants.** *J Orthop Res* 1998, **16**(4)**:**490-499.

77. Maroudas AI: **Balance between swelling pressure and collagen tension in normal and degenerate cartilage.** *Nature* 1976, **260**(5554)**:**808-809.

78. Basser PJ, Schneiderman R, Bank RA, Wachtel E, Maroudas A: **Mechanical properties of the collagen network in human articular cartilage as measured by osmotic stress technique.** *Arch Biochem Biophys* 1998, **351**(2)**:**207-219.

79. Jeffrey JE, Gregory DW, Aspden RM: **Matrix damage and chondrocyte viability following a single impact load on articular cartilage.** *Arch Biochem Biophys* 1995, **322**(1)**:**87-96.

80. Redman SN, Dowthwaite GP, Thomson BM, Archer CW: **The cellular responses of articular cartilage to sharp and blunt trauma.** *Osteoarthritis Cartilage* 2004, **12**(2)**:**106-116.

81. Morel V, Quinn TM: **Short-term changes in cell and matrix damage following mechanical injury of articular cartilage explants and modelling of microphysical mediators.** *Biorheology* 2004, **41**(3-4)**:**509-519.

82. Otsuki S, Brinson DC, Creighton L, Kinoshita M, Sah RL, D'Lima D, Lotz M: **The effect of glycosaminoglycan loss on chondrocyte viability: a study on porcine cartilage explants.** *Arthritis Rheum* 2008, **58**(4)**:**1076-1085.

83. Stolberg-Stolberg JA, Furman BD, Garrigues NW, Lee J, Pisetsky DS, Stearns NA, DeFrate LE, Guilak F, Olson SA: **Effects of cartilage impact with**

and without fracture on chondrocyte viability and the release of inflammatory markers. *J Orthop Res* 2013, **31**(8)**:**1283-1292.

84. DeHaven KE: **Diagnosis of acute knee injuries with hemarthrosis.** *Am J Sports Med* 1980, **8**(1)**:**9-14.

85. Roosendaal G, TeKoppele JM, Vianen ME, van den Berg HM, Lafeber FP, Bijlsma JW: **Blood-induced joint damage: a canine in vivo study.** *Arthritis Rheum* 1999, **42**(5)**:**1033-1039.

86. Shapiro F, Koide S, Glimcher MJ: **Cell origin and differentiation in the repair of full-thickness defects of articular cartilage.** *J Bone Joint Surg Am* 1993, **75**(4)**:**532-553.

87. Borsiczky B, Fodor B, Racz B, Gasz B, Jeges S, Jancso G, Roth E: **Rapid leukocyte activation following intraarticular bleeding.** *J Orthop Res* 2006, **24**(4)**:**684-689.

88. Anderson DD, Chubinskaya S, Guilak F, Martin JA, Oegema TR, Olson SA, Buckwalter JA: **Post-traumatic osteoarthritis: improved understanding and opportunities for early intervention.** *J Orthop Res* 2011, **29**(6)**:**802-809.

89. Marks PH, Donaldson ML: **Inflammatory cytokine profiles associated with chondral damage in the anterior cruciate ligament-deficient knee.** *Arthroscopy* 2005, **21**(11)**:**1342-1347.

90. Elsaid KA, Fleming BC, Oksendahl HL, Machan JT, Fadale PD, Hulstyn MJ, Shalvoy R, Jay GD: **Decreased lubricin concentrations and markers of joint inflammation in the synovial fluid of patients with anterior cruciate ligament injury.** *Arthritis Rheum* 2008, **58**(6)**:**1707-1715.

91. Yu Y, Brouillette MJ, Seol D, Zheng H, Buckwalter JA, Martin JA: **Use of recombinant human stromal cell-derived factor 1alpha-loaded fibrin/hyaluronic acid hydrogel networks to achieve functional repair of full-thickness bovine articular cartilage via homing of chondrogenic progenitor cells.** *Arthritis Rheumatol* 2015, **67**(5)**:**1274-1285.

92. D'Lima DD, Hashimoto S, Chen PC, Colwell CW,Jr, Lotz MK: **Impact of mechanical trauma on matrix and cells.** *Clin Orthop Relat Res* 2001, **391**(Suppl)**:**S90-9.

93. Buckwalter JA, Martin JA, Olmstead M, Athanasiou KA, Rosenwasser MP, Mow VC: **Osteochondral repair of primate knee femoral and patellar articular surfaces: implications for preventing post-traumatic osteoarthritis.** *Iowa Orthop J* 2003, **23:**66-74.

94. Meachim G, Roberts C: **Repair of the joint surface from subarticular tissue in the rabbit knee.** *J Anat* 1971, **109**(2)**:**317-327.

95. Johnstone B, Yoo JU: **Autologous mesenchymal progenitor cells in articular cartilage repair.** *Clin Orthop Relat Res* 1999, **367**(Suppl)**:**S156-62.

96. Mitchell N, Shepard N: **The resurfacing of adult rabbit articular cartilage by multiple perforations through the subchondral bone.** *J Bone Joint Surg Am* 1976, **58**(2)**:**230-233.

97. Mitchell N, Shepard N: **Healing of articular cartilage in intra-articular fractures in rabbits.** *J Bone Joint Surg Am* 1980, **62**(4)**:**628-634.

98. Furukawa T, Eyre DR, Koide S, Glimcher MJ: **Biochemical studies on repair cartilage resurfacing experimental defects in the rabbit knee.** *J Bone Joint Surg Am* 1980, **62**(1)**:**79-89.

99. Convery FR, Akeson WH, Keown GH: **The repair of large osteochondral defects. An experimental study in horses.** *Clin Orthop Relat Res* 1972, **82:**253-262.

100. Schinhan M, Gruber M, Vavken P, Dorotka R, Samouh L, Chiari C, Gruebl-Barabas R, Nehrer S: **Critical-size defect induces unicompartmental osteoarthritis in a stable ovine knee.** *J Orthop Res* 2012, **30**(2)**:**214-220.

101. Llinas A, McKellop HA, Marshall GJ, Sharpe F, Kirchen M, Sarmiento A: **Healing and remodeling of articular incongruities in a rabbit fracture model.** *J Bone Joint Surg Am* 1993, **75**(10)**:**1508-1523.

102. Lovasz G, Llinas A, Benya PD, Park SH, Sarmiento A, Luck JV,Jr: **Cartilage changes caused by a coronal surface stepoff in a rabbit model.** *Clin Orthop Relat Res* 1998, **(354)**(354)**:**224-234.

103. Lovasz G, Park SH, Ebramzadeh E, Benya PD, Llinas A, Bellyei A, Luck JV,Jr, Sarmiento A: **Characteristics of degeneration in an unstable knee with a coronal surface step-off.** *J Bone Joint Surg Br* 2001, **83**(3)**:**428-436.

104. Widuchowski W, Widuchowski J, Trzaska T: **Articular cartilage defects: study of 25,124 knee arthroscopies.** *Knee* 2007, **14**(3)**:**177-182.

105. Curl WW, Krome J, Gordon ES, Rushing J, Smith BP, Poehling GG: **Cartilage injuries: a review of 31,516 knee arthroscopies.** *Arthroscopy* 1997, **13**(4)**:**456-460.

106. Outerbridge RE: **The etiology of chondromalacia patellae.** *J Bone Joint Surg Br* 1961, **43-B:**752-757.

107. Gelber AC, Hochberg MC, Mead LA, Wang NY, Wigley FM, Klag MJ: **Joint injury in young adults and risk for subsequent knee and hip osteoarthritis.** *Ann Intern Med* 2000, **133**(5)**:**321-328.

108. Anderson AF, Pagnani MJ: **Osteochondritis dissecans of the femoral condyles. Long-term results of excision of the fragment.** *Am J Sports Med* 1997, **25**(6)**:**830-834.

109. Twyman RS, Desai K, Aichroth PM: **Osteochondritis dissecans of the knee. A long-term study.** *J Bone Joint Surg Br* 1991, **73**(3)**:**461-464.

110. De Smet AA, Ilahi OA, Graf BK: **Untreated osteochondritis dissecans of the femoral condyles: prediction of patient outcome using radiographic and MR findings.** *Skeletal Radiol* 1997, **26**(8)**:**463-467.

111. Wang Y, Ding C, Wluka AE, Davis S, Ebeling PR, Jones G, Cicuttini FM: **Factors affecting progression of knee cartilage defects in normal subjects over 2 years.** *Rheumatology (Oxford)* 2006, **45**(1)**:**79-84.

112. Biswal S, Hastie T, Andriacchi TP, Bergman GA, Dillingham MF, Lang P: **Risk factors for progressive cartilage loss in the knee: a longitudinal magnetic resonance imaging study in forty-three patients.** *Arthritis Rheum* 2002, **46**(11)**:**2884-2892.

113. Guilak F, Fermor B, Keefe FJ, Kraus VB, Olson SA, Pisetsky DS, Setton LA, Weinberg JB: **The role of biomechanics and inflammation in cartilage injury and repair.** *Clin Orthop Relat Res* 2004, **423:**17-26.

114. Martel-Pelletier J, Alaaeddine N, Pelletier JP: **Cytokines and their role in the pathophysiology of osteoarthritis.** *Front Biosci* 1999, **4:**D694-703.

115. Lee JH, Fitzgerald JB, Dimicco MA, Grodzinsky AJ: **Mechanical injury of cartilage explants causes specific time-dependent changes in chondrocyte gene expression.** *Arthritis Rheum* 2005, **52**(8)**:**2386-2395.

116. Dahlberg L, Friden T, Roos H, Lark MW, Lohmander LS: **A longitudinal study of cartilage matrix metabolism in patients with cruciate ligament**

rupture--synovial fluid concentrations of aggrecan fragments, stromelysin-1 and tissue inhibitor of metalloproteinase-1. *Br J Rheumatol* 1994, **33**(12)**:**1107-1111.

117. Lohmander LS, Roos H, Dahlberg L, Hoerrner LA, Lark MW: **Temporal patterns of stromelysin-1, tissue inhibitor, and proteoglycan fragments in human knee joint fluid after injury to the cruciate ligament or meniscus.** *J Orthop Res* 1994, **12**(1)**:**21-28.

118. Bhosale AM, Richardson JB: **Articular cartilage: structure, injuries and review of management.** *Br Med Bull* 2008, **87:**77-95.

119. Honkonen SE: **Degenerative arthritis after tibial plateau fractures.** *J Orthop Trauma* 1995, **9**(4)**:**273-277.

120. Stevens DG, Beharry R, McKee MD, Waddell JP, Schemitsch EH: **The long-term functional outcome of operatively treated tibial plateau fractures.** *J Orthop Trauma* 2001, **15**(5)**:**312-320.

121. Sommerlath K, Lysholm J, Gillquist J: **The long-term course after treatment of acute anterior cruciate ligament ruptures. A 9 to 16 year followup.** *Am J Sports Med* 1991, **19**(2)**:**156-162.

122. McDevitt C, Gilbertson E, Muir H: **An experimental model of osteoarthritis; early morphological and biochemical changes.** *J Bone Joint Surg Br* 1977, **59**(1)**:**24-35.

123. Lohmander LS, Englund PM, Dahl LL, Roos EM: **The long-term consequence of anterior cruciate ligament and meniscus injuries: osteoarthritis.** *Am J Sports Med* 2007, **35**(10)**:**1756-1769.

124. Rasmussen PS: **Tibial condylar fractures as a cause of degenerative arthritis.** *Acta Orthop Scand* 1972, **43**(6)**:**566-575.

125. Cole BJ, Pascual-Garrido C, Grumet RC: **Surgical management of articular cartilage defects in the knee.** *Instr Course Lect* 2010, **59:**181-204.

126. Badekas T, Takvorian M, Souras N: **Treatment principles for osteochondral lesions in foot and ankle.** *Int Orthop* 2013, **37**(9)**:**1697-1706.

127. Versier G, Dubrana F, French Arthroscopy Society: **Treatment of knee cartilage defect in 2010.** *Orthop Traumatol Surg Res* 2011, **97**(8 Suppl)**:**S140-53.

128. Kramer DE, Pace JL: **Acute traumatic and sports-related osteochondral injury of the pediatric knee.** *Orthop Clin North Am* 2012, **43**(2)**:**227-36.

129. Kumai T, Takakura Y, Kitada C, Tanaka Y, Hayashi K: **Fixation of osteochondral lesions of the talus using cortical bone pegs.** *J Bone Joint Surg Br* 2002, **84**(3)**:**369-374.

130. Schepers T, De Rooij PP, Van Lieshout EM, Patka P: **Reinsertion of an inverted osteochondral lesion of the talus: a case report.** *J Foot Ankle Surg* 2011, **50**(4)**:**486-489.

131. Chotel F, Knorr G, Simian E, Dubrana F, Versier G, French Arthroscopy Society: **Knee osteochondral fractures in skeletally immature patients: French multicenter study.** *Orthop Traumatol Surg Res* 2011, **97**(8 Suppl)**:**S154-9.

132. Lee BJ, Christino MA, Daniels AH, Hulstyn MJ, Eberson CP: **Adolescent patellar osteochondral fracture following patellar dislocation.** *Knee Surg Sports Traumatol Arthrosc* 2013, **21**(8)**:**1856-1861.

133. Uchida R, Toritsuka Y, Yoneda K, Hamada M, Ohzono K, Horibe S: **Chondral fragment of the lateral femoral trochlea of the knee in adolescents.** *Knee* 2012, **19**(5)**:**719-723.

134. Giannini S, Vannini F: **Operative treatment of osteochondral lesions of the talar dome: current concepts review.** *Foot Ankle Int* 2004, **25**(3)**:**168-175.

135. Enea D, Busilacchi A, Cecconi S, Gigante A: **Late-diagnosed large osteochondral fracture of the lateral femoral condyle in an adolescent: a case report.** *J Pediatr Orthop B* 2013, **22**(4)**:**344-349.

136. Li R, Guo G, Chen B, Zhu L, Lin A: **Arthroscopically-assisted reduction and fixation of an old osteochondral fracture of the lateral femoral condyle.** *Med Sci Monit* 2012, **18**(12)**:**CS117-20.

137. Bert JM: **Abandoning microfracture of the knee: has the time come?** *Arthroscopy* 2015, **31**(3)**:**501-505.

138. Steinwachs MR, Guggi T, Kreuz PC: **Marrow stimulation techniques.** *Injury* 2008, **39**(Suppl 1)**:**S26-31.

139. Kim HK, Moran ME, Salter RB: **The potential for regeneration of articular cartilage in defects created by chondral shaving and subchondral abrasion. An experimental investigation in rabbits.** *J Bone Joint Surg Am* 1991, **73**(9)**:**1301-1315.

140. Stanish WD, McCormack R, Forriol F, Mohtadi N, Pelet S, Desnoyers J, Restrepo A, Shive MS: **Novel scaffold-based BST-CarGel treatment results in superior cartilage repair compared with microfracture in a randomized controlled trial.** *J Bone Joint Surg Am* 2013, **95**(18)**:**1640-1650.

141. Bert JM, Maschka K: **The arthroscopic treatment of unicompartmental gonarthrosis: a five-year follow-up study of abrasion arthroplasty plus arthroscopic debridement and arthroscopic debridement alone.** *Arthroscopy* 1989, **5**(1)**:**25-32.

142. Gudas R, Gudaite A, Pocius A, Gudiene A, Cekanauskas E, Monastyreckiene E, Basevicius A: **Ten-year follow-up of a prospective, randomized clinical study of mosaic osteochondral autologous transplantation versus microfracture for the treatment of osteochondral defects in the knee joint of athletes.** *Am J Sports Med* 2012, **40**(11)**:**2499-2508.

143. Steadman JR, Miller BS, Karas SG, Schlegel TF, Briggs KK, Hawkins RJ: **The microfracture technique in the treatment of full-thickness chondral**

lesions of the knee in National Football League players. *J Knee Surg* 2003, **16**(2)**:**83-86.

144. Steadman JR, Briggs KK, Rodrigo JJ, Kocher MS, Gill TJ, Rodkey WG: **Outcomes of microfracture for traumatic chondral defects of the knee: average 11-year follow-up.** *Arthroscopy* 2003, **19**(5)**:**477-484.

145. Kon E, Filardo G, Berruto M, Benazzo F, Zanon G, Della Villa S, Marcacci M: **Articular cartilage treatment in high-level male soccer players: a prospective comparative study of arthroscopic second-generation autologous chondrocyte implantation versus microfracture.** *Am J Sports Med* 2011, **39**(12)**:**2549-2557.

146. Becher C, Driessen A, Hess T, Longo UG, Maffulli N, Thermann H: **Microfracture for chondral defects of the talus: maintenance of early results at midterm follow-up.** *Knee Surg Sports Traumatol Arthrosc* 2010, **18**(5)**:**656-663.

147. Sansone V, de Girolamo L, Pascale W, Melato M, Pascale V: **Long-term results of abrasion arthroplasty for full-thickness cartilage lesions of the medial femoral condyle.** *Arthroscopy* 2015, **31**(3)**:**396-403.

148. Choi GW, Choi WJ, Youn HK, Park YJ, Lee JW: **Osteochondral lesions of the talus: are there any differences between osteochondral and chondral types?** *Am J Sports Med* 2013, **41**(3)**:**504-510.

149. Chuckpaiwong B, Berkson EM, Theodore GH: **Microfracture for osteochondral lesions of the ankle: outcome analysis and outcome predictors of 105 cases.** *Arthroscopy* 2008, **24**(1)**:**106-112.

150. Gobbi A, Francisco RA, Lubowitz JH, Allegra F, Canata G: **Osteochondral lesions of the talus: randomized controlled trial comparing chondroplasty, microfracture, and osteochondral autograft transplantation.** *Arthroscopy* 2006, **22**(10)**:**1085-1092.

151. Goyal D, Keyhani S, Lee EH, Hui JH: **Evidence-based status of microfracture technique: a systematic review of level I and II studies.** *Arthroscopy* 2013, **29**(9)**:**1579-1588.

152. Ferkel RD, Zanotti RM, Komenda GA, Sgaglione NA, Cheng MS, Applegate GR, Dopirak RM: **Arthroscopic treatment of chronic osteochondral lesions of the talus: long-term results.** *Am J Sports Med* 2008, **36**(9)**:**1750-1762.

153. Kon E, Gobbi A, Filardo G, Delcogliano M, Zaffagnini S, Marcacci M: **Arthroscopic second-generation autologous chondrocyte implantation compared with microfracture for chondral lesions of the knee: prospective nonrandomized study at 5 years.** *Am J Sports Med* 2009, **37**(1)**:**33-41.

154. Giannini S, Buda R, Faldini C, Vannini F, Bevoni R, Grandi G, Grigolo B, Berti L: **Surgical treatment of osteochondral lesions of the talus in young active patients.** *J Bone Joint Surg Am* 2005, **87**(Suppl 2):28-41.

155. Hangody L, Kish G, Karpati Z, Szerb I, Udvarhelyi I: **Arthroscopic autogenous osteochondral mosaicplasty for the treatment of femoral condylar articular defects. A preliminary report.** *Knee Surg Sports Traumatol Arthrosc* 1997, **5**(4)**:**262-267.

156. Hangody L, Vasarhelyi G, Hangody LR, Sukosd Z, Tibay G, Bartha L, Bodo G: **Autologous osteochondral grafting--technique and long-term results.** *Injury* 2008, **39**(Suppl 1)**:**S32-9.

157. Hangody L, Rathonyi GK, Duska Z, Vasarhelyi G, Fules P, Modis L: **Autologous osteochondral mosaicplasty. Surgical technique.** *J Bone Joint Surg Am* 2004, **86-A**(Suppl 1)**:**65-72.

158. Giannini S, Vannini F, Buda R: **Osteoarticular grafts in the treatment of OCD of the talus: mosaicplasty versus autologous chondrocyte transplantation.** *Foot Ankle Clin* 2002, **7**(3)**:**621-633.

159. Marcacci M, Kon E, Delcogliano M, Filardo G, Busacca M, Zaffagnini S: **Arthroscopic autologous osteochondral grafting for cartilage defects of the knee: prospective study results at a minimum 7-year follow-up.** *Am J Sports Med* 2007, **35**(12)**:**2014-2021.

160. Solheim E, Hegna J, Oyen J, Harlem T, Strand T: **Results at 10 to 14 years after osteochondral autografting (mosaicplasty) in articular cartilage defects in the knee.** *Knee* 2013, **20**(4)**:**287-290.

161. Solheim E, Hegna J, Oyen J, Austgulen OK, Harlem T, Strand T: **Osteochondral autografting (mosaicplasty) in articular cartilage defects in the knee: results at 5 to 9 years.** *Knee* 2010, **17**(1)**:**84-87.

162. Ollat D, Lebel B, Thaunat M, Jones D, Mainard L, Dubrana F, Versier G, French Arthroscopy Society: **Mosaic osteochondral transplantations in the knee joint, midterm results of the SFA multicenter study.** *Orthop Traumatol Surg Res* 2011, **97**(8 Suppl)**:**S160-6.

163. Gudas R, Gudaite A, Mickevicius T, Masiulis N, Simonaityte R, Cekanauskas E, Skurvydas A: **Comparison of osteochondral autologous transplantation, microfracture, or debridement techniques in articular cartilage lesions associated with anterior cruciate ligament injury: a prospective study with a 3-year follow-up.** *Arthroscopy* 2013, **29**(1)**:**89-97.

164. Reverte-Vinaixa MM, Joshi N, Diaz-Ferreiro EW, Teixidor-Serra J, Dominguez-Oronoz R: **Medium-term outcome of mosaicplasty for grade III-IV cartilage defects of the knee.** *J Orthop Surg (Hong Kong)* 2013, **21**(1)**:**4-9.

165. Hangody L, Dobos J, Balo E, Panics G, Hangody LR, Berkes I: **Clinical experiences with autologous osteochondral mosaicplasty in an athletic population: a 17-year prospective multicenter study.** *Am J Sports Med* 2010, **38**(6)**:**1125-1133.

166. Valderrabano V, Leumann A, Rasch H, Egelhof T, Hintermann B, Pagenstert G: **Knee-to-ankle mosaicplasty for the treatment of osteochondral lesions of the ankle joint.** *Am J Sports Med* 2009, **37**(Suppl 1)**:**105S-111S.

167. Gortz S, Bugbee WD: **Allografts in articular cartilage repair.** *J Bone Joint Surg Am* 2006, **88**(6)**:**1374-1384.

168. Strauss EJ, Sershon R, Barker JU, Kercher J, Salata M, Verma NN: **The basic science and clinical applications of osteochondral allografts.** *Bull NYU Hosp Jt Dis* 2012, **70**(4)**:**217-223.

169. Bugbee WD, Pallante-Kichura AL, Gortz S, Amiel D, Sah R: **Osteochondral allograft transplantation in cartilage repair: Graft storage paradigm, translational models, and clinical applications.** *J Orthop Res* 2016, **34**(1)**:**31-38.

170. Gracitelli GC, Meric G, Pulido PA, McCauley JC, Bugbee WD: **Osteochondral Allograft Transplantation for Knee Lesions after Failure of Cartilage Repair Surgery.** *Cartilage* 2015, **6**(2)**:**98-105.

171. Vangsness CT,Jr, Garcia IA, Mills CR, Kainer MA, Roberts MR, Moore TM: **Allograft transplantation in the knee: tissue regulation, procurement, processing, and sterilization.** *Am J Sports Med* 2003, **31**(3)**:**474-481.

172. McDermott AG, Langer F, Pritzker KP, Gross AE: **Fresh small-fragment osteochondral allografts. Long-term follow-up study on first 100 cases.** *Clin Orthop Relat Res* 1985, **(197)**(197)**:**96-102.

173. Levy YD, Gortz S, Pulido PA, McCauley JC, Bugbee WD: **Do fresh osteochondral allografts successfully treat femoral condyle lesions?** *Clin Orthop Relat Res* 2013, **471**(1)**:**231-237.

174. Gross AE, Shasha N, Aubin P: **Long-term followup of the use of fresh osteochondral allografts for posttraumatic knee defects.** *Clin Orthop Relat Res* 2005, **(435)**(435)**:**79-87.

175. Williams SK, Amiel D, Ball ST, Allen RT, Wong VW, Chen AC, Sah RL, Bugbee WD: **Prolonged storage effects on the articular cartilage of fresh human osteochondral allografts.** *J Bone Joint Surg Am* 2003, **85-A**(11)**:**2111-2120.

176. Ball ST, Amiel D, Williams SK, Tontz W, Chen AC, Sah RL, Bugbee WD: **The effects of storage on fresh human osteochondral allografts.** *Clin Orthop Relat Res* 2004, **(418):**246-252.

177. Pennock AT, Robertson CM, Wagner F, Harwood FL, Bugbee WD, Amiel D: **Does subchondral bone affect the fate of osteochondral allografts during storage?** *Am J Sports Med* 2006, **34**(4)**:**586-591.

178. Pennock AT, Wagner F, Robertson CM, Harwood FL, Bugbee WD, Amiel D: **Prolonged storage of osteochondral allografts: does the addition of fetal bovine serum improve chondrocyte viability?** *J Knee Surg* 2006, **19**(4)**:**265-272.

179. Malinin TI, Mnaymneh W, Lo HK, Hinkle DK: **Cryopreservation of articular cartilage. Ultrastructural observations and long-term results of experimental distal femoral transplantation.** *Clin Orthop Relat Res* 1994, **(303):**18-32.

180. Enneking WF, Campanacci DA: **Retrieved human allografts : a clinicopathological study.** *J Bone Joint Surg Am* 2001, **83-A**(7)**:**971-986.

181. Jomha NM, Elliott JA, Law GK, Maghdoori B, Forbes JF, Abazari A, Adesida AB, Laouar L, Zhou X, McGann LE: **Vitrification of intact human articular cartilage.** *Biomaterials* 2012, **33**(26)**:**6061-6068.

182. Abazari A, Jomha NM, Elliott JA, McGann LE: **Cryopreservation of articular cartilage.** *Cryobiology* 2013, **66**(3)**:**201-209.

183. Shasha N, Krywulak S, Backstein D, Pressman A, Gross AE: **Long-term follow-up of fresh tibial osteochondral allografts for failed tibial plateau fractures.** *J Bone Joint Surg Am* 2003, **85-A**(Suppl 2)**:**33-39.

184. Gracitelli GC, Meric G, Briggs DT, Pulido PA, McCauley JC, Belloti JC, Bugbee WD: **Fresh osteochondral allografts in the knee: comparison of**

primary transplantation versus transplantation after failure of previous subchondral marrow stimulation. *Am J Sports Med* 2015, **43**(4)**:**885-891.

185. Ghazavi MT, Pritzker KP, Davis AM, Gross AE: **Fresh osteochondral allografts for post-traumatic osteochondral defects of the knee.** *J Bone Joint Surg Br* 1997, **79**(6)**:**1008-1013.

186. Jamali AA, Emmerson BC, Chung C, Convery FR, Bugbee WD: **Fresh osteochondral allografts: results in the patellofemoral joint.** *Clin Orthop Relat Res* 2005, **(437):**176-185.

187. Gross AE, Agnidis Z, Hutchison CR: **Osteochondral defects of the talus treated with fresh osteochondral allograft transplantation.** *Foot Ankle Int* 2001, **22**(5)**:**385-391.

188. Adams SB,Jr, Viens NA, Easley ME, Stinnett SS, Nunley JA,2nd: **Midterm results of osteochondral lesions of the talar shoulder treated with fresh osteochondral allograft transplantation.** *J Bone Joint Surg Am* 2011, **93**(7)**:**648-654.

189. Ahmad J, Jones K: **Comparison of Osteochondral Autografts and Allografts for Treatment of Recurrent or Large Talar Osteochondral Lesions.** *Foot Ankle Int* 2016, **37**(1)**:**40-50.

190. Giannini S, Buda R, Grigolo B, Bevoni R, Di Caprio F, Ruffilli A, Cavallo M, Desando G, Vannini F: **Bipolar fresh osteochondral allograft of the ankle.** *Foot Ankle Int* 2010, **31**(1)**:**38-46.

191. Gross CE, Adams SB, Easley ME, Nunley JA,2nd: **Role of Fresh Osteochondral Allografts for Large Talar Osteochondral Lesions.** *J Am Acad Orthop Surg* 2016, **24**(1)**:**e9-e17.

192. Choi WJ, Choi GW, Kim JS, Lee JW: **Prognostic significance of the containment and location of osteochondral lesions of the talus: independent adverse outcomes associated with uncontained lesions of the talar shoulder.** *Am J Sports Med* 2013, **41**(1)**:**126-133.

193. Kon E, Delcogliano M, Filardo G, Busacca M, Di Martino A, Marcacci M: **Novel nano-composite multilayered biomaterial for osteochondral regeneration: a pilot clinical trial.** *Am J Sports Med* 2011, **39**(6)**:**1180-1190.

194. Filardo G, Kon E, Roffi A, Di Martino A, Marcacci M: **Scaffold-based repair for cartilage healing: a systematic review and technical note.** *Arthroscopy* 2013, **29**(1)**:**174-186.

195. Verhaegen J, Clockaerts S, Van Osch GJ, Somville J, Verdonk P, Mertens P: **TruFit Plug for Repair of Osteochondral Defects-Where Is the Evidence? Systematic Review of Literature.** *Cartilage* 2015, **6**(1)**:**12-19.

196. Bekkers JE, Bartels LW, Vincken KL, Dhert WJ, Creemers LB, Saris DB: **Articular cartilage evaluation after TruFit plug implantation analyzed by delayed gadolinium-enhanced MRI of cartilage (dGEMRIC).** *Am J Sports Med* 2013, **41**(6)**:**1290-1295.

197. Dell'Osso G, Bottai V, Bugelli G, Manisco T, Cazzella N, Celli F, Guido G, Giannotti S: **The biphasic bioresorbable scaffold (Trufit) in the osteochondral knee lesions: long-term clinical and MRI assessment in 30 patients.** *Musculoskelet Surg* 2015, in press.

198. Gelber PE, Batista J, Millan-Billi A, Patthauer L, Vera S, Gomez-Masdeu M, Monllau JC: **Magnetic resonance evaluation of TruFit(R) plugs for the treatment of osteochondral lesions of the knee shows the poor characteristics of the repair tissue.** *Knee* 2014, **21**(4)**:**827-832.

199. Dhollander A, Verdonk P, Almqvist KF, Verdonk R, Victor J: **Clinical and MRI outcome of an osteochondral scaffold plug for the treatment of cartilage lesions in the knee.** *Acta Orthop Belg* 2015, **81**(4)**:**629-638.

200. Kon E, Delcogliano M, Filardo G, Pressato D, Busacca M, Grigolo B, Desando G, Marcacci M: **A novel nano-composite multi-layered biomaterial for treatment of osteochondral lesions: technique note and an early stability pilot clinical trial.** *Injury* 2010, **41**(7)**:**693-701.

201. Kon E, Filardo G, Di Martino A, Busacca M, Moio A, Perdisa F, Marcacci M: **Clinical results and MRI evolution of a nano-composite multilayered**

biomaterial for osteochondral regeneration at 5 years. *Am J Sports Med* 2014, **42**(1)**:**158-165.

202. Lee YHD, Suzer F, Thermann H: **Autologous Matrix-Induced Chondrogenesis in the Knee: A Review.** *Cartilage* 2014, **5**(3)**:**145-153.

203. Gille J, Schuseil E, Wimmer J, Gellissen J, Schulz AP, Behrens P: **Mid-term results of Autologous Matrix-Induced Chondrogenesis for treatment of focal cartilage defects in the knee.** *Knee Surg Sports Traumatol Arthrosc* 2010, **18**(11)**:**1456-1464.

204. Patrascu JM, Freymann U, Kaps C, Poenaru DV: **Repair of a post-traumatic cartilage defect with a cell-free polymer-based cartilage implant: a follow-up at two years by MRI and histological review.** *J Bone Joint Surg Br* 2010, **92**(8)**:**1160-1163.

205. Dhollander AA, Verdonk PC, Lambrecht S, Almqvist KF, Elewaut D, Verbruggen G, Verdonk R: **The combination of microfracture and a cell-free polymer-based implant immersed with autologous serum for cartilage defect coverage.** *Knee Surg Sports Traumatol Arthrosc* 2012, **20**(9)**:**1773-1780.

206. Kusano T, Jakob RP, Gautier E, Magnussen RA, Hoogewoud H, Jacobi M: **Treatment of isolated chondral and osteochondral defects in the knee by autologous matrix-induced chondrogenesis (AMIC).** *Knee Surg Sports Traumatol Arthrosc* 2012, **20**(10)**:**2109-2115.

207. Methot S, Changoor A, Tran-Khanh N, Hoemann CD, Stanish WD, Restrepo A, Shive MS, Buschmann MD: **Osteochondral Biopsy Analysis Demonstrates That BST-CarGel Treatment Improves Structural and Cellular Characteristics of Cartilage Repair Tissue Compared With Microfracture.** *Cartilage* 2016, **7**(1)**:**16-28.

208. Wiewiorski M, Miska M, Kretzschmar M, Studler U, Bieri O, Valderrabano V: **Delayed gadolinium-enhanced MRI of cartilage of the ankle joint: results after autologous matrix-induced chondrogenesis (AMIC)-aided reconstruction of osteochondral lesions of the talus.** *Clin Radiol* 2013, **68**(10)**:**1031-1038.

209. Valderrabano V, Barg A, Alattar A, Wiewiorski M: **Osteochondral lesions of the ankle joint in professional soccer players: treatment with autologous matrix-induced chondrogenesis.** *Foot Ankle Spec* 2014, **7**(6)**:**522-528.

210. Kubosch EJ, Erdle B, Izadpanah K, Kubosch D, Uhl M, Sudkamp NP, Niemeyer P: **Clinical outcome and T2 assessment following autologous matrix-induced chondrogenesis in osteochondral lesions of the talus.** *Int Orthop* 2016, **40**(1)**:**65-71.

211. Haddo O, Mahroof S, Higgs D, David L, Pringle J, Bayliss M, Cannon SR, Briggs TW: **The use of chondrogide membrane in autologous chondrocyte implantation.** *Knee* 2004, **11**(1)**:**51-55.

212. Behrens P, Ehlers EM, Kochermann KU, Rohwedel J, Russlies M, Plotz W: **New therapy procedure for localized cartilage defects. Encouraging results with autologous chondrocyte implantation.** *MMW Fortschr Med* 1999, **141**(45)**:**49-51.

213. Behrens P, Bitter T, Kurz B, Russlies M: **Matrix-associated autologous chondrocyte transplantation/implantation (MACT/MACI)--5-year follow-up.** *Knee* 2006, **13**(3)**:**194-202.

214. Brittberg M: **Autologous chondrocyte implantation--technique and long-term follow-up.** *Injury* 2008, **39**(Suppl 1)**:**S40-9.

215. Bartlett W, Skinner JA, Gooding CR, Carrington RW, Flanagan AM, Briggs TW, Bentley G: **Autologous chondrocyte implantation versus matrix-induced autologous chondrocyte implantation for osteochondral defects of the knee: a prospective, randomised study.** *J Bone Joint Surg Br* 2005, **87**(5)**:**640-645.

216. Marlovits S, Zeller P, Singer P, Resinger C, Vecsei V: **Cartilage repair: generations of autologous chondrocyte transplantation.** *Eur J Radiol* 2006, **57**(1)**:**24-31.

217. Kon E, Filardo G, Di Matteo B, Perdisa F, Marcacci M: **Matrix assisted autologous chondrocyte transplantation for cartilage treatment: A systematic review.** *Bone Joint Res* 2013, **2**(2)**:**18-25.

218. Saris DB, Vanlauwe J, Victor J, Almqvist KF, Verdonk R, Bellemans J, Luyten FP, TIG/ACT/01/2000&EXT Study Group: **Treatment of symptomatic cartilage defects of the knee: characterized chondrocyte implantation results in better clinical outcome at 36 months in a randomized trial compared to microfracture.** *Am J Sports Med* 2009, **37**(Suppl 1)**:**10S-19S.

219. Dell'Accio F, De Bari C, Luyten FP: **Molecular markers predictive of the capacity of expanded human articular chondrocytes to form stable cartilage in vivo.** *Arthritis Rheum* 2001, **44**(7)**:**1608-1619.

220. Dhollander AA, Verdonk PC, Lambrecht S, Verdonk R, Elewaut D, Verbruggen G, Almqvist KF: **Short-term outcome of the second generation characterized chondrocyte implantation for the treatment of cartilage lesions in the knee.** *Knee Surg Sports Traumatol Arthrosc* 2012, **20**(6)**:**1118-1127.

221. Minas T, Von Keudell A, Bryant T, Gomoll AH: **The John Insall Award: A Minimum 10-year Outcome Study of Autologous Chondrocyte Implantation.** *Clin Orthop Relat Res* 2014, **472**(1)**:**41-51.

222. Moradi B, Schonit E, Nierhoff C, Hagmann S, Oberle D, Gotterbarm T, Schmitt H, Zeifang F: **First-generation autologous chondrocyte implantation in patients with cartilage defects of the knee: 7 to 14 years' clinical and magnetic resonance imaging follow-up evaluation.** *Arthroscopy* 2012, **28**(12)**:**1851-1861.

223. Vijayan S, Bartlett W, Bentley G, Carrington RW, Skinner JA, Pollock RC, Alorjani M, Briggs TW: **Autologous chondrocyte implantation for osteochondral lesions in the knee using a bilayer collagen membrane and bone graft: a two- to eight-year follow-up study.** *J Bone Joint Surg Br* 2012, **94**(4)**:**488-492.

224. Ferruzzi A, Buda R, Faldini C, Vannini F, Di Caprio F, Luciani D, Giannini S: **Autologous chondrocyte implantation in the knee joint: open compared with arthroscopic technique. Comparison at a minimum follow-up of five years.** *J Bone Joint Surg Am* 2008, **90** (Suppl 4)**:**90-101.

225. Giannini S, Buda R, Ruffilli A, Cavallo M, Pagliazzi G, Bulzamini MC, Desando G, Luciani D, Vannini F: **Arthroscopic autologous chondrocyte implantation in the ankle joint.** *Knee Surg Sports Traumatol Arthrosc* 2014, **22**(6)**:**1311-1319.

226. Bentley G, Biant LC, Vijayan S, Macmull S, Skinner JA, Carrington RW: **Minimum ten-year results of a prospective randomised study of autologous chondrocyte implantation versus mosaicplasty for symptomatic articular cartilage lesions of the knee.** *J Bone Joint Surg Br* 2012, **94**(4)**:**504-509.

227. Peterson L, Vasiliadis HS, Brittberg M, Lindahl A: **Autologous chondrocyte implantation: a long-term follow-up.** *Am J Sports Med* 2010, **38**(6)**:**1117-1124.

228. Moseley JB,Jr, Anderson AF, Browne JE, Mandelbaum BR, Micheli LJ, Fu F, Erggelet C: **Long-term durability of autologous chondrocyte implantation: a multicenter, observational study in US patients.** *Am J Sports Med* 2010, **38**(2)**:**238-246.

229. Peterson L, Minas T, Brittberg M, Nilsson A, Sjogren-Jansson E, Lindahl A: **Two- to 9-year outcome after autologous chondrocyte transplantation of the knee.** *Clin Orthop Relat Res* 2000, **374:**212-234.

230. Vasiliadis HS, Danielson B, Ljungberg M, McKeon B, Lindahl A, Peterson L: **Autologous chondrocyte implantation in cartilage lesions of the knee: long-term evaluation with magnetic resonance imaging and delayed gadolinium-enhanced magnetic resonance imaging technique.** *Am J Sports Med* 2010, **38**(5)**:**943-949.

231. Nehrer S, Dorotka R, Domayer S, Stelzeneder D, Kotz R: **Treatment of full-thickness chondral defects with hyalograft C in the knee: a prospective clinical case series with 2 to 7 years' follow-up.** *Am J Sports Med* 2009, **37**(Suppl 1)**:**81S-87S.

232. Nawaz SZ, Bentley G, Briggs TW, Carrington RW, Skinner JA, Gallagher KR, Dhinsa BS: **Autologous chondrocyte implantation in the knee: mid-term to long-term results.** *J Bone Joint Surg Am* 2014, **96**(10)**:**824-830.

233. Zeifang F, Oberle D, Nierhoff C, Richter W, Moradi B, Schmitt H: **Autologous chondrocyte implantation using the original periosteum-cover**

technique versus matrix-associated autologous chondrocyte implantation: a randomized clinical trial. *Am J Sports Med* 2010, **38**(5)**:**924-933.

234. Erggelet C, Kreuz PC, Mrosek EH, Schagemann JC, Lahm A, Ducommun PP, Ossendorf C: **Autologous chondrocyte implantation versus ACI using 3D-bioresorbable graft for the treatment of large full-thickness cartilage lesions of the knee.** *Arch Orthop Trauma Surg* 2010, **130**(8)**:**957-964.

235. Vanlauwe J, Saris DB, Victor J, Almqvist KF, Bellemans J, Luyten FP, TIG/ACT/01/2000&EXT Study Group: **Five-year outcome of characterized chondrocyte implantation versus microfracture for symptomatic cartilage defects of the knee: early treatment matters.** *Am J Sports Med* 2011, **39**(12)**:**2566-2574.

236. Basad E, Ishaque B, Bachmann G, Sturz H, Steinmeyer J: **Matrix-induced autologous chondrocyte implantation versus microfracture in the treatment of cartilage defects of the knee: a 2-year randomised study.** *Knee Surg Sports Traumatol Arthrosc* 2010, **18**(4)**:**519-527.

237. Kon E, Filardo G, Berruto M, Benazzo F, Zanon G, Della Villa S, Marcacci M: **Articular cartilage treatment in high-level male soccer players: a prospective comparative study of arthroscopic second-generation autologous chondrocyte implantation versus microfracture.** *Am J Sports Med* 2011, **39**(12)**:**2549-2557.

238. Baums MH, Heidrich G, Schultz W, Steckel H, Kahl E, Klinger HM: **Autologous chondrocyte transplantation for treating cartilage defects of the talus.** *J Bone Joint Surg Am* 2006, **88**(2)**:**303-308.

239. Giannini S, Battaglia M, Buda R, Cavallo M, Ruffilli A, Vannini F: **Surgical treatment of osteochondral lesions of the talus by open-field autologous chondrocyte implantation: a 10-year follow-up clinical and magnetic resonance imaging T2-mapping evaluation.** *Am J Sports Med* 2009, **37**(Suppl 1)**:**112S-8S.

240. Anders S, Goetz J, Schubert T, Grifka J, Schaumburger J: **Treatment of deep articular talus lesions by matrix associated autologous chondrocyte implantation--results at five years.** *Int Orthop* 2012, **36**(11)**:**2279-2285.

241. Giannini S, Buda R, Vannini F, Di Caprio F, Grigolo B: **Arthroscopic autologous chondrocyte implantation in osteochondral lesions of the talus: surgical technique and results.** *Am J Sports Med* 2008, **36**(5)**:**873-880.

242. Battaglia M, Vannini F, Buda R, Cavallo M, Ruffilli A, Monti C, Galletti S, Giannini S: **Arthroscopic autologous chondrocyte implantation in osteochondral lesions of the talus: mid-term T2-mapping MRI evaluation.** *Knee Surg Sports Traumatol Arthrosc* 2011, **19**(8)**:**1376-1384.

243. Harrison PE, Ashton IK, Johnson WE, Turner SL, Richardson JB, Ashton BA: **The in vitro growth of human chondrocytes.** *Cell Tissue Bank* 2000, **1**(4)**:**255-260.

244. Barbero A, Grogan S, Schafer D, Heberer M, Mainil-Varlet P, Martin I: **Age related changes in human articular chondrocyte yield, proliferation and post-expansion chondrogenic capacity.** *Osteoarthritis Cartilage* 2004, **12**(6)**:**476-484.

245. Bolton MC, Dudhia J, Bayliss MT: **Age-related changes in the synthesis of link protein and aggrecan in human articular cartilage: implications for aggregate stability.** *Biochem J* 1999, **337**(1)**:**77-82.

246. Stokes DG, Liu G, Dharmavaram R, Hawkins D, Piera-Velazquez S, Jimenez SA: **Regulation of type-II collagen gene expression during human chondrocyte de-differentiation and recovery of chondrocyte-specific phenotype in culture involves Sry-type high-mobility-group box (SOX) transcription factors.** *Biochem J* 2001, **360**(2)**:**461-470.

247. Schnabel M, Marlovits S, Eckhoff G, Fichtel I, Gotzen L, Vecsei V, Schlegel J: **Dedifferentiation-associated changes in morphology and gene expression in primary human articular chondrocytes in cell culture.** *Osteoarthritis Cartilage* 2002, **10**(1)**:**62-70.

248. Marlovits S, Hombauer M, Tamandl D, Vecsei V, Schlegel W: **Quantitative analysis of gene expression in human articular chondrocytes in monolayer culture.** *Int J Mol Med* 2004, **13**(2)**:**281-287.

249. Marlovits S, Hombauer M, Truppe M, Vecsei V, Schlegel W: **Changes in the ratio of type-I and type-II collagen expression during monolayer culture of human chondrocytes.** *J Bone Joint Surg Br* 2004, **86**(2)**:**286-295.

250. Mayne R, Vail MS, Mayne PM, Miller EJ: **Changes in type of collagen synthesized as clones of chick chondrocytes grow and eventually lose division capacity.** *Proc Natl Acad Sci U S A* 1976, **73**(5)**:**1674-1678.

251. Martin JA, Buckwalter JA: **Telomere erosion and senescence in human articular cartilage chondrocytes.** *J Gerontol A Biol Sci Med Sci* 2001, **56**(4)**:**B172-9.

252. Martin JA, Buckwalter JA: **Aging, articular cartilage chondrocyte senescence and osteoarthritis.** *Biogerontology* 2002, **3**(5)**:**257-264.

253. Moussavi-Harami F, Duwayri Y, Martin JA, Moussavi-Harami F, Buckwalter JA: **Oxygen effects on senescence in chondrocytes and mesenchymal stem cells: consequences for tissue engineering.** *Iowa Orthop J* 2004, **24:**15-20.

254. Buda R, Vannini F, Cavallo M, Grigolo B, Cenacchi A, Giannini S: **Osteochondral lesions of the knee: a new one-step repair technique with bone-marrow-derived cells.** *J Bone Joint Surg Am* 2010, **92**(Suppl 2)**:**2-11.

255. Pastides P, Chimutengwende-Gordon M, Maffulli N, Khan W: **Stem cell therapy for human cartilage defects: a systematic review.** *Osteoarthritis Cartilage* 2013, **21**(5)**:**646-654.

256. Sakaguchi Y, Sekiya I, Yagishita K, Muneta T: **Comparison of human stem cells derived from various mesenchymal tissues: superiority of synovium as a cell source.** *Arthritis Rheum* 2005, **52**(8)**:**2521-2529.

257. Saw KY, Anz A, Siew-Yoke Jee C, Merican S, Ching-Soong Ng R, Roohi SA, Ragavanaidu K: **Articular cartilage regeneration with autologous peripheral blood stem cells versus hyaluronic acid: a randomized controlled trial.** *Arthroscopy* 2013, **29**(4)**:**684-694.

258. da Silva Meirelles L, Caplan AI, Nardi NB: **In search of the in vivo identity of mesenchymal stem cells.** *Stem Cells* 2008, **26**(9)**:**2287-2299.

259. Crisan M, Yap S, Casteilla L, Chen CW, Corselli M, Park TS, Andriolo G, Sun B, Zheng B, Zhang L, Norotte C, Teng PN, Traas J, Schugar R, Deasy BM, Badylak S, Buhring HJ, Giacobino JP, Lazzari L, Huard J, Peault B: **A perivascular origin for mesenchymal stem cells in multiple human organs.** *Cell Stem Cell* 2008, **3**(3)**:**301-313.

260. De Bari C, Dell'Accio F, Tylzanowski P, Luyten FP: **Multipotent mesenchymal stem cells from adult human synovial membrane.** *Arthritis Rheum* 2001, **44**(8)**:**1928-1942.

261. Johnstone B, Hering TM, Caplan AI, Goldberg VM, Yoo JU: **In vitro chondrogenesis of bone marrow-derived mesenchymal progenitor cells.** *Exp Cell Res* 1998, **238**(1)**:**265-272.

262. Dominici M, Le Blanc K, Mueller I, Slaper-Cortenbach I, Marini F, Krause D, Deans R, Keating A, Prockop D, Horwitz E: **Minimal criteria for defining multipotent mesenchymal stromal cells. The International Society for Cellular Therapy position statement.** *Cytotherapy* 2006, **8**(4)**:**315-317.

263. Baksh D, Davies JE: **Culture of mesenchymal stem/progenitor cells in adhesion-independent conditions.** *Methods Cell Biol* 2008, **86:**279-293.

264. Di Maggio N, Mehrkens A, Papadimitropoulos A, Schaeren S, Heberer M, Banfi A, Martin I: **Fibroblast growth factor-2 maintains a niche-dependent population of self-renewing highly potent non-adherent mesenchymal progenitors through FGFR2c.** *Stem Cells* 2012, **30**(7)**:**1455-1464.

265. Kfoury Y, Scadden DT: **Mesenchymal cell contributions to the stem cell niche.** *Cell Stem Cell* 2015, **16**(3)**:**239-253.

266. Papadimitropoulos A, Piccinini E, Brachat S, Braccini A, Wendt D, Barbero A, Jacobi C, Martin I: **Expansion of human mesenchymal stromal cells from fresh bone marrow in a 3D scaffold-based system under direct perfusion.** *PLoS One* 2014, **9**(7)**:**e102359.

267. Denker AE, Nicoll SB, Tuan RS: **Formation of cartilage-like spheroids by micromass cultures of murine C3H10T1/2 cells upon treatment with transforming growth factor-beta 1.** *Differentiation* 1995, **59**(1)**:**25-34.

268. Noble BS, Dean V, Loveridge N, Thomson BM: **Dextran sulfate promotes the rapid aggregation of porcine bone-marrow stromal cells.** *Bone* 1995, **17**(4)**:**375-382.

269. Murdoch AD, Grady LM, Ablett MP, Katopodi T, Meadows RS, Hardingham TE: **Chondrogenic differentiation of human bone marrow stem cells in transwell cultures: generation of scaffold-free cartilage.** *Stem Cells* 2007, **25**(11)**:**2786-2796.

270. de Vries-van Melle ML, Narcisi R, Kops N, Koevoet WJ, Bos PK, Murphy JM, Verhaar JA, van der Kraan PM, van Osch GJ: **Chondrogenesis of mesenchymal stem cells in an osteochondral environment is mediated by the subchondral bone.** *Tissue Eng Part A* 2014, **20**(1-2)**:**23-33.

271. Vinardell T, Thorpe SD, Buckley CT, Kelly DJ: **Chondrogenesis and integration of mesenchymal stem cells within an in vitro cartilage defect repair model.** *Ann Biomed Eng* 2009, **37**(12)**:**2556-2565.

272. Naderi-Meshkin H, Andreas K, Matin MM, Sittinger M, Bidkhori HR, Ahmadiankia N, Bahrami AR, Ringe J: **Chitosan-based injectable hydrogel as a promising in situ forming scaffold for cartilage tissue engineering.** *Cell Biol Int* 2014, **38**(1)**:**72-84.

273. Choi JW, Choi BH, Park SH, Pai KS, Li TZ, Min BH, Park SR: **Mechanical stimulation by ultrasound enhances chondrogenic differentiation of mesenchymal stem cells in a fibrin-hyaluronic acid hydrogel.** *Artif Organs* 2013, **37**(7)**:**648-655.

274. Zscharnack M, Hepp P, Richter R, Aigner T, Schulz R, Somerson J, Josten C, Bader A, Marquass B: **Repair of chronic osteochondral defects using predifferentiated mesenchymal stem cells in an ovine model.** *Am J Sports Med* 2010, **38**(9)**:**1857-1869.

275. Hofmann S, Knecht S, Langer R, Kaplan DL, Vunjak-Novakovic G, Merkle HP, Meinel L: **Cartilage-like tissue engineering using silk scaffolds and mesenchymal stem cells.** *Tissue Eng* 2006, **12**(10)**:**2729-2738.

276. Marsano A, Millward-Sadler SJ, Salter DM, Adesida A, Hardingham T, Tognana E, Kon E, Chiari-Grisar C, Nehrer S, Jakob M, Martin I: **Differential cartilaginous tissue formation by human synovial membrane, fat pad, meniscus cells and articular chondrocytes.** *Osteoarthritis Cartilage* 2007, **15**(1)**:**48-58.

277. Mahmoudifar N, Doran PM: **Chondrogenic differentiation of human adipose-derived stem cells in polyglycolic acid mesh scaffolds under dynamic culture conditions.** *Biomaterials* 2010, **31**(14)**:**3858-3867.

278. Matsuda C, Takagi M, Hattori T, Wakitani S, Yoshida T: **Differentiation of Human Bone Marrow Mesenchymal Stem Cells to Chondrocytes for**

Construction of Three-dimensional Cartilage Tissue. *Cytotechnology* 2005, **47**(1-3)**:**11-17.

279. Zhao YH, Yang Q, Xia Q, Peng J, Lu SB, Guo QY, Ma XL, Xu BS, Hu YC, Zhao B, Zhang L, Wang AY, Xu WJ, Miao J, Liu Y: **In vitro cartilage production using an extracellular matrix-derived scaffold and bone marrow-derived mesenchymal stem cells.** *Chin Med J (Engl)* 2013, **126**(16)**:**3130-3137.

280. Darling EM, Athanasiou KA: **Biomechanical strategies for articular cartilage regeneration.** *Ann Biomed Eng* 2003, **31**(9)**:**1114-1124.

281. Uematsu K, Hattori K, Ishimoto Y, Yamauchi J, Habata T, Takakura Y, Ohgushi H, Fukuchi T, Sato M: **Cartilage regeneration using mesenchymal stem cells and a three-dimensional poly-lactic-glycolic acid (PLGA) scaffold.** *Biomaterials* 2005, **26**(20)**:**4273-4279.

282. Masuoka K, Asazuma T, Hattori H, Yoshihara Y, Sato M, Matsumura K, Matsui T, Takase B, Nemoto K, Ishihara M: **Tissue engineering of articular cartilage with autologous cultured adipose tissue-derived stromal cells using atelocollagen honeycomb-shaped scaffold with a membrane sealing in rabbits.** *J Biomed Mater Res B Appl Biomater* 2006, **79**(1)**:**25-34.

283. Shao X, Goh JC, Hutmacher DW, Lee EH, Zigang G: **Repair of large articular osteochondral defects using hybrid scaffolds and bone marrow-derived mesenchymal stem cells in a rabbit model.** *Tissue Eng* 2006, **12**(6)**:**1539-1551.

284. Shao XX, Hutmacher DW, Ho ST, Goh JC, Lee EH: **Evaluation of a hybrid scaffold/cell construct in repair of high-load-bearing osteochondral defects in rabbits.** *Biomaterials* 2006, **27**(7)**:**1071-1080.

285. Dragoo JL, Carlson G, McCormick F, Khan-Farooqi H, Zhu M, Zuk PA, Benhaim P: **Healing full-thickness cartilage defects using adipose-derived stem cells.** *Tissue Eng* 2007, **13**(7)**:**1615-1621.

286. Koga H, Muneta T, Ju YJ, Nagase T, Nimura A, Mochizuki T, Ichinose S, von der Mark K, Sekiya I: **Synovial stem cells are regionally specified according to local microenvironments after implantation for cartilage regeneration.** *Stem Cells* 2007, **25**(3)**:**689-696.

287. Han SH, Kim YH, Park MS, Kim IA, Shin JW, Yang WI, Jee KS, Park KD, Ryu GH, Lee JW: **Histological and biomechanical properties of regenerated articular cartilage using chondrogenic bone marrow stromal cells with a PLGA scaffold in vivo.** *J Biomed Mater Res A* 2008, **87**(4)**:**850-861.

288. Koga H, Shimaya M, Muneta T, Nimura A, Morito T, Hayashi M, Suzuki S, Ju YJ, Mochizuki T, Sekiya I: **Local adherent technique for transplanting mesenchymal stem cells as a potential treatment of cartilage defect.** *Arthritis Res Ther* 2008, **10**(4)**:**R84.

289. Koga H, Muneta T, Nagase T, Nimura A, Ju YJ, Mochizuki T, Sekiya I: **Comparison of mesenchymal tissues-derived stem cells for in vivo**

chondrogenesis: suitable conditions for cell therapy of cartilage defects in rabbit. *Cell Tissue Res* 2008, **333**(2)**:**207-215.

290. Pei M, He F, Boyce BM, Kish VL: **Repair of full-thickness femoral condyle cartilage defects using allogeneic synovial cell-engineered tissue constructs.** *Osteoarthritis Cartilage* 2009, **17**(6)**:**714-722.

291. Dashtdar H, Rothan HA, Tay T, Ahmad RE, Ali R, Tay LX, Chong PP, Kamarul T: **A preliminary study comparing the use of allogenic chondrogenic pre-differentiated and undifferentiated mesenchymal stem cells for the repair of full thickness articular cartilage defects in rabbits.** *J Orthop Res* 2011, **29**(9)**:**1336-1342.

292. Li Q, Tang J, Wang R, Bei C, Xin L, Zeng Y, Tang X: **Comparing the chondrogenic potential in vivo of autogeneic mesenchymal stem cells derived from different tissues.** *Artif Cells Blood Substit Immobil Biotechnol* 2011, **39**(1)**:**31-38.

293. Qi Y, Zhao T, Xu K, Dai T, Yan W: **The restoration of full-thickness cartilage defects with mesenchymal stem cells (MSCs) loaded and cross-linked bilayer collagen scaffolds on rabbit model.** *Mol Biol Rep* 2012, **39**(2)**:**1231-1237.

294. Tay LX, Ahmad RE, Dashtdar H, Tay KW, Masjuddin T, Ab-Rahim S, Chong PP, Selvaratnam L, Kamarul T: **Treatment outcomes of alginate-embedded allogenic mesenchymal stem cells versus autologous chondrocytes**

for the repair of focal articular cartilage defects in a rabbit model. *Am J Sports Med* 2012, **40**(1)**:**83-90.

295. Dashtdar H, Murali MR, Abbas AA, Suhaeb AM, Selvaratnam L, Tay LX, Kamarul T: **PVA-chitosan composite hydrogel versus alginate beads as a potential mesenchymal stem cell carrier for the treatment of focal cartilage defects.** *Knee Surg Sports Traumatol Arthrosc* 2013, **23**(5)**:**1368-1377.

296. Deng J, She R, Huang W, Dong Z, Mo G, Liu B: **A silk fibroin/chitosan scaffold in combination with bone marrow-derived mesenchymal stem cells to repair cartilage defects in the rabbit knee.** *J Mater Sci Mater Med* 2013, **24**(8)**:**2037-2046.

297. Chang NJ, Lam CF, Lin CC, Chen WL, Li CF, Lin YT, Yeh ML: **Transplantation of autologous endothelial progenitor cells in porous PLGA scaffolds create a microenvironment for the regeneration of hyaline cartilage in rabbits.** *Osteoarthritis Cartilage* 2013, **21**(10)**:**1613-1622.

298. Shimomura K, Moriguchi Y, Ando W, Nansai R, Fujie H, Hart DA, Gobbi A, Kita K, Horibe S, Shino K, Yoshikawa H, Nakamura N: **Osteochondral Repair Using a Scaffold-Free Tissue-Engineered Construct Derived from Synovial Mesenchymal Stem Cells and a Hydroxyapatite-Based Artificial Bone.** *Tissue Eng Part A* 2014, **20**(17-18)**:**2291-2304.

299. Park J, Gelse K, Frank S, von der Mark K, Aigner T, Schneider H: **Transgene-activated mesenchymal cells for articular cartilage repair: a**

comparison of primary bone marrow-, perichondrium/periosteum- and fat-derived cells. *J Gene Med* 2006, **8**(1)**:**112-125.

300. Hori J, Deie M, Kobayashi T, Yasunaga Y, Kawamata S, Ochi M: **Articular cartilage repair using an intra-articular magnet and synovium-derived cells.** *J Orthop Res* 2011, **29**(4)**:**531-538.

301. Guo X, Wang C, Zhang Y, Xia R, Hu M, Duan C, Zhao Q, Dong L, Lu J, Qing Song Y: **Repair of large articular cartilage defects with implants of autologous mesenchymal stem cells seeded into beta-tricalcium phosphate in a sheep model.** *Tissue Eng* 2004, **10**(11-12)**:**1818-1829.

302. Ando W, Tateishi K, Hart DA, Katakai D, Tanaka Y, Nakata K, Hashimoto J, Fujie H, Shino K, Yoshikawa H, Nakamura N: **Cartilage repair using an in vitro generated scaffold-free tissue-engineered construct derived from porcine synovial mesenchymal stem cells.** *Biomaterials* 2007, **28**(36)**:**5462-5470.

303. Lee KB, Hui JH, Song IC, Ardany L, Lee EH: **Injectable mesenchymal stem cell therapy for large cartilage defects--a porcine model.** *Stem Cells* 2007, **25**(11)**:**2964-2971.

304. Saw KY, Hussin P, Loke SC, Azam M, Chen HC, Tay YG, Low S, Wallin KL, Ragavanaidu K: **Articular cartilage regeneration with autologous marrow aspirate and hyaluronic Acid: an experimental study in a goat model.** *Arthroscopy* 2009, **25**(12)**:**1391-1400.

305. Shimomura K, Ando W, Tateishi K, Nansai R, Fujie H, Hart DA, Kohda H, Kita K, Kanamoto T, Mae T, Nakata K, Shino K, Yoshikawa H, Nakamura N: **The influence of skeletal maturity on allogenic synovial mesenchymal stem cell-based repair of cartilage in a large animal model.** *Biomaterials* 2010, **31**(31)**:**8004-8011.

306. Wegener B, Schrimpf FM, Bergschmidt P, Pietschmann MF, Utzschneider S, Milz S, Jansson V, Muller PE: **Cartilage regeneration by bone marrow cells-seeded scaffolds.** *J Biomed Mater Res A* 2010, **95**(3)**:**735-740.

307. Fortier LA, Potter HG, Rickey EJ, Schnabel LV, Foo LF, Chong LR, Stokol T, Cheetham J, Nixon AJ: **Concentrated bone marrow aspirate improves full-thickness cartilage repair compared with microfracture in the equine model.** *J Bone Joint Surg Am* 2010, **92**(10)**:**1927-1937.

308. Marquass B, Schulz R, Hepp P, Zscharnack M, Aigner T, Schmidt S, Stein F, Richter R, Osterhoff G, Aust G, Josten C, Bader A: **Matrix-associated implantation of predifferentiated mesenchymal stem cells versus articular chondrocytes: in vivo results of cartilage repair after 1 year.** *Am J Sports Med* 2011, **39**(7)**:**1401-1412.

309. McIlwraith CW, Frisbie DD, Rodkey WG, Kisiday JD, Werpy NM, Kawcak CE, Steadman JR: **Evaluation of intra-articular mesenchymal stem cells to augment healing of microfractured chondral defects.** *Arthroscopy* 2011, **27**(11)**:**1552-1561.

310. Ando W, Fujie H, Moriguchi Y, Nansai R, Shimomura K, Hart DA, Yoshikawa H, Nakamura N: **Detection of abnormalities in the superficial zone of cartilage repaired using a tissue engineered construct derived from synovial stem cells.** *Eur Cell Mater* 2012, **24:**292-307.

311. Zhang Y, Wang F, Chen J, Ning Z, Yang L: **Bone marrow-derived mesenchymal stem cells versus bone marrow nucleated cells in the treatment of chondral defects.** *Int Orthop* 2012, **36**(5)**:**1079-1086.

312. Bekkers JE, Tsuchida AI, van Rijen MH, Vonk LA, Dhert WJ, Creemers LB, Saris DB: **Single-stage cell-based cartilage regeneration using a combination of chondrons and mesenchymal stromal cells: comparison with microfracture.** *Am J Sports Med* 2013, **41**(9)**:**2158-2166.

313. Kamei G, Kobayashi T, Ohkawa S, Kongcharoensombat W, Adachi N, Takazawa K, Shibuya H, Deie M, Hattori K, Goldberg JL, Ochi M: **Articular cartilage repair with magnetic mesenchymal stem cells.** *Am J Sports Med* 2013, **41**(6)**:**1255-1264.

314. Nam H, Karunanithi P, Loo W, Naveen S, Chen H, Hussin P, Chan L, Kamarul T: **The effects of staged intra-articular injection of cultured autologous mesenchymal stromal cells on the repair of damaged cartilage: a pilot study in caprine model.** *Arthritis Research & Therapy* 2013, **15:**R129.

315. Loken S, Jakobsen RB, Aroen A, Heir S, Shahdadfar A, Brinchmann JE, Engebretsen L, Reinholt FP: **Bone marrow mesenchymal stem cells in a**

hyaluronan scaffold for treatment of an osteochondral defect in a rabbit model. *Knee Surg Sports Traumatol Arthrosc* 2008, **16**(10)**:**896-903.

316. Haleem AM, Singergy AA, Sabry D, Atta HM, Rashed LA, Chu CR, El Shewy MT, Azzam A, Abdel Aziz MT: **The Clinical Use of Human Culture-Expanded Autologous Bone Marrow Mesenchymal Stem Cells Transplanted on Platelet-Rich Fibrin Glue in the Treatment of Articular Cartilage Defects: A Pilot Study and Preliminary Results.** *Cartilage* 2010, **1**(4)**:**253-261.

317. Nejadnik H, Hui JH, Feng Choong EP, Tai BC, Lee EH: **Autologous bone marrow-derived mesenchymal stem cells versus autologous chondrocyte implantation: an observational cohort study.** *Am J Sports Med* 2010, **38**(6)**:**1110-1116.

318. Kasemkijwattana C, Hongeng S, Kesprayura S, Rungsinaporn V, Chaipinyo K, Chansiri K: **Autologous bone marrow mesenchymal stem cells implantation for cartilage defects: two cases report.** *J Med Assoc Thai* 2011, **94**(3)**:**395-400.

319. Gigante A, Cecconi S, Calcagno S, Busilacchi A, Enea D: **Arthroscopic knee cartilage repair with covered microfracture and bone marrow concentrate.** *Arthrosc Tech* 2012, **1**(2)**:**e175-80.

320. Enea D, Cecconi S, Calcagno S, Busilacchi A, Manzotti S, Kaps C, Gigante A: **Single-stage cartilage repair in the knee with microfracture covered with**

a resorbable polymer-based matrix and autologous bone marrow concentrate. *Knee* 2013, **20**(6)**:**562-569.

321. Buda R, Vannini F, Cavallo M, Baldassarri M, Luciani D, Mazzotti A, Pungetti C, Olivieri A, Giannini S: **One-step arthroscopic technique for the treatment of osteochondral lesions of the knee with bone-marrow-derived cells: three years results.** *Musculoskelet Surg* 2013, **97**(2)**:**145-151.

322. Buda R, Vannini F, Cavallo M, Baldassarri M, Natali S, Castagnini F, Giannini S: **One-step bone marrow-derived cell transplantation in talarosteochondral lesions: mid-term results.** *Joints* 2014, **1**(3)**:**102-107.

323. Buda R, Vannini F, Castagnini F, Cavallo M, Ruffilli A, Ramponi L, Pagliazzi G, Giannini S: **Regenerative treatment in osteochondral lesions of the talus: autologous chondrocyte implantation versus one-step bone marrow derived cells transplantation.** *Int Orthop* 2015, **39**(5)**:**893-900.

324. Teo BJ, Buhary K, Tai BC, Hui JH: **Cell-based therapy improves function in adolescents and young adults with patellar osteochondritis dissecans.** *Clin Orthop Relat Res* 2013, **471**(4)**:**1152-1158.

325. Adachi N, Ochi M, Deie M, Ito Y: **Transplant of mesenchymal stem cells and hydroxyapatite ceramics to treat severe osteochondral damage after septic arthritis of the knee.** *J Rheumatol* 2005, **32**(8)**:**1615-1618.

326. Sekiya I, Muneta T, Horie M, Koga H: **Arthroscopic Transplantation of Synovial Stem Cells Improves Clinical Outcomes in Knees With Cartilage Defects.** *Clin Orthop Relat Res* 2015, **473**(7)**:**2316-2326.

327. Saw KY, Anz A, Merican S, Tay YG, Ragavanaidu K, Jee CS, McGuire DA: **Articular cartilage regeneration with autologous peripheral blood progenitor cells and hyaluronic acid after arthroscopic subchondral drilling: a report of 5 cases with histology.** *Arthroscopy* 2011, **27**(4)**:**493-506.

328. Wakitani S, Okabe T, Horibe S, Mitsuoka T, Saito M, Koyama T, Nawata M, Tensho K, Kato H, Uematsu K, Kuroda R, Kurosaka M, Yoshiya S, Hattori K, Ohgushi H: **Safety of autologous bone marrow-derived mesenchymal stem cell transplantation for cartilage repair in 41 patients with 45 joints followed for up to 11 years and 5 months.** *J Tissue Eng Regen Med* 2011, **5**(2)**:**146-150.

329. Gigante A, Calcagno S, Cecconi S, Ramazzotti D, Manzotti S, Enea D: **Use of collagen scaffold and autologous bone marrow concentrate as a one-step cartilage repair in the knee: histological results of second-look biopsies at 1 year follow-up.** *Int J Immunopathol Pharmacol* 2011, **24**(1 Suppl 2)**:**69-72.

330. Ryan JM, Barry FP, Murphy JM, Mahon BP: **Mesenchymal stem cells avoid allogeneic rejection.** *J Inflamm (Lond)* 2005, **2:**8.

331. Mukonoweshuro B, Brown CJ, Fisher J, Ingham E: **Immunogenicity of undifferentiated and differentiated allogeneic mouse mesenchymal stem cells.** *J Tissue Eng* 2014, **5:**2041731414534255.

332. Adesida AB, Mulet-Sierra A, Jomha NM: **Hypoxia mediated isolation and expansion enhances the chondrogenic capacity of bone marrow mesenchymal stromal cells.** *Stem Cell Res Ther* 2012, **3**(2)**:**9.

333. Banfi A, Muraglia A, Dozin B, Mastrogiacomo M, Cancedda R, Quarto R: **Proliferation kinetics and differentiation potential of ex vivo expanded human bone marrow stromal cells: Implications for their use in cell therapy.** *Exp Hematol* 2000, **28**(6)**:**707-715.

334. Wagner W, Horn P, Castoldi M, Diehlmann A, Bork S, Saffrich R, Benes V, Blake J, Pfister S, Eckstein V, Ho AD: **Replicative senescence of mesenchymal stem cells: a continuous and organized process.** *PLoS One* 2008, **3**(5)**:**e2213.

335. Schallmoser K, Bartmann C, Rohde E, Bork S, Guelly C, Obenauf AC, Reinisch A, Horn P, Ho AD, Strunk D, Wagner W: **Replicative senescence-associated gene expression changes in mesenchymal stromal cells are similar under different culture conditions.** *Haematologica* 2010, **95**(6)**:**867-874.

336. Izadpanah R, Kaushal D, Kriedt C, Tsien F, Patel B, Dufour J, Bunnell BA: **Long-term in vitro expansion alters the biology of adult mesenchymal stem cells.** *Cancer Res* 2008, **68**(11)**:**4229-4238.

337. Digirolamo CM, Stokes D, Colter D, Phinney DG, Class R, Prockop DJ: **Propagation and senescence of human marrow stromal cells in culture: a simple colony-forming assay identifies samples with the greatest potential to propagate and differentiate.** *Br J Haematol* 1999, **107**(2)**:**275-281.

338. Phinney DG, Kopen G, Righter W, Webster S, Tremain N, Prockop DJ: **Donor variation in the growth properties and osteogenic potential of human marrow stromal cells.** *J Cell Biochem* 1999, **75**(3)**:**424-436.

339. Banfi A, Bianchi G, Notaro R, Luzzatto L, Cancedda R, Quarto R: **Replicative aging and gene expression in long-term cultures of human bone marrow stromal cells.** *Tissue Eng* 2002, **8**(6)**:**901-910.

340. Bruder SP, Jaiswal N, Haynesworth SE: **Growth kinetics, self-renewal, and the osteogenic potential of purified human mesenchymal stem cells during extensive subcultivation and following cryopreservation.** *J Cell Biochem* 1997, **64**(2)**:**278-294.

341. Walenda G, Hemeda H, Schneider RK, Merkel R, Hoffmann B, Wagner W: **Human platelet lysate gel provides a novel three dimensional-matrix for enhanced culture expansion of mesenchymal stromal cells.** *Tissue Eng Part C Methods* 2012, **18**(12)**:**924-934.

342. Wise JK, Alford AI, Goldstein SA, Stegemann JP: **Comparison of uncultured marrow mononuclear cells and culture-expanded mesenchymal stem cells in 3D collagen-chitosan microbeads for orthopedic tissue engineering.** *Tissue Eng Part A* 2014, **20**(1-2)**:**210-224.

343. Godara P, McFarland CD, Nordon RE: **Design of bioreactors for mesenchymal stem cell tissue engineering.** *Journal of Chemical Technology and Biotechnology* 2008, **83:**408-420.

344. Gronthos S, Simmons PJ: **The biology and application of human bone marrow stromal cell precursors.** *J Hematother* 1996, **5**(1)**:**15-23.

345. Martin I, Muraglia A, Campanile G, Cancedda R, Quarto R: **Fibroblast growth factor-2 supports ex vivo expansion and maintenance of osteogenic precursors from human bone marrow.** *Endocrinology* 1997, **138**(10)**:**4456-4462.

346. Solchaga LA, Penick K, Goldberg VM, Caplan AI, Welter JF: **Fibroblast growth factor-2 enhances proliferation and delays loss of chondrogenic potential in human adult bone-marrow-derived mesenchymal stem cells.** *Tissue Eng Part A* 2010, **16**(3)**:**1009-1019.

347. Martin I, Vunjak-Novakovic G, Yang J, Langer R, Freed LE: **Mammalian chondrocytes expanded in the presence of fibroblast growth factor 2 maintain the ability to differentiate and regenerate three-dimensional cartilaginous tissue.** *Exp Cell Res* 1999, **253**(2)**:**681-688.

348. Khan WS, Tew SR, Adesida AB, Hardingham TE: **Human infrapatellar fat pad-derived stem cells express the pericyte marker 3G5 and show enhanced chondrogenesis after expansion in fibroblast growth factor-2.** *Arthritis Res Ther* 2008, **10**(4)**:**R74.

349. Engler AJ, Sen S, Sweeney HL, Discher DE: **Matrix elasticity directs stem cell lineage specification.** *Cell* 2006, **126**(4)**:**677-689.

350. Murphy CM, Matsiko A, Haugh MG, Gleeson JP, O'Brien FJ: **Mesenchymal stem cell fate is regulated by the composition and mechanical properties of collagen-glycosaminoglycan scaffolds.** *J Mech Behav Biomed Mater* 2012, **11:**53-62.

351. Xue R, Li JY, Yeh Y, Yang L, Chien S: **Effects of matrix elasticity and cell density on human mesenchymal stem cells differentiation.** *J Orthop Res* 2013, **31**(9)**:**1360-1365.

352. Filardo G, Kon E, Perdisa F, Di Matteo B, Di Martino A, Iacono F, Zaffagnini S, Balboni F, Vaccari V, Marcacci M: **Osteochondral scaffold reconstruction for complex knee lesions: a comparative evaluation.** *Knee* 2013, **20**(6)**:**570-576.

353. Steinwachs M, Peterson L, Bobic V, Verdonk P, Niemeyer P: **Cell-Seeded Collagen Matrix-Supported Autologous Chondrocyte Transplantation (ACT-CS): A Consensus Statement on Surgical Technique.** *Cartilage* 2012, **3**(1)**:**5.

354. Sekiya I, Larson BL, Vuoristo JT, Reger RL, Prockop DJ: **Comparison of effect of BMP-2, -4, and -6 on in vitro cartilage formation of human adult stem cells from bone marrow stroma.** *Cell Tissue Res* 2005, **320**(2)**:**269-276.

355. Schwarz RI, Kleinman P, Owens N: **Ascorbate can act as an inducer of the collagen pathway because most steps are tightly coupled.** *Ann N Y Acad Sci* 1987, **498:**172-185.

356. Munir S, Foldager CB, Lind M, Zachar V, Soballe K, Koch TG: **Hypoxia enhances chondrogenic differentiation of human adipose tissue-derived stromal cells in scaffold-free and scaffold systems.** *Cell Tissue Res* 2014, **355**(1)**:**89-102.

357. Acharya C, Adesida A, Zajac P, Mumme M, Riesle J, Martin I, Barbero A: **Enhanced chondrocyte proliferation and mesenchymal stromal cells chondrogenesis in coculture pellets mediate improved cartilage formation.** *J Cell Physiol* 2012, **227**(1)**:**88-97.

358. Mizuno S, Tateishi T, Ushida T, Glowacki J: **Hydrostatic fluid pressure enhances matrix synthesis and accumulation by bovine chondrocytes in three-dimensional culture.** *J Cell Physiol* 2002, **193**(3)**:**319-327.

359. Lai CH, Chen SC, Chiu LH, Yang CB, Tsai YH, Zuo CS, Chang WH, Lai WF: **Effects of low-intensity pulsed ultrasound, dexamethasone/TGF-beta1 and/or BMP-2 on the transcriptional expression of genes in human mesenchymal stem cells: chondrogenic vs. osteogenic differentiation.** *Ultrasound Med Biol* 2010, **36**(6)**:**1022-1033.

360. Kafienah W, Mistry S, Dickinson SC, Sims TJ, Learmonth I, Hollander AP: **Three-dimensional cartilage tissue engineering using adult stem cells from osteoarthritis patients.** *Arthritis Rheum* 2007, **56**(1)**:**177-187.

361. Mo XT, Guo SC, Xie HQ, Deng L, Zhi W, Xiang Z, Li XQ, Yang ZM: **Variations in the ratios of co-cultured mesenchymal stem cells and**

chondrocytes regulate the expression of cartilaginous and osseous phenotype in alginate constructs. *Bone* 2009, **45**(1)**:**42-51.

362. Winter A, Breit S, Parsch D, Benz K, Steck E, Hauner H, Weber RM, Ewerbeck V, Richter W: **Cartilage-like gene expression in differentiated human stem cell spheroids: a comparison of bone marrow-derived and adipose tissue-derived stromal cells.** *Arthritis Rheum* 2003, **48**(2)**:**418-429.

363. Bornes TD, Adesida AB, Jomha NM: **Mesenchymal stem cells in the treatment of traumatic articular cartilage defects: a comprehensive review.** *Arthritis Res Ther* 2014, **16**(5)**:**432.

364. Leijten JC, Moreira Teixeira LS, Landman EB, van Blitterswijk CA, Karperien M: **Hypoxia inhibits hypertrophic differentiation and endochondral ossification in explanted tibiae.** *PLoS One* 2012, **7**(11)**:**e49896.

365. Harrison JS, Rameshwar P, Chang V, Bandari P: **Oxygen saturation in the bone marrow of healthy volunteers.** *Blood* 2002, **99**(1)**:**394.

366. Lund-Olesen K: **Oxygen tension in synovial fluids.** *Arthritis Rheum* 1970, **13**(6)**:**769-776.

367. Grayson WL, Zhao F, Bunnell B, Ma T: **Hypoxia enhances proliferation and tissue formation of human mesenchymal stem cells.** *Biochem Biophys Res Commun* 2007, **358**(3)**:**948-953.

368. Tsai CC, Chen YJ, Yew TL, Chen LL, Wang JY, Chiu CH, Hung SC: **Hypoxia inhibits senescence and maintains mesenchymal stem cell properties through down-regulation of E2A-p21 by HIF-TWIST.** *Blood* 2011, **117**(2)**:**459-469.

369. Zscharnack M, Poesel C, Galle J, Bader A: **Low oxygen expansion improves subsequent chondrogenesis of ovine bone-marrow-derived mesenchymal stem cells in collagen type I hydrogel.** *Cells Tissues Organs* 2009, **190**(2)**:**81-93.

370. Sheehy EJ, Buckley CT, Kelly DJ: **Oxygen tension regulates the osteogenic, chondrogenic and endochondral phenotype of bone marrow derived mesenchymal stem cells.** *Biochem Biophys Res Commun* 2012, **417**(1)**:**305-310.

371. Muller J, Benz K, Ahlers M, Gaissmaier C, Mollenhauer J: **Hypoxic conditions during expansion culture prime human mesenchymal stromal precursor cells for chondrogenic differentiation in three-dimensional cultures.** *Cell Transplant* 2011, **20**(10)**:**1589-1602.

372. Leijten J, Georgi N, Moreira Teixeira L, van Blitterswijk CA, Post JN, Karperien M: **Metabolic programming of mesenchymal stromal cells by oxygen tension directs chondrogenic cell fate.** *Proc Natl Acad Sci U S A* 2014, **111**(38)**:**13954-13959.

373. Boyette LB, Creasey OA, Guzik L, Lozito T, Tuan RS: **Human bone marrow-derived mesenchymal stem cells display enhanced clonogenicity but impaired differentiation with hypoxic preconditioning.** *Stem Cells Transl Med* 2014, **3**(2)**:**241-254.

374. Garg T, Singh O, Arora S, Murthy R: **Scaffold: a novel carrier for cell and drug delivery.** *Crit Rev Ther Drug Carrier Syst* 2012, **29**(1)**:**1-63.

375. Aigner J, Tegeler J, Hutzler P, Campoccia D, Pavesio A, Hammer C, Kastenbauer E, Naumann A: **Cartilage tissue engineering with novel nonwoven structured biomaterial based on hyaluronic acid benzyl ester.** *J Biomed Mater Res* 1998, **42**(2)**:**172-181.

376. Livak KJ, Schmittgen TD: **Analysis of relative gene expression data using real-time quantitative PCR and the 2(-Delta Delta C(T)) Method.** *Methods* 2001, **25**(4)**:**402-408.

377. Lee CR, Grodzinsky AJ, Spector M: **Modulation of the contractile and biosynthetic activity of chondrocytes seeded in collagen-glycosaminoglycan matrices.** *Tissue Eng* 2003, **9**(1)**:**27-36.

378. McMahon LA, Reid AJ, Campbell VA, Prendergast PJ: **Regulatory effects of mechanical strain on the chondrogenic differentiation of MSCs in a collagen-GAG scaffold: experimental and computational analysis.** *Ann Biomed Eng* 2008, **36**(2)**:**185-194.

379. Studer D, Millan C, Ozturk E, Maniura-Weber K, Zenobi-Wong M: **Molecular and biophysical mechanisms regulating hypertrophic differentiation in chondrocytes and mesenchymal stem cells.** *Eur Cell Mater* 2012, **24:**118-135.

380. Demoor M, Maneix L, Ollitrault D, Legendre F, Duval E, Claus S, Mallein-Gerin F, Moslemi S, Boumediene K, Galera P: **Deciphering chondrocyte behaviour in matrix-induced autologous chondrocyte implantation to undergo accurate cartilage repair with hyaline matrix.** *Pathol Biol (Paris)* 2012, **60**(3)**:**199-207.

381. Leitinger B, Hohenester E: **Mammalian collagen receptors.** *Matrix Biol* 2007, **26**(3)**:**146-155.

382. Peach RJ, Hollenbaugh D, Stamenkovic I, Aruffo A: **Identification of hyaluronic acid binding sites in the extracellular domain of CD44.** *J Cell Biol* 1993, **122**(1)**:**257-264.

383. Yin Z, Chen X, Song HX, Hu JJ, Tang QM, Zhu T, Shen WL, Chen JL, Liu H, Heng BC, Ouyang HW: **Electrospun scaffolds for multiple tissues regeneration in vivo through topography dependent induction of lineage specific differentiation.** *Biomaterials* 2015, **44:**173-185.

384. Dalby MJ, Gadegaard N, Tare R, Andar A, Riehle MO, Herzyk P, Wilkinson CD, Oreffo RO: **The control of human mesenchymal cell differentiation using nanoscale symmetry and disorder.** *Nat Mater* 2007, **6**(12)**:**997-1003.

385. Chen G, Lv Y, Dong C, Yang L: **Effect of internal structure of collagen/hydroxyapatite scaffold on the osteogenic differentiation of mesenchymal stem cells.** *Curr Stem Cell Res Ther* 2015, **10**(2)**:**99-108.

386. Phadke A, Hwang Y, Kim SH, Kim SH, Yamaguchi T, Masuda K, Varghese S: **Effect of scaffold microarchitecture on osteogenic differentiation of human mesenchymal stem cells.** *Eur Cell Mater* 2013, **25:**114-129.

387. Fiedler T, Belova IV, Murch GE, Poologasundarampillai G, Jones JR, Roether JA, Boccaccini AR: **A comparative study of oxygen diffusion in tissue engineering scaffolds.** *J Mater Sci Mater Med* 2014, **25**(11)**:**2573-2578.

388. Kinner B, Spector M: **Smooth muscle actin expression by human articular chondrocytes and their contraction of a collagen-glycosaminoglycan matrix in vitro.** *J Orthop Res* 2001, **19**(2)**:**233-241.

389. Okada T, Hayashi T, Ikada Y: **Degradation of collagen suture in vitro and in vivo.** *Biomaterials* 1992, **13**(7)**:**448-454.

390. Shingleton WD, Hodges DJ, Brick P, Cawston TE: **Collagenase: a key enzyme in collagen turnover.** *Biochem Cell Biol* 1996, **74**(6)**:**759-775.

391. Caplan AI: **Effects of the nicotinamide-sensitive teratogen3-acetylpyridine on chick limb cells in culture.** *Exp Cell Res* 1970, **62**(2)**:**341-355.

392. Awad HA, Butler DL, Harris MT, Ibrahim RE, Wu Y, Young RG, Kadiyala S, Boivin GP: **In vitro characterization of mesenchymal stem cell-seeded collagen scaffolds for tendon repair: effects of initial seeding density on contraction kinetics.** *J Biomed Mater Res* 2000, **51**(2)**:**233-240.

393. Francioli SE, Candrian C, Martin K, Heberer M, Martin I, Barbero A: **Effect of three-dimensional expansion and cell seeding density on the cartilage-forming capacity of human articular chondrocytes in type II collagen sponges.** *J Biomed Mater Res A* 2010, **95**(3)**:**924-931.

394. Pearle AD, Warren RF, Rodeo SA: **Basic science of articular cartilage and osteoarthritis.** *Clin Sports Med* 2005, **24**(1)**:**1-12.

395. Makris EA, Hu JC, Athanasiou KA: **Hypoxia-induced collagen crosslinking as a mechanism for enhancing mechanical properties of engineered articular cartilage.** *Osteoarthritis Cartilage* 2013, **21**(4)**:**634-641.

396. Ronziere MC, Perrier E, Mallein-Gerin F, Freyria AM: **Chondrogenic potential of bone marrow- and adipose tissue-derived adult human mesenchymal stem cells.** *Biomed Mater Eng* 2010, **20**(3)**:**145-158.

397. Pachence JM: **Collagen-based devices for soft tissue repair.** *J Biomed Mater Res* 1996, **33**(1)**:**35-40.

398. Rowland CR, Lennon DP, Caplan AI, Guilak F: **The effects of crosslinking of scaffolds engineered from cartilage ECM on the chondrogenic differentiation of MSCs.** *Biomaterials* 2013, **34**(23)**:**5802-5812.

399. Vasara AI, Hyttinen MM, Lammi MJ, Lammi PE, Langsjo TK, Lindahl A, Peterson L, Kellomaki M, Konttinen YT, Helminen HJ, Kiviranta I: **Subchondral bone reaction associated with chondral defect and attempted cartilage repair in goats.** *Calcif Tissue Int* 2004, **74**(1)**:**107-114.

400. Lee JE, Park JC, Hwang YS, Kim JK, Kim JG, Sub H: **Characterization of UV-irradiated dense/porous collagen membranes: morphology, enzymatic degradation, and mechanical properties.** *Yonsei Med J* 2001, **42**(2)**:**172-179.

401. Zaleskas JM, Kinner B, Freyman TM, Yannas IV, Gibson LJ, Spector M: **Growth factor regulation of smooth muscle actin expression and contraction of human articular chondrocytes and meniscal cells in a collagen-GAG matrix.** *Exp Cell Res* 2001, **270**(1)**:**21-31.

402. Weadock KS, Miller EJ, Keuffel EL, Dunn MG: **Effect of physical crosslinking methods on collagen-fiber durability in proteolytic solutions.** *J Biomed Mater Res* 1996, **32**(2)**:**221-226.

403. Lee CR, Grodzinsky AJ, Spector M: **The effects of cross-linking of collagen-glycosaminoglycan scaffolds on compressive stiffness, chondrocyte-mediated contraction, proliferation and biosynthesis.** *Biomaterials* 2001, **22**(23)**:**3145-3154.

404. Huang-Lee LL, Cheung DT, Nimni ME: **Biochemical changes and cytotoxicity associated with the degradation of polymeric glutaraldehyde derived crosslinks.** *J Biomed Mater Res* 1990, **24**(9)**:**1185-1201.

405. Bornes TD, Jomha NM, Mulet-Sierra A, Adesida AB: **Hypoxic culture of bone marrow-derived mesenchymal stromal stem cells differentially enhances in vitro chondrogenesis within cell-seeded collagen and hyaluronic acid porous scaffolds.** *Stem Cell Res Ther* 2015, **6**(1)**:**84.

406. Farhadi J, Fulco I, Miot S, Wirz D, Haug M, Dickinson SC, Hollander AP, Daniels AU, Pierer G, Heberer M, Martin I: **Precultivation of engineered human nasal cartilage enhances the mechanical properties relevant for use in facial reconstructive surgery.** *Ann Surg* 2006, **244**(6)**:**978-85; discussion 985.

407. Lee CR, Grodzinsky AJ, Hsu HP, Spector M: **Effects of a cultured autologous chondrocyte-seeded type II collagen scaffold on the healing of a chondral defect in a canine model.** *J Orthop Res* 2003, **21**(2)**:**272-281.

408. Mallya SK, Mookhtiar KA, Van Wart HE: **Kinetics of hydrolysis of type I, II, and III collagens by the class I and II Clostridium histolyticum collagenases.** *J Protein Chem* 1992, **11**(1)**:**99-107.

409. Sumanasinghe RD, Osborne JA, Loboa EG: **Mesenchymal stem cell-seeded collagen matrices for bone repair: effects of cyclic tensile strain, cell density, and media conditions on matrix contraction in vitro.** *J Biomed Mater Res A* 2009, **88**(3)**:**778-786.

410. Nirmalanandhan VS, Levy MS, Huth AJ, Butler DL: **Effects of cell seeding density and collagen concentration on contraction kinetics of mesenchymal stem cell-seeded collagen constructs.** *Tissue Eng* 2006, **12**(7)**:**1865-1872.

411. Krinner A, Zscharnack M, Bader A, Drasdo D, Galle J: **Impact of oxygen environment on mesenchymal stem cell expansion and chondrogenic differentiation.** *Cell Prolif* 2009, **42**(4)**:**471-484.

412. Hansen OM, Foldager CB, Christensen BB, Everland H, Lind M: **Increased chondrocyte seeding density has no positive effect on cartilage repair in an MPEG-PLGA scaffold.** *Knee Surg Sports Traumatol Arthrosc* 2013, **21**(2)**:**485-493.

413. Grogan SP, Barbero A, Winkelmann V, Rieser F, Fitzsimmons JS, O'Driscoll S, Martin I, Mainil-Varlet P: **Visual histological grading system for the evaluation of in vitro-generated neocartilage.** *Tissue Eng* 2006, **12**(8)**:**2141-2149.

414. Gronthos S, Simmons PJ, Graves SE, Robey PG: **Integrin-mediated interactions between human bone marrow stromal precursor cells and the extracellular matrix.** *Bone* 2001, **28**(2)**:**174-181.

415. Fortier LA, Barker JU, Strauss EJ, McCarrel TM, Cole BJ: **The role of growth factors in cartilage repair.** *Clin Orthop Relat Res* 2011, **469**(10)**:**2706-2715.

416. Hoggatt J, Scadden DT: **The stem cell niche: tissue physiology at a single cell level.** *J Clin Invest* 2012, **122**(9)**:**3029-3034.

417. Fortier L, Cassano J, Kennedy J, Ross K, Fraser E, Goodale M: **Chondrogenic Molecules in Bone Marrow Concentrate and Platelet Rich Plasma [abstract].** *International Cartilage Repair Society World Congress 2015 Abstracts* 2015; No 2.1.2.

418. Both SK, van der Muijsenberg AJ, van Blitterswijk CA, de Boer J, de Bruijn JD: **A rapid and efficient method for expansion of human mesenchymal stem cells.** *Tissue Eng* 2007, **13**(1)**:**3-9.

419. Lode A, Bernhardt A, Gelinsky M: **Cultivation of human bone marrow stromal cells on three-dimensional scaffolds of mineralized collagen: influence of seeding density on colonization, proliferation and osteogenic differentiation.** *J Tissue Eng Regen Med* 2008, **2**(7)**:**400-407.

420. Bartmann C, Rohde E, Schallmoser K, Purstner P, Lanzer G, Linkesch W, Strunk D: **Two steps to functional mesenchymal stromal cells for clinical application.** *Transfusion* 2007, **47**(8)**:**1426-1435.

421. Colter DC, Class R, DiGirolamo CM, Prockop DJ: **Rapid expansion of recycling stem cells in cultures of plastic-adherent cells from human bone marrow.** *Proc Natl Acad Sci U S A* 2000, **97**(7)**:**3213-3218.

422. Foldager CB: **Advances in autologous chondrocyte implantation and related techniques for cartilage repair.** *Dan Med J* 2013, **60**(4)**:**B4600.

423. Mahmoudifar N, Doran PM: **Effect of seeding and bioreactor culture conditions on the development of human tissue-engineered cartilage.** *Tissue Eng* 2006, **12**(6)**:**1675-1685.

424. Vunjak-Novakovic G, Obradovic B, Martin I, Bursac PM, Langer R, Freed LE: **Dynamic cell seeding of polymer scaffolds for cartilage tissue engineering.** *Biotechnol Prog* 1998, **14**(2)**:**193-202.

425. Huang CY, Reuben PM, D'Ippolito G, Schiller PC, Cheung HS: **Chondrogenesis of human bone marrow-derived mesenchymal stem cells in agarose culture.** *Anat Rec A Discov Mol Cell Evol Biol* 2004, **278**(1)**:**428-436.

426. Mauck RL, Seyhan SL, Ateshian GA, Hung CT: **Influence of seeding density and dynamic deformational loading on the developing structure/function relationships of chondrocyte-seeded agarose hydrogels.** *Ann Biomed Eng* 2002, **30**(8)**:**1046-1056.

427. Kim DH, Kim DD, Yoon IS: **Proliferation and chondrogenic differentiation of human adipose-derived mesenchymal stem cells in sodium alginate beads with or without hyaluronic acid.** *Journal of Pharmaceutical Investigation* 2013, **43:**145.

428. Vickers SM, Squitieri LS, Spector M: **Effects of cross-linking type II collagen-GAG scaffolds on chondrogenesis in vitro: dynamic pore reduction promotes cartilage formation.** *Tissue Eng* 2006, **12**(5)**:**1345-1355.

429. Hurtig MB, Buschmann MD, Fortier LA, Hoemann CD, Hunziker EB, Jurvelin JS, Mainil-Varlet P, McIlwraith CW, Sah RL, Whiteside RA: **Preclinical Studies for Cartilage Repair: Recommendations from the International Cartilage Repair Society.** *Cartilage* 2011, **2**(2)**:**137-152.

430. Matsumoto T, Kubo S, Meszaros LB, Corsi KA, Cooper GM, Li G, Usas A, Osawa A, Fu FH, Huard J: **The influence of sex on the chondrogenic potential of muscle-derived stem cells: implications for cartilage regeneration and repair.** *Arthritis Rheum* 2008, **58**(12)**:**3809-3819.

431. Payne KA, Didiano DM, Chu CR: **Donor sex and age influence the chondrogenic potential of human femoral bone marrow stem cells.** *Osteoarthritis Cartilage* 2010, **18**(5)**:**705-713.

432. Chiang H, Liao CJ, Wang YH, Huang HY, Chen CN, Hsieh CH, Huang YY, Jiang CC: **Comparison of articular cartilage repair by autologous chondrocytes with and without in vitro cultivation.** *Tissue Eng Part C Methods* 2010, **16**(2)**:**291-300.

433. Izadpanah R, Trygg C, Patel B, Kriedt C, Dufour J, Gimble JM, Bunnell BA: **Biologic properties of mesenchymal stem cells derived from bone marrow and adipose tissue.** *J Cell Biochem* 2006, **99**(5)**:**1285-1297.

434. Bornes TD, Jomha NM, Mulet-Sierra A, Adesida AB: **Optimal Seeding Densities for In Vitro Chondrogenesis of Two- and Three-Dimensional-Isolated and -Expanded Bone Marrow-Derived Mesenchymal Stromal Stem Cells Within a Porous Collagen Scaffold.** *Tissue Eng Part C Methods* 2016, **22**(3)**:**208-220.

435. Cassano JM, Kennedy JG, Ross KA, Fraser EJ, Goodale MB, Fortier LA: **Bone marrow concentrate and platelet-rich plasma differ in cell distribution and interleukin 1 receptor antagonist protein concentration.** *Knee Surg Sports Traumatol Arthrosc* 2016, **:**.

436. Allen MJ, Houlton JE, Adams SB, Rushton N: **The surgical anatomy of the stifle joint in sheep.** *Vet Surg* 1998, **27**(6)**:**596-605.

437. O'Driscoll SW, Keeley FW, Salter RB: **The chondrogenic potential of free autogenous periosteal grafts for biological resurfacing of major full-thickness defects in joint surfaces under the influence of continuous passive motion. An experimental investigation in the rabbit.** *J Bone Joint Surg Am* 1986, **68**(7)**:**1017-1035.

438. O'Driscoll SW, Keeley FW, Salter RB: **Durability of regenerated articular cartilage produced by free autogenous periosteal grafts in major full-thickness defects in joint surfaces under the influence of continuous passive motion. A follow-up report at one year.** *J Bone Joint Surg Am* 1988, **70**(4)**:**595-606.

439. Frenkel SR, Bradica G, Brekke JH, Goldman SM, Ieska K, Issack P, Bong MR, Tian H, Gokhale J, Coutts RD, Kronengold RT: **Regeneration of articular cartilage--evaluation of osteochondral defect repair in the rabbit using multiphasic implants.** *Osteoarthritis Cartilage* 2005, **13**(9)**:**798-807.

440. Hoemann CD, Sun J, Legare A, McKee MD, Buschmann MD: **Tissue engineering of cartilage using an injectable and adhesive chitosan-based cell-delivery vehicle.** *Osteoarthritis Cartilage* 2005, **13**(4)**:**318-329.

441. Goebel L, Orth P, Muller A, Zurakowski D, Bucker A, Cucchiarini M, Pape D, Madry H: **Experimental scoring systems for macroscopic articular cartilage repair correlate with the MOCART score assessed by a high-field MRI at 9.4 T--comparative evaluation of five macroscopic scoring systems in a large animal cartilage defect model.** *Osteoarthritis Cartilage* 2012, **20**(9)**:**1046-1055.

442. Lam J, Lu S, Meretoja VV, Tabata Y, Mikos AG, Kasper FK: **Generation of osteochondral tissue constructs with chondrogenically and osteogenically predifferentiated mesenchymal stem cells encapsulated in bilayered hydrogels.** *Acta Biomater* 2014, **10**(3)**:**1112-1123.

443. Oldershaw RA, Tew SR, Russell AM, Meade K, Hawkins R, McKay TR, Brennan KR, Hardingham TE: **Notch signaling through Jagged-1 is necessary to initiate chondrogenesis in human bone marrow stromal cells but must be switched off to complete chondrogenesis.** *Stem Cells* 2008, **26**(3)**:**666-674.

444. Chung C, Burdick JA: **Influence of three-dimensional hyaluronic acid microenvironments on mesenchymal stem cell chondrogenesis.** *Tissue Eng Part A* 2009, **15**(2)**:**243-254.

445. Xu J, Wang W, Ludeman M, Cheng K, Hayami T, Lotz JC, Kapila S: **Chondrogenic differentiation of human mesenchymal stem cells in three-dimensional alginate gels.** *Tissue Eng Part A* 2008, **14**(5)**:**667-680.

446. Lisignoli G, Cristino S, Piacentini A, Toneguzzi S, Grassi F, Cavallo C, Zini N, Solimando L, Mario Maraldi N, Facchini A: **Cellular and molecular events during chondrogenesis of human mesenchymal stromal cells grown in a three-dimensional hyaluronan based scaffold.** *Biomaterials* 2005, **26**(28)**:**5677-5686.

447. Grad S, Eglin D, Alini M, Stoddart MJ: **Physical stimulation of chondrogenic cells in vitro: a review.** *Clin Orthop Relat Res* 2011, **469**(10)**:**2764-2772.

448. Ben-Yishay A, Grande DA, Schwartz RE, Menche D, Pitman MD: **Repair of articular cartilage defects with collagen-chondrocyte allografts.** *Tissue Eng* 1995, **1**(2)**:**119-133.

449. Munirah S, Samsudin OC, Chen HC, Salmah SH, Aminuddin BS, Ruszymah BH: **Articular cartilage restoration in load-bearing osteochondral defects by implantation of autologous chondrocyte-fibrin constructs: an experimental study in sheep.** *J Bone Joint Surg Br* 2007, **89**(8)**:**1099-1109.

450. van den Borne MP, Raijmakers NJ, Vanlauwe J, Victor J, de Jong SN, Bellemans J, Saris DB, International Cartilage Repair Society: **International Cartilage Repair Society (ICRS) and Oswestry macroscopic cartilage evaluation scores validated for use in Autologous Chondrocyte Implantation (ACI) and microfracture.** *Osteoarthritis Cartilage* 2007, **15**(12)**:**1397-1402.

451. Madry H, van Dijk CN, Mueller-Gerbl M: **The basic science of the subchondral bone.** *Knee Surg Sports Traumatol Arthrosc* 2010, **18**(4)**:**419-433.

452. Rubin DA, Harner CD, Costello JM: **Treatable chondral injuries in the knee: frequency of associated focal subchondral edema.** *AJR Am J Roentgenol* 2000, **174**(4)**:**1099-1106.

453. Li G, Yin J, Gao J, Cheng TS, Pavlos NJ, Zhang C, Zheng MH: **Subchondral bone in osteoarthritis: insight into risk factors and microstructural changes.** *Arthritis Res Ther* 2013, **15**(6)**:**223.

454. Schmitt A, Imhoff AB, Vogt S: **Predifferentiated mesenchymal stem cells for osteochondral defects: letter.** *Am J Sports Med* 2011, **39**(6)**:**NP12-3; author reply NP13-5.

455. Dorotka R, Bindreiter U, Macfelda K, Windberger U, Nehrer S: **Marrow stimulation and chondrocyte transplantation using a collagen matrix for cartilage repair.** *Osteoarthritis Cartilage* 2005, **13**(8)**:**655-664.

456. O'Driscoll SW, Marx RG, Beaton DE, Miura Y, Gallay SH, Fitzsimmons JS: **Validation of a simple histological-histochemical cartilage scoring system.** *Tissue Eng* 2001, **7**(3)**:**313-320.

457. Schumacher BL, Su JL, Lindley KM, Kuettner KE, Cole AA: **Horizontally oriented clusters of multiple chondrons in the superficial zone of ankle, but not knee articular cartilage.** *Anat Rec* 2002, **266**(4)**:**241-248.

458. Lotz MK, Otsuki S, Grogan SP, Sah R, Terkeltaub R, D'Lima D: **Cartilage cell clusters.** *Arthritis Rheum* 2010, **62**(8)**:**2206-2218.

459. Hoshiyama Y, Otsuki S, Oda S, Kurokawa Y, Nakajima M, Jotoku T, Tamura R, Okamoto Y, Lotz MK, Neo M: **Chondrocyte clusters adjacent to sites of cartilage degeneration have characteristics of progenitor cells.** *J Orthop Res* 2015, **33**(4)**:**548-555.

Appendix 1

Methods of Isolation and Expansion of Bone Marrow-Derived Mesenchymal Stromal Stem Cells, Porous Scaffold Seeding and Chondrogenic Differentiation

Troy D. Bornes, Nadr M. Jomha, Aillette Mulet-Sierra, and Adetola B. Adesida

This chapter has been published in part in Bio-protocol.
Bornes TD, Jomha NM, Mulet-Sierra A, Adesida AB: **Porous Scaffold Seeding and Chondrogenic Differentiation of BMSC-seeded Scaffolds.** *Bio-protocol* 2015, **5**(24):e1693.

A1.1 Introduction

Bone marrow-derived mesenchymal stromal stem cells (BMSCs) are a promising cell source for treating articular cartilage defects [363]. BMSCs can be seeded within porous biomaterial scaffolds that support three-dimensional (3D) cell organization, chondrogenic differentiation and extracellular matrix (ECM) deposition for the creation of bioengineered cartilage. This protocol describes our defined methods for isolation and expansion of human and ovine BMSCs, seeding of BMSCs within porous scaffolds and *in vitro* chondrogenic differentiation [332, 405].

A1.2 Materials and Reagents

1. Bone marrow aspirate, human or ovine, collected through needle aspiration at the iliac crest
2. Crystal violet solution (Sigma-Aldrich, catalog number: HT90132)
3. Alpha minimal essential medium (αMEM), containing Earle's salts, ribonucleosides, deoxyribonucleosides and L-glutamine (Corning, Mediatech, catalog number: 10022CV)
4. Fetal bovine serum (FBS), heat inactivated at 56 °C in the laboratory (Life Technologies, Gibco, catalog number: 12483)
5. Penicillin-streptomycin-glutamine (Life Technologies, Gibco®, catalog number: 1248310378, see Recipes)
6. 4-(2-hydroxyethyl)-1-piperazineethanesulfonic acid (HEPES), 1 M (Life Technologies, Gibco, catalog number: 15630)
7. Sodium pyruvate, 100 mM (Life Technologies, Gibco, catalog number: 11360)
8. Fibroblast growth factor-two (FGF-2), human recombinant (Neuromics, catalog number: PR80001)
9. Trypsin-ethylenediaminetetraacetic acid (EDTA) (Corning, Mediatech, catalog number: 25052, see Recipes)
10. Dulbecco's phosphate buffered saline (PBS), sterile filtered (Sigma-Aldrich, catalog number: D8537)

11. Dulbecco's modified Eagle's medium (DMEM) (Sigma-Aldrich, catalog number: D6429, see Recipes)
12. Insulin-transferrin-selenium (ITS+) premix (BD Biosciences, catalog number: 354352, see Recipes)
13. Human serum albumin (Sigma-Aldrich, catalog number: A4327)
14. Transforming growth factor-beta three (TGF-β3), human recombinant, HEK (ProSpec, catalog number: CYT-113)
15. Ascorbic acid 2-phosphate (Sigma-Aldrich, catalog number: A8960)
16. Dexamethasone (Sigma-Aldrich, catalog number: D2915)
17. L-proline (Sigma-Aldrich, catalog number: P5607)
18. Trypan blue solution, 0.4% (Sigma-Aldrich, catalog number: T8154)
19. Porous scaffolds, collagen I or esterified hyaluronic acid (described in detail by Bornes *et al*., [405])
20. Culture plate, 24 wells (Becton Dickinson Labware, catalog number: 353047)
21. Expansion medium (see Recipes)
22. Serum-free medium (see Recipes)
23. TGF-β3 working solution (see Recipes)
24. Chondrogenic medium (see Recipes)

A1.3 Equipment

1. Biosafety cabinet (Microzone, catalog number: BK-2-6 A2)

2. Incubator, containing humidified air at 37 °C with 5% carbon dioxide, and 3% oxygen (Thermo Scientific, catalog number: Forma Series II Water Jacket CO_2)
3. Centrifuge, 1,500 revolutions per min (rpm) (Beckman Coulter, Allegra, catalog number: X-22R)
4. Light microscope (Omano, catalog number: OM159T)
5. Pipette (Drummond Scientific, catalog number: Pipet Aid XP)
6. Micropipettes, volumes of 100-1000 µl, 20-200 µl, 2-20 µl, and 0.5-10 µl (Bio-Rad, catalog numbers: 1660508, 1660507, 1660506, and 1660505)
7. Pipette tips, 1000 µl, 200 µl and 10 µl volumes (Corning, DeckWorks, catalog numbers: 4124, 4121 and 4120)
8. Suction source
9. Pasteur pipettes, 230 mm length (Wheaton, catalog number: 4500448667)
10. Forceps
11. Water bath, set to 37 °C (vWR, catalog number: 89501)
12. Cell strainer, nylon with 100 µm pores (BD Biosciences, catalog number: 352360)
13. Conical tube, 50 ml volume (Falcon, catalog number: 352070)
14. Neubauer hemocytometer, 0.1 mm deep (Reichert Bright-Line, Sigma-Aldrich, catalog number: Z359629)
15. Tissue-culture flask, 150 cm^2 surface area (T150) (Falcon, catalog number: 355000)

16. Conical microtube, 1.5 ml volume (Bio Basic Canada, catalog number: TC152SN)
17. Biopsy punch, circular with 6 mm diameter (Miltex, catalog number: 3336)

A1.4 Procedure

Methods involving manipulation of bone marrow aspirate, cells and porous scaffolds must be performed within a biosafety cabinet. Instruments, solutions and media in contact with bone marrow aspirate, cells and porous scaffolds must be sterile. Solutions and medium should be preheated to 37 °C in a closed container submersed in a water bath.

A1.4.1 Isolation and expansion of bone marrow-derived mesenchymal stromal stem cells

1. Obtain a sterile bone marrow aspirate. Collection of heparinized human and ovine iliac crest aspirates has been described in detail previously [254, 405]. Aspirate volumes of 15-60 ml and 20-40 ml may be obtained from human and ovine donors, respectively [43, 254, 274, 317, 405]. Aspirates should be taken to the laboratory directly following collection for processing in order to avoid cell death.
2. Filter the bone marrow aspirate using a 100 µm cell strainer to remove clots and tissue. Collect the filtrate in a sterile 50 ml conical tube.
3. For mononucleated cell counting, micropipette 50 µl of diluted bone marrow aspirate filtrate (1:10 in PBS; dilution might have to be increased to 1:50 if

cells are highly concentrated) and 50 µl of diluted crystal violet solution (1:50 in PBS) into a 1.5 ml conical microtube and mix thoroughly. Micropipette 20 µl of this mixture into a hemocytometer. Count the number of mononucleated cells within the four grid squares of the hemocytometer using a light microscope. Divide the number of cells counted by four (number of grid squares in hemocytometer), multiply by 20 (dilution of aspirate filtrate) and multiply by 10,000 (hemocytometer factor) to calculate the concentration of mononucleated cells per ml of aspirate filtrate. The total number of mononucleated cells is then determined my multiplying the concentration by the total volume (in ml) of the aspirate filtrate.

4. Calculate the volume of bone marrow aspirate filtrate containing 15 million human mononucleated cells or 80 million ovine mononucleated cells and pipette this volume into a sterile 50 ml conical tube [332, 405]. Pipette 20 ml of expansion medium into the 50 ml conical tube and mix with the aspirate filtrate. Transfer the aspirate filtrate-medium mixture into a T150 flask (passage 0). If large numbers of mononucleated cells are present in the aspirate filtrate, multiple T150 flasks may be seeded.
5. Statically incubate each T150 flask for seven days undisturbed at 37 °C. No media changes should be performed during this period.
6. After seven days, aspirate off medium and wash adherent BMSCs with 10 ml of PBS. Pipette 20 ml of fresh expansion medium into each T150 flask.
7. Statically incubate each T150 flask at 37 °C, and change the medium twice per week until 80% confluence is obtained based on microscopy.

8. Once 80% confluence has been reached, aspirate off medium and wash cells with 10 ml of PBS.
9. Pipette 6 ml of trypsin-EDTA into each T150 flask and incubate at 37 °C for 5 min. Agitate the flask to promote detachment of BMSCs from the flask surface. Microscopy may be used to confirm detachment of cells.
10. Pipette the BMSC-trypsin-EDTA mixture into a 50-ml conical tube and add 2 ml of serum-containing medium (expansion medium or αMEM with FBS) to deactivate trypsin.
11. Centrifuge the resulting mixture for 10 min (1,500 rpm) and aspirate off the liquid component. The BMSC collection will be present at the bottom of the 50 ml conical tube.
12. For BMSC counting, re-suspend the BMSC collection within a known quantity of expansion medium (*e.g.* 10 ml). Micropipette 50 µl of BMSC collection and 50 µl of trypan blue into a 1.5-ml conical microtube and mix thoroughly. Micropipette 20 µl of this mixture into a hemocytometer. Count the number of BMSCs within the four grid squares of the hemocytometer using a light microscope. Divide the number of cells by four (number of grid squares), multiply by 2 (dilution of BMSC suspension) and multiply by 10,000 (hemocytometer factor) to calculate the concentration of cells (BMSCs per ml of suspension). The total number of BMSCs is then determined by multiplying this concentration by total volume (in ml) of the BMSC suspension. Each T150 flask can be expected to yield 1-3 million BMSCs for human donors and 3-10 million BMSCs for ovine donors.

13. Add expansion medium to the BMSCs and re-suspend. BMSCs derived from one T150 flask during passage 0 should be re-suspended in 40 ml of expansion medium and divided into two T150 flasks for passage 1. There are a total of two T150 flasks during passage 1 per one T150 flask during passage 0.
14. Repeat steps A7-12 for passage 1.
15. Add expansion medium to the BMSCs and re-suspend. BMSCs derived from each T150 flask during passage 1 should be re-suspended in 40 ml of expansion medium and divided into two T150 flasks for passage 2. There are a total of four T150 flasks during passage 2 per one T150 flask during passage 0.
16. Repeat steps A7-12 for passage 2 BMSCs (Figures A1.1A and A1.1B). Subsequent passaging may be performed beyond passage 2 to increase the number of BMSCs available for use, although prolonged BMSC expansion has been shown to result in de-differentiation and loss of multipotent differentiation capacity of BMSCs [334, 368]. Therefore, the authors recommend using passage 2 BMSCs for use in chondrogenic differentiation.

A1.4.2 Seeding of porous biomaterial scaffolds with bone marrow-derived mesenchymal stromal stem cells and chondrogenic differentiation

1. Porous scaffold composition and size should be based on the goals of the study. For *in vitro* assessment of chondrogenesis, porous scaffold sheets

composed of collagen I sponge or esterified hyaluronic acid mesh (Bornes *et al.,* 2015) may be cut into 6 mm-diameter cylinders using a biopsy punch. Dimensions of the scaffold of choice must be known to calculate BMSC seeding density.

2. Calculate the number of BMSCs required to create a seeding density of 10 million BMSCs per cm^3 of scaffold. Other densities may be considered, although the authors recommend a seeding density of 5-10 million BMSCs per cm^3 of scaffold to be used in chondrogenic differentiation. For cylindrical collagen I scaffolds with a diameter of 6 mm and height of 3.5 mm, 989,602 BMSCs are required per scaffold for a density of 10 million BMSCs per cm^3. For cylindrical esterified hyaluronic acid scaffolds with a diameter of 6 mm and height of 2 mm, 565,487 BMSCs are required per scaffold.
3. Following counting of passage 2 BMSCs, centrifuge the resulting mixture for 10 min (1,500 rpm) and aspirate off the liquid component. The BMSC collection will be present at the bottom of the 50 ml conical tube.
4. Re-suspend BMSCs in chondrogenic medium with a total volume dependent on the number of scaffolds to be seeded (Figure A1.1C). For each 6 mm diameter scaffold, BMSCs (number calculated in step 2) should be re-suspended in 20 µl of chondrogenic medium.
5. Place scaffolds within empty wells of a 24 well culture plate using forceps (Figure A1.1D).
6. Micropipette the 20 µl BMSC-medium suspension onto the central area of the flat surface of each scaffold (Figure A1.1E). If the suspension does not spread

throughout the entirety of the surface of the scaffold, pre-soaking the scaffold with 20 µl of cell-free chondrogenic medium may be required to promote full dispersion of the BMSC-medium suspension over the scaffold. If a larger scaffold is to be used, multiple BMSC-medium suspensions may be micropipetted onto different areas of the scaffold to promote uniform seeding.

7. Incubate BMSC-seeded scaffolds at 37 °C for 15 min.
8. Micropipette 100 µl of chondrogenic medium onto the base of each BMSC-seeded scaffold.
9. Incubate BMSC-seeded scaffolds at 37 °C for 30 min.
10. Micropipette 1 ml of chondrogenic medium into each well to submerse the BMSC-seeded scaffolds.
11. Statically incubate 24 well plates at 37 °C for 2-3 weeks. Change the chondrogenic medium twice per week. BMSCs will differentiate into cells capable of producing cartilaginous extracellular matrix (Figure A1.1F).

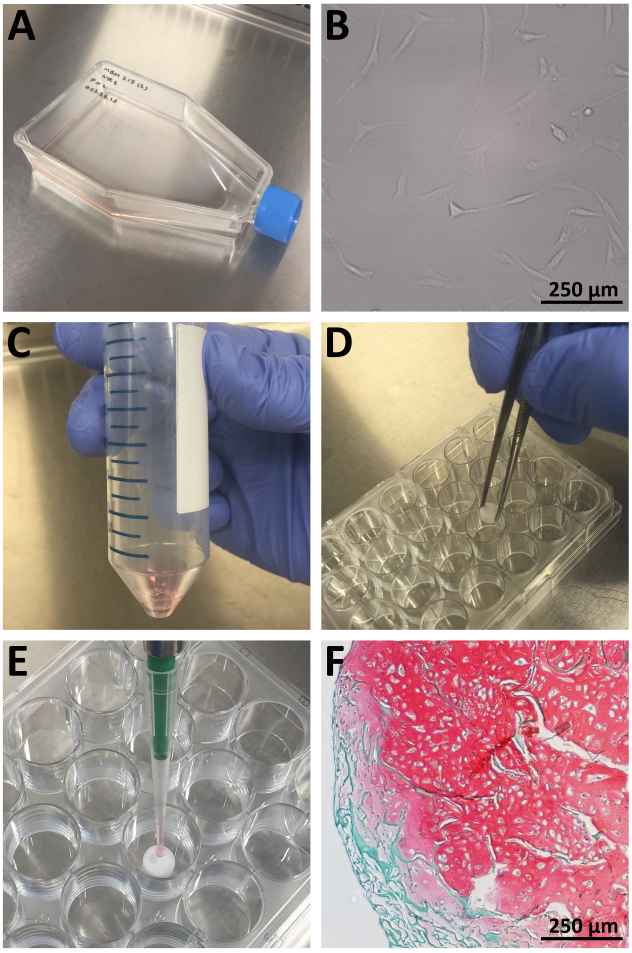

Figure A1.1 Isolation, expansion, seeding, and chondrogenic differentiation of bone marrow-derived mesenchymal stromal stem cells. (A) A tissue-culture flask (T150) containing isolated bone marrow-derived mesenchymal stromal stem cells (BMSCs0 and expansion medium. (B) Adherent, human BMSCs on the surface of a tissue-culture flask demonstrating a characteristic spindle-shaped morphology during expansion. (C) Re-suspension of BMSCs in chondrogenic medium within a 50 ml conical tube prior to scaffold seeding. (D) Collagen I scaffold placement into the empty well of a 24-well culture plate using forceps. (E) Micropipetting of a BMSC-chondrogenic medium suspension onto the central area of a collagen I scaffold. (F) Extracellular cartilaginous proteoglycans stained with safranin O following 3 weeks of chondrogenic differentiation of human BMSCs seeded within a collagen I scaffold. Remnant collagen I scaffold is stained with fast green counterstain (7× combined magnification of objective and camera lenses).

A1.5 Recipes

Penicillin-streptomycin-glutamine

10,000 units/ml penicillin

10 mg/ml streptomycin

29.2 mg/ml L-glutamine

Trypsin-ethylenediaminetetraacetic acid (EDTA)

0.05% trypsin

0.53 mM EDTA without sodium bicarbonate

Calcium and magnesium

Dulbecco's modified Eagle's medium (DMEM)

4.5 mg/ml glucose,

110 μg/ml sodium pyruvate

L-glutamine

Insulin-transferrin-selenium (ITS+) premix

625 μg/ml insulin

625 μg/ml transferrin

625 μg/ml selenium

125 μg/ml bovine serum albumin

535 μg/ml linoleic acid

Expansion medium, 565 ml total volume with final concentrations listed

500 ml αMEM

50 ml FBS [8.8% volume/volume (v/v)]

5 ml penicillin-streptomycin-glutamine

a. 88.5 units/ml penicillin

b. 88.5 µg/ml streptomycin

c. 258.4 µg/ml L-glutamine

5 ml HEPES (8.8 mM)

5 ml sodium pyruvate (885.0 µM)

282.5 µl FGF-2, 10 µg/ml stock solution (5 ng/ml)

Serum-free medium, 182 ml total volume with final concentrations listed

166 ml DMEM

2 ml HEPES (11.0 mM)

2 ml penicillin-streptomycin-glutamine

109.9 units/ml penicillin

109.9 µg/ml streptomycin

320.9 µg/ml L-glutamine

2 ml ITS+ premix

10 ml human serum albumin, 25 mg/ml stock solution (1.4 mg/ml)

TGF-β3 working solution, 10 ml total volume with final concentrations listed

9.4 ml DMEM

100 µl TGF-β3, 10 µg/ml stock solution (100 ng/ml)

500 µl human serum albumin, 25 mg/ml stock solution (1.3 mg/ml)

Chondrogenic medium, 100 ml total volume with final concentrations listed

87 ml serum-free medium

DMEM

9.6 mM HEPES

95.6 units/ml penicillin

95.6 µg/ml streptomycin

279.2 µg/ml L-glutamine

1 ml ITS+ premix

10 ml TGF-β3 working solution

DMEM

10.0 ng/ml TGF-β3

125 µg/ml human serum albumin

1 ml ascorbic acid 2-phosphate, 3.65 mg/ml stock solution (365 µg/ml)

1 ml dexamethasone, 10 µM stock solution (100 nM)

1 ml L-proline, 4 mg/ml stock solution (40 µg/ml)

Appendix 2

Reverse-Transcription Quantitative Polymerase Chain Reaction Product Sequencing

Troy D. Bornes

This chapter has been published in part in Stem Cell Research & Therapy. Bornes TD, Jomha NM, Mulet-Sierra A, Adesida AB: **Hypoxic culture of bone marrow-derived mesenchymal stromal stem cells differentially enhances in vitro chondrogenesis within cell-seeded collagen and hyaluronic acid porous scaffolds.** *Stem Cell Res Ther* 2015, **6:**84.

A2.1 Introduction

Reverse-transcription quantitative polymerase chain reaction (RT-qPCR) products from Chapter 3 were sequenced to confirm that expression levels were based on appropriate sequences for each gene. RT-qPCR products were purified using a QIAquick Gel Extraction Kit (Qiagen Canada, Toronto, Canada), combined with each primer – forward and reverse primers separately – and sequenced using the Sanger method (The Applied Genomics Centre, University of Alberta, Edmonton, Canada). The resulting traces were read using FinchTV Software Version 1.5 (Geospiza, Seattle, USA) and matched to corresponding regions within characterized gene sequences using the nucleotide Basic Local Alignment Search

Tool (BLAST) of the National Center for Biotechnology Information (NCBI, Bethesda, USA).

A2.2 Beta-actin (*ACTB*)

Forward primer for *ACTB*:

5'-cggcgggaccaccat-3' NCBI sequence base pairs: 986-1000

Reverse primer for *ACTB*:

5'-gcagtgatctctttctgcatcct-3' NCBI sequence base pairs: 1020-1042

PCR product within NCBI sequence for *ACTB*:

Ovis aries actin, beta (*ACTB*), mRNA – starting at base pair 981

5'-ctgtccggcg ggaccaccat gtaccctggc atcgcagaca ggatgcagaa agagatcact gccctg-3'

3'-gacaggccgc cctggtggta catgggaccg tagcgtctgt cctacgtctt tctctagtga cgggac-5'

Sanger sequencing of PCR product using forward primer of *ACTB*:

Clearly sequenced region on chromatograph: 5'-gaaagagatcactgc-3'

BLAST of sequenced region: Ovis aries actin, beta (*ACTB*), mRNA (100% coverage, 100% identification)

5'-ctgtccggcg ggaccaccat gtaccctggc atcgcagaca ggatgcagaa agagatcact gccctg-3'

3'-gacaggccgc cctggtggta catgggaccg tagcgtctgt cctacgtctt tctctagtga cgggac-5'

Sanger sequencing of PCR product using reverse primer of *ACTB*:

Clearly sequenced region on chromatograph: 5'-catggtggtcccgccg-3'

BLAST of sequenced region: Ovis aries actin, beta (*ACTB*), mRNA (100% coverage, 100% identification)

5’-ctgtccggcg ggaccaccat gtaccctggc atcgcagaca ggatgcagaa agagatcact gccctg-3’

3’-gacaggccgc cctggtggta catgggaccg tagcgtctgt cctacgtctt tctctagtga cgggac-5’

A2.3 Aggrecan (*ACAN*)

Foward primer for *ACAN*:

5’-tggaatgatgtcccatgcaa-3’ NCBI sequence base pairs: 6019-6038

Reverse primer for *ACAN*:

5’-gccactgtgccctttttacag-3’ NCBI sequence base pairs: 6077-6057

PCR product within NCBI sequence for *ACAN*:

Ovis aries aggrecan (*ACAN*), mRNA (predicted) - starting at base pair 6015

5’-cgagtg gaatgatgtc ccatgcaatt accagctgcc cttcacctgt aaaaagggca cagtggcctg-3’

3’-gctcac cttactacag ggtacgttaa tggtcgacgg gaagtggaca tttttcccgt gtcaccggac-5’

Sanger sequencing of PCR product using forward primer for ACAN:

Clearly sequenced region on chromatograph: 5’-cccttcacctgtaaaaagggcacagtggc-3’

BLAST of sequenced region: Ovis aries aggrecan (*ACAN*), mRNA (100% coverage, 100% identification)

5’-cgagtg gaatgatgtc ccatgcaatt accagctgcc cttcacctgt aaaaagggca cagtggcctg-3’

3’-gctcac cttactacag ggtacgttaa tggtcgacgg gaagtggaca tttttcccgt gtcaccggac-5’

Sanger sequencing of PCR product using reverse primer for ACAN:

Clearly sequenced region on chromatograph: 5’-ctggtaattgcatgggacatcattcca-3’

BLAST of sequenced region: Ovis aries aggrecan (*ACAN*), mRNA (100% coverage, 100% identification)

5’-cgagtg gaatgatgtc ccatgcaatt accagctgcc cttcacctgt aaaaagggca cagtggcctg-3’

3’-gctcac cttactacag ggtacgttaa tggtcgacgg gaagtggaca tttttcccgt gtcaccggac-5’

A2.4 Cartilage oligomeric matrix protein (*COMP*)

Forward primer for *COMP*:

5’-cctaactgggtggtgctcaac-3’ NCBI sequence base pairs: 1654-1674

Reverse primer for *COMP*:

5’-ctgggtcgctgttcatcgt-3’ NCBI sequence base pairs: 1714-1696

PCR product within NCBI sequence for *COMP*:

Ovis aries cartilage oligomeric matrix protein (COMP), mRNA (predicted) - starting at base pair 1651

5’-gacctaact gggtggtgct caaccagggt atggagatcg tgcagacgat gaacagcgac ccaggcct-3’

3’-ctgggattga cccaccacga gttggtccca tacctctagc acgtctgcta cttgtcgctg ggtccgga-5’

Sanger sequencing of PCR product using forward primer for *COMP*

Clearly sequenced region on chromatograph: 5’-tgcagacgatgaacagcgacccag-3’

BLAST of sequenced region: Ovis aries cartilage oligomeric matrix protein (*COMP*), mRNA (100% coverage and 100% identification)

5’-gacctaact gggtggtgct caaccagggt atggagatcg tgcagacgat gaacagcgac ccaggcct-3’

3’-ctgggattga cccaccacga gttggtccca tacctctagc acgtctgcta cttgtcgctg ggtccgga-5’

Sanger sequencing of PCR product using reverse primer for *COMP*

Clearly sequenced region on chromatograph: 5'-ccctggttgagcaccacccagttagg-3'

BLAST of sequenced region: Ovis aries cartilage oligomeric matrix protein (*COMP*), mRNA (100% coverage and 100% identification)

5'-gaccctaact gggtggtgct caaccagggt atggagatcg tgcagacgat gaacagcgac ccaggcct-3'

3'-ctggattga cccaccacga gttggtccca tacctctagc acgtctgcta cttgtcgctg ggtccgga-5'

A2.5 Collagen I (*COL1A1*)

Forward primer for *COL1A1*:

5'-cgccccagaccaggaatt-3' NCBI sequence base pairs: 4419-4436

Reverse primer for *COL1A1*:

5'-gtggaaggagtttacaggaagca-3' NCBI sequence base pairs: 4481-4459

PCR product within NCBI sequence for *COL1A1*:

Ovis aries collagen, type I, alpha 1 (*COL1A1*), mRNA (predicted) - starting at base pair 4415

5'-ttggcg ccccagacca ggaattcggc ttcgacatcg gctctgtctg cttcctgtaa actccttcca ccc-3'

3'-aaccgc ggggtctggt ccttaagccg aagctgtagc cgagacagac gaaggacatt tgaggaaggt ggg-5'

Sanger sequencing of PCR product using forward primer for *COL1A1*:

Clearly sequenced region on chromatograph: 5'-gtctgcttcctgtaaactccttccac-3'

BLAST of sequenced region: Ovis aries collagen, type I, alpha 1 (*COL1A1*), mRNA (100% coverage and 100% identification)

5'-ttggcg ccccagacca ggaattcggc ttcgacatcg gctctgtctg cttcctgtaa actccttcca ccc-3'

3'-aaccgc ggggtctggt ccttaagccg aagctgtagc cgagacagac gaaggacatt tgaggaaggt ggg-5'

Sanger sequencing of PCR product using reverse primer *COL1A1*:

Clearly sequenced region on chromatograph: 5'-tcgaagccgaattcctggtctggggcg-3'

BLAST of sequenced region: Ovis aries collagen, type I, alpha 1 (*COL1A1*), mRNA (100% coverage and 100% identification)

5'-ttggcg ccccagacca ggaattcggc ttcgacatcg gctctgtctg cttcctgtaa actccttcca ccc-3'

3'-aaccgc ggggtctggt ccttaagccg aagctgtagc cgagacagac gaaggacatt tgaggaaggt ggg-5'

A2.6 Collagen II (*COL2A1*)

Forward primer for *COL2A1*:

5'-acctcacgtctccccatca-3' NCBI sequence base pairs: 4372-4390

Reverse primer for *COL2A1*:

5'-ctgctcgggccctcctat-3' NCBI sequence base pairs: 4428-4411

PCR product within NCBI sequence for *COL2A1*:

Ovis aries collagen, type II, alpha 1 (*COL2A1*), mRNA (predicted) - starting at base pair 4371

5'-gacctcacgt ctccccatca ttgacattgc acccatggac ataggagggc ccgagcagga attc-3'

3'-ctggagtgca gaggggtagt aactgtaacg tgggtacctg tatcctcccg ggctcgtcct taag-5'

Sanger sequencing of PCR product using forward primer

Clearly sequenced region on chromatograph: 5'-tggacataggagggcccgagcag-3'

BLAST of sequenced region: Ovis aries collagen, type II, alpha 1 (COL2A1), mRNA (100% coverage and 100% identification)

5'-gacctcacgt ctccccatca ttgacattgc acccatggac ataggagggc ccgagcagga attc-3'

3’-ctggagtgca gaggggtagt aactgtaacg tgggtacctg tatcctcccg ggctcgtcct taag-5’

Sanger sequencing of PCR product using reverse primer for *COL2A1*:

Clearly sequenced region on chromatograph: 5’-caatgatggggagacgtgaggt-3’

BLAST of sequenced region: Ovis aries collagen, type II, alpha 1 (*COL2A1*), mRNA (100% coverage and 100% identification

5’-gacctcacgt ctccccatca ttgacattgc acccatggac ataggagggc ccgagcagga attcg-3’

3’-ctggagtgca gaggggtagt aactgtaacg tgggtacctg tatcctcccg ggctcgtcct taagc-5’

A2.7 Collagen X (*COL10A1*)

Forward primer for *COL10A1*:

5’-caggctcgaatgggctgtac-3’ NCBI sequence base pairs: 2000-2019

Reverse primer for *COL10A1*:

5’-ccaccaagaatcctgagaaagag-3’ NCBI sequence base pairs: 2062-2040

PCR product within NCBI sequence for *COL10A1*:

Ovis aries collagen, type X, alpha 1 (*COL10A1*), mRNA (predicted) - starting at base pair 1996

5’-aatgc aggctcgaat gggctgtact cctctgagta cgtccactcc tctttctcag gattcttggt ggct-3’

3’-ttacg tccgagctta cccgacatga ggagactcat gcaggtgagg agaaagagtc ctaagaacca ccga-5’

Sanger sequencing of PCR product using forward primer for *COL10A1*:

Clearly sequenced region on chromatograph: 5’-ccactcctctttctcaggattcttggtgg-3’

BLAST of sequenced region: Ovis aries collagen, type X, alpha 1 (*COL10A1*), mRNA (100% coverage and 100% identification)

5’-aatgc aggctcgaat gggctgtact cctctgagta cgtccactcc tctttctcag gattcttggt ggct-3’

3’-ttacg tccgagctta cccgacatga ggagactcat gcaggtgagg agaaagagtc ctaagaacca ccga-5’

Sanger sequencing of PCR product using reverse primer for *COL10A1*:

Clearly sequenced region on chromatograph: 5’-ctcagaggagtacagcccattcgagcctg-3’

BLAST of sequenced region: Ovis aries collagen, type X, alpha 1 (*COL10A1*), mRNA (100% coverage and 100% identification)

5’-aatgc aggctcgaat gggctgtact cctctgagta cgtccactcc tctttctcag gattcttggt ggct-3’

3’-ttacg tccgagctta cccgacatga ggagactcat gcaggtgagg agaaagagtc ctaagaacca ccga-5’

A2.8 Sex determining region Y-box 9 (*SOX9*)

Forward primer for *SOX9*:

5’-gctgctggccgtgatga-3’ NCBI sequence base pairs: 956-972

Reverse primer for *SOX9*:

5’-gggtcgcgcgtttgttt-3’ NCBI sequence base pairs: 1007-995

PCR product within NCBI sequence for *SOX9*:

Ovis aries SRY (sex determining region Y)-box 9 (*SOX9*), mRNA (predicted) - starting at base pair 951

5’-cccacgctgc tggccgtgat gatcgcagaa agaacccaag aaacaaacgc gcgacccttt-3’

3’-gggtgcgacg accggcacta ctagcgtctt tcttgggttc tttgtttgcg cgctgggaaa-5’

Sanger sequencing of PCR product using forward primer for *SOX9*:

Clearly sequenced region on chromatograph: 5’-aaacgcgcgaccc-3’

BLAST of sequenced region: Ovis aries SRY (sex determining region Y)-box 9 (*SOX9*), mRNA (100% coverage and 100% identification)

5’-cccacgctgc tggccgtgat gatcgcagaa agaacccaag aaacaaacgc gcgacccttt-3’

3’-gggtgcgacg accggcacta ctagcgtctt tcttgggttc tttgtttgcg cgctgggaaa-5’

Sanger sequencing of PCR product using reverse primer for *SOX9*:

Clearly sequenced region on chromatograph: 5’-catcacggccagcagc-3’

BLAST of sequenced region: Ovis aries SRY (sex determining region Y)-box 9 (*SOX9*), mRNA (100% coverage and 100% identification)

5’-cccacgctgc tggccgtgat gatcgcagaa agaacccaag aaacaaacgc gcgacccttt-3’

3’-gggtgcgacg accggcacta ctagcgtctt tcttgggttc tttgtttgcg cgctgggaaa-5’

Appendix 3

Histological Scoring using the Modified O'Driscoll Scoring System

Troy D. Bornes

A3.1 Introduction

The modified O'Driscoll scoring system was used in Chapter 6 to assess sections of distal femoral defect sites stained with safranin O and fast green.

A3.2 History of the O'Driscoll scoring system

A3.2.1 Original system

Parameters of the O'Driscoll scoring system were first described by O'Driscoll *et al.* in 1986 to assess cartilaginous repair tissue following transplantation of autologous periosteum into patellar groove osteochondral defects in rabbits [437]. These parameters and others were subsequently combined into a defined, 24-point scoring system that was used to evaluate cartilage regeneration in the same model in 1988 [438]. O'Driscoll *et al.* later analyzed the subjective assessment of parameters of the scoring system relative to computerized methods [456]. It was shown that untrained observers – orthopaedic surgeons with no experience in cartilage research – were able to grade cartilage based on cellular morphology and safranin O staining in a similar fashion to a validated, computerized image

analysis system. It was also demonstrated that expert observers – researchers experienced in cartilage histology – were able to visually estimate the percentage of cartilage within safranin O-stained sections with a strong correlation to actual percentage measured using image analysis software with good inter-observer reliability. Subsequently, the original scoring system was used to assess femoral condyle cartilage regeneration in sheep following matrix-assisted microfracture, matrix-associated autologous chondrocyte implantation (MACI) and bone marrow-derived mesenchymal stem cell (BMSC) transplantation [274, 306, 308].

A3.2.2 Previously modified systems

Multiple modified scoring systems have been created based on the original system. Ben-Yishay *et al.* developed a 24-point scoring system to assess femoral trochlea repair tissue following MACI in rabbits [448]. Parameters of *cellular morphology* (maximal score of 4 points) and *safranin O staining of the matrix* (maximal score of 3 points) from the original system were replaced with *percentage of hyaline articular cartilage* (maximal score of 8 points) to provide a quantitative assessment of hyaline cartilage. The maximal score of *hypocellularity* was reduced from 3 to 2 points. Frenkel *et al.* subsequently modified the scoring system into a 27-point scoring system to assess repair tissue in the medial femoral condyles of rabbits following scaffold implantation [439]. This group maintained the *percentage of hyaline articular cartilage* addition of Ben-Yishay *et al*., but reinstated *safranin O staining* from the original score that was removed by Ben-Yishay *et al* [439, 448]. Parameters for *reconstitution of subchondral bone*

(maximal score of 2 points) and *bonding of repair cartilage to de novo subchondral bone* (maximal score of 2 points) were added. *Hypocellularity* (maximal score of 2 points) and *chondrocyte clustering* (maximal score of 2 points) were replaced with a combined parameter of *freedom from cellular changes of degeneration* (maximal score of 3 points). The maximal score of *surface regularity* was reduced from 3 to 2 points. Munirah *et al.* used the system modified by Frenkel *et al.* to assess femoral condyle regeneration following MACI in sheep [449]. The percentage ranges used in scoring were clarified. For example, ranges of 80-100% (8 points) and 60-80% (6 points) were modified to 80-100% (8 points) and 60-79% (6 points) to reduce ambiguity related to percentages at the division between two ranges. In our study, a system based on the work of Frenkel *et al*. was modified and adapted for use in assessing cartilage regeneration in full-thickness cartilage defects [439, 449].

A3.3 Analysis using the current modified system

The system used in this study involved several modifications in comparison to previously modified systems [439, 448]. The definition of hyaline-like cartilaginous repair tissue was clarified. *Hyaline-like cartilaginous tissue* and *percentage of safranin O staining* parameters were normalized to: area of repair tissue / area of defect site. *Thickness* of repair tissue was normalized to: width of the defect site containing repair tissue / total width of defect site. With respect to *changes in repair tissue* and *changes in adjacent native cartilage* parameters, the definitions for cellularity and cell clusters were updated. The parameters of the

score are listed in Table A2.1 described in detail below given the complexity of the system.

Table A3.1 Modified O'Driscoll histological scoring system

Nature of repair tissue		
Hyaline-like cartilaginous repair tissue*:	80 – 100% of all repair tissue	8
	60 – 79% of all repair tissue	6
	40 – 59% of all repair tissue	4
	20 – 39% of all repair tissue	2
	0 – 19% of all repair tissue	0
Safranin O staining*:	80 – 100% of all repair tissue	2
	40 – 79% of all repair tissue	1
	0 – 39% of all repair tissue	0
Structural characteristics of repair tissue		
Surface regularity:	Smooth and intact	2
	Fissures present	1
	Severe disruption and/or fibrillation	0
Structural integrity:	Normal	2
	Slight disruption and/or including cysts	1
	Severe lack of integrity	0
Thickness[&]:	100% of adjacent native cartilage	2
	50 – 99% of adjacent native cartilage	1
	0 – 49% of adjacent native cartilage	0
Bonding to adjacent cartilage:	Both ends bonded fully	2
	Bonded at one end or partially at both ends	1
	Not bonded	0
Bonding to subchondral bone:	100% of repair tissue bonded	2
	50 – 99% of repair tissue bonded	1
	0 – 49% of repair tissue bonded	0
Freedom from degeneration		
Changes in repair tissue:	Normal cellularity, no clusters	2
	Slight hypocellularity, <25% clusters	1
	Moderate hypocellularity/hypercellularity, ≥25% clusters	0
Changes in adjacent native cartilage:	Normal cellularity, no clusters, and normal staining	3
	Normal cellularity, mild clusters, moderate staining	2
	Mild-moderate hypocellularity, slight staining	1
	Severe hypocellularity, poor or no staining	0
Intactness of subchondral bone plate:	100% of defect width intact	2
	50 – 99% of defect width intact	1
	0 – 49% of defect width intact	0

* Normalized to the area of repair tissue / area of defect site

[&] Normalized to the width of repair tissue / width of defect site

A3.3.1 Hyaline-like cartilaginous repair tissue

In 1986, O'Driscoll *et al*. provided a definition of "hyaline-like cartilage" [437]:

> To be called hyaline-like cartilage, the [extracellular] matrix of the tissue had to stain normally or nearly normally with safranin O and, under high-power magnification, its cells had to demonstrate the normal morphological characteristics of chondrocytes (well demarcated lacunae containing round or oval nuclei with one or more nucleoli). The term hyaline-like is used rather than hyaline in order to indicate that, although the newly formed tissue resembled normal hyaline articular cartilage histologically and histochemically, the ultrastructure of this tissue was not assessed by electron microscopy, and the tissue frequently was more cellular and less organized into specific zones than is normal articular cartilage.

The original O'Driscoll scoring system was subsequently published in 1988 [438]. *Cellular morphology* and *safranin O staining of the matrix* served as parameters under *nature of predominant tissue* [438]. The term "hyaline articular cartilage" was used in the system instead of "hyaline-like cartilage" although presumably the authors were defining hyaline articular cartilage with the description provided in the previous article [437]. In the modification of Ben-Yishay *et al*., *percentage of hyaline articular cartilage* was introduced with a maximal score of 8 points [448]. This parameter replaced both *cellular*

morphology and *safranin O staining* from the original score. Through this revision, it appeared as though the definition of hyaline articular cartilage was based on cellular morphology and safranin O staining. However, it was not described in detail whether positive staining with safranin O was required to define tissue as hyaline articular cartilage. Furthermore, the heading *cellular morphology* alone was used in the table above *percentage of hyaline articular cartilage*. There was not another parameter included to assess for safranin O staining.

In the modification by Frenkel *et al*., the 8-point parameter described as *percentage of hyaline- or articular-appearing repair tissue* – and termed more simply as *percentage of hyaline articular cartilage* in Figure 3 of the article – was used with no heading describing cellular morphology or or safranin O staining. However, it was stated in the Materials and methods section that "hyaline-like appearance was judged by comparison with normal, unoperated host tissue, with respect to the type and density of cells populating the repair, and columnar arrangement of these cells." This raises the question of whether safranin O staining was used in addition to cellular morphology to confirm the presence of hyaline-like cartilaginous tissue. Is a cell located within a lacuna considered to be a chondrocyte with hyaline properties if it is not surrounded by extracellular matrix that stains positive for safranin O? A separate parameter called *safranin O staining* related to percentage of tissue stained homogeneously with safranin O.

During analysis in our study, we used the term “hyaline-like cartilage” as this was the term initially used by O’Driscoll *et al.* [437]. To determine *hyaline-like cartilaginous repair tissue*, we utilized the following definition to describe repair tissue that was deemed to be hyaline-like cartilage:

> Hyaline-like cartilaginous repair tissue is tissue that contains predominantly circular cells (≥75% of cells present within the area of tissue) within lacunae surrounded by extracellular matrix that stains positively with safranin O. Superficial repair tissue may be considered hyaline-like if it contains flattened, non-circular cells, lacks lacunae and safranin O staining, and is adjacent to deeper tissue containing predominantly circular cells within lacunae and positive safranin O staining given that this phenotype resembles the structural organization of native hyaline articular cartilage.

With respect to positive safranin O staining in our study, tissue had to be stained moderately (light pink) or strongly (deep pink-red-orange) to fulfill the requirement of the definition. In the event that the extracellular matrix appeared to be stained with both safranin O and fast green, the tissue was only considered as moderately stained with safranin O if it was closer in color to pink (safranin O) than green (fast green). The staining did not have to be uniform throughout the matrix to fulfill the definition. The quality and uniformity of the staining was assessed more thoroughly with a separate parameter called *safranin O staining*.

The density and organization of the cells (i.e. columnar arrangement) was not included in our definition as it was in the definition of Frenkel *et al*. given that we presumed that our repair tissue would be relatively immature as it was derived from BMSCs and assessed after a 6-month period. Consistent with this, O'Driscoll *et al*. stated that: "hyaline-like is used rather than hyaline in order to indicate that, although the newly formed tissue resembled normal hyaline articular cartilage histologically and histochemically… the tissue frequently was more cellular and less organized into specific zones than is normal articular cartilage" [437]. Tissue containing clustered cells was also considered to be hyaline-like if they were seen within lacunae.

Percentage of repair tissue area present fulfilling the definition described was documented during analysis and used for scoring. If a thin portion of the superficial repair tissue contained circular or flattened cells and lacked the presence of lacunae and safranin O staining, it was considered as hyaline-like tissue only if the tissue deep to it was rich in round cells surrounded by lacunae and safranin O staining. Although this tissue would meet the requirements of hyaline-like cartilage for this parameter, the superficial portion would not fulfill the requirements for the parameter *safranin O staining*.

A tidemark stained with safranin O that was present below the repair tissue was considered to be native tissue and not repair tissue for this analysis. In the event that the subchondral bone plate appeared to have shifted superficially

due to bony ingrowth, the level of the original, native subchondral plate was estimated from surrounding native tissues and the percentage of all repair tissue including bony repair tissue and cartilaginous repair tissue in the proposed defect site was assessed.

We normalized percentage of tissue with hyaline-like features to: area of repair tissue / area of defect site. All repair tissue, including tissue located both inside and outside of the defect site was used to estimate the area of repair tissue. The defect site was defined as the area created by the level of the native subchondral bone plate, top of lesion based on surface of the adjacent native cartilage, and interfaces between native cartilage and the defect on each side. The normalized value was documented following calculation using: percentage of repair tissue containing hyaline-like cartilage × (area of repair tissue / area of defect site). This value was used to determine a normalized score for this parameter.

A3.3.2 Safranin O staining

The parameter of *hyaline-like cartilaginous tissue* described above was used to assess tissue containing a specific cell morphology and extracellular matrix confirmed with positive safranin O staining, whereas *safranin O staining* was used to quantify the amount of tissue containing homogeneous staining, regardless of cell type or morphology.

During analysis, the percentage of repair tissue area that was stained with safranin O to at least a moderate intensity and in a homogeneous fashion was documented and used for scoring. To fulfill the requirements of safranin O staining, tissue had to be stained moderately (light pink) or strongly (deep pink-red-orange). In the event that an area of extracellular matrix appeared to be stained with both safranin O and fast green, the tissue was only considered to be moderately stained with safranin O if it was closer in color to pink (safranin O) than green (fast green). If there were areas with more intense staining within the homogeneously and moderately stained tissue, they were included in the percentage area, although less intensely stained areas were not included.

A tidemark that stained positively below the repair tissue was considered to be native tissue and not repair tissue for this analysis. In the event that the subchondral bone plate appeared to have shifted superficially due to bony ingrowth, the level of the native subchondral plate was estimated from surrounding osteochondral interfaces and all repair tissue including bony repair tissue and cartilaginous repair tissue in the proposed defect site was assessed.

Similar to the parameter of *hyaline-like cartilaginous repair tissue*, *safranin O staining* was also normalized to: area of repair tissue / area of defect site (see description within *hyaline-like cartilaginous repair tissue*). The normalized value was documented following calculation using: percentage of

repair tissue stained homogeneously with safranin O × (area of repair tissue / area of defect site). This value was used to determine a normalized score.

A3.3.3 Surface regularity

Surface regularity was used for assessment of the surface architecture of the repair tissue. For this parameter, fissures were defined as focal or linear disruptions in the surface that course downward towards the subchondral bone, whereas fibrillation was considered to be shredding of the superficial tissue.

During analysis, the entire defect site was assessed for irregularities in the surface. A score of 2 points was given only if there were no irregularities or disruptions in the surface architecture. If any irregularities were present, a score of 1 or 0 points was considered depending on the level of disruption.

A score of 1 point was given if one or more fissures were present. A defect noted centrally was considered to be a fissure to prevent over-scoring of sections containing an unfilled defect centrally with only small amounts of repair tissue near the repair tissue – native cartilage junctions. Lack of bonding between repair tissue located adjacent to native tissue and native cartilage was *not* considered as a fissure given that this finding was considered to be an indication of lack of integration rather than surface compromise of repair tissue. Lack of integration was assessed with a separate parameter called *bonding to adjacent cartilage*. Therefore, if there were no irregularities in the defect site other than lack of

integration between the repair tissue and native cartilage, a score of 2 points rather than 1 point was given.

Severe disruption related to the presence of many fissures or fibrillation in the surface, or complete lack of repair tissue present in the defect site was given a score of 0 points.

A3.3.4 Structural integrity

Structural integrity was "considered separately from the surface regularity" and referred to "the degree to which tissue below the surface appears to be intact histologically" [437]. However, *structural integrity* may be affected by surface irregularities in the setting of a fissure coursing downward to the subchondral bone through the repair tissue.

During analysis, a score of 2 points was awarded if the sub-surface tissue appeared to be completely intact. If any irregularities were present, a score of 1 or 0 points was considered depending on the level of disruption.

A score of 1 point was given if there were only minor horizontal cleavage planes or if fissures were found to extend from the surface to the subchondral bone [437]. A focal break or narrow fissure between repair tissue and native tissue localized to the junction was *not* considered to be a fissure extending to subchondral bone as this finding was considered to be an indication of lack of

integration rather than structural compromise (assessed with *bonding to adjacent cartilage*). However, areas of the defect site that lacked repair tissue with exposed subchondral bone – considered to be unfilled defects – were considered to be fissures extending to subchondral bone and received a score of 1 point, regardless of whether they were located centrally or near the junction with native cartilage.

A score of 0 points was given if there were large horizontal clefts within the newly formed tissue or if there was no repair tissue present. Lack of integration between repair tissue and subchondral bone was *not* considered a horizontal cleft. In the initial O'Driscoll scoring system, disruptions between the repair tissue and subchondral bone were considered as disruptions of structural integrity [438]. However, a separate parameter was not used to assess this condition. Given that the modified system used in our study contained a parameter called *bonding to subchondral bone* to assess bonding of repair tissue to subchondral bone, disruptions between repair tissue and bone were not included in analysis of structure.

A3.3.5 Thickness

Thickness of repair tissue is determined as a percentage relative to adjacent native cartilage.

During analysis, the average thickness of the repair tissue was estimated as a percentage relative to the height of the defect site. The defect site was defined as

the area created by the level of the native subchondral plate, top of lesion based on surface of the adjacent native cartilage, and interfaces between native cartilage and the defect on each side. The percentage calculated by repair tissue / native cartilage × 100 was documented and used for scoring.

In the event that there was a subchondral bone plate defect and cellular repair tissue into the underlying bone that was noted to be different than adjacent native bone, the thickness of the repair tissue found in the subchondral area was included in the thickness analysis. As a result, it was possible for the calculated thickness to be higher than that estimated by including only tissue within the chondral defect site superficial to the presumed height of the original subchondral plate. If the subchondral plate appeared to have shifted superficially due to bony ingrowth into the defect site, the level of the native subchondral plate was estimated from surrounding native osteochondral interfaces. In this latter case, bony repair tissue was considered to be repair tissue in the measurement of thickness along with cartilaginous tissue.

The value of thickness was normalized to the percentage of defect width that was occupied by repair tissue in the defect site. The normalized value was documented following calculation using: percentage of thickness of repair tissue relative to adjacent native cartilage × (width of the defect site containing repair tissue / total width of defect site). This value was used to determine a normalized score.

A3.3.6 Bonding to adjacent cartilage

Bonding to adjacent cartilage was used in the assessment of integration of repair tissue with surrounding native cartilage. Based on the description by O'Driscoll *et al*., bonding is defined as "perfect apposition of the two tissues" [437].

During analysis, the two interfaces between the repair tissue and adjacent native cartilage were assessed. A score of 2 points was awarded only if there was full bonding noted at both interfaces, i.e. the entire thickness of the repair tissue adjacent to the native cartilage was bonded to the native cartilage, and this occurred on both sides. A score of 1 point was given if there was full bonding on one interface only with some or no bonding on the other interface, or if both interfaces displayed partial bonding. A score of 0 points was given if one side of the repair tissue displayed no bonding and the other side displayed either partial or no bonding.

A3.3.7 Bonding to subchondral bone

Bonding to subchondral bone was not included in the original O'Driscoll scoring system [438]. Frenkel *et al*. introduced this parameter to assess repair cartilage bonding to *de novo* subchondral bone generated within osteochondral defects [439]. Our study involved full-thickness chondral defects without destruction of the subchondral bone prior to implantation. Therefore, the goal was to look at the

integration between repair tissue and native subchondral bone, not *de novo* subchondral bony repair tissue.

During analysis, bonding to subchondral bone was based on the quantity of width of the repair tissue that was bonded to underlying bone. The native tidemark was present in some sections between the subchondral bone and repair tissue. In these sections, attachment of the repair tissue to the tidemark served as an assessment of integration of repair tissue with subchondral bone.

A score of 2 points was awarded when 100% of the repair tissue width was bonded to the subchondral bone (or native tidemark). A score of 1 point was given when 50-99% of the width of the repair tissue was bonded to the subchondral bone (or tidemark), while a score of 0 points was given for 0-49% bonding.

A3.3.8 Changes in repair tissue

Changes in repair tissue is a parameter focused on cell density and the presence of cell clusters that relate to degeneration. The original O'Driscoll scoring system included *hypocellularity* and *presence of clusters* as separate parameters [438]. Frenkel *et al*. combined these parameters into one parameter [439]. This group also introduced hypercellularity into the parameter.

Hypercellularity referred to tissue that was very hypercellular with respect to native cartilage and appeared to have a significantly reduced quantity of extracellular matrix surrounding each cell. Tissue that had mild hypercellularity relative to the native cartilage but still contained prominent extracellular matrix stained either green (fast green) or red-orange-pink (safranin O) was not be defined as demonstrating hypercellularity based on our definition, but was considered to display normocellularity. The reason for this was that the repair tissue in our study was derived from BMSCs and it was anticipated that the tissue formed would still display at least some characteristics of immaturity after 6 months. Based on the work of O'Driscoll *et al*., the term "hyaline-like" was used to describe tissue that resembled "normal hyaline articular cartilage histologically and histochemically" although the tissue was "frequently more cellular and less organized into specific zones than normal articular cartilage" [437]. Therefore, to score all immature hyaline-like tissues containing mild hypercellularity relative to native cartilage the same (hypercellularity yields a score of 0 points) would not be appropriate as it would lead to underscoring and would not decipher between immature tissues that varied in cell density and clustering.

In order to define hypercellularity, we employed a technique reported by Grogan *et al.* in the Bern score, a scale used to evaluate *in vitro*-generated neo-cartilage. This technique involved quantifying the distance between cells using cell size or diameter [413]. In our modified scale, tissue was defined as displaying hypercellularity when there was an average of <2 cell diameters of distance

between adjacent cells. Tissue containing cells that were separated on average by ≥2 cell diameters of extracellular matrix was defined as displaying either normal cellularity or hypocellularity. Hypocellularity was used to refer to tissue with a cell density that was lower than the native cartilage in the section. Therefore, normal cellularity was defined as tissue containing cells that were separated by ≥2 cell diameters of extracellular matrix but with a density that was equivalent or greater than the native cartilage in the section.

Cell clustering was not clearly defined in the studies by O'Driscoll *et al*. and Frenkel *et al*. [437-439]. It has been shown in human knees without osteoarthritis that cells in the superficial zone of native, articular cartilage naturally occur as single cells (90%) and doublets [457]. Within the deep zone of native cartilage, cells are typically oriented in vertical columns of multiple cells, often in groups of 3-4 cells [457]. Clusters in arthritic native tissue are typically larger and more prevalent than those in non-arthritic tissue, and are characteristically round and located within large lacunae [458]. One group recently defined a cluster as >6 cells within one lacuna [459]. Therefore, in our analysis, a clusters was defined as a group of >6 cells within a large lacuna. Cells in a vertical column consistent with the structure of native cartilage were not considered as clustered cells [457].

During analysis, the repair tissue was assessed in whole if quality was consistent throughout. When there were clear differences in tissue quality

between regions within a section, each region was assessed separately and given a sub-score. Sub-scores from multiple regions were then averaged and rounded to the nearest whole number to determine the score for the section. In the event that the subchondral plate appeared to have shifted superficially due to bony ingrowth, the level of the native subchondral plate was estimated from surrounding osteochondral interfaces and all repair tissue including bony repair tissue and cartilaginous repair tissue in the proposed defect area was assessed.

Normal cellularity and lack of cell clusters were necessary to award a score of 2 points.

For a score of 1 point, both slight hypocellularity and <25% of cells present in clusters were required, or just one of these findings with the other sub-parameter being normal. For example, if normal cellularity – that would yield a score of 2 points if no clusters were present – and clusters with <25% involvement were present, then 1 point was given. On the other hand, if there were no clusters – that would yield a score of 2 points if normal cellularity was present – and slight hypocellularity, then a score of 1 point was given.

For a score of 0 points, both moderate (to severe) hypocellularity (or hypercellularity) and ≥25% clusters were required, or just one of either moderate (to severe) hypocellularity (or hypercellularity) or the presence of clusters with ≥25% of cell involvement. If there was slight hypocellularity - that would yield a

score of 1 point with no clusters or <25% clusters - and clusters present to ≥25%, then a score of 0 points was given. If there was <25% clusters - that would yield a score of 1 point with slight hypocellularity or normal cellularity - and moderate (or severe) hypocellularity or hypercellularity, then a score of 0 points was given.

A3.3.9 Changes in adjacent cartilage

Changes in adjacent cartilage is a parameter based on cellular density, presence of cell clusters and safranin O staining in the native cartilage adjacent to the defect site.

During analysis, the adjacent cartilage was assessed over a width equivalent to 1× thickness of the native cartilage at the junction of the defect and native cartilage. Given that this parameter involved assessment of two separate areas of adjacent cartilage on each side of the defect, sub-scores were determined for each side and averaged. The averaged score was rounded to the nearest whole number. Cell clusters were defined as described under *changes in repair tissue*.

Normal cellularity, lack of cell clusters and normal safranin O staining were required to award a score of 3 points.

For a score of 2 points, all of normal cellularity, mild clusters and moderate staining were required, or normal cellularity was noted with either mild clusters and normal staining or no clusters and moderate staining.

For a score of 1 point, mild-moderate hypocellularity and slight staining were required, or mild-moderate hypocellularity was noted with either moderate or normal staining. On the other hand, if there was slight staining combined with normal cellularity, a score of 1 point was given.

For a score of 0 points, severe hypocellularity and poor or no staining were required, or severe hypocellularity was noted with slight, moderate or normal staining. On the other hand, a score of 0 points was also given for poor or no staining combined with mild-moderate hypocellularity or normal cellularity.

A3.3.10 Intactness of subchondral bone plate

Intactness of subchondral bone plate was not present in the original scoring system [438]. Frenkel *et al*. introduced this parameter for assessment of reconstitution of subchondral bone following surgical intervention for osteochondral lesions [439]. Given that the model in our study involved a full-thickness chondral defect without destruction of the subchondral bone prior to implantation, the goal was to assess intactness of subchondral bone in the context of degeneration. Presumably, destruction of the subchondral plate in a full-thickness cartilage model related to degenerative changes that occurred with time following implantation.

During analysis, the width of the subchondral plate that was intact was assessed. In some cases, the tidemark was present, while in others it was not. The presence or absence of the tidemark was not used to assess the subchondral plate, even if presence of the tidemark was variable within a section. Rather, the level of the subchondral bone located deep to the tidemark was assessed relative to the adjacent bone in the defect site and adjacent native cartilage. A small defect that appears to be related to a superficial bone sinusoid was not considered to be a subchondral plate defect. The presence of an obvious depression or disruption within the plate was required to consider the plate as not intact. If the subchondral plate has shifted superficially due to bony ingrowth, the subchondral plate was considered to be intact provided that the repair tissue that resembles bone was intact.

A score of 2 points was awarded when 100% of a plate's width was intact. A score of 1 point was given for 50-99% of width intactness, while 0 points was given for 0-49% of width intactness.

Appendix 4

Macroscopic Scoring using the Modified Goebel Scoring System

Troy D. Bornes

A4.1 Introduction

The modified Goebel scoring system was used in Chapter 6 to assess photographs taken of distal femoral defect sites.

A4.2 Original system

The system was created in 2012 by Goebel *et al.* to assess treatment of full-thickness cartilage defects in sheep treated with subchondral drilling [441]. The authors compared their new system to the International Cartilage Repair Society (ICRS) cartilage repair assessment score, Oswestry arthroscopy score, O'Driscoll macroscopic scoring system, and Jung macroscopic scoring system. The Goebel scoring system had the best intra- and inter-observer reliabilities and the highest correlation with *defect fill* on the magnetic resonance observation of cartilage repair score (MOCART).

A4.3 Analysis using the current modified system

There were several modifications made in comparison to the original Goebel scoring system [441]. The point scale was numbered inversely. *Color of repair tissue*, *presence of blood vessels*, and *degeneration of adjacent cartilage* parameters were analyzed as described by Goebel *et al*. and shown in Table A3.1 [441]. The *surface quality* parameter was clarified with respect to the definition of incomplete repair tissue. The *defect fill* parameter was assessed based on percentage of the defect filled to the level of the adjacent native cartilage rather than depth, which we believe is difficult to assess when viewing a defect from above.

Table A4.1 Modified Goebel macroscopic scoring system

Characteristics of repair tissue		
Color of repair tissue:	Hyaline or white (100%)	4
	Predominantly white (50 – 99%)	3
	Predominantly translucent or empty (50 – 99%)	2
	Translucent (100%)	1
	Empty	0
Presence of blood vessels:	0% of tissue	4
	0 – 24% of tissue	3
	25 – 49% of tissue	2
	50 – 74% of tissue	1
	75 – 100% of tissue	0
Surface quality:	Full resurfacing with smooth, homogeneous tissue	4
	Full resurfacing with smooth, heterogeneous tissue	3
	Full resurfacing with presence of fibrillated tissue	2
	Incomplete repair tissue with subchondral bone exposed	1
	No repair tissue with subchondral bone exposed	0
Characteristics of defect site		
Defect fill:	100% of defect filled to level of adjacent cartilage	4
	50 – 99% of defect filled to level of adjacent cartilage	3
	<50% of defect filled to level of adjacent cartilage	2
	Empty defect	1
	Subchondral bone damage in at least part of the defect site	0
Characteristics of native cartilage		
Degeneration of adjacent cartilage:	No changes in normal cartilage	4
	Cracks or fibrillations in integration zone	3
	Diffuse degenerative changes	2
	Extension of defect into adjacent cartilage	1
	Subchondral bone damage	0